Institute for Molecular Science

annual review

2009

Published by
Institute for Molecular Science
National Institutes of Natural Sciences
Myodaiji, Okazaki 444-8585, Japan
Phone: +81-564-55-7418 (Secretary Room)
Fax: +81-564-54-2254 (Secretary Room)
URL: http://www.ims.ac.jp/

Editorial Committee 2009

This is the last year of the first term of incorporation (privatization) of all the National Universities and Inter-University Research Institutes. Thanks to the efforts of all the staff members of IMS, we have enjoyed the high ranking evaluation. However, the severe conditions of academic research in Japan are still continuing, being badly affected also by the financial crisis.

The six special programs of IMS are going well and some nice achievements have been attained so far. These six programs are (i) Nano-science simulations for the "Grand Challenge Applications" of the next generation supercomputer project, (ii) Nano-network project, including the joint research initiative using the cutting-edge 920MHz NMR, (iii) Extreme photonics in collaboration with RIKEN, (iv) COE of molecular and materials simulations as a joint program of NINS, (v) Quantum Beam Development Program in collaboration with Kyoto University and Nagoya University, and (vi) Networked Laboratories for the Frontiers of Photon Science and Technology in collaboration with Japan Atomic Energy Research Institute, Osaka University and Kyoto University.

The network system for efficient and mutual use of experimental equipments covering 72 universities has been financially supported by the 2009-fiscal year government subsidiary budget. Thirty six new equipments will be installed at thirty two national universities including IMS.

In addition to the Asian Core Program, our JENESYS (Japan-East Asia Network of Exchange for Students and Youths) program has been approved by JSPS and active young scientists have been invited to IMS from various East Asian countries to carry out collaborative researches. Based on these activities we want to eventually establish an Asian Molecular Science Research Center at IMS.

In this 2009 fiscal year two new faculty members have joined us: Associate Professor Yuji Furutani of Division of Biomolecular Sensing, Department of Life and Coordination-Complex Molecular Science, and Associate Professor Hisashi Okumura of Research Center for Computational Science. In spite of the continuing unfortunate financial situation of academic research in Japan, we always have to strive to carry out excellent original researches at IMS as a Center of Excellence.

This volume of Annual Review is a summary of research activities performed at IMS in the period of September 2008–August 2009. As usual, a lot of activities are going on and we are proud of that. Any constructive comments and/or questions are heartily welcome. It is also a great pleasure to announce that many colleagues received various prizes as explained in this volume.

This is actually the last year of my director-ship. I would like to take this opportunity to thank all the members of IMS and also many people outside the institute for having supported me in many respects. I really hope that the financial situation will be substantially improved and many more wonderful researches will be carried out in future.

September, 2009

H. Nakamura

NAKAMURA, Hiroki
Director-General, Institute for Molecular Science

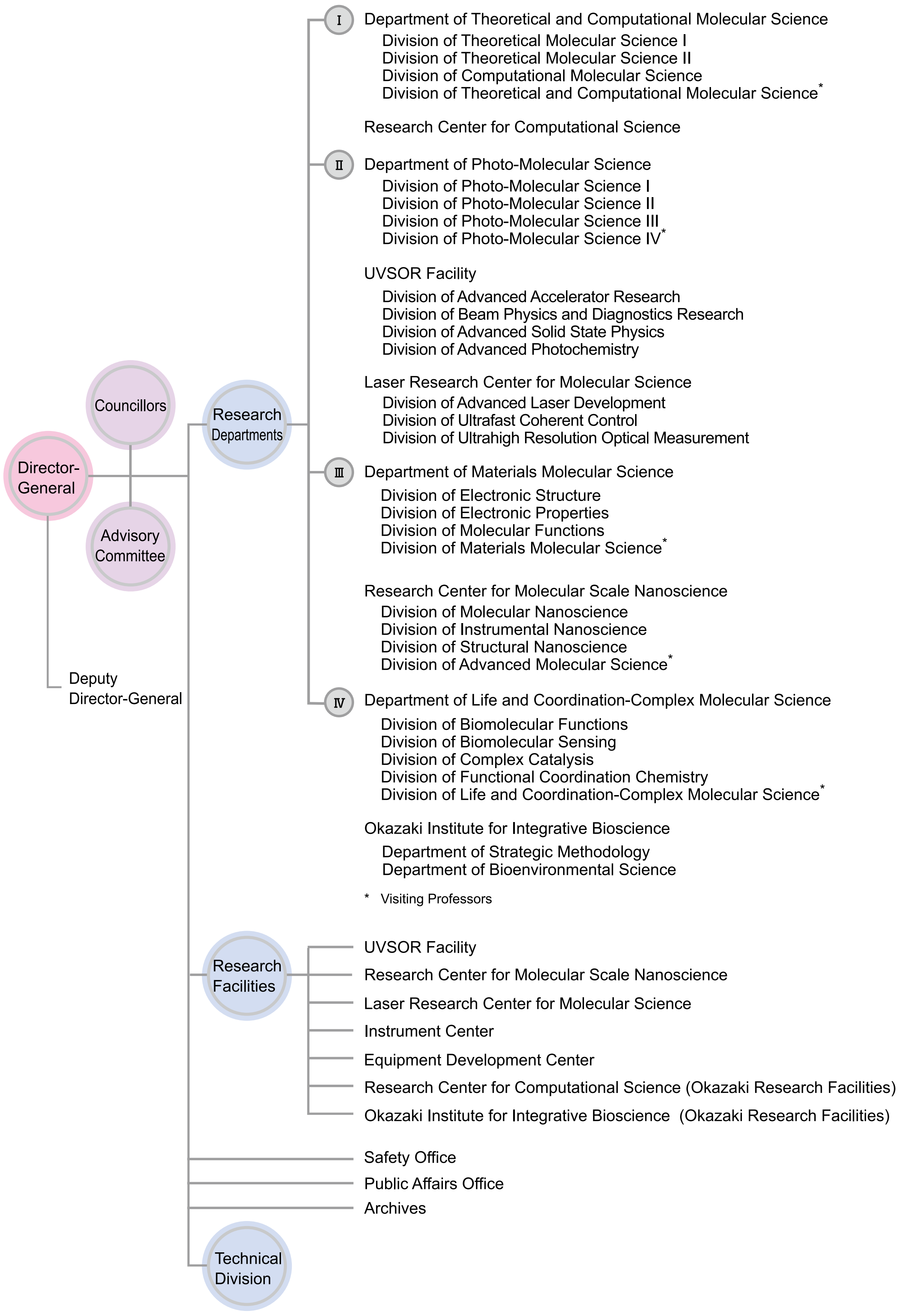

- Director-General
  - Councillors
  - Advisory Committee
  - Deputy Director-General
  - Research Departments
    - I Department of Theoretical and Computational Molecular Science
      - Division of Theoretical Molecular Science I
      - Division of Theoretical Molecular Science II
      - Division of Computational Molecular Science
      - Division of Theoretical and Computational Molecular Science*
    - Research Center for Computational Science
    - II Department of Photo-Molecular Science
      - Division of Photo-Molecular Science I
      - Division of Photo-Molecular Science II
      - Division of Photo-Molecular Science III
      - Division of Photo-Molecular Science IV*
    - UVSOR Facility
      - Division of Advanced Accelerator Research
      - Division of Beam Physics and Diagnostics Research
      - Division of Advanced Solid State Physics
      - Division of Advanced Photochemistry
    - Laser Research Center for Molecular Science
      - Division of Advanced Laser Development
      - Division of Ultrafast Coherent Control
      - Division of Ultrahigh Resolution Optical Measurement
    - III Department of Materials Molecular Science
      - Division of Electronic Structure
      - Division of Electronic Properties
      - Division of Molecular Functions
      - Division of Materials Molecular Science*
    - Research Center for Molecular Scale Nanoscience
      - Division of Molecular Nanoscience
      - Division of Instrumental Nanoscience
      - Division of Structural Nanoscience
      - Division of Advanced Molecular Science*
    - IV Department of Life and Coordination-Complex Molecular Science
      - Division of Biomolecular Functions
      - Division of Biomolecular Sensing
      - Division of Complex Catalysis
      - Division of Functional Coordination Chemistry
      - Division of Life and Coordination-Complex Molecular Science*
    - Okazaki Institute for Integrative Bioscience
      - Department of Strategic Methodology
      - Department of Bioenvironmental Science

    * Visiting Professors
  - Research Facilities
    - UVSOR Facility
    - Research Center for Molecular Scale Nanoscience
    - Laser Research Center for Molecular Science
    - Instrument Center
    - Equipment Development Center
    - Research Center for Computational Science (Okazaki Research Facilities)
    - Okazaki Institute for Integrative Bioscience (Okazaki Research Facilities)
  - Safety Office
  - Public Affairs Office
  - Archives
  - Technical Division

COUNCIL

NAKAMURA, Hiroki	**Director-General**

Councillors

KATO, Shinichi	Chief Executive Officer, Toyota Central Research & Development Laboratories, Inc.
TSUCHIYA, Soji	Professor Emeritus, The University of Tokyo ; Visiting Professor, National Chiao Tung University
TOKITOH, Norihiro	Director, Institute for Chemical Research, Kyoto University
TANAKA, Hiroaki	Culture News Editor, The Chunichi Shinbun Press
STACE, Anthony John*	Professor, The University of Nottingham
SAUVAGE, Jean-Pierre*	Director, University of Strasbourg

The Council is the advisory board for the Director-General.
* Two of the councillors are selected among distinguished foreign scientists.

Distinguished Consultants

NAGAKURA, Saburo	Professor Emeritus, Institute for Molecular Science, The Graduate University for Advanced Studies, and The University of Tokyo
INOKUCHI, Hiroo	Advisor, Japan Aerospace Exploration Agency
ITO, Mitsuo	Professor Emeritus, Institute for Molecular Science, The Graduate University for Advanced Studies, and Tohoku University
KAYA, Koji	Director, Advanced Computational Science Department, RIKEN Advanced Science Institute

Research Consultants

HIROTA, Noboru	Professor Emeritus, Kyoto University
IRIE, Masahiro	Professor, Rikkyo University

Advisory Committee

EBATA, Takayuki	Professor, Hiroshima University
ENOKI, Toshiaki	Professor, Tokyo Institute of Technology
FUKE, Kiyokazu	Professor, Kobe University (Vice chair)
KATO, Masako	Professor, Hokkaido University
NAKAJIMA, Atsushi	Professor, Keio University
SEKIYA, Hiroshi	Professor, Kyushu University
SHINOHARA, Hisanori	Professor, Nagoya University
WATANABE, Yoshihito	Professor, Nagoya University
YAMASHITA, Kouichi	Professor, The University of Tokyo
YAMASHITA, Masahiro	Professor, Tohoku University
HIRATA, Fumio	Professor, Institute for Molecular Science
KOSUGI, Nobuhiro	Professor, Institute for Molecular Science
NAGASE, Shigeru	Professor, Institute for Molecular Science
NISHI, Nobuyuki	Professor, Institute for Molecular Science
OKAMOTO, Hiromi	Professor, Institute for Molecular Science
OHMORI, Kenji	Professor, Institute for Molecular Science
TANAKA, Koji	Professor, Institute for Molecular Science
URISU, Tsuneo	Professor, Institute for Molecular Science (Chair)
YAKUSHI, Kyuya	Professor, Institute for Molecular Science
YOKOYAMA, Toshihiko	Professor, Institute for Molecular Science

Administration Bureau

MAEDA, Toshio	Director, Okazaki Administration Office Director, General Affairs Department
YOSHIDA, Hideo	Director, Financial Affairs Department
HIRANO, Shigeichi	Head, General Affairs Division
ISHIKAWA, Shinji	Head, International Relations and Research Cooperation Division
SUEMURA, Shinichiro	Head, Financial Affairs Division
SAKAMOTO, Kazuhiro	Head, Procurement Division
TORAZAWA, Takahiko	Head, Facilities Division

Emeritus Professors

NAGAKURA, Saburo	Professor Emeritus, The Graduate University for Advanced Studies and The University of Tokyo
HIROTA, Eizi	Professor Emeritus, The Graduate University for Advanced Studies
KIMURA, Katsumi	IMS, Professor Emeritus, Japan Advanced Institute of Science and Technology
MOROKUMA, Keiji	Research Leader, Fukui Institute for Fundamental Chemistry, Kyoto University
INOKUCHI, Hiroo	Advisor, Japan Aerospace Exploration Agency
MARUYAMA, Yusei	Professor, Hosei University
YOSHIHARA, Keitaro	Fellow, Toyota Physical and Chemical Research Institute
HANAZAKI, Ichiro	Professor Emeritus, The Graduate University for Advanced Studies
IWAMURA, Hiizu	Professor, Nihon University
SAITO, Shuji	Professor Emeritus, The Graduate University for Advanced Studies
IWATA, Suehiro	Fellow, Toyota Physical and Chemical Research Institute
ITO, Mitsuo	Professor Emeritus, The Graduate University for Advanced Studies and Tohoku University
KAYA, Koji	Director, Advanced Computational Science Department, RIKEN Advanced Science Institute
KITAGAWA, Teizo	Fellow, Toyota Physical and Chemical Research Institute
KOABAYASHI, Hayao	Visiting Professor, Nihon University

Graduate Programs

IMS promotes pioneering and outstanding research by young scientists as a core academic organization in Japan. IMS trains graduate students in the Departments of Structural Molecular Science and Functional Molecular Science, Graduate School of Physical Sciences, the Graduate University for Advanced Studies (SOKENDAI). By virtue of open seminars in each research division, Colloquiums and the Molecular Science Forum to which speakers are invited from within Japan and all over the world, as well as other conferences held within IMS, graduate students have regular opportunities to be exposed to valuable information related to their own fields of research as well as other scientific fields. Graduate students can benefit from these liberal and academic circumstances, all of which are aimed at extending the frontiers of fundamental molecular science and to facilitate their potential to deliver outstanding scientific contributions.

For more details on the Departments of Structural Molecular Science and Functional Molecular Science, young scientists are encouraged to visit IMS through many opportunities such as the IMS Open Campus in May, Graduate-School Experience Program (Taiken Nyugaku) in August, Open Lectures in summer and winter, *etc*.

International Collaboration and International Exchange

IMS has accepted many foreign scientists and hosted numerous international conferences (e.g. Okazaki Conference) since its establishment and is now universally recognized as an institute that is open to foreign countries. In 2004, IMS initiated a program to further promote international collaborations. As a part of this program, IMS faculty members can (1) nominate senior foreign scientists for short-term visits, (2) invite young scientists for long-term stays, and (3) undertake visits overseas to conduct international collaborations. In 2006, IMS started JSPS Asian CORE Program on “Frontiers of material, photo- and theoretical molecular sciences” (2006–2011). This program aims to develop a new frontier in the molecular sciences and to foster the next generation of leading researchers through the collaboration and exchange among IMS and core Asian institutions: ICCAS (China), KAIST (Korea), and IAMS (Taiwan). From 2008, IMS also started JSPS JENESYS Program on “Improvement of Fundamental Research Base for Environmental and Energy Problems.” IMS provides the opportunity for young researchers from ASEAN countries to stay in the laboratories related to the basic research for environmental and energy problem for 14–90 days. Through the experience, we encourage them to continue the basic research in their own countries as well as to build up the future collaboration.

Joint Studies Programs

As one of the important functions of an inter-university research institute, IMS facilitates joint studies programs for which funds are available to cover the costs of research expenses as well as the travel and accommodation expenses of individuals. Proposals from domestic scientists are reviewed and selected by an interuniversity committee. See the details in pages 110–113.

The programs are conducted under one of the following categories:

(1) Joint Studies on Special Projects (a special project of significant relevance to the advancement of molecular science can be carried out by a team of several groups of scientists).
(2) Research Symposia (a symposium on timely topics organized as a collaborative effort between outside and IMS scientists).
(3) Cooperative Research (a research program conducted by outside scientists with collaboration from an IMS scientist).
(4) Use of Facilities (a research program conducted by outside scientists using the research facilities of IMS, except the UVSOR facility).
(5) Joint Studies Programs using beam lines of UVSOR Facility.
(6) Use of Facility Program of the Computer Center (research programs conducted by outside scientists at research facilities in the Research Center for Computational Science).

RESEARCH ACTIVITIES

Theoretical and Computational Molecular Science

It is our goal to develop new theoretical and computational methods based on quantum mechanics, statistical mechanics, and molecular simulation in order to predict and understand the structures, reactions, and functions of molecules in gas, solution, and condensed phases as well as in nano- and bio-systems prior to or in cooperation with experiment.

Theoretical Study and Design of Functional Molecules: New Bonding, Structures, and Reactions

Department of Theoretical and Computational Molecular Science
Division of Theoretical Molecular Science I

NAGASE, Shigeru	Professor
GADRE, Shridhar R.	Visiting Professor
JANG, Joonkyung	Visiting Associate Professor*
OHTSUKA, Yuki	Assistant Professor
TANAKA, Masato	IMS Fellow
KATOUDA, Michio	Post-Doctoral Fellow
GAO, Xingfa	Post-Doctoral Fellow
GUO, Jing-Doing	Post-Doctoral Fellow
WANG, Lu	Post-Doctoral Fellow
MIYAKE, Toshiko	Post-Doctoral Fellow
WON, Jongok	Visiting Scientist†
RAHALKAR, Anuja P.	Graduate Student‡
YAMADA, Mariko	Secretary
KONDO, Naoko	Secretary

In theoretical and computational chemistry, it is an important goal to develop functional molecules prior to or in cooperation with experiment. Thus, new bonds and structures provided by heavier atoms are investigated together with the reactivities. In addition, chemical modification and properties of large molecules are investigated to develop functional nanomolecular systems. Efficient computational methods are also developed to perform reliable quantum chemistry calculations for small and large molecular systems.

1. Efficient Parallel Algorithm of Second-Order Møller-Plesset Perturbation Theory with Resolution-of-Identity Approximation (RI-MP2)[1)]

Density functional theory (DFT) is widely used to calculate large molecules as well as small molecules because of its accuracy and low computational cost. However, the generally used DFT methods fail to describe noncovalent interactions that play an essential role in host-guest molecules, self-assembly, molecular recognition, and three-dimensional structures of proteins, and usually underestimate reaction barriers. Therefore, many attempts have been made to develop new functionals. However, no widely applicable method has emerged yet.

Second-order Møller-Plesset perturbation theory (MP2) is the simplest and effective method that accounts for electron correlation effects important for noncovalent interactions and reaction barriers. MP2 is also helpful for checking DFT results. Despite these advantages, the formal scaling of MP2 calculations is $O(n^5)$ (n is the number of basis functions), much higher than that of DFT calculations. We have recently developed a new parallel algorithm of MP2 calculations. Despite this new algorithm, MP2 calculations of huge molecules are considerably time-consuming and require very large sizes of fast memory and hard disk. Therefore, we have developed an efficient parallel algorithm of RI-MP2 calculations to reduce highly the computational cost as well as the sizes of memory and disk by employing the resolution-of the identity (RI) approximation for two-electron repulsion integrals. The parallel algorithm aims at reducing I/O overheads and achieving good load balancing.

Test parallel calculations were carried out using 6-31G* and 6-311G basis sets for taxol ($C_{47}H_{51}NO_{14}$), valinomycin ($C_{54}H_{90}N_6O_{18}$), two-layer nanographene sheets ($C_{192}H_{28}$), and the noncovalent complex of C_{60} and $C_{60}H_{28}$. All the RI-MP2 calculations were performed on a Linux cluster of 3.2 GHz EM64T Pentium 4 processors connected by a Gigabit Ethernet network. These calculations confirm the high parallel efficiency of the developed algorithm. For taxol, the speedup, defined as the ratio of elapsed time, was almost linear, 27.0 (6-31G*) and 29.6 (6-311G*) for 32 processors. For valinomycin with the larger number of basis functions, super-linear scaling was achieved, the speedup being 36.6 (6-31G*) and 34.8 (6-311G*) for 32 processors. As the calculations of the noncovalent complex of C_{60} and $C_{60}H_{28}$ show (Figure 1), the high parallel efficiency is kept up to 64 CPU cores. The parallel efficiency depends on the speed of network communication because the amount of network communication increases linearly as the number of processors. It is expected that the high parallel efficiency is kept up to much more processors when more efficient network communication is employed. As shown by the RI-MP2 calculation of two-layer nanographene sheets with the 6-311 G* basis set (3,932 basis functions), only 2.3 GB memory per processor and a total of 228 GB disk are required, unlike the MP2 calculation that requires 14.6 GB memory and a total of 7.9 TB disk. In addition, RI-MP2 energies deviate from MP2 energies only by 1-3 mHartree.

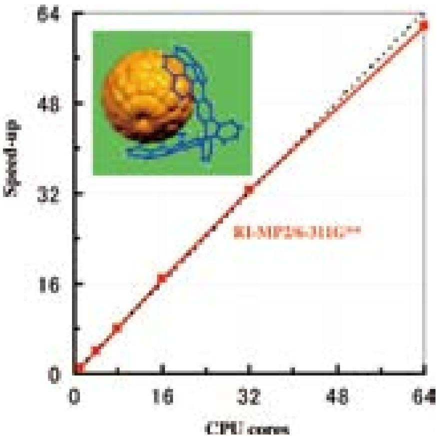

Figure 1. The RI-MP2 parallel calculations of the complex of C_{60} and $C_{60}H_{20}$.

2. Computational Approach to the Structures, Reactions, and Functionalization of Large Molecules

There has been much interest in silicon-silicon triply bonded compounds. Therefore, the structure and properties of 1,2-diaryldisilyne ($ArSi{\equiv}SiAr$), isolated by introducing bulky aryl groups ($Ar = C_6H_2\text{-}2,6\{CH(SiMe_3)_2\}_2\text{-}4\text{-}C(SiMe_3)_3$), were investigated by theoretical calculations.[2,3] The mechanisms of unique reactions of $R^{Si}Si{\equiv}SiR^{Si}$ protected by bulky silyl groups ($R^{Si} = Si^{i}Pr\{CH(SiMe_3)_2\}_2$) were theoretically disclosed.[4] In addition, neutral organogallium aryl dimeres and monomers were investigated to characterize the gallium-gallium bonds in digallenes and digallynes.[5]

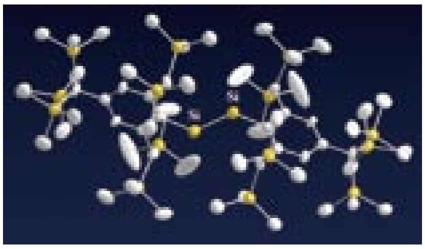

Endohedral metallofullerenes are of great interest in developing functional nanomolecules. It is an important task to observe the ^{13}C NMR chemical shifts of metal carbides in $Sc_2C_2@C_{82}$, $Sc_2C_2@C_{84}$, and $Sc_3C_2@C_{80}$ in an attempt to provide insight into its electronic and magnetic properties. The ^{13}C NMR chemical shifts were theoretically predicted and experimentally confirmed using ^{13}C-enriched samples.[6] In addition, calculations were performed for the radical coupling reactions of paramagnetic endohedral metallofullerenes,[7] anisotropic behavior of anionic carbene derivatives,[8] and missing metallofullerenes.[9]

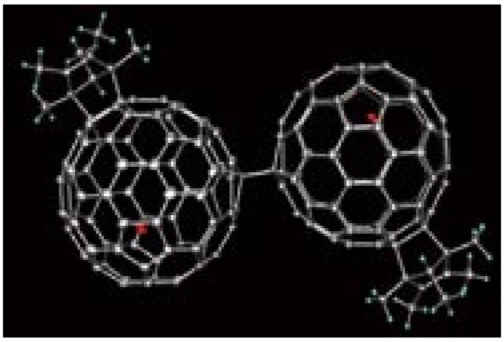

Nanographene (NG) has attracted great interest as the new generation of carbon electronics. We predicted how the oxidation unzipping of stable NG leads to spin-rich fragments in an attempt to realize NG-based molecular magnets.[10]

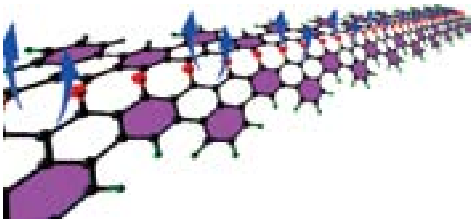

References

1) M. Katouda and S. Nagase, *Int. J. Quant. Chem.* **109**, 2121–2130 (2009).
2) T. Sasamori, K. Hironaka, Y. Sugiyama, N. Takagi, S. Nagase, Y. Hosoi, Y. Furukawa and N. Tokitoh, *J. Am. Chem. Soc.* **130**, 13856–13857 (2008).
3) T. Sasamori, J. S. Han, K. Hironaka, N. Takagi, S. Nagase and N. Tokitoh, *Pure Appl. Chem.* in press.
4) K. Takeuchi, M. Ichinohe, A. Sekiguchi, J. -D. Guo and S. Nagase, *Organometallics* **28**, 2658–2660 (2009).
5) Z. Zhu, R. C. Fischer, B. D. Ellis, E. Rivard, W. A. Merrill, M. M. Olmstead, P. P. Power, J. -D. Guo, S. Nagase and L. Pu, *Chem. Eur. J.* **15**, 5263–5272 (2009).
6) Y. Yamada, K. Nakajima, T. Wakahara, T. Tsuchiya, M. O. Ishitsuka, Y. Maeda, T. Akasaka, M. Waelchli, N. Mizorogi and S. Nagase, *Angew. Chem., Int. Ed.* **47**, 7905–7908 (2008).
7) Y. Takano, A. Yomogida, H. Nikawa, M. Yamada, T. Wakahara, T. Tsuchiya, Y. Maeda, T. Akasaka, T. Kato, Z. Slanina, N. Mizorogi and S. Nagase, *J. Am. Chem. Soc.* **130**, 16224–16230 (2009).
8) Y. Takano, M. Aoyagi, M. Yamada, H. Nikawa, Z. Slanina, N. Mizorogi, M. O. Ishitsuka, T. Tsuchiya, Y. Maeda, T. Akasaka, T. Kato and S. Nagase, *J. Am. Chem. Soc.* **131**, 9340–9346 (2009).
9) H. Nikawa, Y. Yamada, B. Gao, N. Mizorogi, Z. Slanina, T. Tsuchiya, T. Akasaka, K. Yoza and S. Nagase. *J. Am. Chem. Soc.* **131**, 10950–10954 (2009).
10) X. Gao, L. Wang, Y. Ohtsuka, D. -E. Jiang, Y. Xhao, S. Nagase and Z. Chen, *J. Am. Chem. Soc.* **131**, 9663–9669 (2009).

---

* Present Address; Present Address; Department of Nanomaterials Engineering, Pusan National University, Miryang 627-706, Korea

† Present Address; Department of Applied Chemistry, Sejong University, Seoul 143-747, Korea

‡ Present Address; Department of Chemistry, University of Pune, Pune 411007, India

Electronic Structure and Electron-Nuclear Dynamics of Molecules in Contact with an Electron Reservoir

Department of Theoretical and Computational Molecular Science
Division of Theoretical Molecular Science I

NOBUSADA, Katsuyuki	Associate Professor
YASUIKE, Tomokazu	Assistant Professor
IWASA, Takeshi	JSPS Post-Doctral Fellow
KUBOTA, Yoji	Post-Doctoral Fellow
NODA, Masashi	Post-Doctoral Fellow
YAMADA, Mariko	Secretary

Electronic structures and electron dynamics of molecules or nanostructured materials in contact with an electron reservoir play important roles in heterogeneous catalysis, surface photochemistry, and also electrochemistry. We have developed theoretical methods to calculate electronic structures of adsorbate-surface systems and electron-nuclear dynamics on their electronic potential-energy-surfaces. We have also investigated exciton transfer dynamics in an array of quantum dot. Furthermore, a generalized theoretical description of a light-matter interaction beyond a dipole approximation is developed on the basis of the multipolar Hamiltonian with the aim of understanding the near-field excitation of molecules at the 1 nm scale.

1. Photoinduced Coherent Adsorbate Dynamics on a Metal Surface: Nuclear Wave-Packet Simulation with Quasi-Diabatic Potential Energy Curves Using an Open-Boundary Cluster Model Approach[1)]

We present a nuclear wave-packet simulation of photoinduced coherent adsorbate dynamics on a metal surface with quasi-diabatic potential energy curves obtained from our recently developed open-boundary cluster model approach. Photoexcitation to the resonant adsorbate state and the subsequent ultrafast decay to the electronically excited substrate states were found to cause a coherent vibration of the adsorbate on the metal surface. This process competes with a Raman scattering process, which is generally believed to explain the coherent adsorbate vibration. These two mechanisms induce vibrations with a common frequency, and therefore cannot be distinguished from each other in a frequency-domain experiment. However, they can be distinguished by determining the initial vibrational phase through a time domain experiment such as ultrafast pump-probe spectroscopy. We further demonstrate that for near-resonant excitation the oscillation amplitude induced by our proposed mechanism largely exceeds the amplitude due to the Raman mechanism.

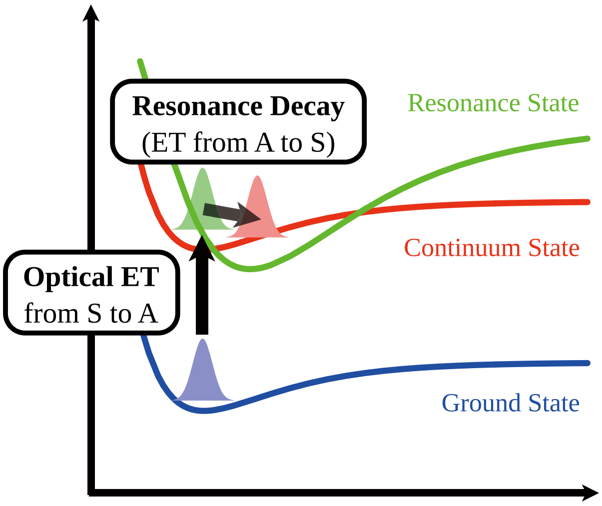

Figure 1. Schematic diagram of the TAM mechanism of causing coherent vibrational motion of the adsorbate on the continuum state.

2. Nonuniform Light-Matter Interaction Theory for Near-Field-Induced Electron Dynamics

A generalized theoretical description of a light-matter interaction beyond a dipole approximation is developed on the basis of the multipolar Hamiltonian with the aim of understanding the near-field excitation of molecules at the 1 nm scale. The theory is formulated for a system consisting of a molecule and a near-field, where a nonuniform electric field plays a crucial role. The nonuniform light-matter interaction is expressed in terms of a spatial integral of the inner product of the total polarization of a molecule and an electric field so that the polarization is treated rigorously without invoking the conventional dipole approximation. A nonuniform electronic excitation of a molecule is demonstrated by solving a time-dependent Kohn-Sham equation in real-space and real-time with an implementation of the nonuniform light-matter interaction. The computations are performed to a linear chain molecule of dicyanodiacetylene (NC_6N). The nonuniform electronic excitation clearly shows inhomogeneous electron dynamics in sharp contrast to the dynamics induced by a uniform electronic excitation under the dipole approximation. Despite the inversion symmetry of NC_6N, the nonuniform excitation generates even harmonics in addition to the odd ones. Higher-order nonlinear optical response and quadrupole excitation are also observed.

3. Applicability of Site-Basis Time-Evolution Equation for Thermalization of Exciton States in a Quantum Dot Array[2)]

We verify the practical applicability of the conventional site-basis time-evolution equation to exciton transfer processes in a quantum-dot array model. The time-evolution equation has proved to work under the rather limited conditions of the zero temperature limit and/or a minimal two-dot system. The computed results dramatically change with the temperature, the number of quantum dots, and the intensity of transition rates between adjacent sites. This is due to the fact that the higher-order perturbation terms, which are neglected in deriving the site-basis equation, have a great influence on the exciton dynamics. We found that the thermal relaxation can be suppressed by controlling the dot size and interdot distance.

4. Oscillator Strength Distribution of C_{60} in the Time-Dependent Density Functional Theory[3)]

An oscillator strength distribution of the fullerene C_{60} molecule is calculated in the time-dependent density functional theory. A real-time method is employed to obtain the spectrum of a wide energy region extending up to 120 eV. The orbitals are expressed on the uniform grid points in the three-dimensional Cartesian coordinates inside a large cubic box area. The calculated distribution shows an intense peak centered at around 20 eV, accompanying a number of sharp structures on it up to 35 eV. Absolute values and gross features of the oscillator strength distribution are in reasonable agreement with measurements.

5. Thiolated Gold Nanowires: Metallic *versus* Semiconducting[4)]

Tremendous research efforts have been spent on thiolated gold nanoparticles and self-assembled monolayers of thiolates on gold, but thiolated gold nanowires have received almost no attention. Here we computationally design two such one-dimensional nanosystems by creating a linear chain of Au icosahedra, fused together by either vertex sharing or face sharing. Then neighboring Au icosahedra are bridged by five thiolate groups for the vertex-sharing model and three RS Au SR motifs for the face-sharing model. We show that the vertex-sharing thiolated gold nanowire can be made either semiconducting or metallic by tuning the charge, while the face-sharing one is always metallic. We explain this difference between the two nanowires by examining their band structures and invoking a previously proposed electron-count rule. Implications of our findings for previous experimentation of gold nanowires are discussed, and a potential way to make thiolated gold nanowires is proposed.

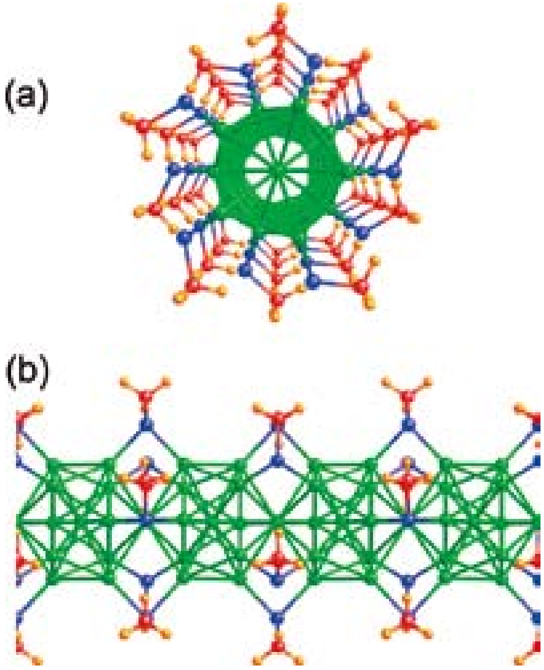

Figure 2. Vertex-sharing icosahedral thiolated gold nanowire: (a) viewed along the wire; (b) side view. Au, green; S, blue; C, red; H, orange.

References

1) T. Yasuike and K. Nobusada, *Phys. Rev. B* **80**, 035430 (8 pages) (2009).
2) Y. Kubota and K. Nobusada, *J. Phys. Soc. Jpn.* **78**, 114603 (7 pages) (2009).
3) Y. Kawashita, K. Yabana, M. Noda, K. Nobusada and T. Nakatsukasa, *THEOCHEM* **914**, 130–135 (2009).
4) D. -E. Jiang, K. Nobusada, W. Luo and R. L. Whetten, *ACS NANO* **3**, 2351–2357 (2009).

Advanced Electronic Structure Theory in Quantum Chemistry

Department of Theoretical and Computational Molecular Science
Division of Theoretical Molecular Science I

YANAI, Takeshi	Associate Professor
KURASHIGE, Yuki	Assistant Professor
MIZUKAMI, Wataru	Graduate Student
YAMADA, Mariko	Secretary

Aiming at predictive computational modelings of molecular electronic structures with *ab initio* quantum chemistry calculations, our scientific exploration is to establish a cutting-edge theoretical methodology that allows one to compute accurately and efficiently the complex electronic structures, in which strongly-interacting electrons play a crucial role to characterize the nature of molecules. The complicated electronic structures can be handled accurately with the multireference theory, which deals with multiple important electronic configurations on equal footing. However, with the standard multireference methods such as the complete active space self-consistent field (CASSCF), the tractable size of the reference space is limited to small active space because the complexity of the calculations grows exponentially with the reference size. The existing multireference methods are nevertheless usefully applied to chemical theory problems such as exploring chemical reactions of bonding, dissociation and isomerization along the reaction coordinates, electronically excited states, unstable electronic structures of radical systems, and multiple covalent bindings in molecular metal complexes, *etc*. Our resultant works to be reported here are (1) to develop a type of the multireference correlation model named Canonical Transformation (CT) theory, which can efficiently describe short-range dynamic correlation on top of the multi-configurational staring wave function, and (2) to construct the extensive complete active space self-consistent field (CASSCF) method combined with *ab initio* density matrix renormalization group (DMRG) method for making unprecedentedly larger active spaces available for the CASSCF calculations.

1. High-Performance *ab initio* Density Matrix Renormalization Group Method Multireference Application for Metal Compounds[1)]

The density matrix renormalization group (DMRG) algorithm has recently attracted significant attention as a robust quantum chemical approach to multireference electronic structure problems in which a large number of electrons have to be highly correlated in a large-size orbital space. It can be seen as a substitute for the exact diagonalization method that is able to diagonalize large-size Hamiltonian matrices. It comprises only a polynomial number of parameters and computational operations, but is able to involve a full set of the Slater determinants or electronic configurations in the Hilbert space, of which the size nominally scales exponentially with the number of active electrons and orbitals. In this work, we have presented a new efficient and parallelized implementation of the DMRG algorithm that is oriented towards applications for poly-nuclear transition metal compounds. The difficulty in DMRG calculations for these systems lies in the large active space and the non-1D nature of the electron correlation. A straightforward extension of the DMRG algorithm has been proposed with further improvements and aggressive optimizations to allow its application with large multireference active space, which is often demanded for metal compound calculations. Special efficiency is achieved by making better use of sparsity and symmetry in the operator and wavefunction representations. By accomplishing computationally intensive DMRG calculations, the authors have found that a large number of renormalized basis states are required to represent high entanglement of the electron correlation for metal compound applications, and it is crucial to adopt auxiliary perturbative correction to the projected density

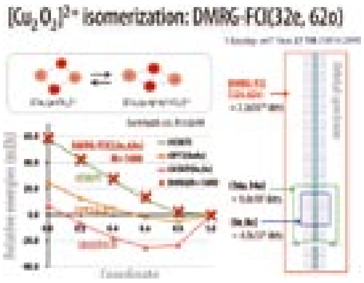

Figure 1. DMRG-FCI application to the potential curve of Cu_2O_2 isomerization, which is recently under hot debate. The behaviors of the single reference calculations and those of the multireference calculations exhibit clear differences. For this problem, we modeled a fairly large orbital space (32e,62o) to execute the DMRG diagonalization with.It has been shown thatDMRG energies nearly overlap with CCSD(T) results..

matrix during the DMRG sweep optimization in order to attain proper convergence to the solution. Potential energy curve calculations for the Cr_2 molecule near the known equilibrium precisely predicted the full configuration interaction (FCI) energies with a correlation space of 24 electrons in 30 orbitals (denoted by (24e,30o)). The energies are demonstrated to be accurate to 0.6 mE_h (the error from the extrapolated best value) when as many as ten thousand renormalized basis states are employed for the left and right DMRG block representations. The relative energy curves for $[Cu_2O_2]^{2+}$ along the isomerization coordinate were obtained from DMRG and other correlated calculations, for which a fairly large orbital space (32e,62o) is modeled as a full correlation space (Figure 1). The DMRG prediction nearly overlaps with the energy curve from the coupled-cluster with singles, doubles and perturbative triples (CCSD(T)) calculations, while the multireference complete active space self-consistent field (CASSCF) calculations with the small reference configuration (8e,8o) are found to overestimate the biradical character of the electronic state of $[Cu_2O_2]^{2+}$, according to the one-electron density matrix analysis.

2. DMRG-CASSCF: Spin States of Poly-Carbene[2)]

Posing the multireference problems in quantum chemistry, the complex electronic structures troubling the problems ought to be described by handling multiple electronic configurations, several of which should be equally important in the description. We have recently presented an extensively large-scale CASSCF approach, which is realized by implementing the orbital optimization with the density matrix renormalization group (DMRG) wavefunction (DMRG-CASSCF). By virtue of the compact nature of the DMRG wavefunction, which provides an efficient description of the strongly correlated electronic structures, the DMRG-CASSCF approach enables us to handle much larger active spaces than are possible with the traditional CASSCF algorithm. Using the DMRG-CASSCF method, we investigated the spin states of poly(phenyl)carbenes (Figure 2). These molecules involve a characteristic electronic structure, and the higher-spin states are known to be more stable than the lower-spin states. We examined stability of high-spin state by computing highest and singlet spin states. The table shows energy gaps of 1,2,3-carbene between highest and singlet spin states. For comparison, reference numbers are computed with several single-reference (mean-field + perturbation) methods. In DMRG-CASSCF on 3-carbene, a large CAS(30,30) was used for active space. As expected, all the calculations predicted that high-spin states are more stable than singlet state. However, in terms of the energy gaps, we observed surprisingly large discrepancy between single-reference methods and DMRG-CASSCF. Electronic structure of carbene sites can be represented in sp2 hybridization. Then the high-spin state is described as parallel spins occupying sp2 and p_z orbitals. This description is consistently observed in one-electron density matrix elements of DMRG-CASSCF as well as single determinant wavefunctions. For singlet state, however, as can be seen in the electron density elements, DMRG-CASSCF and single-determinant method chose different configuration. It is found that the single-reference methods describe the lone pair configuration, while DMRG-CASSCF chose this biradical configuration as the stable singlet state. For this reason, DMRG-CASSCF stabilizes the description of the singlet state, and thus the small energy gaps are estimated.

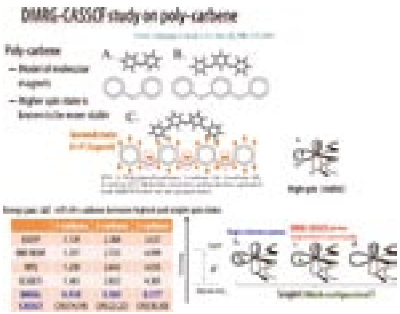

Figure 2. DMRG-CASSCF study of poly(phenyl) carbene. This molecule involves a characteristic electronic structure, and the high-spin state is known to be more stable. For 3-carbene, the septet state is thought to be the most stable spin state where you see there are parallel spins on three carbene sites. The table shows energy gaps of 1,2,3-carbene between highest and singlet spin states. For comparison, reference numbers are computed with several single-reference methods.

3. Canonical Transformation (CT) Theory for Efficient Multireference Method[3–4)]

We have been developing a many-body technique based on canonical transformation (CT) for realizing large-scale multireference calculations for the purpose of attaining the chemical accuracy, for which dynamical correlations are described by using cluster expansion on top of muticonfigurational setting (*e.g.* DMRG-CASSCF). We are working on extending the implementation to the wider applications in terms of tractable size of molecules of target. The ongoing reimplementation fixes some of problems in the extant implementation that relies on infinite computer memory. We have demonstrated the recent application of CT to the description of an energy curve along the isomerization coordinate between bis and peroxo cores of $Cu_2O_2^{2+}$.

References

1) Y. Kurashige and T. Yanai, *J. Chem. Phys.* **130**, 234114 (2009).
2) T. Yanai, Y. Kurashige, D. Ghosh and G. K-L. Chan, *Int. J. Quantum Chem.* **109**, 2178 (2009).
3) E. Neuscamman, T. Yanai and G. K-L. Chan, *J. Chem. Phys.* **130**, 124102 (2009).
4) G. K-L. Chan, J. J. Dorando, D. Ghosh, J. Hachmann, E. Neuscamman, H. Wang and T. Yanai, *Frontiers in Quantum Systems in Chemistry and Physics*, S. Wilson *et al.*, Eds., Springer, **Vol. 18**, pp. 49–64 (2008).

Award

YANAI, Takeshi; The Wiley-International Journal of Quantum Chemistry Young Investigator Award (The 49th Sanibel Symposium, 2009).

Developing the Statistical Mechanics Theory of Liquids in Chemistry and Biophysics

Department of Theoretical and Computational Molecular Science
Division of Theoretical Molecular Science II

HIRATA, Fumio	Professor
CHONG, Song-ho	Assistant Professor
YOSHIDA, Norio	Assistant Professor
MARUYAMA, Yutaka	Post-Doctoral Fellow
MIYATA, Tatsuhiko	Post-Doctoral Fellow
ISHIZUKA, Ryosuke	Post-Doctoral Fellow
PHONGPHANPHANEE, Saree	Post-Doctoral Fellow
KIYOTA, Yasuomi	Graduate Student
SUETAKE, Yasumi	Secretary
KONDO, Naoko	Secretary
YAMADA, Mariko	Secretary

We have been developing a new theory for the molecular recognition by protein based on the statistical mechanics of liquids, or the 3D-RISM/RISM theory. The theory has demonstrated its amazing capability of "predicting" the process from the first principle.1–3) However, what we have investigated so far is an entirely equilibrium process both in protein conformation and solvation.

Recently, we have started to incorporate the conformational fluctuation of protein into the molecular recognition process in two ways. The first of those is a "static" one in which we just shake the protein conformation to find the local minimum of the free energy surface by the combined 3D-RISM/RISM with conformational sampling algorithms, and to see if one can find the distribution of a guest molecule in the recognition site.4) The other method is to take the "dynamic" fluctuation of protein conformation into account. The process can be described by hybridized 3D-RISM/RISM with the generalized Langevin theories.5) The methodology is currently under construction, and some prospective view of the theory will be presented in the lecture.

1. 3D-RISM/RISM Studies on the Dissociation Pathway of CO in Myoglobin6)

Myoglobin (Mb) is a globular protein which has important biological functions, or oxygen storage. Due to its biochemical function, many researchers have made intensive efforts to identify the escaping pathway of the ligand, experimentally and theoretically.7)

Among many unresolved questions with respect to the CO escaping pathway, the dependence of the pathway on Xe concentration has recently been highlighted by Terazima based on the time-resolved partial molar volume (PMV) measured with the transient grating spectroscopy. The experimental results indicate that CO is trapped at the Xe site before escaping to solvent at room temperature. The difference of Xe and CO affinity of each Xe trapping site makes the CO escaping pathway different depending on Xe concentration. It is believed that the dissociated CO escapes to the solvent through the Xe1 trapping site under the Xe-free condition, dominantly, while CO escapes through the Xe4 site in a Xe-rich solution.

Shown in Figure 1 is the 3D-distribution of CO in the four Xe-sites calculated from 3D-RISM in the ternary mixture composed of water, Xe, and CO. It is apparent that each Xe-site has some affinity to a CO molecule. The comaprison of the population of CO and Xe in each Xe-site at high concentration revealed that Xe has greater affinity to the Xe1 site than CO, while CO is dominant in the Xe4-site.

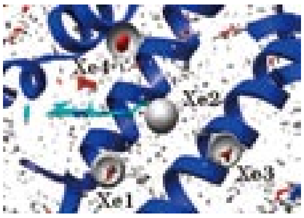

Figure 1. CO distribution in the Xe-sites: red, O; gray, C.

Table 1. The partial molar volume of the different association state of the CO-Mb complex. (ΔV_1 = (Mb:CO) – (MbCO), ΔV_2 = (Mb+CO) – (Mb:CO), and ΔV_{total} = (Mb+CO) – (MbCO)).

models	PMV[cm^3/mol]
MbCO	9029.0
Mb:CO(Xe1)	9030.4
Mb:CO(Xe4)	9032.8
MB+CO	9019.6

	Xe1	Xe4	(expt.7))
ΔV_1 =	1.4	3.8	(3±1)
ΔV_2 =	–10.8	–13.2	(–12.6±1.0)
ΔV_{total} =	–9.4	–9.4	(–10.7±0.5)

(MbCO, CO bound at the Heme; Mb:CO(Xe1), CO is bound at the Xe1 site: Mb:CO(Xe4), CO is bound at the Xe4-site; MB+CO, CO is dissociated from Mb.)

In order to examine the hypothesis made by Terazima with respect to the escaping pathway, we have calculated PMV of the CO-Mb complexes in each of which a CO molecule is explicitly bound in one of the Xe-sites. The results are shown in Table 1. As is obvious from the table, the theoretical results for Mb:CO(Xe4) show much better agreement with the experiment, indicating that CO escapes from the Xe4-site. The hypothesis made by Terazima is thus verified by the theory.

2. An Attempt toward the Generalized Langevin Dynamics Simulation$^{5)}$

It has been five decades since the molecular simulation scored its first step in the study of liquids and solutions. Accelerated by the increasing power of computer, the method has been enjoying the status of a standard tool to explore the molecular aspects of physical, chemical, and biological processes in liquids and solutions. However, the method is facing high barriers which may not be overcome by the improvement of computing power alone. One of those is the large and slow fluctuations taking place in a protein in solutions, which touches the zero wavelength and frequency limits. Straightforward applications of the molecular simulation to the limits are in danger to end up with an “animation” or a “science fiction.”

In this report, we have attempted a new step toward the molecular dynamics simulation which is not based on the Newton equation, but on the generalized Langevin theory, in which all the degrees of freedom concerning the solvent molecules are “coarse-grained” or “projected” in term of the pair correlation functions. Choosing the coordinates ***R*** of protein atoms and the density field ρ of solvent atoms, as well as their conjugated momentum, as dynamic variables in the phase space, we have derived the generalized Langevin equations for protein dynamics in solutions.

$$\frac{d\mathbf{R}(t)}{dt}=\frac{\mathbf{P}(t)}{M}$$

$$\frac{d\mathbf{P}(t)}{dt}=-k_BT\mathbf{L}^{-1}\cdot\mathbf{R}(t)-\frac{1}{Mk_BT}\int_0^t ds\left\langle \mathbf{W}e^{i(t-s)QL}\right\rangle\cdot\mathbf{P}(s)+e^{itQL}\mathbf{W}$$

$$\frac{d\rho_k(t)}{dt}=ikJ_k^L(t)$$

$$\frac{dJ_k^L(t)}{dt}=\frac{ikk_BT}{mS_k}\delta\rho_k(t)-\frac{m}{Nk_BT}\int_0^t\left\langle R_{-k}e^{i(t-s)QL}R_k\right\rangle J_k^L(s)+e^{itQL}f_k$$

where ***R*** and ***P*** denote the coordinates and conjugated momenta of protein atoms, ρ and *J* the density and momentum field of solvent atoms, respectively. The first two equations describe the dynamics of protein, while the last two are concerned with the solvent dynamics. However, they should be solved simultaneously, since the equations are closely coupled each other. It is our plan to solve the equation in the way just as is done in the molecular dynamic simulation, or the numerical integration of the equation.

The equations for protein have a typical expression of the original Langevin equation, but each term in the right hand side has a microscopic description in contrast to the original one. The first term is related to the variance-covariance matrix of mean square displacement of protein, which signifies the conformational fluctuation of the molecule. The factor $k_B\boldsymbol{TL}^{-1}$ is related to a frequency matrix of the fluctuation, or the variance-covariance matrix (<Δ*R*Δ*R*>), diagonalization of which gives rise to an “effective normal mode” of the fluctuation. The second term is the damping or drag term. In the original Langevin equation, this term is local in time, and is described by the phenomenological expression such as the Oseen tensor which models the hydrodynamic interactions. The third term stands for the “random” force acting on the solute, which of course is orthogonal to the dynamic variables at time zero.

It is a highly nontrivial problem to solve the equation by means of the numerical integration. Our working hypothesis to solve the equations is following.

(1) For each time step Δ*t*, the protein structure is at “local equilibrium,” and the fluctuation around the equilibrium follows the “central limiting theorem,” or the “Gaussian fluctuation.”

(2) By virtue of the Gaussian fluctuation, the variance-covariance matrix (<Δ*R*Δ*R*>) can be the second derivative of the free energy of protein (conformational energy + solvation free energy) with respect to protein atom positions.

(3) The solvation free energy of protein and its derivatives can be evaluated from the 3D-RISM theory. (The variance-covariance matrix (<Δ*R*Δ*R*>) is proportional to the second derivative.

(4) The time step Δ*t* of integration should be sufficiently large so that the central limiting theorem is valid, while it should be small enough so that the memory term can be approximated with a short time memory.

(5) The perturbation onto solution from protein can be treated by a renormalized potential or the direct correlation functions.

There is another concern in the actual implementation of the theory to the computational science. Each time step of the numerical integration requires the solution of the 3D-RISM equation, which has been notorious with respect to the computational time. For example, when the equation was first solved for protein about five years ago, it took “a month” by ordinary workstations to get the 3D-distribution around “one” conformation of the solute. It was essentially due to the 3D-FFT program which is notorious about the parallelization. If it is the case, the new approach described above is useless, because the simulation requires thousands of steps to explore a meaningful region of the conformational space. However, we could have made a dramatic progress during the year of 2009, thanks to the collaboration with the computer scientists in Tsukuba: The current achievement is “a minute per a conformation” of protein with T2K in Tsukuba.

References

1) F. Hirata, *Molecular Theory of Solvation*, Kluwer; Dordrecht, Netherlands (2003).

2) A. Kovalenko and F. Hirata, *J. Chem. Phys.* **110**, 10095–10112 (1999).

3) T. Imai, R. Hiraoka, A. Kovalenko and F. Hirata, *J. Am. Chem. Soc. (Communication)* **127**, 15334–15335 (2005).

4) T. Miyata and F. Hirata, *J. Comput. Chem.* **29**, 872 (2007).

5) B. Kim, S-H. Chong, R. Ishizuka and F. Hirata, *Cond. Matt. Phys.* **11**, 179 (2008).

6) Y. Kiyota, R. Hiraoka, N. Yoshida, Y. Maruyama, T. Imai and F. Hirata, *J. Am. Chem. Soc. (Communication)* **131**, 3852 (2009).

7) M. Sakakura, S. Yamaguchi, N. Hirota and M. Terazima, *J. Am. Chem. Soc.* **123**, 4286 (2001).

Theory of Nonequilibrium Quantum Dynamics and Transport

Department of Theoretical and Computational Molecular Science
Division of Theoretical Molecular Science II

YONEMITSU, Kenji	Associate Professor
YAMASHITA, Yasufumi	Assistant Professor*
TANAKA, Yasuhiro	IMS Research Assistant Professor
MIYASHITA, Satoshi	Post-Doctoral Fellow†
KONDO, Naoko	Secretary

Nonequilibrium properties of low-dimensional correlated electron systems are investigated from different aspects. Among them, photoinduced transitions are now widely achieved between metals and insulators, between paraelectric and ferroelectric phases, among nonmagnetic, paramagnetic and ferromagnetic phases, and so on.[1)] Most of them are realized by changing the temperature also. Here, we focus on a quantum phase transition between neutral quantum- paraelectric and ionic (anti)ferroelectric ground (*i.e.*, zero temperature) states, where photoinduced dynamics are experimentally demonstrated to be different from ordinary ones. In addition, we continue the research for the mechanisms of different rectifying actions. Here, we employ nonequilibrium Green's functions to elucidate differences between strongly-correlated and weakly-correlated insulators.

1. Enhanced Coherent Dynamics near a Quantum Phase Transition[2)]

A quantum phase transition between neutral quantum-paraelectric and ionic antiferroelectric phases is realized in mixed-stack charge-transfer complexes composed of 4,4'-dimethyltetrathiafulvalene (DMTTF) and tetrahalo-*p*-benzoquinones ($\mathrm{QBr}_n\mathrm{Cl}_{4-n}$). Recently, photoinduced reflectivity changes are reported. The reflectivity in the energy range where it is sensitive to the ionicity change shows a large-amplitude oscillation near the quantum phase transition point. Then, nonequilibrium dynamics is studied near the quantum phase transition point in the one-dimensional quantum Blume-Emery-Griffiths model. Its pseudospin component S^z represents an electric polarization, and $(S^z)^2$ corresponds to ionicity. This model is one-dimensional and does not distinguish between ferroelectric and antiferroelectric phases. The time-dependent Schrödinger equation is solved for the exact many-body wave function in the quantum-paraelectric phase. After impact force is introduced on a polarization locally in space and time, polarizations [Figure 1(a)] and ionicity [Figure 1(b)] coherently oscillate. The oscillation amplitudes are large near the quantum phase transition point. The dependences of these oscillation amplitudes on the total-energy increment ΔE are shown in Figure 2 for different quantum-tunneling amplitudes h.

The energy supplied by the impact flows linearly into these oscillations, so that the nonequilibrium behavior is uncooperative.

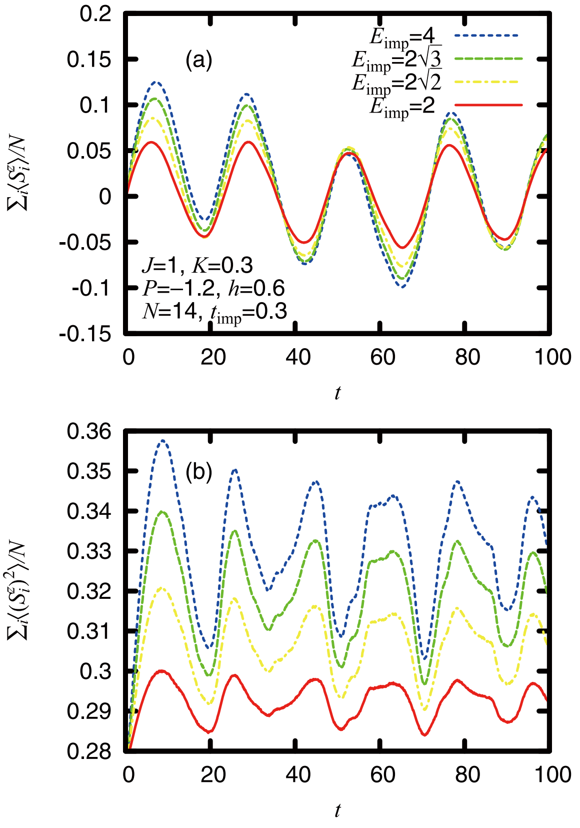

Figure 1. (a) Spatial average of electric polarization S^z and (b) spatial average of ionicity $(S^z)^2$, as a function of time t, after impact force of strength E_{imp} is locally introduced on a polarization.

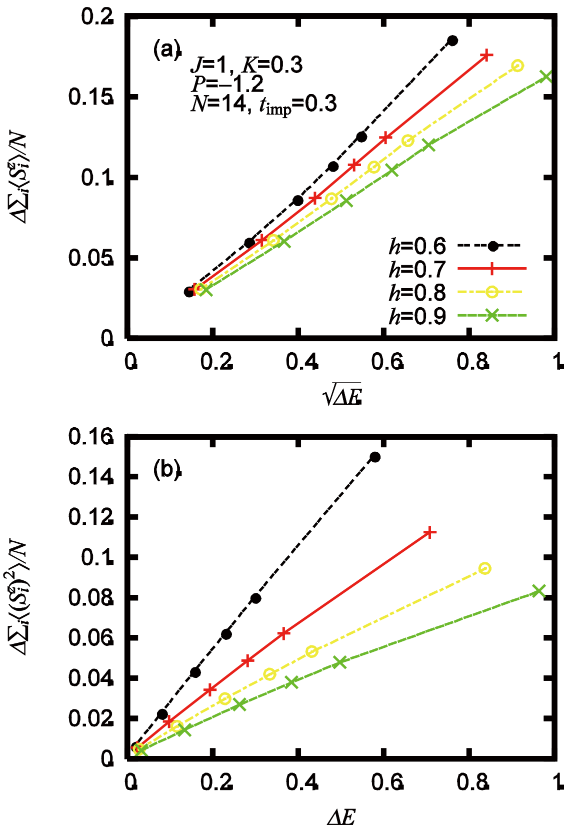

Figure 2. (a) Amplitude of oscillation in spatial average of electric polarization S^z, as a function of square root of energy supplied, and (b) amplitude of oscillation in spatial average of ionicity $(S^z)^2$, as a function of energy supplied ΔE. The quantity h denotes the quantum-tunneling amplitude.

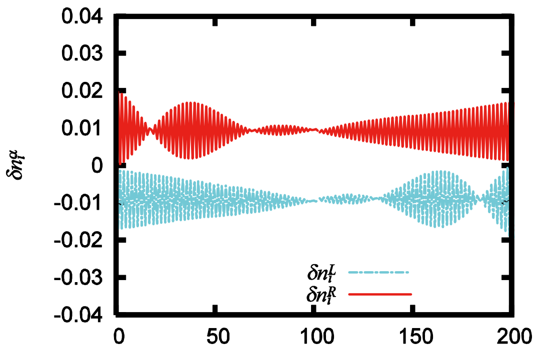

Figure 3. Nonequilibrium part of charge density due to coupling with left electrode, $\delta n^L{}_i$ (light blue), and that with right electrode, $\delta n^R{}_i$ (red), for Mott insulator with left-going bias.

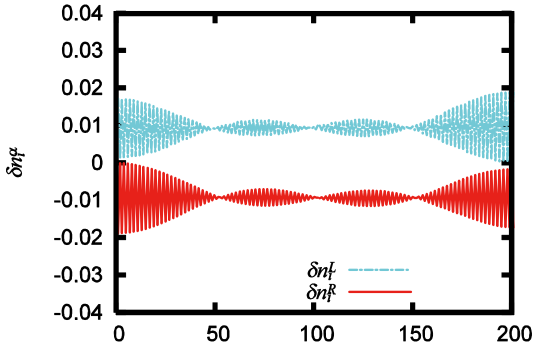

Figure 4. Nonequilibrium part of charge density due to coupling with left electrode, $\delta n^L{}_i$ (light blue), and that with right electrode, $\delta n^R{}_i$ (red), for Mott insulator with right-going bias.

2. Nonequilibrium Green's Functions for Rectification at Metal–Insulator Interfaces[3)]

The suppression of rectification at metal–Mott-insulator interfaces, which was previously shown by numerical solutions to the time-dependent Schrödinger equation and experiments on real devices, is reinvestigated theoretically using nonequilibrium Green's functions. The one-dimensional Hubbard model is used for a Mott insulator. The effects of attached metallic electrodes are incorporated into the self-energy. A scalar potential originating from work-function differences and satisfying the Poisson equation is added to the model. For electron density, we decompose it into three parts. One is obtained by integrating the local density of states over energy to the midpoint of the electrodes' chemical potentials.

The others, obtained by integrating lesser Green's functions, are due to couplings with the electrodes and correspond to an inflow and an outflow of electrons (Figures 3 and 4). In Mott insulators, incoming electrons and holes are extended over the whole system, avoiding further accumulation of charges relative to that in the case without bias. Furthermore, the inflow and the outflow of electrons are insensitive to the polarity of the bias. This induces collective charge transport and results in the suppression of rectification.

References

1) K. Yonemitsu and K. Nasu, *Phys. Rep.* **465**, 1–60 (2008).
2) K. Yonemitsu, *Phys. Rev. B* **78**, 205102 (5 pages) (2008).
3) K. Yonemitsu, *J. Phys. Soc. Jpn.* **78**, 054705 (8 pages) (2009).

Award

YAMASHITA, Yasufumi; Young Scientist Award of the Physical Society of Japan.

---

* Present Address: General Studies, College of Engineering, Nihon University, Koriyama, Fukushima 963-8642

† Present Address: Japan Science and Technology Agency, Chiyoda-ku, Tokyo 102-0075

Theoretical Studies on Condensed Phase Dynamics

Department of Theoretical and Computational Molecular Science
Division of Computational Molecular Science

SAITO, Shinji	Professor
KIM, Kang	Assistant Professor
HIGASHI, Masahiro	IMS Fellow
KOBAYASHI, Chigusa	Post-Doctoral Fellow
YAGASAKI, Takuma	Post-Doctoral Fellow
SUMIKAMA, Takashi	Post-Doctoral Fellow
IMOTO, Sho	Graduate Student*
UENO, Harumi	Secretary

Liquids and biological systems show complicated dynamics because of their structural flexibility and dynamical hierarchy. Understanding these complicated dynamics is indispensable to elucidate chemical reactions and relaxation in solutions and functions of proteins. We have been investigating complex dynamics in supercooled liquids[1–3] and chemical reactions in biological systems using molecular dynamics simulation and electronic structure calculation. In addition, we have been analyzing liquid dynamics by using multi-dimensional spectroscopy.[4,5]

1. Multiple Time Scales Hidden in Heterogeneous Dynamics of Glass-Forming Liquids[1]

A multi-time probing of density fluctuations is introduced to investigate hidden time scales of heterogeneous dynamics in glass-forming liquids. Molecular-dynamics simulations for simple glass-forming liquids are performed and a three-time correlation function is numerically calculated for general time intervals. It is demonstrated that the three-time correlation function is sensitive to the heterogeneous dynamics and that it reveals couplings of correlated motions over a wide range of time scales. Furthermore, the time scale of the heterogeneous dynamics τ_{hetero} is determined by the change in the second time interval in the three-time correlation function. The present results show that the time scale of the heterogeneous dynamics τ_{hetero} becomes larger than the α-relaxation time at low temperatures and large wavelengths. We also find a dynamical scaling relation between the time scale τ_{hetero} and the length scale ξ of dynamical heterogeneity as $\tau_{\mathrm{hetero}} \sim \xi^z$ with $z = 3$.

2. Slow Dynamics in Random Media: Crossover from Glass to Localization Transition[2]

We study slow dynamics of particles moving in a matrix of immobile obstacles using molecular dynamics simulation. The glass transition point decreases drastically as the obstacle density increases. At higher obstacle densities, dynamics of mobile particles changes qualitatively from glass-like to a Lorentz-gas-like relaxation. This crossover is studied by the density correlation functions, non-ergodic parameters, mean square displacement, and nonlinear dynamic susceptibility. Our finding is qualitatively consistent with results of recent numerical and theoretical studies on various spatially heterogeneous systems. Furthermore, we show that slow dynamics is surprisingly rich and sensitive to the obstacle configurations. Especially, reentrant transition is observed for a particular configuration, though its origin is not directly linked to the similar prediction based on the mode-coupling theory.

3. Conformational Changes and Fluctuations of Molecular Switch Ras

Ras superfamily works as a molecular switch for cell growth. Ras is cycled between two states of guanine nucleotide, the GTP- and GDP-bound states, by hydrolysis. Ras binds to effectors for regulation of cell proliferation in the GTP-bound state, whereas it is inactivated in the GDP-bound state. X-ray crystallography studies revealed conformational changes of two regions, *i.e.* switch I and switch II, around a nucleotide binding site in these two states. We analyze the conformational changes and fluctuations between these states by carrying out molecular dynamics (MD) simulation. We find that the change in the coordinations of Thr35-Mg^{2+} and Gly60-γ-phosphate due to the hydrolysis of GTP induces the changes in the conformations of sidechains as well as the backbone in the GTP- and GDP-bound states. We perform the principle coordinate analysis of the structural change between these states and indeed find the important structural change arising from the switch regions.

In addition to the GTP-bound state with the function of the cell growth, another GTP-bound state with different conformation has been observed experimentally. The GTP-bound state with the function is called state 2, while the other state is referred to as state 1. It is known that state 2 is a predominant form of Ras and interacts with effectors. ^{31}P NMR spectroscopy of some mutants shows the absence of the coordination of Thr35-Mg^{2+} in state 1. It is also shown in X-ray structural analysis that the coordination of Gly60-γ-phosphate is lost in the state 1 of another mutant. We investigate the conformational changes and fluctuations in these two kinds of state 1 by using MD simulation. It is found that the breaking of the coordination of Thr35-Mg^{2+} causes the large scale structural change in the switch I region followed by the steric hindrance between Pro34 and γ-phosphate and then the break of hydrogen bond between ribose in GTP and switch I region. We also find that the conformational fluctuation in the switch I region is substantially large in state 1. We show that the global structural changes of loop4 and α2 helix in the switch II region are induced by the loss of the coordination between Gly60 and γ-phosphate. The presence of multiple states with different conformations in the GTP-bound state is consistent with the experimentally observed interconversion between multiple conformations and with the low affinity to effectors.

We also analyze the GAP-GTP-bound state to understand the role of GAP. We find that the binding of GAP significantly suppressed the unnecessary thermal motions of the water molecule which is involved in the hydrolysis of GTP.

In addition to the above analyses based on MD simulation, we are currently analyzing the reaction pathway of hydrolysis of GTP in the GAP-GTP-bound state, by using the so-called QM/MM method.

4. Molecular Dynamics Simulation of Nonlinear Spectroscopies of Intermolecular Motions in Liquid Water[4,5]

Water is the most extensively studied of liquids because of both its ubiquity and its anomalous thermodynamic and dynamic properties. The properties of water are dominated by hydrogen bonds and hydrogen bond network rearrangements. Fundamental information on the dynamics of liquid water has been provided by linear infrared (IR), Raman, and neutron-scattering experiments; molecular dynamics simulations have also provided insights. Recently developed higher-order nonlinear spectroscopies open new windows into the study of the hydrogen bond dynamics of liquid water. For example, the vibrational lifetimes of stretches and a bend, intramolecular features of water dynamics, can be accurately measured and are found to be on the femtosecond time scale at room temperature. Higher-order nonlinear spectroscopy is expressed by a multi-time correlation function, whereas traditional linear spectroscopy is given by a one-time correlation function. Thus, nonlinear spectroscopy yields more detailed information on the dynamics of condensed media than linear spectroscopy. In this Account, we describe the theoretical background and methods for calculating higher-order nonlinear spectroscopy; equilibrium and non-equilibrium molecular dynamics simulations, and a combination of both, are used. We also present the intermolecular dynamics of liquid water revealed by fifth-order two-dimensional (2D) Raman spectroscopy and third order IR spectroscopy. 2D Raman spectroscopy is sensitive to couplings between modes; the calculated 2D Raman signal of liquid water shows large anharmonicity in the translational motion and strong coupling between the translational and librational motions. Third-order IR spectroscopy makes it possible to examine the time-dependent couplings. The 2D IR spectra and three-pulse photon echo peak shift show the fast frequency modulation of the librational motion. A significant effect of the translational motion on the fast frequency modulation of the librational motion is elucidated by introducing the "translation-free" molecular dynamics simulation. The isotropic pump-probe signal and the polarization anisotropy decay show fast transfer of the librational energy to the surrounding water molecules, followed by relaxation to the hot ground state.

Reference

1) K. Kim and S. Saito, *Phys. Rev. E* **79**, 060501(R) (4 pages) (2009).
2) K. Kim, K. Miyazaki and S. Saito, *Europhys. Lett.* **88**, 36002 (5 pages) (2009).
3) A. Furukawa, K. Kim, S. Saito and H. Tanaka, *Phys. Rev. Lett.* **102**, 016001 (4 pages) (2009).
4) T. Yagasaki and S. Saito, *Acc. Chem. Res.* **42**, 1250–1259 (2009).
5) T. Yagasaki, J. Ono and S. Saito, *J Chem. Phys.* **131**, 164511 (11 pages) (2009).

* carrying out graduate research on Cooperative Education Program of IMS with Nagoya University

Theoretical Study on Molecular Excited States and Chemical Reactions

Department of Theoretical and Computational Molecular Science
Division of Computational Molecular Science

EHARA, Masahiro	Professor
FUKUDA, Ryoichi	Assistant Professor
TASHIRO, Motomichi	IMS Research Assistant Professor
VONGACHARIYA, Arthit	Research Fellow
KAWAGUCHI, Ritsuko	Secretary

Molecules in the excited states show characteristic photophysical properties and reactivity. We investigate the molecular excited states and chemical reactions which are relevant in chemistry, physics, and chemical biology with developing the highly accurate electronic structure theory. We are also interested in the excited-state dynamics and energy relaxation so that we also develop the methodology of large-scale quantum dynamics. In this report, we report our recent studies on the development of the active-space method,[1)] molecular excited states,[2–4)] in particular the inner- shell spectroscopy[3,4)] and catalytic reaction on surface.[5)]

1. Development of Active-Space Method[1)]

Radicals show characteristic spectroscopic properties and reactivity in their ground and excited states. Since they are unstable and short-lived, their spectroscopic properties and reactions have to be examined through suitably designed experimental procedures, such as flash photolysis and matrix isolation spectroscopy, to mention a few examples. Excellent experimental techniques using argon and solid parahydrogen matrices have been developed for this purpose. Thanks to these and related advances, a large amount of experimental data has been accumulated for radicals, and a highly accurate theoretical analysis has become an indispensable tool for obtaining a detailed interpretation of these data.

In this work, we have developed the active-space method based on the SAC-CI method and applied the theory to the molecular spectroscopy of open-shell systems. The low-lying valence excited states of four open-shell triatomic molecules, CNC, C_2N, N_3, and NCO, were investigated using the electron-attached (EA) and ionized (IP) SAC-CI general-*R* as well as the full and active-space EA and IP EOMCC methods. A comparison was made with experiment and with the results of the completely renormalized (CR) CC calculations with singles, doubles, and non-iterative triples defining the CR-CC (2,3) approach. Adiabatic excitation energies of the calculated states were in reasonable agreement with the experimental values, provided that the 3-particle–2-hole (3p-2h) components in the electron attaching operator, as in the EA SAC-CI SDT-*R* and EA EOMCCSD(3p-2h) approaches, are included in the calculations for the excited states of C_2N and CNC which have a predominantly two-electron character. The results also revealed that the active-space EA/IP EOMCC schemes with up to 3p-2h/3h-2p excitations are able to accurately reproduce the results of their much more expensive parent methods while requiring significantly less computational effort. Furthermore, the more “black-box” CR-CC(2,3) approach calculated the lowest state of each symmetry with the same accuracy as that obtained with the EA/IP SAC-CI SDT-*R* and EA/IP EOMCCSD (3p-2h/3h-2p) methods, confirming the significance of higher-order correlation effects in obtaining an accurate description of excited states of radicals, particularly the valence excited states of the CNC and C_2N species dominated by two-electron processes. Table 1 summarizes the results of the ground and excited states of C_2N.

Table 1. Spectroscopic constants of the ground and excited states of C_2N.

State	Method	Exc. level	R_{CC} (Å)	R_{CN} (Å)	T_e (eV)
X $^2\Pi$	SD-*R*	1	1.405	1.191	---
	SDT-*R*{4,4}	1	1.400	1.185	---
	Expt.		---		---
A $^2\Delta$	SD-*R*	2	1.352	1.185	6.004
	SDT-*R*{4,4}	2	1.315	1.207	2.837
	Expt.		---		2.636
B $^2\Sigma^-$	SD-*R*	2	1.354	1.188	7.632
	SDT-*R*{4,4}	2	1.302	1.223	3.640
	Expt.		---		2.779
C $^2\Sigma^+$	SD-*R*	2	1.341	1.192	6.578
	SDT-*R*{4,4}	2	1.311	1.214	3.594
	Expt.		---		3.306

2. Relativistic Effects in *K*-Shell Ionizations: SAC-CI General-*R* Study Based on the DK2 Hamiltonian[3)]

Core-electron binding energies (CEBEs) contain information not only about inner-core electrons but also about valence electrons and chemical bonds. Extensive experimental studies have provided the CEBEs of numerous molecules. Siegbahn *et al.* summarized the electron spectroscopy for chemical analysis (ESCA) data in 1969 and Bakke *et al*. reported further ESCA data in 1980. They also clarified the important chemical implications involved in the CEBE data. The recent development of high-resolution soft X-ray photoelectron spectroscopy (XPS) has enabled accurate experimental observations of the CEBEs, resolving the vibrational structure.

It is now generally recognized that the relativistic effect is important in chemistry in particular for the molecular properties of the heavy elements. The methodologies of relativistic quantum chemistry have been developed and established. The relativistic effect is also important in core-electron processes. Although the spin-orbit splitting of the inner-shell P and D states has been intensively investigated, the relativistic effect has not been so much focused in the accurate calculation of the CEBEs for the heavy elements. Most calculations including both electron correlations and relativistic effect have been performed for molecules containing first-row atoms except for the recent work of Barysz and Leszczynski for the rare gas atoms.

In this work, we investigated the relativistic effects in the CEBEs of molecules containing the second-row atoms, Si, P, S, and Cl as well as the F atom. We performed the SAC-CI general-*R* calculations based on the spin-free part of the second-order Douglass-Kroll-Hess (DK2) Hamiltonian.3) Table 2 summarizes the results of the relativistic and non-relativistic SAC-CI calculations. The relativistic effect in the CEBEs of the second-row atoms was found to be 4–9 eV. The effect was mostly overestimated by the Koopmans' theorem and was reduced to the extent of 0.15–0.4 eV by including the orbital relaxation and electron correlations.

Table 2. Calculated and observed Si, P, S, and Cl 1s CEBE (eV).

Mol.	Exptl.	Rel. SAC-CI	Non-Rel. SAC-CI	Rel. effect (eV) SAC-CI	Rel. effect (eV) Koopmans'
$\underline{Si}H_4$	1847.1	1848.24	1843.96	4.28	3.97
$\underline{P}H_3$	2150.5	2151.25	2146.32	4.93	5.30
$H_2\underline{S}$	2478.5	2479.51	2472.98	6.53	6.94
$OC\underline{S}$	2480.3	2481.84	2475.06	6.78	6.93
$CH_3\underline{Cl}$	2829.4	2832.15	2823.35	8.80	8.95

3. Theoretical Study of the Methanol Dehydrogeneation Reaction on Pt and Ag Surfaces/Clusters5)

The mechanism of the methanol dehydrogenation reaction on a Pt surface has been investigated using the dipped adcluster model (DAM) combined with density functional theory (DFT) calculations. Reaction pathways starting from CH and OH dissociations (Figure 1), both of which were proposed experimentally, but, not fully understood, have been examined.

Figure 1. Reaction pathways of the dehydrogenation of CH_3OH to CO.

Starting from O–H bond scission, methanol decomposes to form CO exothermically on the Pt surface, where the Pt-dσ orbital effectively interacts with the O–H antibonding orbital. The donative interaction of the Pt dσ orbitals was found to be important for catalytic activation on the Pt surface. Figure 2 shows the overall energy diagram of the methanol dehydrogenation reaction starting. The reaction pathway starting from C–H bond scission has a larger activation barrier and, therefore, is less kinetically favorable. Electron transfer from the bulk, which is included in the present DAM calculation, plays an important role in the reaction pathway from O–H bond scission, in particular for the dehydrogenation of formaldehyde. On the other hand, the Ag surface has been shown to be effective for formaldehyde synthesis, because formaldehyde desorbs spontaneously from the Ag surface. The present reaction has also been examined and discussed in view of the nanoscale clusters and nanorods.

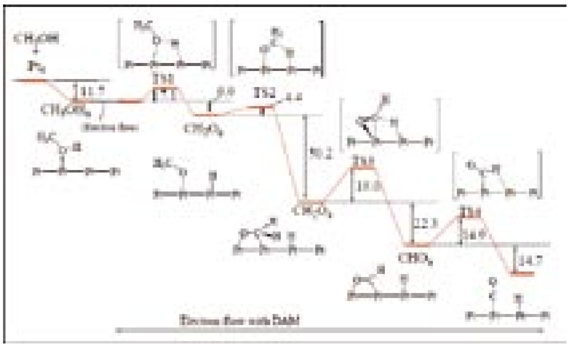

Figure 2. Overall energy diagram of methanol dehydrogenation starting from OH bond dissociation.

References

1) M. Ehara, J. R. Gour and P. Piecuch, *Mol. Phys.* **107**, 871–880 (2009).
2) S. Arulmozhiraja, M. Ehara and H. Nakatsuji, *J. Chem. Phys.* **129**, 174506 (8 pages) (2008).
3) M. Ehara, K. Kuramoto and H. Nakatsuji, *Chem. Phys.* **356**, 195–198 (2009).
4) K. Ueda, R. Puttner, N. A. Cherepkov, F. Gel'mukhanov and M. Ehara, *Eur. Phys. J.* **169**, 95–107 (2009).
5) T. Watanabe, M. Ehara, K. Kuramoto, H. Nakatsuji, *Surf. Sci.* **603**, 641–646 (2009).

Award

EHARA, Masahiro; APATCC (Asia-Pacific Association of Theoretical & Computational Chemists) 2009 Pople Medal.

Development of New Algorithms for Molecular Dynamics Simulation and Its Application to Biomolecular Systems

Department of Theoretical and Computational Molecular Science
Division of Computational Molecular Science

OKUMURA, Hisashi	Associate Professor
KAWAGUCHI, Ritsuko	Secretary

1. Temperature and Pressure Dependence of Alanine Dipeptide Studied by Multibaric-Multithermal Molecular Dynamics Simulations1)

We applied the multibaric-multithermal (MUBATH) molecular dynamics (MD) algorithm to an alanine dipeptide in explicit water (Figure 1). The MUBATH MD simulation covered a wide range of conformational space and sampled the states of $P_{\rm II}$, C_5, α_R, α_P, α_L, and C_7^{ax}. On the other hand, the conventional isobaric-isothermal simulation was trapped in local-minimum free-energy states and sampled only a few of them. Temperature and pressure dependences of the population of these states were investigated by the MUBATH MD simulations as shown in Figure 2. Such temperature and pressure dependences by molecular simulations were calculated for the first time. We calculated the partial molar enthalpy difference ΔH and partial molar volume difference ΔV among these states by the MUBATH simulation using the AMBER parm99 and AMBER parm96 force fields and two sets of initial conditions as listed in Tables 1 and 2. We compared these results with those from Raman spectroscopy experiments. The Raman spectroscopy data of ΔH for the C_5 state against the $P_{\rm II}$ state agreed with both MUBATH data with the AMBER parm96 and parm99 force fields. The partial molar enthalpy difference ΔH for the α_R state and the partial molar volume difference ΔV for the C_5 state by the Raman spectroscopy agreed with those for the AMBER parm96 force field. On the other hand, ΔV for the α_R state by the Raman spectroscopy was consistent with our AMBER-parm99 force-field result. All the experimental results fall in between those of simulations using AMBER parm96 and parm99 force fields, suggesting that the ideal force field parameter lie between those of AMBER parm96 and parm99.

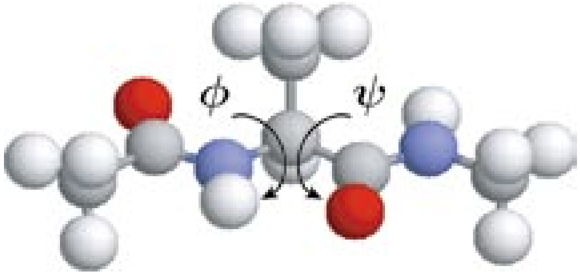

Figure 1. The initial conformations of alanine dipeptide for the MD simulation.

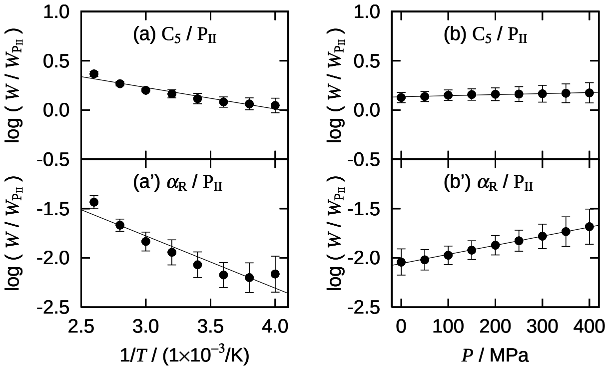

Figure 2. The population ratios of (a) the C_5 state and (a') the α_R state against the $P_{\rm II}$ state as functions of the inverse of temperature $1/T$ at constant pressure of P = 0.1 MPa. The population ratios of (b) the C_5 state and (b') the α_R state against the $P_{\rm II}$ state as functions of pressure P at constant temperature of T = 298 K.

Table 1. Differences ΔH/(kJ/mol) in partial molar enthalpy of the C_5, and α_R states from that of the P_{II} state calculated by the MUBATH MD simulations. Raman experimental data are also listed.

State	AMBER 96	AMBER 99	Raman exp.
C_5	1.8±0.5	3.6±2.2	2.5±0.3
α_R	4.4±1.1	–1.5±2.0	4.4±1.5

Table 2. Differences ΔV/(cm^3/mol) in partial molar volume of the C_5, and α_R states from that of the P_{II} state calculated by the MUBATH MD simulations. Raman experimental data are also listed.

State	AMBER 96	AMBER 99	Raman exp.
C_5	–0.3±0.7	1.5±0.9	0.1±0.3
α_R	–2.3±1.3	1.8±0.8	1.1±0.2

2. Partial Multicanonical Algorithm for Molecular Dynamics and Monte Carlo Simulations[2)]

Partial multicanonical algorithm is proposed for molecular dynamics and Monte Carlo simulations. The partial multicanonical simulation samples a wide range of a part of the potential energy terms which is necessary to sample the conformational space widely, whereas a wide range of total potential energy is sampled in the multicanonical algorithm. Thus, one can concentrate the effort to determine the weight factor only on the important energy terms in the partial multicanonical simulation. The partial multicanonical, multicanonical, and canonical molecular dynamics algorithms were applied to an alanine dipeptide in explicit water solvent. The canonical simulation sampled the states of P_{II}, C_5, α_R, and α_P. The multicanonical simulation covered the α_L state as well as these states. The partial multicanonical simulation also sampled the C_7^{ax} state in addition to the states which were sampled by the multicanonical simulation as shown in Figure 3. In the partial multicanonical simulation, furthermore, backbone dihedral angles ϕ and ψ rotated more frequently than in the multicanonical and canonical simulations. These results mean that the partial multicanonical algorithm has higher sampling efficiency than the multicanonical and canonical algorithms.

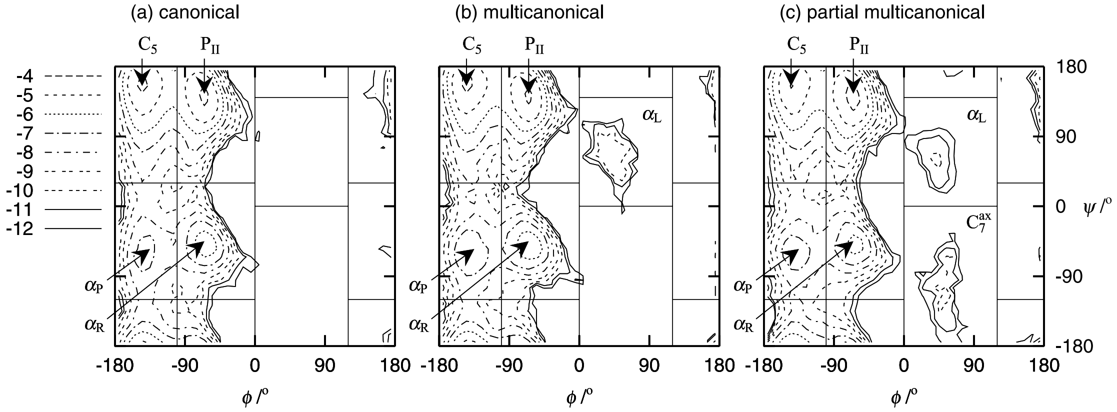

Figure 3. Contour maps of the logarithms of the probability distributions $\log P_{NVT}(\phi,\psi)$ of the backbone dihedral angles ϕ and ψ at T = 300 K obtained (a) by the canonical MD simulation, (b) by the reweighting techniques from the results of the multicanonical MD simulation, and (c) by the reweighting techniques from the results of the partial multicanonical MD simulation.

References

1) H. Okumura and Y. Okamoto, *J. Phys. Chem. B* **112**, 12038–12049 (2008).

2) H. Okumura, *J. Chem. Phys.* **129**, 124116 (9 pages) (2008).

Theory and Computation of Reactions and Properties in Solutions and Liquids

Department of Theoretical and Computational Molecular Science
Division of Computational Molecular Science

ISHIDA, Tateki Assistant Professor

We focus on the projects both on ultrafast photoinduced reaction and on ionic liquids. The project on photoinduced reaction processes in solution focuses on the development of a theoretical method to describe solvent motion and dynamics around a solute molecule in short-time region. Also, it includes the application of the developed theoretical treatment to solvation processes and excited-state intramolecular processes in Betaine dye molecule solution. On the other hand, the project on ionic liquids is collaborating work with the experimental studies by Prof. Shirota at Chiba University.

1. Solvent Motions and Solvation Processes in a Short-Time Regime: Effects on Excited-State Intramolecular Processes in Solution[1)]

We propose a method for treating equation of motions for atoms taking into account the inertial term with an interaction site model for capturing solvent dynamics attributed to solvent motions in a short-time regime, $t < 100$ fs. We show a prescription for solving the equation which governs the development of the fluctuation of solvent number density with the inertial term, and, also, the procedure is applied to the study of solvation dynamics of the simplest betaine dye molecule pyridinium *N*-phenoxide in water in the excited state. It is shown that the coupling between solvation and a fast intramolecular reaction such as charge transfer is likely to play an important role in solvation dynamics of the simplest betaine.

2. Atom Substitution Effects of $[XF_6]^-$ in Ionic Liquids. 1. Experimental Study[2)]

We have investigated the interionic vibrational dynamics of 1-butyl-3-methylimidazolium cation ($[BMIm]^+$) based ionic liquids with the anions of $[PF_6]^-$, $[AsF_6]^-$, and $[SbF_6]^-$ as well as the static physical properties, such as shear viscosity and liquid density. Shear viscosity for the ionic liquids becomes lower with the heavier atom anion: $[BMIm][PF_6]$ > $[BMIm][AsF_6]$ > $[BMIm][SbF_6]$. Femtosecond optically heterodyne-detected Raman-induced Kerr effect spectroscopy has been used to observe the interionic vibrational dynamics of ionic liquids. The interionic vibration in the frequency region of less than 50 cm^{-1} clearly shows the heavy atom substitution effect; that is, the heavy atom substitution of $[XF_6]^-$ critically affects the interaction-induced motion.

3. Atom Substitution Effects of $[XF_6]^-$ in Ionic Liquids. 2. Theoretical Study[3)]

We have carried out the molecular dynamics simulations for 1-butyl-3-methylimidazolium cation based ILs ($[BMIm][PF_6]$, $[BMIm][AsF_6]$, and $[BMIm][SbF_6]$) including the calculations of density of state (DOS) profiles, polarizability time correlation function (TCF), and Kerr spectra (with the development of the force fields of $[AsF_6]^-$ and $[SbF_6]^-$ by an ab initio calculation). From these computational studies, we find that the contribution of the reorientation of cations and anions mainly governs the Kerr spectrum profile in all three ILs, while the contribution of the collision-induced and cross terms, which are related to translational motions including coupling with librational motion, is not large at higher frequencies than 50 cm^{-1}. In addition, it is emphasized in this study that atomic mass effects in ILs are accessible through a complementary approach of both experimental and theoretical approaches.

References

1) T. Ishida, *J. Phys. Chem. B* **113**, 9255–9264 (2009).
2) H. Shirota, K. Nishikawa and T. Ishida, *J. Phys. Chem. B* **113**, 9831–9839 (2009).
3) T. Ishida, K. Nishikawa and H. Shirota, *J. Phys. Chem. B* **113**, 9840–9851 (2009).

Visiting Professors

Visiting Professor

TAKETSUGU, Tetsuya *(from Hokkaido University)*

Ab Initio Dynamics Study of Excited-State Chemical Reactions

We have developed an ab initio molecular dynamics (AIMD) program code for excited-state reaction dynamics, combined with the quantum chemistry program packages, MOLPRO and GAMESS, and applied it to several significant photoreactions at the state-averaged CASSCF level. In the current code, nonadiabatic transitions are treated by the Tully's surface hopping algorithm, while the solvent effects are treated by QM/MM approach. The applications include the excited-state dynamics of 7-azaindole-H_2O cluster (excited-state proton transfer), coumarin 151 in water solution (large solvent effects), cytosine (examination of photostability), photoisomerization of azobenzene (examination of reaction pathways), dissociative recombination reactions of small molecules (surface hopping dynamics), and photodissociation of CH_3I (spin-orbit coupling effects). Through these applications, the code has been extended for general use to examine excited-state dynamics of real molecular system.

Visiting Associate Professor

NAKAJIMA, Takahito *(from The University of Tokyo)*

Development of Large-Scale Molecular Theory

With the emergence of peta-scale computing platforms we are entering a new period of the molecular simulation. The computer simulations can be carried out for larger, more complex, and more realistic molecular systems such as nano- and bio-materials than ever before. To make the most of the computer resource, we should achieve some breakthroughs of conventional theoretical approaches. We have proposed several efficient molecular theories to treat large molecular systems accurately via relativistic and non-relativistic treatments. These approaches include several types of auxiliary basis approaches, such as the pseudospectral method, the resolution of the identity method, the augmented plane-waves method, and the augmented finite-elements method. We expect that these approaches will be capable of the clarification of chemical phenomena in nano- and bio-materials with the help of the next generation supercomputer.

Visiting Associate Professor

HAYASHI, Shigehiko *(from Kyoto University)*

Molecular Simulation Studies of Protein Functions

Protein functional activities involve dynamic molecular conformational changes of complex protein systems. Hence molecular dynamics underlying functional activities are necessary to be revealed for understanding of molecular nature of protein functions. We performed molecular dynamics (MD) simulations on photochemical dynamics of rhodopsins (Rh) and ligand migration dynamics in myoglobin (Mb). We carried out an ab initio quantum mechanical/molecular mechanical MD simulation for the retinal photoisomerization processes in Rh, and revealed a dynamic regulation mechanism for the fast photoisomerization. We also examined the ligand migration dynamics in Mb by a meta-dynamics simulation and a linear response theory, and identified remarkable collective protein motions coupled to the transient ligand migrations through the migration channels.

RESEARCH ACTIVITIES

Photo-Molecular Science

Molecules respond to photon irradiation in a variety of ways, including photo-induced transitions and photochemical reactions. We have employed various light sources and experimental schemes to elucidate molecular structures and properties, and to control chemical reactions and molecular functions. We have also developed novel and advanced light sources for molecular science. Two of research facilities, the Laser Research Center for Molecular Science and the UVSOR Facility, conduct collaborative researches having intimate contacts with the Department of Photo-Molecular Science.

The main topics pursued in the Department include: Development of novel laser spectroscopic methods to reveal fundamental properties of molecules, development of high-resolution optical microscopic methods and application to nanomaterials, coherent control of molecules with ultrafast techniques, spectroscopy of inner-shell excited molecules and fundamental vacuum-UV photochemistry, investigation of the functionality of solid-state materials, developments of novel laser and synchrotron-orbit radiation sources, and so on.

Development of Advanced Near-Field Spectroscopy and Application to Nanometric Systems

Department of Photo-Molecular Science
Division of Photo-Molecular Science I

OKAMOTO, Hiromi	Professor
IMURA, Kohei	Assistant Professor*
NARUSHIMA, Tetsuya	Assistant Professor
JIANG, Yuqiang	Post-Doctoral Fellow
HARADA, Yosuke	Post-Doctoral Fellow
WU, Huijun	Graduate Student
NOMURA, Emiko	Secretary

There is much demand for the study of local optical properties of molecular assemblies and materials, to understand mesoscopic phenomena and/or to construct optoelectronic devices in the nanometric scale. Scanning near-field optical microscopy (SNOM) is an imaging method that enables spatial resolution beyond the diffraction limit of light. Combination of this technique with various advanced spectroscopic methods may offer a direct probe of dynamical processes in nanomaterials. It may provide essential and basic knowledge for analyzing origins of characteristic features and functionalities of the nanometric systems. We have constructed apparatuses of near-field spectroscopy for excited-state studies of nanomaterials, with the feasibilities of nonlinear and time-resolved measurements. They enable near-field measurements of two-photon induced emission and femtosecond transient transmission, in addition to conventional transmission, emission, and Raman-scattering. Based on these methods, we are investigating the characteristic spatiotemporal behaviors of various metal-nanoparticle systems and molecular assemblies.

1. Visualization of Plasmon Wavefunctions and Enhanced Optical Fields Induced in Metal Nanoparticles

We recently reported that wavefunctions of localized plasmon resonances of chemically synthesized metal (Au and Ag) nanoparticles are visualized by near-field transmission or two-photon excitation measurements.[1,2] Figure 1 shows typical near-field transmission images of longitudinal plasmon modes on a Au nanorod, which correspond to the square moduli of the plasmon wavefunctions. We also visualized optical fields in Au nanoparticle assemblies by the near-field two-photon excitation imaging method.[1,3] It was revealed for the dimers that highly localized optical field is generated at the interstitial sites between the particles. In many-particle assemblies, the localized fields were especially intensified at the rim parts of the assemblies.

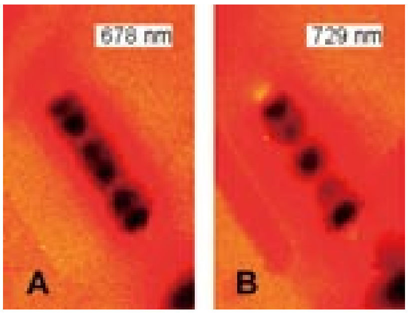

Figure 1. Near-field transmission images of a Au nanorod (diameter 20 nm, length 510 nm), observed at 678 nm (A) and 729 nm (B).

We are now extending the studies to metal nanostructures manufactured by the electron-beam lithography technique, in collaboration with researchers of other institution. Peculiar nano-optical characteristics and characteristic plasmon waves have been found for some metal nanostructures. Near-field properties of nano-void structures opened on thin gold metallic films on substrates have been also characterized, and the field distributions in the vicinities of the voids have been visualized. The detailed analyses of the characteristic optical fields are now under way. Such a study is essential as a basis for designing unique optical properties and functions of metal nanostructures, and their applications to highly sensitive spectroscopic methods and exotic photochemical fields.

2. Properties of Two-Photon Induced Photoluminescence from Au and Ag Nanoparticles

We investigated properties of photoluminescence from Au and Ag nanorods induced by near-field two-photon excitation. For Au nanorods,[4] photoluminescence spectrum showed two peaks around 550 and 650 nm regardless of the rod dimensions, whereas the intensity ratio of the two spectral components varies from rod to rod. The observed spectral features were discussed based on electromagnetic calculations. We found that the spectral components were attributable to the interband transition of gold, and the intensity variation was explainable in terms of local field enhancement in the vicinity of the nanorod due to plasmon-mode excitation.

We also discussed the mechanism of the luminescence from Ag nanowires.[5)] The luminescence was most probably attributed to emission from the oxidized surface layer of the nanowires, which was enhanced in resonance with plasmons on the wires. In a similar way to the Au case, we succeeded in visualization of enhanced electric fields and plasmon modes for Ag nanowires (Figure 2) by the near-field two-photon excitation imaging, by detecting the luminescence from silver.

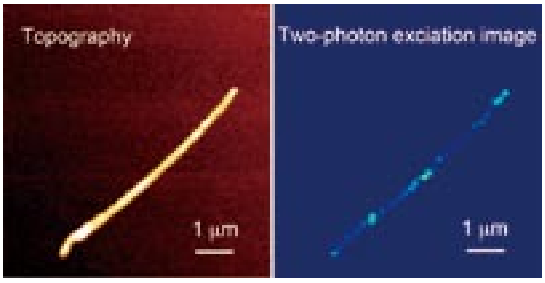

Figure 2. Topography (left) and near-field two-photon excitation (right) images of a silver nanowire (diameter 25 nm, length 6 µm).[5)] © 2009 Royal Society of Chemistry.

3. Bioimaging with Two-Photon-Induced Luminescence from Triangular Nanoplates and Nanoparticle Aggregates of Gold

Two-photon laser scanning microscopy (TPLSM) has been widely used recently in the field of biological imaging because of its merit in *z*-axis resolution and in effective avoidance of photodamage. Since it is difficult to completely eliminate the photobleaching for ordinary fluorophores, ideal optical imaging agents for TPLSM still have to be found. Recently, our group and some others found that two-photon-induced photoluminescence (TPIPL) from Au nanoparticles in the visible region shows quite high efficiency upon femtosecond near-infrared excitation. Based on detailed experimental and theoretical studies on the luminescence characteristics, we found that TPIPL from triangular Au nanoplates is especially efficient. Chemically stable (and as a consequence nontoxic) nature of Au is also beneficial in practical applications. Au nanoplates thus have the potential to be ideal agents for biosensing for microanlysis or bioimaging with TPIPL by TPLSM. In the present study we have demonstrated that Au nanoplate could be indeed a promising material for bioimaging studies by TPLSM.[6)]

Images of yeast cells conjugated to nanoplates were recorded by (far-field) TPLSM for biological use (Figure 3). We found that dried yeast as well as living cells in water can be clearly imaged by this method. We also found that cells conjugated with aggregated Au nanospheres give bright TPIPL, while isolated nanospheres were TPIPL-inactive.

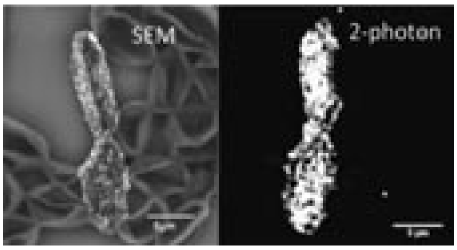

Figure 3. SEM (left) and far-field TPIPL (right) images of dried yeast cells conjugated to triangular Au nanoplates (base length ~300 nm) and some naked dried yeast cells.[6)] Scale bar: 5 µm. © 2009 Wiley-VCH Verlag.

4. Construction of Apparatuses for Nonlinear and Ultrafast Near-Field Spectroscopy

In previous studies we achieved ultrafast near-field imaging with a time resolution of ~100 fs.[2,7)] To further extend the dynamical studies of plasmons, we are now developing basic technologies to achieve near-field time-resolved measurements with <20 fs time resolution. We are also constructing an apparatus for near-field/far-field microscopic nonlinear optical measurements based on the technique of atomic-force microscope.

5. Near-Field Imaging of Organic Molecular Assemblies and Hybrid Systems

We are studying nanometric structures and optical properties of organic molecular assemblies such as carbon nanotubes embedded in sugar polymer chains, LB films of functional conjugated molecules, and hybrid systems consist of metal nanoparticles and organic functional materials, mainly as collaborations with other research groups.

References

1) H. Okamoto and K. Imura, *Prog. Surf. Sci.* **84**, 199–229 (2009).
2) K. Imura, T. Nagahara and H. Okamoto, *J. Phys. Chem. B* **108**, 16344–16347 (2004).
3) K. Imura, H. Okamoto, M. K. Hossain and M. Kitajima, *Nano Lett.* **6**, 2173–2176 (2006).
4) K. Imura and H. Okamoto, *J. Phys. Chem. C* **113**, 11756–11759 (2009).
5) K. Imura, Y. C. Kim, S. Kim, D. H. Jeong and H. Okamoto, *Phys. Chem. Chem. Phys.* **11**, 5876–5881 (2009).
6) Y. Jiang, N. N. Horimoto, K. Imura, H. Okamoto, K. Matsui and R. Shigemoto, *Adv. Mater.* **21**, 2309–2313 (2009).
7) K. Imura and H. Okamoto, *Phys. Rev. B* **77**, 041401(R) (4 pages) (2008).

---

* Present address; Graduate School of Advanced Science and Engineering, Waseda University, Shinjuku, Tokyo 169-8555

Quantum-State Manupulation of Molecular Motions

Department of Photo-Molecular Science
Division of Photo-Molecular Science I

OHSHIMA, Yasuhiro	Professor
HASEGAWA, Hirokazu	Assistant Professor
BAEK, Dae Yul	IMS Fellow
HAYASHI, Masato	Post-Doctoral Fellow
KITANO, Kenta	Graduate Student
MIYAKE, Shinichiro	Graduate Student
INAGAKI, Itsuko	Secretary

Molecules in gas phase undergo translational, rotational and vibrational motions in a random manner, and the total molecular system is a statistical ensemble that contains a number of molecules in many different states of motions. This research group aims to establish methods to manipulate the quantum-state distribution pertinent to molecular motions, by utilizing the coherent interaction with laser lights. Here lasers with ultimate resolution in time and energy domains are employed complementally and cooperatively for manipulation of molecular motions.

1. Nonadiabatic Rotational Excitation of Molecules by Nonresonant Intense Femtosecond Laser Fields

When a gaseous molecular sample is irradiated by an intense nonresonant ultrafast laser pulse, the laser field exerts a torque that aligns the molecular axis along the laser polarization vector, due to the interaction with the molecular anisotropic polarizability. The process has now been termed commonly as "nonadiabatic molecular alignment," and has been attracting much attention because of interesting physics involved and possible broader applications.$^{1)}$ Here the field–molecule interaction only remains in much shorter duration than the characteristic time for molecular rotation, and thus the nonadiabatic alignment is inherently accomplished by nonadiabatic rotational excitation (NAREX), where rotation of the molecules is coherently excited to create a rotational quantum wave packet (WP), a non-stationary superposition of rotational eigenstates.

This research group has developed a method for exploring the NAREX process in a quantum-state resolved manner by using resonance-enhanced multiphoton ionization (REMPI), and reported state distributions after the impulsive excitation with a fundamental output of a femtosecond (fs) Ti:Sapphire laser.$^{2,3)}$ It has been shown that the state distribution is a useful experimental source for verifying the excitation process, since population for each rotational level is proportional to the square of the probability amplitude of the corresponding eigenstate in the rotational WP thus created.

The state-resolved REMPI probe has also been coupled successfully with double-pulse fs excitation. The population for each rotational eigenstate changes oscillatory against the delay between the excitation pulses. When the population of the initial pure state is probed, the delay-time dependent signals provide the phases as well as amplitudes of the WP. Such an experimental reconstruction of WP has recently been demonstrated on the adiabatically cooled molecular sample of benzene by this research group.$^{4)}$ The determined phases show a clear signature for impulsive rotational excitation in non-perturbative regime driven by the intense ultrashort pulse.

The double-pulse excitation study has been extended to probe population changes in various eigenstates with different rotational quantum numbers. For benzene molecules, states with J ranging from 0 to 4 with K = 0–3 have been examined. This systematic investigation experimentally verifies the K dependence of the excitation pathways in the NAREX process for symmetric-top molecules.

2. Ultrafast Angular-Momentum Orientation by Linearly Polarized Laser Fields

In a quantum-mechanical description, the anisotropy of molecular system is represented as a non-uniform distribution of projections, M, of angular momenta onto a space-fixed (Z) axis. In particular, the system is designated as being *oriented* when the populations for $+M$ and $-M$ are different, while it is *aligned* when the populations for $\pm M$ are the same, but those for different $|M|$ differ from one another. In previous studies, the application of circularly polarized radiations had been exclusively considered for the realization of orientation, because it is regarded as being the only way to induce the required helical interaction that breaks the right/left-handed symmetry around the Z axis. The molecular-axis orientation has already been reported in several studies with intense nonresonant radiation, but all of them implemented linearly polarized light, and thus were related to the angular-momentum alignment. Quite recently, this research group theoretically shows and experimentally verifies that a pair of linearly-polarized intense ultrafast pulses creates molecular ensembles with oriented rotational angular momentum in ultrafast time scale, when the delay and the mutual polarization between them are appropriately arranged (as shown in Figure 1). Asymmetric distribution for +*M* and –*M* sublevels relies on quantum interference between the rotational WPs created in the stimulated Raman excitation by the first and the second pulses. The present approach provides spatiotemporally propagating ensembles, of which classical perspective are molecules rotating in clockwise or counter-clockwise direction.

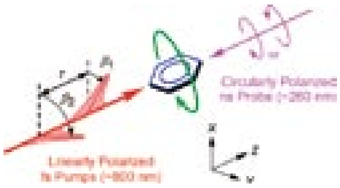

Figure 1. Experimental scheme to create and observe the angular-momentum orientation in molecular rotation.

3. Nonadiabatic Vibrational Excitation by Nonresonant Intense Ultrafast Laser Fields

Nonadiabatic interaction with a nonresonant intense ultrafast laser field can also coherently excite the vibration of molecules, because the molecular polarizability depends on vibrational coordinates. By adopting the similar method to the NAREX studies, nonadiabatic vibrational excitation (NAVEX) of intermolecular vibrations has been successfully realized for benzene clusters by this research group. Here, benzene clusters generated in a supersonic expansion were irradiated with laser pulses (~800 nm, 40–200 fs duration, up to 40 TW/cm^2 in intensity) from the fs Ti:Sapphire laser. Observed changes in intensities of vibronic bands of the benzene dimer indicated the population transfer pertinent to intermolecular vibrational excitation induced by impulsive Raman process. Double-pulse experiments have also been performed, to show that the populations in the ground and excited intermolecular vibrational states oscillatory changed against the delay between the two pulses (see Figure 2). The beat frequencies for the population changes match well with those of the intermolecular modes obtained by the previous ns stimulated Raman spectroscopic studies.[5] This fact confirms that quantum WPs pertinent to intermolecular vibrations in the ground state manifold were created via impulsive stimulated Raman process by a single fs laser pulse. The similar experiment has been performed to record the time-domain spectrum of benzene trimer, which provides the first experimental information on its intermolecular vibrations.

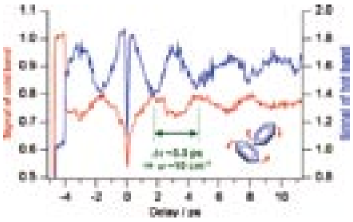

Figure 2. Double-pulse NAVEX spectra of benzene dimer, recorded by probing cold (red) and hot (blue) band transitions.

4. New Experimental Setup for NAREX and NAVEX Studies

A new vacuum chamber and a high-reputation rate dye laser system have been installed for REMPI-probed studies on NAREX/NAVEX processes. The chamber is differentially pumped in two stages and equipped with a high-pressure pulsed valve, which can be operated up to 80 atm at 1 kHz. The laser system runs also at 1 kHz by pumping with a third harmonic of a Nd:YLF laser with the pulse duration of <10 ns, and affords the doubled output of ~50 μJ/pulse at 220–260 nm. High reputation in data acquisition will greatly improve the quality of REMPI spectra to be observed. The performance of the new setup is now examined in the investigation of the intermolecular vibrational excitation of NO–Ar.

5. Development of Coherent ns Pulsed Light Sources and Its Application to Adiabatic Population Transfer

Adiabatic interactions with coherent pulsed radiation can accomplish highly efficient population transfer between quantum states. For realizing such an adiabatic quantum-state manipulation, we are constructing laser systems which deriver single-longitudinal mode (SLM) ns pulses. Among various coherent population transfer methods, we are planning to mainly adopt chirped adiabatic Raman passage (CARP),[6] where one or both of the laser frequency to drive stimulated Raman transitions is swept so as to cross over the two-photon resonance. This method affords multiple advantages, e.g., robustness in transfer probability against variation in laser parameters and broader applicability without necessity for radiation in one-photon resonance to molecular transitions. The laser system for CARP experiments under construction is based on the optical parametric oscillation (OPO), which is injection-seeded by an extra-cavity cw diode laser to achieve the SLM operation. The seeding laser frequency is phase modulated at appropriate RF frequency to attain the frequency chirp to drive the CARP process. The OPO operates near the degenerate condition, so that its signal and idler waves can be used for pump and Stokes fields for stimulated Raman transitions. This design greatly reduces the complication in the setup and will provide much simpler and reliable operation for CARP experiments.

References

1) H. Stapelfeldt and T. Seideman, *Rev. Mod. Phys.* **75**, 543 (2003).
2) H. Hasegawa and Y. Ohshima, *Phys. Rev. A* **74**, 061401 (2006).
3) H. Hasegawa and Y. Ohshima, *Chem. Phys. Lett.* **454**, 148 (2008).
4) H. Hasegawa and Y. Ohshima, *Phys. Rev. Lett.* **101**, 053002 (2008).
5) V. A. Venturo and P. M. Felker, *J. Chem. Phys.* **99**, 748 (1993); M. W. Schaeffer, P. M. Maxton and P. M. Felker, *Chem. Phys. Lett.* **224**, 544 (1994).
6) S. Chelkowski and A. D. Bandrauk, *J. Raman Spectrosc.* **28**, 459 (1997).

Development of High-Precision Coherent Control and Its Applications

Department of Photo-Molecular Science
Division of Photo-Molecular Science II

OHMORI, Kenji	Professor
KATSUKI, Hiroyuki	Assistant Professor
TAKEI, Nobuyuki	Assistant Professor
VESHAPIDZE, Giorgi	Visiting Scientist; JSPS Post-Doctoral Fellow
IBRAHIM, Heide	Visiting Scientist; JSPS Post-Doctoral Fellow
GOTO, Haruka	Graduate Student
NAKAGAWA, Yoshihiro	Graduate Student
INAGAKI, Itsuko	Secretary

Coherent control is based on manipulation of quantum phases of wave functions. It is a basic scheme of controlling a variety of quantum systems from simple atoms to nanostructures with possible applications to novel quantum technologies such as bond-selective chemistry and quantum computation. Coherent control is thus currently one of the principal subjects of various fields of science and technology such as atomic and molecular physics, solid-state physics, quantum electronics, and information science and technology. One promising strategy to carry out coherent control is to use coherent light to modulate a matter wave with its optical phase. We have so far developed a high-precision wave-packet interferometry by stabilizing the relative quantum phase of the two molecular wave packets generated by a pair of femtosecond laser pulses on the attosecond time scale. We will apply our high-precision quantum interferometry to gas, liquid, solid, and surface systems to explore and control various quantum phenomena.

1. Actively Tailored Spatiotemporal Images of Quantum Interference on the Picometer and Femtosecond Scales[1)]

Interference fringes of quantum waves weave highly regular space-time images, which could be seen in various wave systems such as wave packets in atoms and molecules, Bose Einstein condensates, and Fermions in a box potential. We have experimentally designed and visualized spatiotemporal images of dynamical quantum interferences of two counter-propagating nuclear wave packets in the iodine molecule; the wave packets are generated with a pair of femtosecond laser pulses whose relative phase is locked within the attosecond time scale. The design of the image has picometer and femtosecond resolutions, and changes drastically as we change the relative phase of the laser pulses, providing a direct spatio-temporal control of quantum interferences.

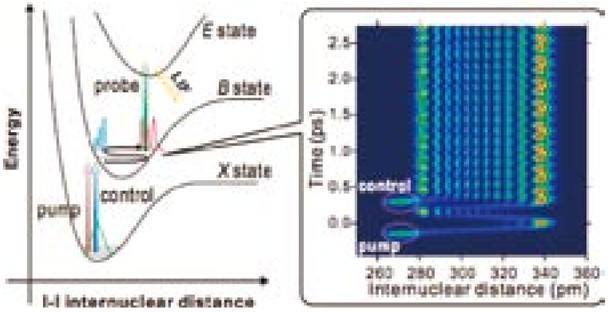

Figure 1. Pump-control-probe scheme for tailoring and visualizing the quantum carpet in the iodine molecule. (Left) Three femtosecond laser pulses are employed. Two of them are phase-locked and used as the pump and control pulses, and the other one is not phase-locked and is used as the probe pulse. The fluorescence signal induced by the probe pulse is measured with a photomultiplier tube attached to a monochromator. (Right) The model simulation of the quantum interference of two wave packets created on the *B*-state potential curve of the iodine molecule by the pump and control pulses. The interference shows a highly regular space-time image that looks like a carpet.

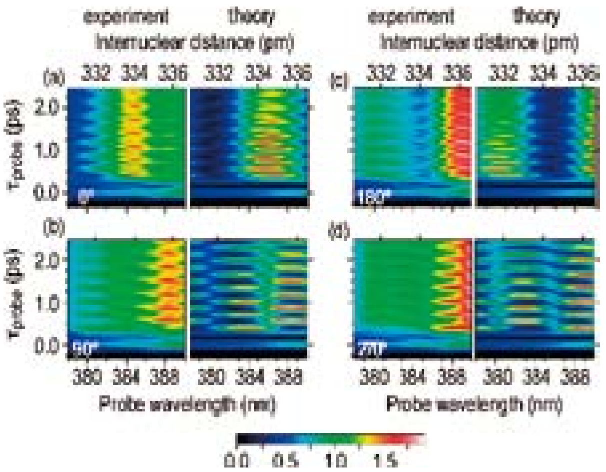

Figure 2. Comparisons of the quantum carpets measured (left) and simulated (right) at the pump-control relative phases θ_{pc} = (a) 0°, (b) 90°, (c) 180°, and (d) 270°. The color scaling is common within each set of measured or simulated carpets; the maxima of those two sets have the same color. The origin $\tau_{probe} = 0$ of the simulated carpet denotes a position of the top of the first oscillation around the outer turning point. The simulations include the interactions with the pump, control, and probe pulses. The parameter $\tau_{control}$, used for the simulation of $\theta_{pc} = 0°$, was 468.920 fs.

2. Optical Control and Mode Selective Excitation of Coherent Phonons in $YBa_2Cu_3O_{7-\delta}$ 2)

Femtosecond time-resolved reflectivity measurement is performed on $YBa_2Cu_3O_{7-\delta}$ films. Coherent phonons of both the Ba–O and Cu–O modes are observed at frequencies of 3.4 and 4.3 THz, respectively. Amplitudes of both Ba–O and Cu–O modes are optically manipulated by using a pair of femtosecond pulses, the separation time of which is controlled. Coherent phonons of the Ba–O and Cu–O modes are completely suppressed at the double-pulse separation times of 135.0 and 108.5 fs and those amplitudes are enhanced at 217 and 270 fs, respectively.

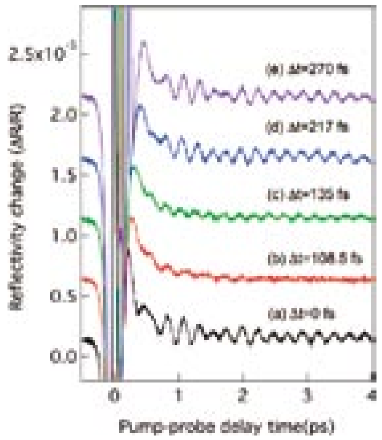

Figure 3. Time-resolved reflectivity of a photo-excited $YBa_2Cu_3O_{7-\delta}$ thin film by irradiation of a pair of femtosecond laser pulses at double-pulse separation time of 0 (a), 108.5 (b), 135 (c), 217 (c), and 270 fs (e).

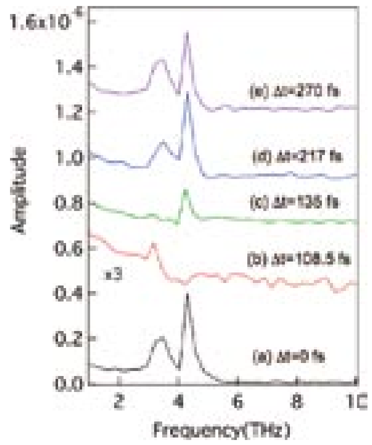

Figure 4. Fourier transformation of the transient relectivity change of a photo-excited $YBa_2Cu_3O_{7-\delta}$ thin film by irradiation of a pair of femtosecond laser pulses at double-pulse separation time of 0 (a), 108.5 (b), 135 (c), 217 (d), and 270 fs (e).

References

1) H. Katsuki, H. Chiba, C. Meier, B. Girard and K. Ohmori, *Phys. Rev. Lett.* **102**, 103602 (2009).
2) H. Takahashi, K. Kato, H. Nakano, M. Kitajima, K. Ohmori and K. G. Nakamua, *Solid State Commun.* in press.

Award

KATSUKI, Hiroyuki; PCCP Prize.

Molecular Inner-Shell Spectroscopy: Electronic Structure and Intermolecular Interaction

Department of Photo-Molecular Science
Division of Photo-Molecular Science III

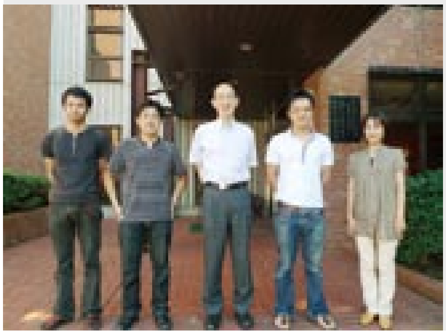

KOSUGI, Nobuhiro	Professor
YAMANE, Hiroyuki	Assistant Professor
NAGASAKA, Masanari	Assistant Professor
NAKANE, Junko	Secretary

In order to reveal electronic structure and intermolecular interaction of molecular solids, liquids, and clusters, we are developing and improving several kinds of soft X-ray spectroscopic techniques and also an original *ab initio* quantum chemical program package GSCF, which is optimized to calculation of molecular inner-shell processes.

1. Development of a Liquid Flow Cell to Measure Soft X-Ray Absorption in Transmission Mode[1)]

We have developed a liquid flow cell for transmission measurement of soft X-ray absorption spectra of liquid samples. The liquid flow cell consists of four regions as shown in Figure 1; (I) vacuum region below 1.0×10^{-4} Pa, connected to the soft X-ray undulator beamline, (II) helium buffer region filled by 1-atm helium, (III) liquid layer and flow region, and (IV) photodiode region in the helium atmosphere. Each region is separated by a 100 nm-thick SiN_x membrane. The window size is 200×200 μm^2 in the region I/II and 2×2 mm^2 in the regions II/III and III/IV. The photon energy calibration is simply carried out by mixing a reference such as oxygen in the helium gas. Fresh liquid samples can be continually supplied to avoid the radiation damage. We have tested this cell for the measurement of O K-edge X-ray absorption spectra in absorbance of liquid water. Thickness of the liquid water layer (region III) is controlled to be ~600 nm by optimizing a water flow speed in a tubing pump system. The present liquid flow cell may enable us to investigate electronic structure of liquid samples confined at a nano-scale space by increasing the helium pressure in the regions IV and II and/or by slowing down the liquid flow.

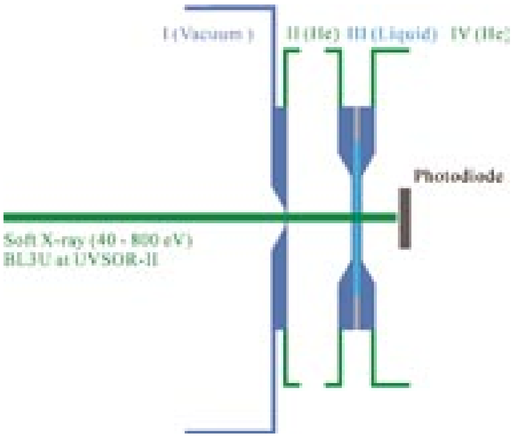

Figure 1. A schematic soft X-ray transmission liquid cell.

2. Strong Double Excitation Features in Soft X-Ray Absorption Spectra of Ferrocene and Ferrocenium Compounds[2)]

We measured the Fe 2p X-ray absorption spectra of decamethyl ferrocene (Fe $3d^6$) and ferrocenium hexafluorophosphate (Fe $3d^5$). The 2p-edge features of 3d transition metal compounds have been attributed, variably, to an atomic multiplet model or a covalent bonding model. A unique covalent bonding between Fe and the two cyclopentadienyl (Cp) rings, especially, the ligand π and out-of-plane $3d^*_{xz,yz}$ (e_{1g}) orbitals, suggests that covalent effects will be most important in the spectral features.

We found the Fe 2p excitation parallel to the π (//*z*) direction cannot be interpreted within a single excitation picture and is split into two strong features as shown in Figure

2. *Ab initio* CI calculations predict a significant role of the double excitation features in the Fe 2p spectra of both $Fe^{II}(Cp)_2$ and the $[Fe^{III}(Cp)_2]^+$ ion. An additional low energy feature (W) observed in $[Fe^{III}(Cp)_2]^+$ is attributed to a Fe 2p to SOMO excitation.

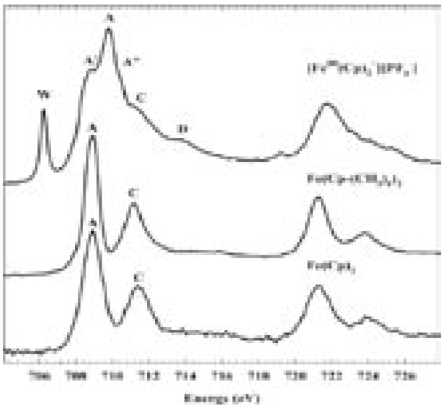

Figure 2. Fe 2p-edge spectra of $[Fe^{III}(Cp)_2{}^+][PF_6{}^-]$, $Fe^{II}(Cp\text{-}(CH_3)_5)_2$ and $Fe^{II}(Cp)_2$.

3. Inner Electronic States beneath Electrodes: Fluorescence-Yield X-Ray Absorption of Pentacene Derivative Films[3)]

The electronic states of inner organic thin films were investigated by X-ray absorption spectroscopy in a bulk-sensitive fluorescence yield (FY) mode. The thin films of the synthesized pentacene derivative (HAPn), 6,13-dihydrodiazapentacence ($C_{20}N_2H_{14}$), on SiO_2-covered Si substrates were fabricated and their morphology and crystallinity were characterized by atomic force microscopy (AFM) and X-ray diffraction (XRD) analysis, respectively. The observed N K-edge FY spectra were different from the surface-sensitive spectra measured in a partial-electron-yield (PEY) mode as shown in Figure 3. The incident angle dependence of the FY spectra was consistent with the expected molecular orientation in the thin films. As a result, we successfully obtained the N and C K-edge FY spectra of the inner HAPn thin films, even beneath the Au electrodes.

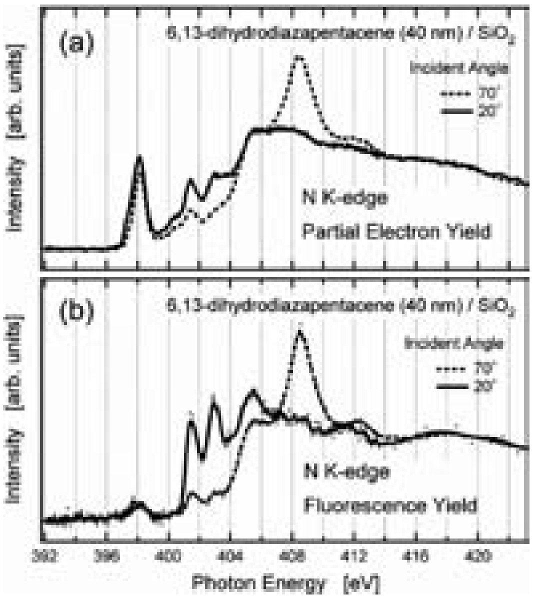

Figure 3. N K-edge X-ray absorption spectra of the HAPn thin film (40 nm thick) deposited on the oxidized Si substrate: Detected in (a) PEY mode and (b) FY mode. The incident angle of X-rays is defined from the surface normal. The spectra are normalized by the signal height at around 420 eV. The sample was stored for 2 weeks in a desiccator at room temperature.

4. Origin of Fine Structures on the Dissociative 1s−σ* Resonance in X-Ray Absorption Spectra of O_2[4)]

We attempted to explain a puzzling long-tailed peak shape of the X-ray absorption spectrum of the oxygen molecule in the energy region around 539 eV by taking into account the Rydberg-valence and vibronic couplings. The long-tailed feature is found to arise from two dissociative σ* states and the sudden drop in intensity is related to decrease in transition dipole near the crossing point between the repulsive σ* and weak 3s Rydberg states with the quartet ion core. This is supported by numerical wave-packet simulations allowing for all inter-channel couplings between the Rydberg and valence manifolds with the quartet (Q) and doublet (D) ion cores in a diabatic representation of the core-excited states as shown in Figure 4.

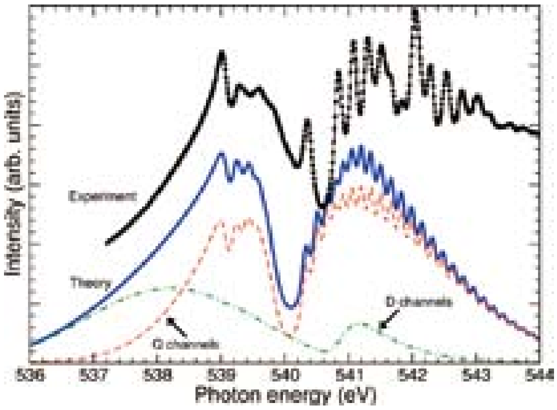

Figure 4. Theoretical X-ray absorption spectra obtained for the excitation to all the channels (solid line), and Q (dashed red line) and D (dash-dotted green line) channels.

References

1) M. Nagasaka, T. Hatsui, T. Horigome, Y. Hamamura and N. Kosugi, *J. Electron Spetrosc.* (2010) in press.
2) E. Otero, N. Kosugi and S. Urquhart, *J. Chem. Phys.* **131**, 114313 (2009).
3) H. S. Kato, R. Hirakawa, F. Yamauchi, T. Minato, M. Kawai, T. Hatsui and N. Kosugi, *J. Electron Spectrosc.* **174**, 93 (2009).
4) Y. Velkov, V. Kimberg, N. Kosugi, P. Sałek and F. Gel'mukhanov, *Chem. Phys. Lett.* **476**, 147 (2009).

Photoabsorption and Photoionization Studies of Fullerenes and Development of High-Efficiency Organic Solar Cells

Department of Photo-Molecular Science
Division of Photo-Molecular Science III

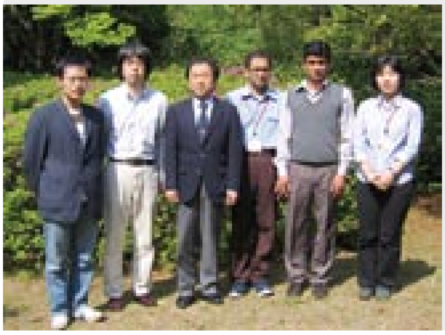

MITSUKE, Koichiro	Associate Professor
KATAYANAGI, Hideki	Assistant Professor
HUANG, Chaoqun	IMS Fellow
YAGI, Hajime	Post-Doctoral Fellow
KAFLE, Bhim Prasad	Post-Doctoral Fellow
PRODHAN, Md. Serajul Islam	Graduate Student (–March ’09) Post-Doctoral Fellow (May ’09–)
NAKAJIMA, Koichi	Visiting Scientist*
BASHYAL, Deepak	Graduate Student
ASARI, Chie	Technical Fellow

The total photoabsorption cross section curves of C_{60} and C_{70} at $h\nu$ = 1.3 to 42 eV were determinined by using photon attenuation method in the UVSOR facility. Moreover, the yield curves of singly- and multiply-charged photoions from fullerenes were measured at $h\nu$ = 25 to 200 eV. We have thus studied the mechanisms and kinetics of sequential C_2-release reactions on the basis of (i) the yield curves for the fragments $C_{60(70)-2n}{}^{z+}$ as a function of the primary internal energy of the parent $C_{60(70)}{}^{z+}$ and (ii) the 3D velocity distributions (velocity map imaging) of the fragments.

In the second topic we have fabricated dye-sensitized solar cells (DSCs) containing Ru dye and iodide electrolyte and measured their short-circuit current density and the intensity of the transmitted light to estimate the wavelength dependence of the incidence photon-to-current conversion efficiency (IPCE) and photoabsorbance (ABS) in the range of 300 to 1000 nm. In addition, we evaluated the quantum yield (APCE) of DSCs for the electron injection from the excited orbital of Ru dye to the conduction band of TiO_2 nano particles. Our final goal is to develop DSCs with high performance and long lifetime by improving ABS and APCE mainly in the near infrared region.

1. Photoabsorption Cross Section of C_{70} Thin Films from the Visible to Vacuum Ultraviolet[1)]

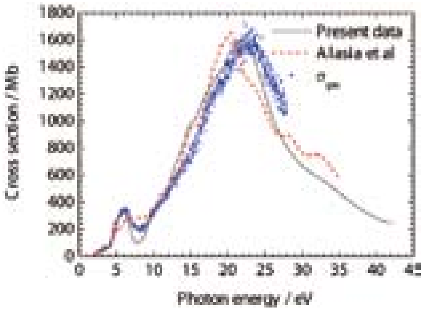

Figure 1. Absolute photoabsorption cross sections of a single C_{70} molecule.

Absolute photoabsorption cross sections of C_{70} thin films were determined for $h\nu$ values from 1.3 to 42 eV using photon attenuation. The spectrum showed a prominent peak of 1320 Mb at 21.4 eV with several fine structures mostly due to $\sigma\rightarrow\sigma^*$ single-electron excitation. The complex refractive index and complex dielectric function were calculated up to 42 eV with Kramers-Kronig analyses. From the present data of C_{70} thin films, the cross section curve of molecular C_{70} was calculated using the standard Clausius-Mossotti relation dealing with correction of the local electromagnetic field, with a plausible assumption that the anisotropy in molecular structure of C_{70} was smeared out by molecular rotation at room temperature.

2. Potential-Switch Mass Gate Incorporated into a TOM Spectrometer[2)]

A photoionization spectrometer for velocity map imaging (VMI) has been developed for measuring the scattering distribution of fragment ions from polyatomic molecules. The mass gate and an ion reflector in the spectrometer are capable of discriminating ions with a particular mass-to-charge ratio m/z. The basic functions and feasibility of these devices were tested experimentally. The photoions from SF_6 were extracted into a time-of-flight (TOF) mass spectrometer by pulsed electrostatic fields. Mass resolution of the fragments was very poor in Figure 2a, because the stationary reverse electric field exists at the ionization region in the absence of the extraction pulses. When the pulse-application timing on the mass gate was tuned to a specific m/z, an exclusive peak of the selected ions was present on a TOF spectrum (Figure 2b).

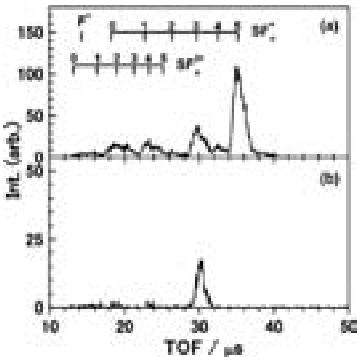

Figure 2. (a) TOF mass spectrum of photofragments from SF_6 at *h*ν = 100 eV. (b) Peak of SF_3^+ selected by applying a 5-V pulsed voltage to the mass gate at an appropriate timing.

3. Mass-Selected Velocity Map Imaging of Fullerenes

The performance of the mass gate in the VMI spectrometer was investigated by the computer simulations of the ion trajectories of photofragments from C_{60}. The initial three-dimensional velocity distribution of C_{58}^+ was projected onto the image plane with an energy resolution better than 10 meV. The C_{58}^+ image was free from the contamination of other ions such as C_{60}^+ and C_{56}^+. We have also tried to deconvolute the effect of the initial beam temperature with the aid of a low pass filter.[3]

4. Measurements of IPCE and Photo-Absorbance of Dye-Sensitized Solar Cells

The IPCE curve a in Figure 3 calculated from the density of the output short-circuit current J_{SC} and the number of the incident photons on the cell I_P agrees with the curve b that was obtained using a laboratory instrument fitting a Xe lamp. An IPCE value was improved to be 0.7 when the layer of TiO_2 film is thicker than 16 μm. Two APCE curves in Figure 4 were calculated in different ways of estimation of ΔI_P, according as whether the scattered SR in the TiO_2 film is partly absorbed by dye (curve b) or not (curve a). It is clear that such multiple absorption may favorably take place in shorter wavelengths and contributes to electron injection from the dye. The quantum yield of the electron injection is expected to be more than 0.8 at shorter wavelengths, whereas it gradually decreases at longer wavelengths.

5. Transient Fluorescence Spectroscopy of DSCs

We observed fluorescence decay by time-resolved single photon counting using free electron laser (FEL) of ~580 nm. Figure 5 shows the dependence of the decay curves of the DSCs on the fluorescence wavelength. The fluorescence lifetime appears to increase with increasing wavelength. This suggests that the conversion rates to other electronic states are comparable to those of the electron injection and fluorescing emission. The decay curves were monitored at 720 nm for a complete DSC and a photovoltaic electrode of TiO_2 film covered with Ru dye. The apparent fluorescence lifetime of the complete DSC is longer than those of the photovoltaic electrode, due to either slower electron injection induced by one of the additives in the electrolyte or aggregation of the dye molecules at the surface of TiO_2.

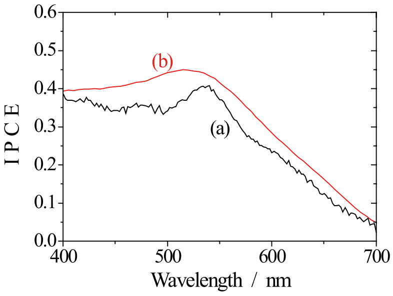

Figure 3. IPCE curves obtained using (a) the SR source and (b) an exclusive IPCE spectrometer.

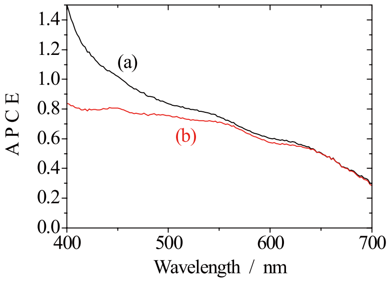

Figure 4. APCE curves calculated in different ways of estimation of ΔI_P.

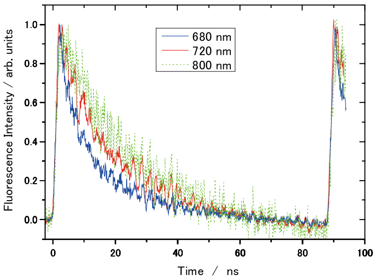

Figure 5. Fluorescence decay curves of DSSC and photovoltaic electrodes, obtained by FEL photolysis.

References

1) H. Yagi, K. Nakajima, K. R. Koswattage, K. Nakagawa, H. Katayanagi and K. Mitsuke, *J. Chem. Phys.* **130**, 234510 (2009).
2) H. Katayanagi, B. P. Kafle, C. Huang, Md. S. I. Prodhan, H. Yagi, and K. Mitsuke, *Nucl. Instrum. Methods Phys. Res., Sect. A* Submitted.
3) Md. S. I. Prodhan, H. Katayanagi, C. Huang, H. Yagi, B. P. Kafle, and K. Mitsuke, *Chem. Phys. Lett.* **469**, 19 (2009).

---

* from Hosei University

Atoms & Molecules in Intense Laser Fields

Department of Photo-Molecular Science
Division of Photo-Molecular Science III

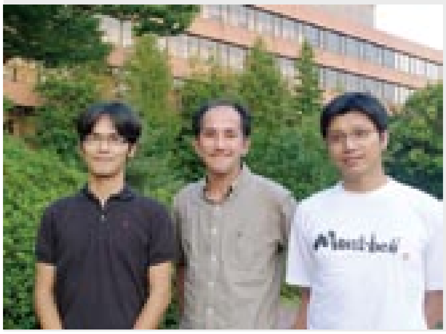

HISHIKAWA, Akiyoshi	Associate Professor
FUSHITANI, Mizuho	Assistant Professor
TSENG, Chien-Ming	IMS Fellow
NAKANE, Junko	Secretary

Intense laser fields, comparable in magnitude with the Coulomb field within atoms and molecules, can be generated by focussing high-energy and ultrashort laser pulses. When exposed to such a strongly perturbing field, molecules exhibit various exotic features that cannot be observed in weak laser fields. We are seeking a deeper understanding of the behavior of molecules in intense laser fields, to elucidate how molecules interact with light, as well as to apply the new features they exhibit to the real-time visualization of ultrafast chemical reactions and their control. In particular, we focus on the following research themes:

(1) Understanding of atomic and molecular dynamics in intense laser fields and the control
(2) Ultrafast reaction imaging by laser Coulomb explosion imaging
(3) Generation and application of ultrashort soft-X-ray pulses by laser high-order harmonics.

1. Electron-Ion Coincidence Momentum Imaging of Molecular Dissociative Ionization in Intense Laser Fields: Application to CS_2[1)]

Molecules in intense laser fields show characteristic reaction processes, such as above-threshold dissociation (ATD), bond softening/hardening and deformation of the geometrical structures, associated with rearrangement of the electron distribution. Here, we performed photoelectron spectroscopy of the dissociative ionization of CS_2 to clarify the electron dynamics in intense laser fields. We developed a new electron–ion coincidence imaging system to label each photoelectron with the counterpart ion, so that the electron dynamics for different pathways can be discussed separately from the corresponding photoelectron images.

Photoelectron images of CS_2 in 35 fs intense laser fields (2 × 10^{13} W/cm^2, 800 nm, linearly polarized) recorded in coincidence with the parent ion, CS_2^+, show clear concentric ring patterns due to the above-threshold ionization (ATI) process. On the other hand, broad structure-less distributions elongated along the direction of the laser polarization are observed in the coincidence electron images for the CS^+ and S^+ fragment ions. The difference in the electron images indicates that the dissociative ionization does not proceed sequentially by the formation and photodissociation of CS_2^+ in intense laser fields. The origin of the difference in the spectra was discussed in terms of the direct ionization to the dissociative state and of the (multiple) electron recollision process.

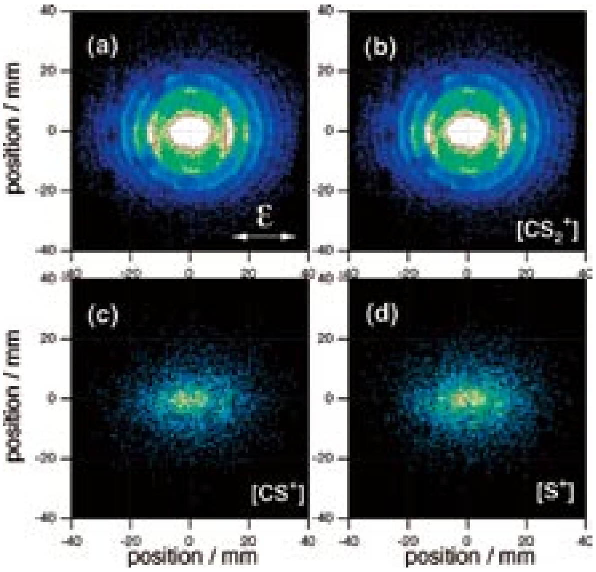

Figure 1. Photoelectron images of CS_2 recorded at a field intensity of 2.1 × 10^{13} W/cm^2 (800 nm, 35 fs) (a) and those recorded in coincidence with CS_2^+ (b), CS^+ (c) and S^+ (d). The concentric ring patterns appearing in (a) are the ATI peaks. The laser pulses are linearly polarized. The total electron-ion coincidence count rate is less than 0.03 per laser shot.

2. Multiple Explosion Pathways of the Deuterated Benzene Trication in 9-fs Intense Laser Fields[2)]

The formation and fragmentation of multiply charged molecular ions are commonly observed as the responses of molecules exposed to intense laser fields. The fragmentation dynamics in these interactions have been extensively studied in recent years as they provide insight into the interplay between the electron and nuclear dynamics with large degrees of nuclear freedom in the presence of strong alternating electric fields. Here we employ the coincidence momentum imaging technique to clarify the fragmentation process of benzene in 9 fs intense laser fields (1×10^{15} W/cm^2). By using this technique we can unambiguously identify the Coulomb explosion pathways from one particular charge state of interest and determine the momenta of the fragment ions in the laboratory frame.

Five two-body and eight three-body Coulomb explosion pathways from the trication ($C_6D_6^{3+}$), associated with the deprotonation and ring-opening reactions, are identified. It is found from the fragment momentum correlation that all the observed three-body explosion processes proceed sequentially via the two-body Coulomb explosion forming molecular dications, $C_mD_n^{2+}$, with (m,n) =(6,5), (5,5), (5,4), (4,4), (4,3) and (3,3), which further dissociate into pairs of monocations (see Figure 2). The branching ratios of the observed Coulomb explosion pathways, estimated from the number of the corresponding coincidence events, largely deviate from the previous RRKM prediction, showing that the dissociation processes are not fully statistical.

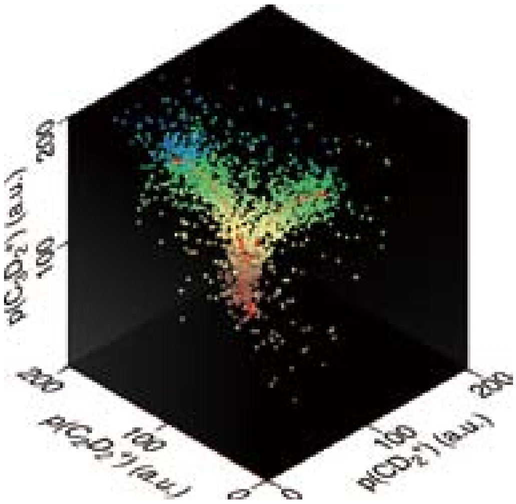

Figure 2. Three-dimensional momentum correlation map, plotting all the coincidence events identified for the three-body Coulomb explosion pathway, $C_6D_6^{3+} \rightarrow C_3D_2^+ + C_2D_2^+ + CD_2^+$, in intense laser fields (9 fs, 1×10^{15} W/cm^2). The results of simulations based on the free-rotor model for the sequential three-body explosion are shown by the red solid lines.

3. Development of Time-Resolved Reaction Imaging System with Laser High-Order Harmonics[3)]

Laser high-order harmonics have novel features such as i) photon energy higher than several 100 eV, ii) extremely short pulse duration in the sub-fs regime, iii) high-quality spatio-temporal coherence, iv) high photon flux comparable to synchrotron radiation and v) simple and precise synchronization with other laser light sources. Because of these aspects, the laser high-order harmonic pulses are of great interest as a potential light source for time-resolved spectroscopy of ultrafast dynamics that could not be elucidated in real time by conventional techniques.

Figure 3 shows the schematic of new time-resolved reaction imaging system developed in our group. It consists of a laser high-order harmonics source, a soft X-ray spectrograph, a beam line equipped with a time delay line as well as a pair of dielectric mirrors to select one of the harmonic orders, and an electron-ion coincidence imaging chamber. The photoelectron spectra recorded for Xe with the 59 th harmonics (~92 eV) show the 4d inner-core photoelectron and the associated Auger electron peaks. Real-time probing of chemical reaction dynamics using this system is in progress.

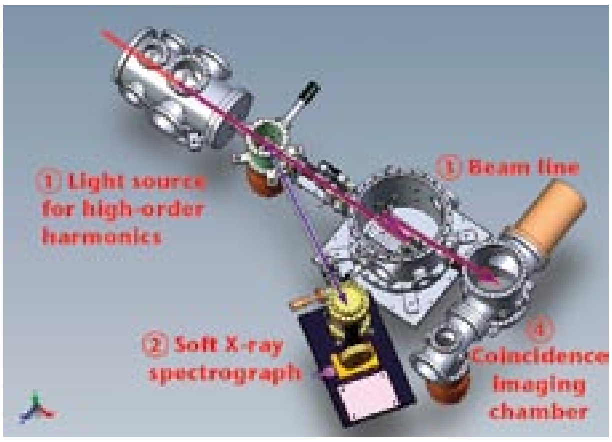

Figure 3. Schematic of time-resolved reaction imaging system developed at IMS, consisting of (i) a high-order harmonics source, (ii) a soft X-ray spectrograph, (iii) a beam line and (iv) a coincidence momentum imaging chamber.

References

1) A. Matsuda, M. Fushitani and A. Hishikawa, *J. Electron Spectrosc. Relat. Phenom.* **169**, 97–101 (2009).
2) A. Matsuda, M. Fushitani, R. D. Thomas, V. Zhaunerchyk and A. Hishikawa, *J. Phys. Chem. A* **113**, 2254–2260 (2009).
3) M. Fushitani, A. Matsuda, E. J. Takanashi and A. Hishikawa, *J. Phys: Conf. Series* **185**, 012009 (4 pages) (2009).

Light Source Developments by Using Relativistic Electron Beams

UVSOR Facility
Division of Advanced Accelerator Research

KATOH, Masahiro	Professor
ADACHI, Masahiro	Assistant Professor
ZEN, Heishun	Assistant Professor
TANIKAWA, Takanori	Graduate Student
TAIRA, Yoshitaka	Graduate Student*
NAGATANI, Atsumune	Graduate Student*
FURUI, Yuta	Graduate Student*
HAJIRI, Tetsuya	Graduate Student*
KIKUCHI, Yoshitaka	Graduate Student*

This project involves researches and developments on synchrotron light source, free electron laser, beam physics and related technologies. Most of these works are performed at the UVSOR-II electron storage ring and its injector.

1. Developments on UVSOR-II Accelerators

After the major upgrade in 2003,[1)] the UVSOR-II electron storage ring has been operated with a small emittance of 27 nm-rad, that enables four undulators to produce highly brilliant synchrotron radiation in the VUV region. This small emittance, on the other hand, makes the beam lifetime short through the intra-beam scattering, so called Touschek effect. To solve this lifetime problem eternally, we have been preparing for top-up injection. In this operation scheme, electron beam is re-filled with a short interval, typically one minute, to keep the beam current almost constant.

In 2008, we have started test operation with the top-up injection on every Thursday night. The electron beam is kept at 300 mA for 12 hours, as shown in Figure 1. We have observed instability on the injection efficiency, which causes gradual reduction of the beam current. We have found that the instability is mainly caused by some drifts of the electron energy from the linear accelerator and also of the high voltage of the injection septum electrode of the booster synchrotron. A feedback system is being developed. It has been demonstrated that this system could stabilize the injection efficiency.

In 2009, we have successfully demonstrated a top-up operation in single bunch mode. Short electron pulse produced by the electron gun was successfully accelerated and transferred to the storage ring. This new operation scheme drastically improves not only the performances of the single bunch users' runs but also the free electron laser and other coherent light sources as described below.

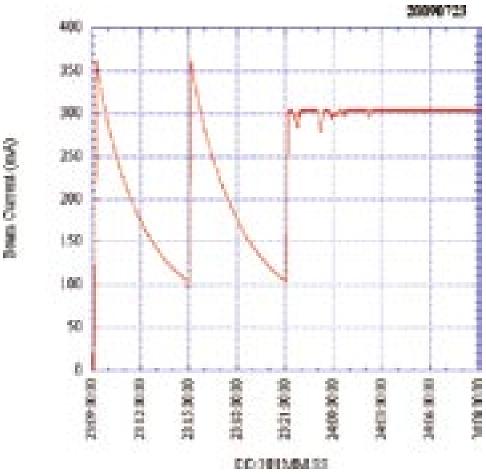

Figure 1. Beam current history in the top-up test operation. After operated for 12 hours in the ordinary operation mode, the ring was operated for about 12 hours in the top-up mode as keeping the beam current at 300 mA.

2. Storage Ring Free Electron Laser

The low emittance and the high peak current of UVSOR-II enable the free electron laser to oscillate in the deep UV region with high output power exceeding 1W.2) During the high power operation of the free electron laser, a rapid change of the output power was observed, which was partly due to the decrease of the electron beam intensity and partly due to the thermal deformation of the mirrors of the optical cavity. To solve this problem, a feedback system has been developed, which control the mirror alignment as monitoring the FEL output power. It was successfully demonstrated to stabilize the output power.3) In adding to this, FEL operation with top-up injection was tried. We have succeeded in lazing for several hours as keeping the output power almost constant.

3. Coherent Synchrotron Radiation by Laser-Electron Interaction

We have developed a system to create micro-density structure on electron bunches circulating in the storage ring.4) By controlling the laser pulse shape, we can create various density structures such as a short dip structure or periodic structure. In the former case, broadband coherent terahertz radiation was produced.4) In the latter case, quasi-monochromatic coherent terahertz radiation was produced.5)

Coherent harmonic generation is a method to produce coherent harmonics of laser light by using relativistic electron beam. The laser-electron interaction in an undulator produces density modulation of a period of the laser wavelength. When the energy modulation is sufficiently larger than the natural energy spread, a density modulation is created which contains higher harmonic component of the laser wavelength. Such an electron bunch emits coherent harmonics of the injected laser. We have successfully observed the coherent third harmonics of Ti:Sa laser.6) We have demonstrated a generation of variable polarization coherent harmonics using a variable polarization undulator.7)

The coherent radiation experiments using laser has come into a new phase as supported by the Quantum Beam Technology Program of JST/MEXT. In the new research project, a part of the storage ring was reconstructed. By moving the injection point to anther short straight section, we will have a new long straight section dedicated for the coherent radiation experiments. A new undulator system is under designing. The laser system is being upgraded. A VUV diagnostic system is under preparation.

4. Developments of Accelerator Technologies

The stabilization of the electron orbit of the storage ring is important to provide stable synchrotron radiation to users. At UVSOR-II, a drift of the orbit in a time scale of minutes to hours has been observed. An orbit feedback system has been developed which observes the orbit drift and control the orbit steering magnets in the ring. It was successfully demonstrated that the system can suppress the orbit drift of a few hundred of microns to a few tens of microns.8)

A 5T super-conducting bending magnet has been designed for a 1.2 GeV synchrotron light source to produce hard X-rays planned at Nagoya University. The bending angle is 12 degree and the peak magnetic field is above 5T. The pole shape was optimized by using a 3D simulation to provide X-rays to three beam-lines separated by a few degrees.

References

1) M. Katoh, M. Hosaka, A. Mochihashi, J. Yamazaki, K. Hayashi, Y. Hori, T. Honda, K. Haga, Y. Takashima, T. Koseki, S. Koda, H. Kitamura, T. Hara and T. Tanaka, *AIP Conf. Proc.* **705**, 49–52 (2004).
2) M. Hosaka, M. Katoh, A. Mochihashi, M. Shimada, T. Hara and Y. Takashima, *Proc. 28th Internat. Free Electron Laser Conf. (Berlin)* 368–370 (2006).
3) M. Koike, M. Hosaka, M. Katoh, Y. Takashima and M. Adachi, *UVSOR Activity Report 2008* 34 (2009).
4) M. Shimada, M. Katoh, S. Kimura, A. Mochihashi, M. Hosaka, Y. Takashima, T. Hara and T. Takahashi, *Jpn. J. Appl. Phys.* **46**, 7939–7944 (2007).
5) (in alphabetic order) S. Bielawski, C. Evain, T. Hara, M. Hosaka, M. Katoh, S. Kimura, A. Mochihashi, M. Shimada, C. Szwaj, T. Takahashi and Y. Takashima, *Nat. Phys.* **4**, 390–393 (2008).
6) M. Labat, M. Hosaka, A. Mochihashi, M. Shimada, M. Katoh, G. Lambert, T. Hara, Y. Takashima and M. E. Couprie, *Eur. Phys. J. D* **44**, 187–200 (2007).
7) M. Labat, M. Hosaka, M. Shimada, M. Katoh and M. E. Couprie, *Phys. Rev. Lett.* **101**, 164803 (2008).
8) Y. Suzuki, M. Katoh, Y. Takashima, M. Hosaka, N. Yamamoto and H. Morimoto, *UVSOR Activity Report 2008* 32 (2009).
9) M. Yoshida, Y. Takashima, M. Katoh, M. Hosaka, N. Yamamoto, H. Morimoto and M. Torikoshi, *UVSOR Activity Report 2008* 33 (2009).

---

* carrying out graduate research on Cooperative Education Program of IMS with Nagoya University

Synchrotron Radiation Spectroscopy on Strongly Correlated Electron Systems

UVSOR Facility
Division of Advanced Solid State Physics

KIMURA, Shin-ichi	Associate Professor
ITO, Takahiro	Assistant Professor[*]
MIYAZAKI, Hidetoshi	IMS Fellow
TERASHIMA, Kensei	JSPS Post-Doctoral Fellow[†]
IM, Hojun	Post-Doctoral Fellow[‡]
TSUNEKAWA, Masanori	Post-Doctoral Fellow[§]
NISHI, Tatsuhiko	Research Fellow[||]
MIZUNO, Takafumi	Graduate Student
IIZUKA, Takuya	Graduate Student
MITANI, Hiroyuki	Graduate Student[¶]

Solids with strong electron–electron interaction, so-called strongly correlated electron systems (SCES), have a various physical properties, such as non-BCS superconducting, colossal magneto-resistance, heavy fermion and so on, which cannot be predicted by first-principle band structure calculation. Thanks to the physical properties, the materials are the candidates of the next generation functional materials. We are investigating the mechanism of the physical properties of SCES, especially rare-earth compounds, organic superconductors and transition-metal compounds, by infrared/THz spectroscopy and angle-resolved photoemission spectroscopy using synchrotron radiation. Since experimental techniques using synchrotron radiation are evolved rapidly, the development of the synchrotron radiation instruments is also one of our research subjects.

1. Direct Observation of Momentum-Dependent Exchange Interaction in a Heisenberg Ferromagnet1)

Local magnetism is generally believed to originate from the direct interaction among isolated electron spins described by the Heisenberg model, in which the electronic states with local magnetic moments are perfectly localized. In rare-earth compounds, instead of direct exchange interaction, superexchange interaction mediated by ligand valence electrons and indirect exchange interaction by conduction electrons among rare-earth ions are dominant because the 4*f* state in rare-earth ions is spatially localized. In the case of the superexchange and indirect exchange interactions, hybridization between the 4*f* electrons with local magnetic moments and the valence/conduction electrons is important. Then we measured the temperature-dependent three-dimensional angle-resolved photoemission spectra of EuO(100) thin film, a typical Heisenberg ferromagnetic semiconductor, to investigate the essential origin of the ferromagnetic transition. We observed sizable energy dispersion and large binding-energy shift of the Eu 4*f* state below the Curie temperature only near the Γ and X points, despite the expected Heisenberg-type local magnetism. The band dispersion and temperature dependence of the Eu 4*f* state indicates that the indirect exchange and superexchange interactions have strong momentum dependence. The observed temperature-dependent energy shift of the 4*f* state is the essential origin of the magnetism of EuO.

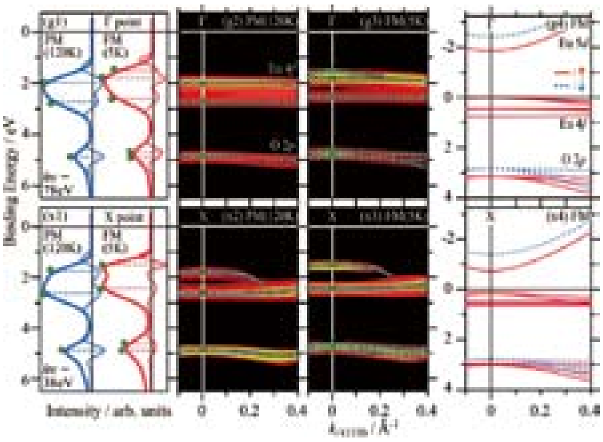

Figure 1. Energy distribution curves (EDCs, thick lines) and their second-derivative EDCs (thin lines) of EuO(100) thin film in the paramagnetic phase (PM) at 120 K and in the ferromagnetic phase (FM) at 5 K at the Γ (g1) and X (x1) points. The dashed lines indicate the peaks in the second-derivative EDCs that correspond to the peaks and shoulders in the EDCs. The 3D ARPES images were derived from the second-derivative EDCs in the paramagnetic phase at 120 K and in the ferromagnetic phase at 5 K near the Γ [(g2), (g3)] and X [(x2), (x3)] points. The open circles in (g2), (g3), (x2), and (x3) indicate the peaks and shoulders in the 3D ARPES images. The band structures calculated by the LSDA+*U* (*U* = 7 eV) method are shown near the Γ (g4) and X (x4) points. The solid and dashed lines in (g4) and (x4) denote the majority (↑) and minority (↓) spin states, respectively.

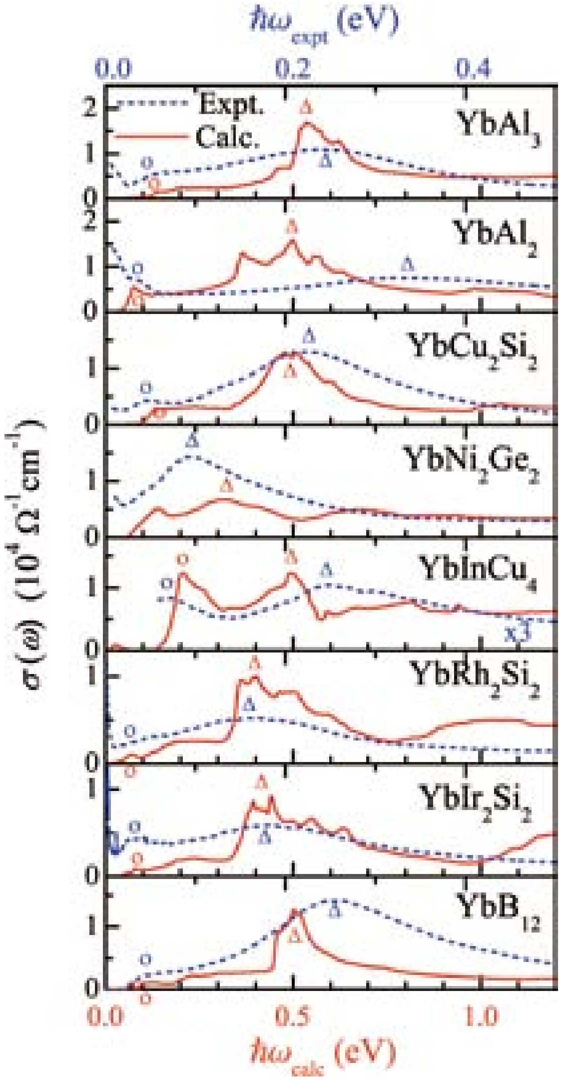

Figure 2. Calculated optical conductivity [σ(ω)] spectra compared with experimental spectra of $YbAl_3$, $YbAl_2$, $YbCu_2Si_2$, $YbNi_2Ge_2$, $YbInCu_4$, $YbRh_2Si_2$, $YbIr_2Si_2$, and YbB_{12}. The σ(ω) spectra of $YbCu_2Si_2$, $YbNi_2Ge_2$, $YbRh_2Si_2$, and $YbIr_2Si_2$ were calculated along the *a*-axis, in the same way as the experimental spectra. The horizontal scales of the experimental and calculated spectra are located at the top and bottom, respectively. Note that the horizontal scale of the calculated σ(ω) spectra is reduced by a factor of 0.42 (= 0.5/1.2) compared with that of the experimental spectra. The vertical scales of the calculated and experimental σ(ω) spectra are identical except in the case of $YbInCu_4$, in which the experimental spectrum is three times as large as the calculated spectrum. The mid-IR peaks and far-IR shoulders of the experimental and calculated spectra are marked by open triangles and open circles, respectively.

2. Origin of Infrared Peaks in the Optical Conductivity of Cerium and Ytterbium Compounds[2,3]

We have demonstrated that the middle-infrared (mid-IR) peaks commonly appearing in the optical conductivity [σ(ω)] spectra of CeX_3 (X = Pd, Sn, In) and ytterbium compounds ($YbAl_3$, $YbAl_2$, $YbCu_2Si_2$, $YbNi_2Ge_2$, $YbInCu_4$, $YbRh_2Si_2$, $YbIr_2Si_2$, and YbB_{12}) can be explained by first-principle band structure calculation with the spin–orbit interaction from the comparison with the results with the experimentally obtained σ(ω) spectra. On CeX_3, the mid-IR peak shapes are not identical to one another: $CePd_3$, $CeSn_3$, and $CeIn_3$ have a triple-peak structure, a double-peak structure, and a broad single-peak structure, respectively. These peaks can be theoretically explained by the optical transition from the occupied state to the spin–orbit splitted Ce 4*f* state. On the other hand, in Yb compounds, the spectral feature of a peak in the middle-infrared (IR) region (mid-IR peak) and a shoulder structure in the far-infrared region (far-IR shoulder) in the experimental σ(ω) spectra can be described by the band calculation with a common renormalization factor of z = 0.42. These results suggested that the infrared spectra of Ce and Yb compounds originate from the own band structure but that the Yb 4*f* state shifts to the Fermi level with strong electron correlation.

References

1) H. Miyazaki, T. Ito, H. J. Im, S. Yagi, M. Kato, K. Soda and S. Kimura, *Phys. Rev. Lett.* **102**, 227203 (2009).
2) S. Kimura, T. Iizuka and Y. S. Kwon, *J. Phys. Soc. Jpn.* **78**, 013710 (2009).
3) S. Kimura, *Phys. Rev. B* **80**, 073103 (2009).

Awards

KIMURA, Shin-ichi; Morita Memorial Award, The Alumni Association of Physics Department “Senshu-kai,” Tohoku University.
MIYAZAKI, Hidetoshi; Best Presentation Award, PF Workshop on Recent Research Activities and Future Prospect of Angle-Resolved Photoemission Spectroscopy.

---

* Present Address; Graduate School of Engineering, Nagoya University, Nagoya 464-8603
† Present Address; Department of Physics, Ritsumeikan University, Kusatsu 525-8577
‡ Present Address; Department of Advanced Physics, Hirosaki University, Hirosaki 036-8561
§ Present Address; Faculty of Education, Shiga University, Otsu 520-0862
|| from Chiba University
¶ carrying out graduate research on Cooperative Education Program of IMS with Shinshu University

Electronic Structure and Decay Dynamics in Atoms and Molecules Following Core Hole Creation

UVSOR Facility
Division of Advanced Photochemistry

SHIGEMASA, Eiji Associate Professor
HIKOSAKA, Yasumasa Assistant Professor

The dynamics of the inner-shell photoexcitation, photoionization, and subsequent decay processes is much more complex, in comparison to outer-shell photo-processes. For instance, the inner-shell photoionization is concomitant with the excitation and ionization of valence electrons, which reveal themselves as shake-up and shake-off satellite structures in the corresponding photoelectron spectrum. The one-photon multi-electron processes, which are entirely due to the electron correlation in the system, are known to happen not only in the primary inner-shell hole creation processes, but also in their relaxation processes. Our research project is focused on elucidating the electronic structures and decay dynamics in core-excited atoms and molecules, by utilizing various spectroscopic techniques together with monochromatized synchrotron radiation in the soft x-ray region.

1. Dissociation Dynamics in Polyatomic Molecules Following Core Hole Creation

The acetylene dication is one of the smallest metastable polyatomic dications, whose dissociation and isomarization from the acetylene (HCCH) into the vinylidene (H_2CC) configurations have been extensively investigated. By using the PEPIPICO technique, it was found that the acetylene dications dissociate from excited states above 34 eV, where five three-body reactions and three two-body reactions including the dissociation channel via the vinylidene form ($CH_2^+ + C^+$: V-channel) have been identified. The isomarization time of the acetylene decation produced following the Auger decay was estimated to proceed within 60 fs. Very lately, the visualization of ultrafast hydrogen migration in deuterated acetylene dication, which occurs in a recurrent manner, was nicely demonstrated by using intense ultrashort laser pulses.[1)]

In the previous work, in addition to the V-channel, the other two channels in the two-body reactions, such as the acetylene channel ($CH^+ + CH^+$: A-channel) and deprotonation channels ($C_2H^+ + H^+$: P-channel), were correlated with some Auger final states. In order to gain a further insight into the dissociation mechanism of the Auger final states, we have performed an Auger-electron–ion coincidence study on fragmentations of deuterated acetylene dication, $C_2D_2^{2+}$, formed via Auger decay. With the use of our Auger-electron–ion coincidence spectrometer,[2)] we have identified Auger final states relevant to the individual fragmentations including the three-body reaction, as well as to the formation of metastable $C_2D_2^{2+}$.

It is found that the atomic fragment ions tend to be produced in the entire region of Auger electrons, while the molecular ions except for CD^+ exhibit specific productions for certain Auger final states. The parent dications are mainly observed at the lowest band, which shows a clear maximum around 33.3 eV. The CD_2^+ fragments related to the V-channel, as well as the atomic fragments C^+ and D^+ yield the highest energy peak in the $1\pi_u^{-2}$ band at 35.0 eV. The highest binding energy band centered at 50 eV enhances violent fragmentation leading to the productions of C^+, D^+, CD^+, and C_2^+.

2. One-Photon Multi-Electron Emission Processes Studied by Multi-Eelectron Coincidence Spectroscopy

Neutral core-excited states of low-Z atoms relax mainly by electron emission, which has been investigated intensively in rare gases. It leads predominantly to singly-charged ions, but formation of doubly-charged ions by emission of two Auger electrons also makes up a considerable fraction of the total decay. Both direct and indirect processes can contribute to resonant double Auger decay. In the direct process, two electrons are simultaneously ejected and the available energy is continuously shared between the two electrons. In the indirect process, two electrons are emitted sequentially with distinct kinetic energies depending on the energy levels of the initial, intermediate, and final electronic states involved. Resonant double Auger decay of molecules is indeed known to exist from mass spectroscopic studies of ions. However, the molecular process is much more complicated than the atomic one, because it can be influenced by nuclear motions at any stage of the decay. In order to clarify the resonant double Auger process in molecules, we have used high-resolution electron spectroscopy and electron-electron coincidence spectroscopy.

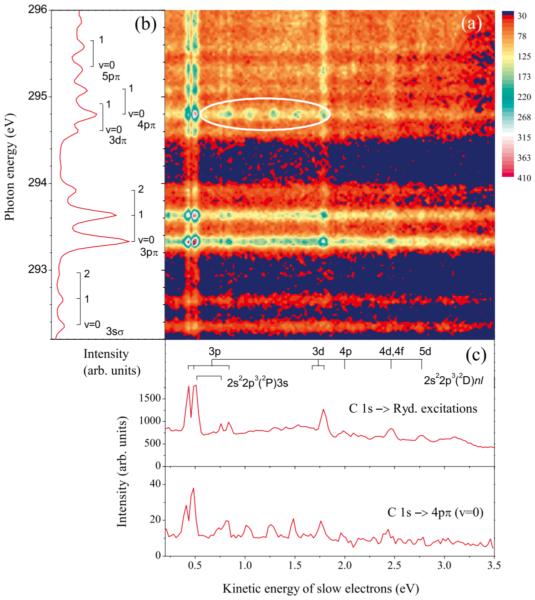

Figure 1. (a) Two-dimensional (2D) map of the slow electron yields in the C1s-to-Rydberg range. (b) Total ion yield spectrum. (c) Top: Sum of the slow electron yields in the Rydberg excitation region which is derived by projecting the electron yields in the 2D map onto the horizontal axis. Bottom: slow electron spectrum at the C 1s → 4pπ (v = 0) resonance.

Figure 1 shows a two-dimensional (2D) map of slow electron yields as a function of the photon energy in the C 1s Rydberg excitation region of CO, with the total ion yield spectrum measured together with the slow electron yields. The 2D map exhibits horizontal stripes in the Rydberg resonances. Knots of enhancement are discernable in each stripe on the 2D map. The locations of some of these knots are common to all different C1s-to-Rydberg excitations. The observation implies that dissociation of CO^+ states formed by first-step Auger decay and subsequent fragment O* atom autoionization constitute a major path for the double Auger decay of the C1s-to-Rydberg states. It is also found that additional spots appearing only on the 4pπ (v = 0) resonance. These spots are spaced at 0.24 eV intervals, as clearly seen in the horizontal cut of the 2D map on this resonance [bottom panel of Figure 1(c)]. The constant intervals suggest that the peaks correspond to vibrational levels of CO^+ or CO_2^+, and are therefore associated with molecular autoionization of CO^+ into CO_2^+. The mechanisms of the complicated molecular double Auger decay has nicely been clarified by the combined use of the two different spectroscopic methods.

3. Construction of New Soft X-Ray Spectroscopy Beamline BL6U

A new project for constructing the undulator beamline BL6U has been initiated. We have decided to choose the entrance slit-less configuration for the monochromator. A varied-line-spacing (VLS) plane grating monochromator (PGM) seems to be one of the most trustworthy ones to realizing high resolution in the soft x-ray range. In order to cover a wide photon energy region (30–500 eV) with one single grating, a variable-included-angle Monk-Gillieson mounting VLS-PGM has been selected.

The monochromator has been designed to cover the photon energy ranging from 30 to 500 eV, with the resolving power higher than 10000 and the photon flux more than 10^{10} photons/sec. The practical construction of BL6U has begun from the summer shutdown in 2008. The first light has been observed in December 2008 and then precise tunings of the monochromator have been continued.

The installation of a new electron spectrometer to BL6U, which can be rotated around the photon beam axis, has been finished in August 2009, and its performance test has begun.

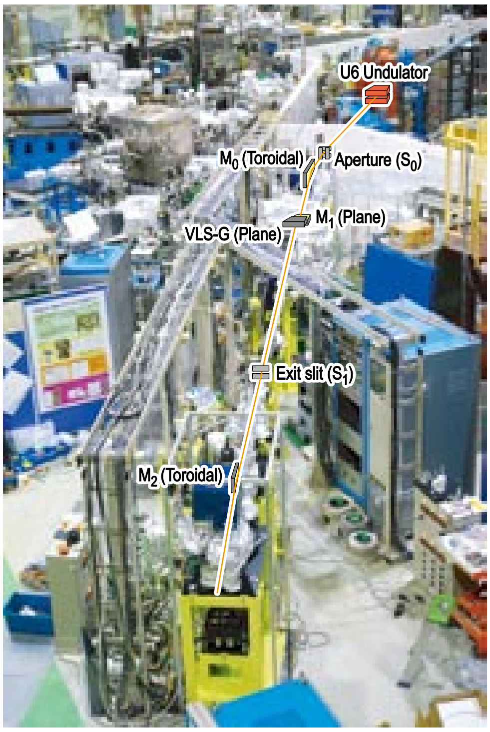

Figure 2. A top view of the newly constructed soft X-ray spectroscopy beamline BL6U.

References

1) A. Hishikawa, A. Matsuda, M. Fushitani and E. Takahashi, *Phys. Rev. Lett.* **99**, 258302 (4 pages) (2007).

2) T. Kaneyasu, Y. Hikosaka and E. Shigemasa, *J. Electron Spectrosc. Relat. Phenom.* **156-158**, 279–282 (2007).

3) T. Kaneyasu, Y. Hikosaka, P. Lablanquie, F. Penent, L. Andric, G. Gamblin, J. H. D. Eland, Y. Tamenori, T. Matsushita and E. Shigemasa, *Phys. Rev. Lett.* **101**, 183003 (4 pages) (2008).

Micro Solid-State Photonics

Laser Research Center for Molecular Science
Division of Advanced Laser Development

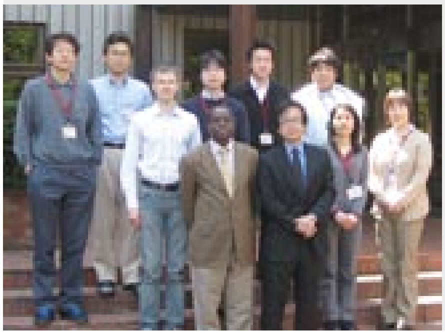

TAIRA, Takunori	Associate Professor
ISHIZUKI, Hideki	Assistant Professor
AKIYAMA, Jun	IMS Fellow
TSUNEKANE, Masaki	Post-Doctoral Fellow*
SATO, Yoichi	Post-Doctoral Fellow
SAIKAWA, Jiro	Post-Doctoral Fellow†
OISHI, Yu	Post-Doctoral Fellow‡
MATSUSHITA, Tomonori	Post-Doctoral Fellow
ONO, Yoko	Secretary
INAGAKI, Yayoi	Secretary

The artistic optical devices should be compact, reliable, efficient and high power light sources. With the approaches of domain structures and boundaries engineering, it is possible to bring the new interaction in their coherent radiation. The high-brightness nature of Yb or Nd doped single crystal or ceramic microchip lasers can realize efficient nonlinear wavelength conversion. In addition, designed nonlinear polarization under coherent length level allows us new function, such as the quasi phase matching (QPM). The development of "***Micro Solid-State Photonics***," which is based on the micro domain structure and boundary controlled materials, opens new horizon in the laser science.

1. High Peak Power, Passively Q-Switched Cr:YAG/Nd:YAG Micro-Laser for Ignition of Engines

Our high peak power, micro-laser igniter was first applied for a real automobile engine. A commercial engine of 1AZ-FSE (TOYOTA Motor Corp.) which is a 2.0 L, straight-4 piston engine with a gasoline direct injection system was prepared. The ignition point of a laser is set to be the same point as a spark plug. In this experiment, three of four cylinders (from #1 to #3) were ignited by conventional spark plugs and a #4 cylinder was ignited by our laser. Each ignition timing was carefully controlled and optimized. The repletion rates of the igniters are 13.3 Hz corresponding to an engine speed of 1600 rpm. Schlieren photographies of the early stage of ignition and subsequent combustion in a real engine are shown in Figure 1. The left figure shows the image of a conventional spark plug ignition and the right shows the laser ignition. The A/F is 14.5 which is a stoichiometric mixture of gasoline and air. It should be emphasized that a single laser pulse with an energy of 2mJ can successfully ignite a real engine. We think it will be the lowest energy ever reported for laser ignition of a real automobile engine. High brightness, passively Q-switched micro-laser could reduce the ignition energy dramatically compared to previous ignition lasers and also a spark plug. We further demonstrated the first prototype micro-laser module which had the same dimension as a spark plug as shown in Figure 2.

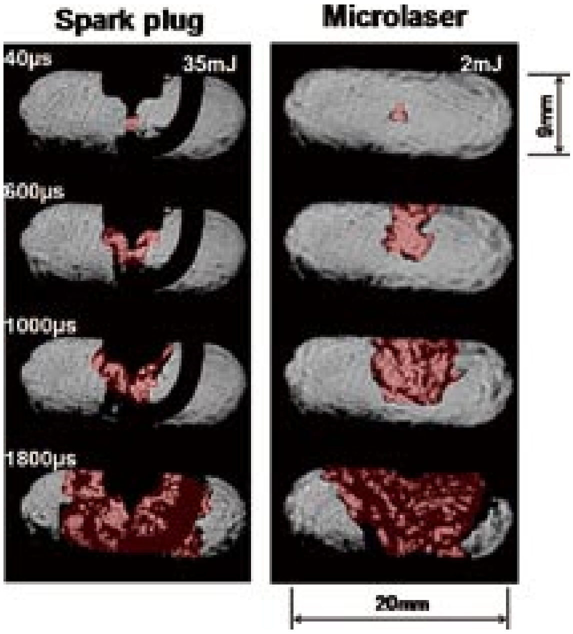

Figure 1. Schlieren photographs of the flame kernel ignited by a spark plug (a) and the micro-laser (b) in a constant volume combustion chamber at 6 ms after ignition trigger.

Figure 2. First prototype micro-laser module (right), which has the same dimension as a spark plug (left).

2. Spectroscopic Characteristics of Nd^{3+}-Doped Photo-Thermo-Refractive Glass

Considering recent spreading of laser resonator control that uses volume Bragg diffraction grating (VBG), it is convenient for VBG to have an ability of laser action. VBG is made of photo-thermo-refractive (PTR) glass, therefore we have evaluated the spectroscopic properties of Nd^{3+}-doped photo-thermo-refractive glass (Nd:PTR). From absorption characteristics we can estimate radiative lifetime of Nd:PTR by Judd-Ofelt analysis to be 861 μs while quantum efficiency of 0.8at.% Nd:PTR is considered to be 57.6%. Authors assures that Nd:PTR is the promised laser medium due to wide absorption and emission bandwidth, long fluorescent lifetime.

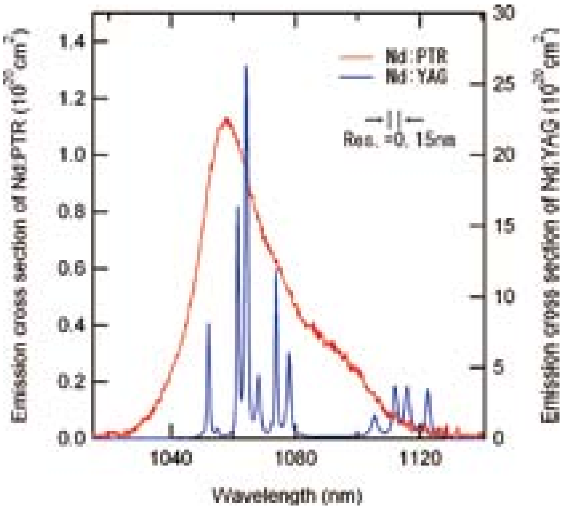

Figure 3. Emission cross section of Nd:PTR. Center wavelength of fluorescence is 1058 nm with a very wide emission bandwidth of 28nm that is useful for tuning by Bragg grating.

3. Broadly and Continuously Tunable, High-Energy Optical Parametric System by Angular Tuning of Tilted QPM Structures

We proposed a broadly and continuously tunable high-energy colinear optical parametric systems by using a periodically poled Mg-dpoped $LiNbO_3$ (MgLN) device with tilted quasi-phase matching (QPM) structures as shown in Figure 4, and experimentally demonstrated expanded tuning characteristics of the tilted QPM devices. The resulting tuning ranges of signal wave were 0.22 μm (1.50 μm ~ 1.72 μm), 0.13 μm (1.45 μm ~ 1.58 μm), for tilted QPM device with QPM period Λ_0 = 28.0, 29.0 μm, in device-rotation angle θ_1 from –10° to +10°. Combination of angular rotation and tilted QPM structure is effective for compact and broadband-tunable coherent light source, especially for high refractive index crystals, as MgLN.

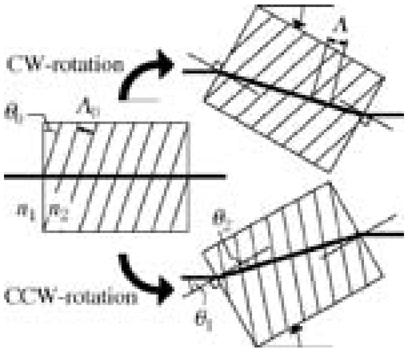

Figure 4. Broad and continuous tuning of optical parametric system by angular tuning of tilted QPM device.

4. Formation of Anisotropic Laser Ceramics

Rare-earth doped transparent ceramics (polycrystalline materials) have attracted considerable attentions as the next generation laser gain media due to their capability for engineered structure and improved mechanical properties. In this study, we have newly established “Rare-earth assisted electromagnetic material processing” which is a precise grain orientation controlling method for transparent *anisotropic* laser ceramics. We applied it for fabrication of rare-earth doped FAP ($Ca_{10}(PO_4)_6F_2$) materials and successfully obtained the uniaxially oriented laser grade Nd^{3+}:FAP ceramics as shown in Figure 5 by imposition of a feeble (1.4 tesla) static magnetic field during slip-casting process.

Figure 5. Macro photograph of Nd^{3+} doped transparent FAP ceramics.

References

1) M. Tsunekane and T. Taira, *Tech. Digest of Conf. on Lasers and Electro-Optics/Europe 2009* CA.P.30 (2009).
2) Y. Sato, T. Taira, V. Smirnov, L. Glebova and L. Glebov, *Technical Digest of Conf. on Lasers and Electro-Optics (CLEO2009)* CTuFF-5 (2009).
3) H. Ishizuki and T. Taira, *Tech. Digest of Conf. on Lasers and Electro-Optics (CLEO2009)* CThZ1 (2009).
4) J. Akiyama, Y. Sato and T. Taira, *OSA Topical Meeting on Advanced Solid-State Photonics 2009* MF1 (2009) (postdeadline papers).

* from JST Innovation Plaza Tokai
† from Tokyo Institute of Technology
‡ from RIKEN

Photo-Induced Dynamics and Reactions at Solid Surfaces

Laser Research Center for Molecular Science
Division of Ultrahigh Resolution Optical Measurement

MATSUMOTO, Yoshiyasu Professor*

Solid surfaces provide an interesting environment where two completely different electronic systems meet to each other: Localized electronic system, *i.e.*, atoms and molecules and delocalized one, *i.e.*, solid bulk surfaces. Charge transfer at surfaces is fundamental to adsorbate-metal interactions and reactions. Moreover, dynamic processes including chemical reactions on surfaces, particularly metal surfaces, are associated with continuous nonadiabatic transitions. This research program aims for understanding electron and nuclear dynamics at surfaces. Photo-induced processes including photochemistry at surfaces are the major focus in this program. Photons are used for not only exciting electronic states of adsorbate and substrate, but also for probing those states with various types of nonlinear optical spectroscopy.

1. Ultrafast Coherent Phonon Dynamics at Well-Defined Surfaces$^{1)}$

To understand the mechanism of surface photochemistry, it is vital to know how photoinduced electronic excitation induces adsorbate nuclear motions that ultimately lead to chemical reactions. We have demonstrated the real-time observations of surface phonons and adsorbate-substrate vibrational modes by fs time-resolved second harmonics generation (TRSHG). If an excitation light pulse has a duration sufficiently shorter than a period of a vibrational mode or a phonon mode, it can excite the mode with a high degree of temporal and spatial coherence. This coherent nuclear motion modulates the second-order susceptibility $\chi^{(2)}$. Thus, by monitoring the intensity modulation of the second harmonics (SH) generation of a probe pulse, we can observe the evolution of the coherent nuclear motion subsequent to the electronic excitation at the surfaces. We have focused on the excitation mechanism of coherent surface phonons at K-covered Cu(111) surfaces in comparison with Na adsorbates.

At the coverages from 0.22 to 0.35 monolayer (ML), TRSHG traces show the oscillatory component with a frequency of 3.05±0.05 THz. The amplitude of this component decreases as coverage increases higher than ~0.35 ML, whereas another oscillating component with a frequency of 1.26±0.03 THz grows. Both components are ascribed to K–Cu stretching motion. The spectral changes with coverage suggest that the overlayer structure varies with lateral compression.

The fast transient peak in TRSHG traces at around zero delay changes its sign from negative to positive when coverage exceeds ~0.22 ML. Since the quantum-well state (QWS) is partly filled at around this coverage, electrons in the QWS are principally responsible for the transition of the electronic response. Furthermore, the excitation photon energy dependence of TRSHG traces indicates that the excitation of substrate d-band electrons, giving rise to rapid charge fluctuations in the QWS, generates the coherent K–Cu stretching vibration. Consequently, the QWS plays a major role in the electronic and nuclear dynamics induced by pump pulses at $h\nu = 2.2$ eV.

2. Ultrafast Vibrational Energy Transfer in Thin Layers on Pt(111) Surfaces$^{2)}$

Ultrafast dynamics of vibrational energy transfer in overlayers of D_2O and CO on Pt(111) have been investigated by femtosecond time-resolved (TR) IR–visible sum-frequency-generation (SFG) spectroscopy under ultrahigh-vacuum conditions. About 10 layers of D_2O ice were epitaxially grown on c(4×2)-CO/Pt(111). The surface was excited by subpicosecond laser pulses, and subsequent energy transfer through low-frequency modes of adsorbates was monitored in terms of peak shifts and broadenings of C–O and O–D stretching bands in SFG spectra as a function of the pump–probe delay. Because D_2O ice forms islands, there are two types of CO: one interacting with D_2O and the other free from D_2O. Simulations of the TR-SFG spectra by using a phenomenological model for the energy-transfer dynamics indicate that the coupling rate of perturbed CO is larger than that of free CO by a factor of 1.7; this is probably because CO $2\pi^*$ states shift toward the Fermi level due to interaction with D_2O. Two isolated bands at 2668 and 2713 cm^{-1} were assignable to the OD stretching bands of D_2O directly interacting with CO at the D_2O/CO interface and D_2O at the vacuum/ice interface, respectively. Analysis of the temporal spectral changes of free D_2O by using a diffusive thermal transport model indicates that heat transfer through low-frequency phonons of the ice layers occurs within 3 ps; this is substantially faster than the pulsed laser-induced melting of thin ice films reported previously.

3. Spectroscopy of Molecules at Interfaces in Organic Field Effect Transistors by a Sum Frequency Generation Microscope

Organic field effect transistors (OFETs) have gained substantial attentions recently. In order to understand the efficiency of the device and the mechanism of charge transport, it is important to know carriers at the interface between a gate electrode and an organic semiconductor thin film. Since the interface is buried in the device, there are a few methods to investigate what is really happening at the interface. Sum frequency generation (SFG) is one of promising methods to realize it, since this is sensitive to the molecules at interfaces. SFG is a nonlinear optical process and, in particular, when visible and infrared beams are used, SFG is a powerful means for vibrational spectroscopy. We have developed a SFG microscope and applied it to the interface between pentacene and silicon oxide at the gate electrode. SFG signals generated at the interface are spatially resolved by the SFG microscope.

We observed clear SFG microscopic images of source and drain electrodes and the channel regions between them of the OFET devices. Upon application of a gate voltage of –50 V while keeping the voltage between the drain and source electrodes zero, the SFG signal intensity homogeneously increased only in the channel region about ten times and clear peak structures emerged in the SFG spectra. The observed peak structures are attributed to poly vinylphenol (PVP) used as a gate insulating layer of this devise; they are enhanced by the local electric field induced by carriers injected into the semiconductor/dielectric interface. Thus, the spatial distributions of carriers in the channel region at the interface were sensitively mapped by use of the vibrational resonance of PVP in the SFG images.

Reference

1) K. Watanabe, K. Inoue, I. F. Nakai, M. Fuyuki and Y. Matsumoto, *Phys. Rev. B* **80**, 075404 (10 gages) (2009).
2) M. Nagao, K. Watanabe and Y. Matsumoto, *J. Phys. Chem. C* **113**, 11712–11719 (2009).

---

* Present Address; Kyoto University, Graduate School of Sciences, Department of Chemistry, Kyoto 606-8502

Visiting Professors

Visiting Professor

MIDORIKAWA, Katsumi *(from RIKEN)*

XUV Nonlinear Optics and Attosecond Dynamics in Atoms and Molecules

Nonlinear optical process in the XUV region is of paramount importance not only in the field of quantum electronic but also in ultrafast optics. From the viewpoint of quantum electronics, new features of the interaction between intense XUV photons and matters are expected to be revealed through observation of those nonlinear phenomena. On the other hand, those nonlinear processes in the XUV region is indispensable for progress of attosecond science including attosecond atomic/molecular physics and chemistry, because it is very useful for investigating ultrafast phenomena directly in attosecond time scale. Using high harmonic generation by intense femtosecond lasers, we are pursuing extreme optical science including XUV nonlinear optics and attosecond physics/chemistry.

Visiting Professor

TOMINAGA, Keisuke *(from Kobe University)*

Molecular Dynamics in Condensed Phases Studied by Ultrafast Laser Spectroscopy

Molecules in liquids interact with each other in a complex manner, and this complicated interaction yields a variety of aspects in the dynamical behaviors of liquids. We have investigated fluctuations of vibrational frequencies of solute in aqueous solutions by infrared three-pulse photon echo experiments. The time-correlation function of the frequency fluctuation can be expressed by a bi-exponential function with a time constant of about 100 fs and that of 1 ps. The temperature dependence experiment shows that the picosecond component is very weakly temperature dependent. In order to compare the vibrational fluctuation with the fluctuation of the electronic state, we have also performed fluorescence dynamic Stokes shift experiment in aqueous solutions. It is found that the different dynamics and interactions are important for the fluctuations of the vibrational and electronic states.

Visiting Associate Professor

AMEMIYA, Kenta *(from High Energy Accelerator Research Organization)*

Development of Soft X-Ray Optics and X-Ray Absorption Techniques

We have developed a high-resolution soft X-ray beamline in UVSOR, where the X-ray absorption spectroscopy (XAS) technique is available in order to investigate the atomic and electronic structures. Since the soft X-ray region includes the K edge of light elements such as carbon, nitrogen and oxygen, as well as the L edges of 3d transition metals, one can study various materials such as organic molecules and complexes by using this new beamline. We are also trying to develop a novel experimental technique, three-dimensional XAS, by combining the soft X-ray microbeam with the depth-resolved XAS technique, in which the probing depth of the electron-yield XAS spectrum is controlled by the electron emission angle. The lateral and depth profiles of the atomic and electronic structures can be determined with lateral and depth resolution of several micron and sub nanometer, respectively.

Visiting Associate Professor

KERA, Satoshi *(from Chiba University)*

Electronic Structure of π-Conjugated Organic Thin Film by Photoelectron Spectroscopy

To clarify the charge transport and injection mechanism in weakly-interacting organic molecular solids, ultraviolet photoelectron spectroscopy (UPS) is considered a conventional and novel powerful technique. Hole-vibronic coupling as well as intermolecular energy-band dispersion is important fundamental properties to reveal mysterious electric properties of organic molecular solids. Moreover, a quantitative analysis of the intensity distribution from angle-resolved UPS using photoelectron scattering theory gives us information on the molecular orbital character as well as bonding nature, leading important aspects on intermolecular and molecule–substrate interaction to electronic/spin configuration. Photoemission related phenomena, *e.g.* scattering, interference and lifetime effect of photogenerated hole on a discrete and delocalized state of molecular orbital, are hot issues.

RESEARCH ACTIVITIES

Materials Molecular Science

Extensive development of new molecules, molecular systems and their higher-order assemblies is being conducted in the four divisions and in the research center for molecular scale nanoscience. Their electronic, optical and magnetic properties as well as reactivities and catalytic activities are being examined in an attempt to discover new phenomena and useful functions.

Structures and Functions of Metal–Carbon Nano-Systems Produced from Metal-Acetylides

Department of Materials Molecular Science
Division of Electronic Structure

NISHI, Nobuyuki	Professor
JUDAI, Ken	Assistant Professor
NISHIJO, Junichi	Assistant Professor
NUMAO, Shigenori	Graduate Student
USUI, Chika	Technical Fellow
UBAHARA, Wakana	Secretary

Metal acetylides or metal ethynyl conpounds are made of the M^+–C^- ionic bonds. However, the ionic states of the acetylides are essentially metastable resulting in the segregation into metal-carbon or metal-organic polymer nanophases. Following to the invention of graphene-walled Mesoporous Carbon Nano Dendrides (MCND) by evaporating silver from dendroid silver acetylide crystals, we have invented copper nanowires and nanonets by removing the carbon, this time, and also 3D nanonets with copper skeletons with carbon mantles. These electron-conductive materials can be used for energy storage devices.

1. Invention of Electron-Conductive 3D Nanostructure Networks for Energy Storage Electrodes

As demonstrated by the invention of graphene-walled Mesoporous Carbon Nano-Dendrites (MCND), metal-acetylides are well suited for generating nanostructured conductive materials. In contrast to silver acetylide, copper acetylide or methylethynyl copper normally produces wire-type crystals. Copper methylacetylide ($Cu–C≡C–CH_3$) also produces wire type crystals bigger than those of copper acetylide as shown in the next section. These wire crystals form bundles of the wires and, owing to the catalytic activity of copper, all carbons are removed as volatile hydrocarbon gases leaving copper wires, or 3D copper nets (Figure 1-a). We also succeeded to generate Hollow Carbon Nets by removing copper and the methyl group from copper methylacetylene wire crystals. After the segregation reaction of the acetylide to copper nanoparticles, light hydrocarbon gases, and the carbon matrices with 3D connected net-type structures of 20~150 nm wires (Figure 1-b), mild thermal activation and nitric acid treatment removes copper components from the hybrid materials leaving hollow carbon networks. This material allow to be heated at a high temperature producing conductive graphene and graphitic components around the wall region.

In the empty space of the carbon networks, one can fill tin nanoparticles or silicon submicron particles to make lithium ion batteries or other active metal particles for new batteries.

a) Copper 2D Nano-Nets (SEM)

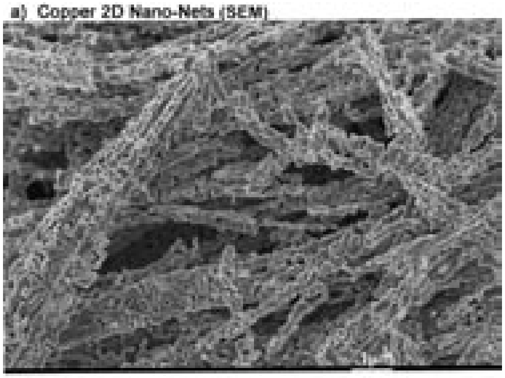

b) Hollow Carbon Alveolus with Graphitic Walls (TEM)

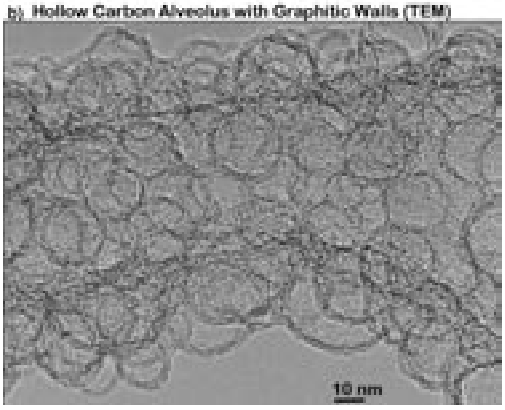

Figure 1. a: a SEM image of the 2D copper nanonets. **b**: Hollow Carbon Alveolus with graphitic walls. The body is a planer belt shape with many carbon balls connected each other.

2. Self-Assembly of Copper Methyl-Acetylide Nanowires

The methods for nanowire production by highly anisotropic materials are usually based upon the binding with covalent bonds. The Cu_2C_2 molecule is a new category of highly anisotropic crystal, which is based on ionic bonding with a highly anisotropic ligand of a C_2^{2-} unit. Crystal growth of metal atoms is expected to be isotropic and nanowire structures cannot be obtained by a normal method of crystal growth. Our strategy is that the insertion of an acetylenic functional group (C_2^{2-} unit) to metal element provides anisotropic properties. Metal acetylides can be a candidate compound to self-assemble into nanowire morphology.

The substituent effect was examined on nanowire generation of Cu_2C_2. We have succeeded in producing the copper methyl-acetylene (CuC_2CH_3) nanowires by the simple self-assembly technique. The methyl substitution on an acetylene molecule, can also self-assemble into nanowire morphology through methyl-methyl hydrophobic intermolecular interaction in an aqueous solution. It may mean that an acetylenic or a methy-ethynyl functional group originally has anisotropic crystal growth properties.

It is very simple to produce CuC_2CH_3 nanowires. The fabrication method for CuC_2CH_3 nanowire involves bubbling methyl acetylene (propyne, HC_2CH_3) gas into an ammonia solution of copper chloride (CuCl).[1,2] Figure 2 shows a scanning electron microscopic (SEM) image of as-grown product of CuC_2CH_3. A mat with copper methyl acetylide nanowires was observed. It should be noticed that the amount of impure, amorphous product (not nanowire) for CuC_2CH_3 is much smaller than that for Cu_2C_2. Not only purity of the CuC_2CH_3 nanowire mats, but also the large surface area of them can link to the capability of good gas adsorbent, gas sensor, or gas storage materials. Indeed, we attempt to check the properties of this nano-material for hydrogen storage, catalysis and so on.

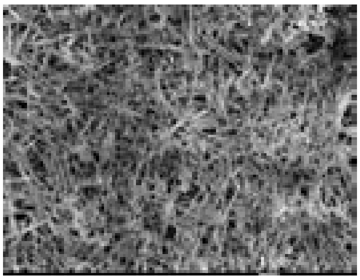

Figure 2. A SEM image of $Cu–C≡C–CH_3$ bundled nanowire crystals. Organometallic crystals are normally space-charged for SEM observation.

3. Weak Ferromagnetism in Chromium Acetylide Based Magnet

The interest in constructing a transition metal acetylide $[M(C≡C–R)_n]^{(m–n)+}$ based magnet has been stimulated, in part, by its superior optical properties that raise the possibility of using the materials in various magneto-optical devices.

Recently, we succeeded in constructing the first transition metal acetylide based magnet $[CrCyclam(C≡C–Ph)_2]$ $[Ni(mdt)_2](H_2O)$. The crystal structure of the material is characterized by the centrosymmetric unit cell containing a pair of a cation $[CrCyclam(C≡C–Ph)_2]^+$ (S = 3/2) and an anion $[Ni(mdt)_2]^-$ (S = 1/2), and one water molecule. The cations and anions form one dimensional [3/2–1/2] ferrimagnetic chains. The inter-chain interaction between adjacent cations along the *a*-axis is mediated by the water molecules which are strongly bound to the cations by hydrogen bonds as shown in Figure 3b. Despite the centrosymmetry of the whole crystal, a water molecule can occupy only one of the two centrosymmetric sites, resulting in the local breakdown of the inversion symmetry between adjacent cations. The observed magnetic susceptibility is in good agreement with the theoretical value of the isolated [3/2–1/2] ferrimagnetic chains down to 3.8 K with the intra-chain interaction $2J/k_B = –5.7$ K. The weak inter-chain interaction through water molecules brings a magnetic phase transition at 3.7 K accompanied with a small spontaneous magnetization as shown in Figure 1d, indicating a weak-ferromagnetic ground state below the temperature. The remanent magnetization monotonically increases from 0.016 to 0.12 μ_B as the temperature decreases from 3.7 to 1.8 K, while coercive force approximately keeps a constant value of 0.8 mT in the temperature range of $2.9 < T < 3.7$ K, followed by a rapid increase below 2.9 K, suggesting the existence of the second phase transition. The existence of the second phase transition is also evidenced by the AC susceptibility, but the detail of the transition remains unclear. The weak ferromagnetism is originated from the local symmetry breakdown that allows the Dzyaloshinsky-Moriya interaction between adjacent cations despite the centrosymmetry of the whole crystal.

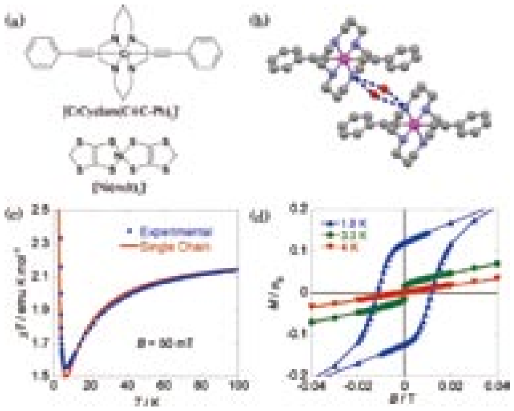

Figure 3. a) The molecular structures. b) The inter-chain interaction path along the *a*-axis mediated by a water molecule. The red spheres indicate two crystallographically equivalent positions of the water molecule, and the dashed blue lines represent the hydrogen bonds between the oxygen atom of a water molecule and the hydrogen atom of cations. c) The temperature dependence of the χT value. The red solid line indicates the theoretical value calculated by the isolated [1/2–3/2] ferrimagnetic chain model with the intra-chain interaction $2J/k_B = –5.7$ K. d) The magnetization curves measured at 1.8, 3.3 and 4 K.

References

1) K. Judai, J. Nishijo and N. Nishi, *Adv. Mater.* **18**, 2842–2846 (2006).
2) K. Judai, S. Numao, A. Furuya, J. Nishijo and N. Nishi, *J. Am. Chem. Soc.* **130**, 1142–1143 (2008).

Characterization of Magnetic Ultrathin Films by Novel Spectroscopic Methods

Department of Materials Molecular Science
Division of Electronic Structure

YOKOYAMA, Toshihiko	Professor
NAKAGAWA, Takeshi	Assistant Professor
TAKAGI, Yasumasa	Assistant Professor
YAMAMOTO, Isamu	Post-Doctoral Fellow
ISAMI, Kyohei	Graduate Student
EGUCHI, Keitaro	Graduate Student
FUNAKI, Yumiko	Secretary
NOTO, Madomi	Secretary

Novel properties of magnetic metal ultrathin films have been attractive both from fundamental interest and from technological requirements. We are interested in drastic modification of metal thin films by surface chemical treatment such as adsorption-induced spin transitions and morphological changes. The magnetic properties are characterized by means of several kinds of spectroscopic methods like MOKE (Magneto-Optical Kerr Effect) using lasers and XMCD (X-ray Magnetic Circular Dichroism) using UV-visible lasers and XMCD (X-ray Magnetic Circular Dichroism) using synchrotron radiation soft X-rays.

Moreover, we have been exploiting new techniques based on UV photoemission magnetic circular dichroism (MCD) such as ultrafast time resolved UV MCD photoelectron emission microscopy (PEEM) for spatiotemporal magnetic imaging.

1. Observation of Two-Photon Photoemission Magnetic Circular Dichroism[1)]

In 2006, we discovered surprising enhancement of the UV-visible photoemission MCD from ultrathin Ni films on Cu (001) when the photon energy was tuned to the work function threshold.[2)] Based on this discovery, we succeeded in the first observation of UV MCD PEEM images of ultrathin magnetic films.[3)] This method allows us to perform in-laboratory MCD PEEM measurements instead of the usage of third-generation synchrotron radiation XMCD PEEM. Moreover, ultrafast UV MCD PEEM images were successfully obtained by using ultrashort pulsed lasers and a pump-and-probe technique.[4)]

Laser two-photon photoemission (2PPE) MCD should be also an attractive technique, because deeper valence bands can easily be detected without using vacuum UV light. In this work, we succeeded in the observation of significant enhancement in the 2PPE MCD near the work function threshold.

Figure 1(a) shows the MCD asymmetry of 12 monolayer (ML) Ni grown on Cu(001) as a function of excitation energy. An wavelength-tunable Ti:sapphire laser (80 MHz, 2.5 W, ~70 fs, 690–1050 nm) was employed in these measurements. The 4th-order harmonics for 1PPE (one-photon photoemission, *h*ν = 5–6 eV) and the 2nd-order for 2PPE (*h*ν = 2.5–3 eV). Noticeable enhancements of both the 1PPE and 2PPE MCD asymmetries are clearly observed in the vicinity of the work function threshold (Φ = 5.15 eV). It is noted that the spectral features of the 1PPE and 2PPE MCD resemble each other and that the negative maximum (~7%) in the 2PPE MCD is strong enough to apply this phenomenon to MCD PEEM measurements.

Figure 1(b) depicts the laser incidence angle (θ) dependence of the 1PPE and 2PPE MCD asymmetries from the same sample. In the 1PPE, the function is rather constant, although the MCD asymmetry should basically be proportional to cosθ (θ corresponds to the angle between the magnetization and the light propagation direction). The deviation from the cosθ function is ascribed to the presence of the reflected light. Actually, the dashed line in Figure 1(b), which shows the calculated result using dielectric constants, agrees well with the observation. On the contrary, huge further enhancement is observed in the 2PPE at the grazing laser incidence (~45°). The negative maximum reaches as much as ~28%. Since

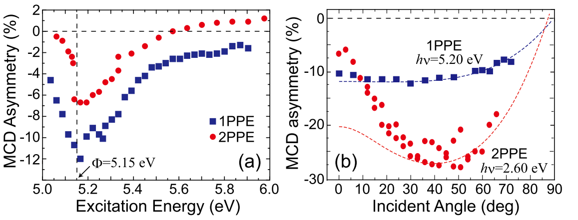

Figure 1. (a) 1PPE and 2PPE MCD asymmetries as a function of excitation energy (*h*ν and 2*h*ν for 1PPE and 2*h*ν, respectively). The sample is perpendicularly magnetized Ni(12ML)/Cu(001) at room temperature and the laser incidence angle was 0° (normal incidence). Noticeable enhancements near the work function threshold (5.15 eV) can be seen as negative maxima. (b) Incidence angle dependence of 1PPE and 2PPE MCD asymmetries. 2PPE MCD shows negative maxima at ~45° incidence. Dashed lines are the calculated results using a simple model.

PEEM experiments require grazing light incidence, the present finding is essentially important for the 2PPE MCD. The dashed line in Figure 1(b) again agrees fairly well with the observation. The calculation was done by assuming that only the first photon contributes to the MCD since the second photon excites the hot electron that is regarded as a free electron without spin-orbit coupling. Theoretical study is needed to understand the present observation in detail.

2. Structural and Magnetic Properties of Ultrathin Iron Nitride Eptaxial Films Grown on Cu(001)

Bulk iron nitrides exhibit various kinds of phases depending on the Fe/N stoichiometry, and many of the Fe-rich phases show ferromagnetism. It is interesting to investigate magnetic and structural properties of ultrathin iron nitride films. We have succeeded in the preparation of very flat ultrathin iron nitride films grown eptaxially on Cu(001) by the sequential process of depositing elemental Fe, subsequent N^+ bombardment, and annealing at ~670 K. Figures 2(a) and 2(b) show respectively the *p4gm*(2×2) LEED (low energy electron diffraction) pattern and the STM (scanning tunnel microscopy) of the 1 ML Fe_2N film. The Fe/N stoichiometry of 2:1 was verified separately by the X-ray absorption spectra (XAS) intensity. A sharp LEED pattern in Figure 2(a) and a wide terrace observed in the STM image of Figure 2(b) confirm the extreme flatness of the film. The LEED *I–V* curves were measured and analyzed to determine quantitative surface structures. The surface structure obtained is shown in Figure 2(c). The surface Fe atoms are squeezed due to embedding of the N atoms, leading to the *p4gm*(2×2) reconstructed surface.

By conducting a similar preparation procedure, a 2 ML iron nitride epitaxial film was also obtained. Interestingly, the Fe/N stoichiometry is found to be 4:1 by XAS, and the tensor LEED analysis has elucidates that the topmost layer structure is nearly identical to that of 1 ML Fe_2N, while the second layer contains only Fe, as seen in Figure 2(d). Such surface structures is found to mimic the bulk γ'-Fe_4N structure, where Fe forms *fcc* lattice with the N atom located at the center of the lattice. By neglecting the occurrence of the *p4gm*(2×2) surface reconstruction, the 1 ML Fe_2N/Cu(001) structure can be regarded as one γ'-Fe_4N layer containing N, while the 2 ML Fe_4N structure corresponds to the unit cell of γ'-Fe_4N.

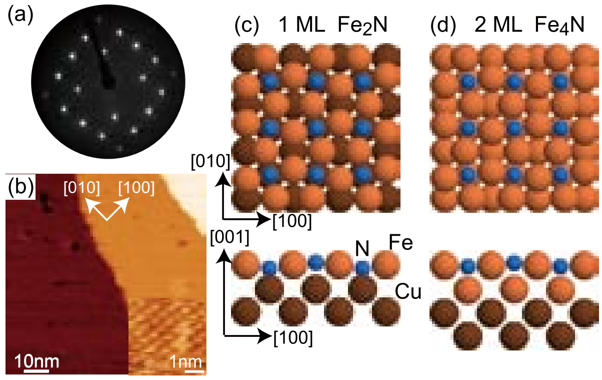

Figure 2. (a) *p4gm*(2×2) LEED pattern, (b) STM images, and (c) surface structure of the 1 ML Fe_2N film on Cu(001), and (d) that of the 2 ML Fe_4N film on Cu(001). The surface structure was determined quantitatively by the tensor LEED analysis.

Magnetic properties were investigated by XMCD using the Beamline 4B of the UVSOR-II synchrotron radiation facility in IMS and our high-field & low-temperature XMCD apparatus recently developed.[5] Figure 3(a) shows the angular dependent magnetization (*M–H*) curves of 1–4 ML iron nitride films on Cu(001). The *M–H* curves along the θ = 0° direction imply that the surface normal is a magnetically hard axis, while the grazing angle (θ = 55°) data indicates an easy axis within the film plane. The total magnetic moments $m = m_{\mathrm{spin}} + m_{\mathrm{orb}}$ and the direction dependent orbital magnetic moments m_{orb} were obtained by the XMCD sum-rule analysis. The total magnetic moment *m* [Figure 3(a)] of 1 ML is rather small possibly due to the formation of strong chemical bonds between Fe and N. It increases with the thickness and seems to approach the bulk γ'-Fe_4N value of 2.2 μ_B. The orbital magnetic moment m_{orb} [Figure 3(b)] is always larger in the in-plane (//) direction than in the perpendicular (⊥) direction. The difference between $m_{\mathrm{orb}}^{//}$ and $m_{\mathrm{orb}}^{\perp}$ is ~0.06 μ_B, which corresponds to the uniaxial magnetic anisotropy constant K_u of ~0.1 meV/atom. This implies semiquantitative agreement in the present macroscopic and microscopic observations. The large in-plane magnetic anisotropy of the present system is resulted from a large anisotropy in the spin-orbit interaction.

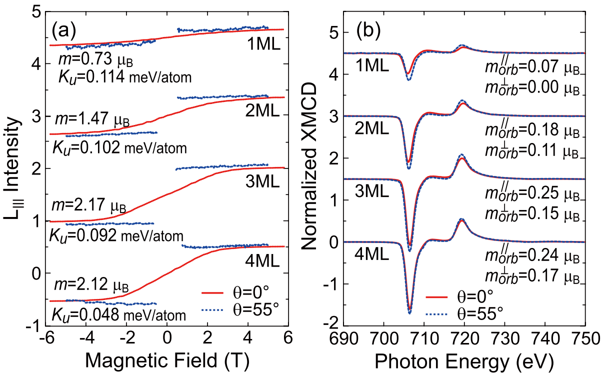

Figure 3. (a) Magnetization curves of 1–4 ML iron nitride films on Cu(001) at *T* = 5 K, recorded by the Fe L3-edge circularly polarized X-ray absorption intensity and (b) the angle dependent XMCD spectra of the same samples at *T* = 5 K and *H* = ±5 T. The X-ray incident angles θ = 0° and 55° correspond respectively to normal and grazing magnetization measurements.

References

1) T. Nakagawa, I. Yamamoto, Y. Takagi, K. Watanabe, Y. Matsumoto and T. Yokoyama, *Phys. Rev. B* **79**, 172404 (2009).
2) T. Nakagawa and T. Yokoyama, *Phys. Rev. Lett.* **96**, 237402 (2006).
3) T. Nakagawa, T. Yokoyama, M. Hosaka and M. Katoh, *Rev. Sci. Instrum.* **78**, 023907 (2007).
4) T. Nakagawa, K. Watanabe, Y. Matsumoto and T. Yokoyama, *J. Phys.: Condens. Matter* **21**, 314010 (2009).
5) T. Nakagawa, Y. Takagi, Y. Matsumoto and T. Yokoyama, *Jpn. J. Appl. Phys.* **47**, 2132 (2008).

Advanced Design and In-Situ Time-Resolved Analysis of Catalyst Surfaces

Department of Materials Molecular Science
Division of Electronic Structure

TADA, Mizuki	Associate Professor
MURATSUGU, Satoshi	Assistant Professor
NAGAMATSU, Shin-ichi	IMS Resarch Assistant Professor
YANG, Yong	Post-Doctoral Fellow
WENG, Zhihuan	Post-Doctoral Fellow
KINOSHITA, Mutsuo	Graduate Student*
MURAKAMI, Daisuke	Graduate Student*
ISHIGURO, Nozomu	Graduate Student*
KUSHIDA, Yuko	Graduate Student*
UBAHARA, Wakana	Secretary

1. Advanced Design of Catalytically Active Structures at Surfaces

Although many useful chemicals have been produced by heterogeneous solid catalysts, the molecular-level design of heterogeneous catalyst surfaces has not been established yet. On heterogeneous catalyst surfaces with the limited accessibility of reactants, rate enhancement and new catalysis can often be obtained on novel unsaturated metal structures, which are hard to be isolated in homogeneous solutions. We have succeeded in preparing novel catalytically active structures on oxide surfaces for selective catalysis by attaching techniques of some organic acid-base catalysts or metal-complex catalysts.1–6)

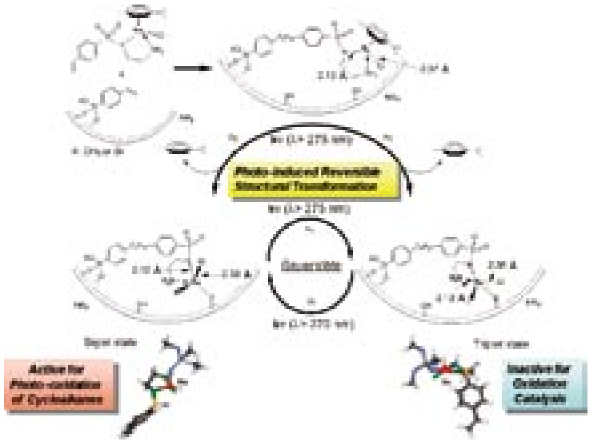

Figure 1. The step-by-step preparation and photo-induced structural transformations of novel unsaturated Ru complexes on a SiO_2 surface for the selective photo-oxidation of cycloalkanes.1)

For examples, the photo-irradiation of a Ru complex supported on a SiO_2 surface was found to promote the selective formation of two different unsaturated Ru complexes under O_2 or N_2 atmosphere, one of whose structures with an appropriate Ru–H conformation efficiently catalyzed the selective photo-oxidation of cycloalkanes with O_2. The active Ru complex immobilized at double sites on SiO_2 was prepared by the photo-induced selective elimination of a *p*-cymene ligand accompanied with dissociative coordination of a surface OH group to the unsaturated Ru center (Figure 1). The two supported Ru complexes were reversible for the structural transformation by photo-excitation with different wavelength and atmospheres.1)

2. Design of Molecular-Imprinted Metal-Complex Catalysts for Regio- and Shape-Selective Catalysis

Molecular imprinting of supported metal complex in which a specific ligand serves as a prescribed template is devoted to tailor-made design of catalyst architecture for selective integrated catalysis. A selective reaction cavity memorized the shape and coordination environment of a ligand, which is a template for molecular imprinting, can be selectively created right beside an unsaturated active metal atom on a support surface. We have designed and prepared a novel molecular-imprinted Ru-complex catalyst on a SiO_2 surface and succeeded in regulating the regio- and shape-selective epoxidation of limoene using O_2.

A molecular-imprinted Ru-complex catalyst was prepared by following step-by-step procedures: (1) the attachment of a precursor Ru complex onto a SiO_2 surface, (2) the coordination of limonene-10-ol (template), which possesses a similar shape to an intermediate of terminal C=C bond epoxidation of limonene, (3) stacking of surface SiO_2-matrix overlayers, and (4) the removal of the template ligand to create a shape-selective reaction space (cavity) on the active Ru site (Figure 2). The structures of the supported and molecular-imprinted catalysts were characterized by means of solid-state NMR, FT-IR, XRD, XRF, UV/Vis, BET, and XAFS. We found that the molecular-imprinted catalyst designed for the terminal C=C bond epoxidation of limonene exhibited fine shape selectivity discriminating a methyl group of alkene reactants and high regioselectivity for the epoxidation of the terminal C=C bond of limonene.

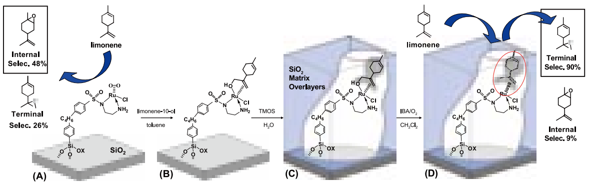

Figure 2. Design of a molecular-imprinted Ru-complex catalyst for the terminal C=C bond epoxidation of limonene.

We have also designed novel molecular-imprinted Ru catalysts for the asymmetric transfer hydrogenation of ketones. Molecular recognition sites spatially locating the imprinted matrix was designed at the molecularly imprinted catalyst surface for the first time.

3. In-Situ Time-Resolved XAFS and Raman Spectroscopy for Reaction Mechanism of Selective Alcohol Oxidation on Supported Vanadium Catalysts

Vanadium is one of the most active metals for oxidation catalysis and supported V catalysts on various oxide surfaces have been utilized for selective alcohol oxidation to aldehyde at low temperatures. Their catalytic activity and aldehyde selectivity highly depend on the structures of supported V species, however the catalytic reaction mechanism of selective alcohol oxidation has not been demonstrated yet. We have developed in-situ time-resolved energy-dispersive XAFS (DXAFS) and in-situ time-resolved Raman spectroscopy, which can monitor dynamic structural changes in active catalysts *under working conditions in real time*,7) and the structural kinetics and reaction mechanism of selective ethanol oxidation on V/SiO$_2$ and V/γ-Al$_2$O$_3$ catalysts were investigated.

Figure 3 shows a series of V K-edge DXAFS spectra recorded every 150 ms for the oxidation of ethanol on a V/γ-Al$_2$O$_3$ catalyst. The analysis of DXANES spectra revealed rate constants and activation energies for the oxidation/reduction and symmetry changes of the active V catalyst. Ethanol smoothly reacted with V^{5+} species, forming the stoichiometric amount of acetoaldehyde, and the V catalyst reduced with the rate constant of 0.19 s^{-1}. The further adsorption of ethanol varied the symmetry of the supported V species with the rate constant of 0.12 s^{-1}. When O$_2$ admitted to the reduced V catalyst, CO and CO$_2$ were obtained as major C products. The rate constants and activation energies for the V oxidation were estimated to be 1.59 s^{-1} and 52 kJ mol^{-1}, respectively. These results suggest that low acetoaldehyde selectivity on the V/γ-Al$_2$O$_3$ catalyst is caused by the oxidation process with O$_2$ on the reduced V species.

On the other hand, a SiO$_2$-supported V catalyst exhibited high acetoaldehyde selectivity and there were no significant changes in in-situ V K-edge XAFS and Raman spectroscopy. On the SiO$_2$ surface, it is suggested that the bond breaking of a V–O–Si bond forms a V–O–Et species, which selectively converts to acetoaldehyde. The in-situ time-resolved DXAFS and Raman spectroscopy revealed the relationship between the structures of supported V species and their ethanol oxidation performances, the structural kinetics of the active V catalysts, and the reaction mechanism of the ethanol oxidation catalysis for the first time.

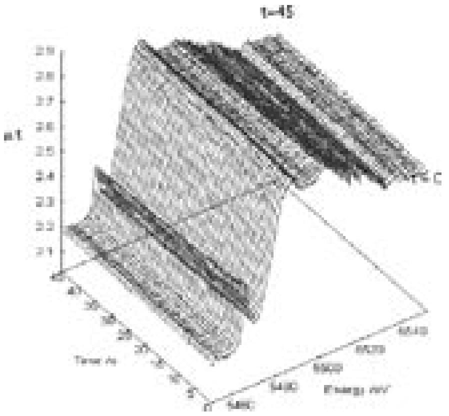

Figure 3. A series of V K-edge DXAFS spectra for the selective oxidation of ethanol on a V/γ-Al$_2$O$_3$ catalyst at 553 K. DXAFS spectra were recorded every 150 ms and presented every 900 ms.

References

1) M. Tada, Y. Akatsuka, Y. Yang, T. Sasaki, M. Kinoshita, K. Motokura and Y. Iwasawa, *Angew. Chem., Int. Ed.* **47**, 9252–9255 (2008).
2) K. Motokura, M. Tada and Y. Iwasawa, *Angew. Chem., Int. Ed.* **47**, 9230–9235 (2008).
3) T. Sasaki, M. Tada, C. Zhong, T. Kume and Y. Iwasawa, *J. Mol. Catal. A: Chem.* **279**, 200–209 (2008).
4) K. Motokura, M. Tada and Y. Iwasawa, *J. Am. Chem. Soc.* **131**, 7944–7945 (2009).
5) T. Sasaki, M. Tada and Y. Iwasawa, *Top. Catal.* **52**, 880–887 (2009).
6) M. Tada, S. Muratsugu, M. Kinoshita, T. Sasaki, Y. Yong and Y. Iwasawa, submitted.
7) M. Tada, *Surface Science (Hyomen)* **30**, 75–83 (2009).

Awards

TADA, Mizuki; The 13th JSSRR Scientific Awards.
TADA, Mizuki; The 1st Inoue Science Research Award.
TADA, Mizuki; The 11th Morita Fellowship Award.

---

* carrying out graduate research on Cooperative Education Program of IMS with The University of Tokyo

Optical Studies of Charge Ordering in Organic Conductors

Department of Materials Molecular Science
Division of Electronic Properties

YAKUSHI, Kyuya	Professor
YAMAMOTO, Kaoru	Assistant Professor
URUICHI, Mikio	Technical Associate
YUE, Yue	Graduate Student
ABE, Hitomi	Secretary

In organic conductors, kinetic energy is comparable with on-site and inter-site Coulomb energy. Due to this reason, many organic conductors are located in a boundary area between metallic and localized states, and thus various organic charge-transfer compounds show metal–insulator phase transition. Recently, charge-ordered (CO) state originated from Coulomb interaction is widely found in organic conductors, and the electronic phase diagrams of typical organic conductors are re-considered taking CO into account. The CO state attracts much attention, first because charge-mediated superconductivity is theoretically predicted in superconducting compounds neighbored on CO phase, second because some compounds in CO phase show ferroelectricity through the crystallization of conduction electrons, third because the narrow-band compounds have a poorly understood intermediate state between metallic and CO states. We have investigated the CO state and metallic state near CO employing infrared and Raman, and reflection spectroscopy.

1. Charge Order–Disorder Phase Transition in α'-(BEDT-TTF)$_2$IBr$_2$$^{1)}$

Among a variety of organic conductors, the α-type BEDT-TTF salts shows rich properties such as charge order, superconductivity, zero-gap state, persistent photoconductivity, photo-induced phase transition, and non-linear optical response. Although α'-(BEDT-TTF)$_2$IBr$_2$ is not isostructural to α-type BEDT-TTF salts, it has a herringbone molecular arrangement similar to α-type BEDT-TTF salts. This compound shows an insulator-insulator phase transition differently from convensional metal-insulator transition. According to the x-ray diffraction study, no distinct structural change was reported at phase transition temperature. We elucidated the mechanism of this phase transition.

Kinetic energy arising from hopping process is directly correlated with bandwidth. To compare the bandwidth with other α-type BEDT-TTF salts, the kinetic energy was estimated from integration of optical conductivity in the far-infrared and infrared region. It was found that the kinetic energy of α'-(BEDT-TTF)$_2$IBr$_2$ is much smaller than other α-type BEDT-TTF) salts, and therefore the bandwidth is narrowest among the α-type BEDT-TTF salts.

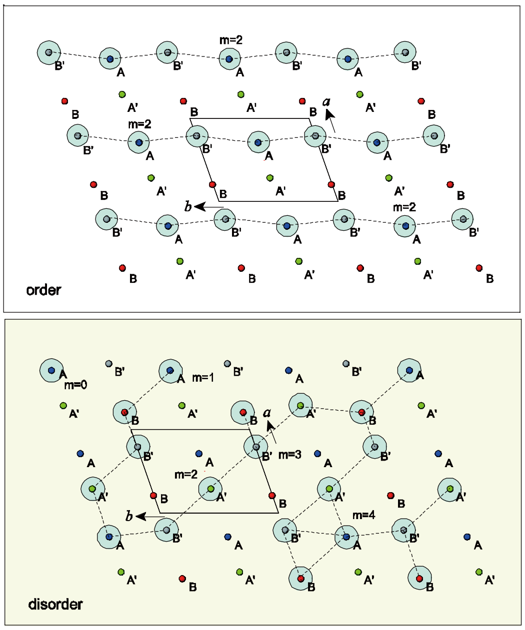

Figure 1. Snapshot of order (top) and disorder (bottom) model. The blue circles denote holes (charge-rich sites). The dashed lines denote the inter-site Coulomb interaction. In ordered state, every charge-rich site is surrouded by two charge-rich sites (m = 2), whereas in disordered state various configurations (m = 0, ..., 6).are accessible as shown in the above figures.

The investigation of infrared and Raman spectra of α'-(BEDT-TTF)$_2$IBr$_2$ with the aid of ^{13}C-substituted compound showed clear evidence that the low-temperature high-resistivity phase is a charge-ordered state. The horizontal stripe of charge order is most stable, but dislocation can be easily generated because a diagonal stripe is energetically very close to the horizontal stripe.

It was found from infrared and Raman spectra that the electrons are localized even in the high-temperature (HT) phase. In HT phase, however, inter-site hopping rate significantly increases, symmetry changes from $P1$ to $P\bar{1}$, diagnostic vibronic mode which reflects order parameter vanishes, and the density of state near Fermi energy appears. All of these observations indicate that the HT phase is a dynamically disordered state. Therefore, this insulator-to-insulator transition is regarded as an order-disorder phase transition of localized charge. This localized electronic state in the whole temperature range is ascribed to the very narrow bandwidth.

Based on this picture, we proposed a simple electronic model using point charge approximation neglecting all transfer integrals. In this model, the energy states can be calculated from the electrostatic inter-site Coulomb energy (see Figure 2). Using this model, the energy states of charge-rich sites (holes) are calculated for ordered and disordered states. The estimation of the activation energies in low-temperature and high-temperature phase, resistivity jump can be qualitatively explained. The optical gap in low-temperature phase and the increase of optical weight in the gap region in high-temperature phase also is well explained by this model. The magnetic susceptibility is also consistent with this localized model.

Hydrostaic pressure suppresses the order-disorder transition temperature down to 100 K at 1.2 GPa, above which the phase transition changes the character such as a metal-insulator transition. The Raman spectrum was measured up to 2.3 GPa at various temperatures. The Raman spectrum also changes spectral features above 1.6 GPa. The author presents a pressure-temperature phase diagram using the spectral characteristic feature and electrical resistivity. The order-disorder transition extends up to 1.3 GP, above which metal-insulator transition appears. The insulating states above 1.3 GPa is a dimer-Mott state or density-wave state.

2. Direct Observation of Ferroelectric Domains Created by the Wigner Crystallisation of Electrons in an Organic Conductor$^{2)}$

In an effort to materialize a novel class of ferroelectrics, the possibility of pure-electronic mechanisms of spontaneous polarization, draws recent attention.$^{3)}$ We have proposed in the previous study that an organic superconductor α-(BEDT-TTF)$_2$I$_3$ could be a promising candidate of a compound corresponding to the above picture.$^{4)}$ In the present study, we examined to reveal the ferroelectric domains created in the organic complex by means of second-harmonic (SH) generation interferometry.

The ferroelectric transition in the compound is driven by Wigner crystallization of valence electrons. Since the charge ordering forms a pattern which is incompatible with the centric crystal symmetry underlying the valence charges. The domains created by such a transition that breaks centric symmetry, 180° polar domains, in which different domains have opposite polarizations, should be formed.

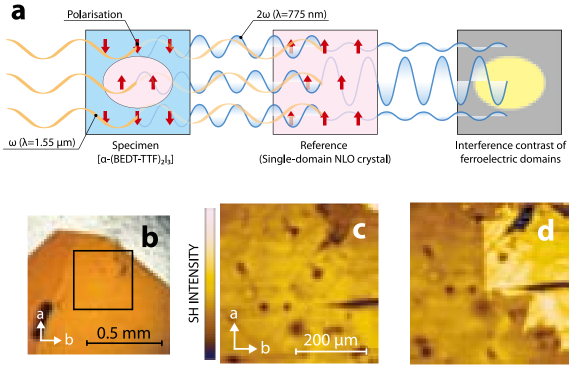

Figure 2. (a) Propagations of the excitation and SH light waves in the SH interferometry. (b) Transmission microscope image of a thin single crystal of α-(BEDT-TTF)$_2$I$_3$ used for the SH interference measurement. (c) and (d) show the SH contrast images measured from the rectangular region in (b) masured at above (140 K) and lower (50 K) temperature than the transition point (135 K), respectively.

The SH intereferometry enables us to observe 180° polar domains that cannot be observed by a conventional microscope. Figure 1(a) illustrates the trajectory of the SH light waves in the interferometry. As shown in this sketch, the phase of SH wave generated from a domain is reversed from that of different domains of opposite polarization. On the SH beam generated by the specimen, harmonic beam produced by a single-domain nonlinear-optical crystal is overlaid as reference wave. The two beams interfere constructively or destructively depending on the phase difference, resulting in the SH contrast of domain structure.

Figure 1(b) shows the microscope image of the crystal used for the domain observations. Figures 1(c) and 1(d) show the SH images observed from the rectangular region in 1(b) at above (140 K) and lower (50 K) temperature than the transition point (T_{CO} = 135 K), respectively. The SH image showed the drastic change from 1(c) to (d); the image was split into bright and dark regions representing the formation of polar domains.

The growth of macroscopic domains manifests that the polar state forms as a stable bulk phase in the complex, materializing the feasibility of the electronic mechanism of ferroelectric polarization. The visualization of domain structures is important as the first step for understanding the nature of the ferroelectric compounds. Furthermore, the ability of discerning different polarizations can be utilized as a means of non-destructive readout of information in memory applications of the compound.

References

1) Y. Yue, *et al.*, *J. Phys. Soc. Jpn.* **78**, 044701 (2009).

2) K. Yamamoto *et al.*, submitted.

3) N. Ikeda, *et al.*, *Nature* **436**, 1136 (2005).

4) K. Yamamoto, *et al.*, *J. Phys. Soc. Jpn.* **77**, 074709 (2008).

Magnetic Resonance Studies for Molecular-Based Conductors

Department of Materials Molecular Science
Division of Electronic Properties

NAKAMURA, Toshikazu	Associate Professor
FURUKAWA, Ko	Assistant Professor
IWASE, Fumitatsu	IMS Fellow
SUGIURA, Koichi	Graduate Student
ABE, Hitomi	Secretary

Magnetic resonance measurements are advantageous for studying fundamental electronic properties and for understanding the detailed electronic structures of molecular based compounds. Developing an understanding of the electronic phases and functionality of these materials enables us to perform systematic investigations of low-dimensional, highly-correlated electron systems and functional materials. Competition between the electronic phases in molecular-based conductors has attracted much attention.[1)] The investigations of such electronic phases by magnetic resonance measurements are important to understanding unsolved fundamental problems in the field of solid state physics, and to explore novel functionalities in the field of material science.

In this study, we performed broad-line NMR and ESR measurements on molecular-based conductors to understand electron spin dynamics and functionality in low-temperature electronic phases.

1. ^{13}C NMR Study of the Chemical Pressure Effect in $(TMTTF)_2[(AsF_6)_x(SbF_6)_{1-x}]$ (x ~ 0.5)

^{13}C NMR measurements of $(TMTTF)_2[(AsF_6)_x(SbF_6)_{1-x}]$ (x ~ 0.5) alloy were performed in order to understand the chemical pressure effect and the electronic state at low temperatures. The charge-ordering transition temperature is the intermediate value between those of SbF_6 and AsF_6 salts. The broadening of NMR spectra and the weak temperature dependence of the spin-lattice relaxation rate at low temperatures indicate that this salt is situated in the vicinity of the phase boundary between the spin-Peierls and antiferromagnetic phases.

2. ^{13}C NMR Investigation of Low-Temperature States in One-Dimensional Organic Cation Radical Salt, $(TMTTF)_2SbF_6$, under High Pressures

^{13}C nuclear magnetic resonance (NMR) measurements under the application of hydrostatic pressure were carried out on the one-dimensional organic conductor, $(TMTTF)_2SbF_6$, to investigate the competed antiferromagnetic and spin-singlet ground states. The charge-ordering (CO) transition temperature, T_{CO}, (155 K at ambient pressure), decreased to 100 K under a pressure of 5 kbar, and was suppressed above 8 kbar. Under pressures between 5 kbar and 14 kbar, the low-pressure side antiferromagnetic state (AF-I) was suppressed. At the same time, a spin-gap phase was stabilized. Above 17 kbar, another antiferromagnetic phase appeared below approximately 15~20 K. A possible reentrant antiferromagnetic phase diagram is discussed from a microscopic point-of-view.

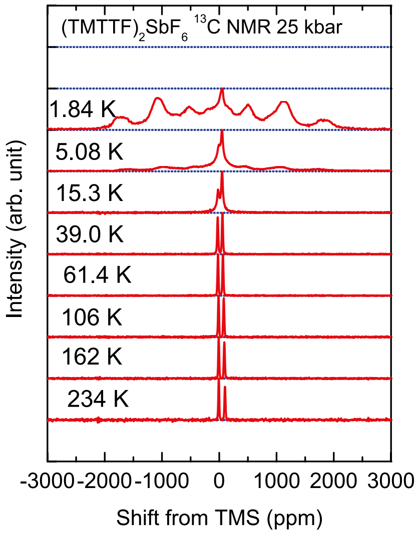

Figure 1. Temperature dependence of the ^{13}C NMR spectra of $(TMTTF)_2SbF_6$ under a pressure of 25 kbar.

3. Anomalous Temperature Dependence of g-Tensor in Organic Conductor, $(TMTTF)_2X$ (X = Br, PF_6 and SbF_6)

The magnetic properties of organic conductor $(TMTTF)_2X$ (X = Br, PF_6 and SbF_6), where TMTTF is tetramethyltetrathiafulvalene, were examined by electron spin resonance (ESR) spectroscopy, X-ray diffraction (XRD) of the single crystals, and quantum-chemical calculation of the *g*-tensor. In the case of salts with bulky counter anions such as the PF_6 and SbF_6, an anomalous temperature dependence of the *g*-tensor was observed in the temperature range from 20 K to 296 K. This anomalous behavior of the *g*-tensor signifies the rotation of the principal axes as well as the shift of the principal values. The *g*-tensor of the Br salt is, however, temperature independent. No remarkable change in the intra-molecular structure as a function of temperature was observed for all salts. On the other hand, the distance between TMTTF and counter-anion molecules obviously decreases as the temperature decreases for the PF_6 and the SbF_6 salts, while thermal contraction is not remarkable for the Br salt. In order to clarify the origin of the anomalous behavior of the *g*-tensor, we investigated the possibility of deformation of the wave-function by the counter-anion potentials using a quantum-chemical calculation for the actual crystal structures measured at low-temperatures. In this paper, we describe the first direct observation of the deformation of the frontier orbital by the counter anion potential for organic conductors. The intra-molecular spin-distribution as a function of temperature also is discussed from the microscopic point of view.

4. Spin-Dynamics in Vicinity of Phase Transition for Organic Conductor $(TMTTF)_2X$

$(TMTTF)_2PF_6$ shows unique electronic state with a charge ordering phase above the ground state. The spin dynamics in the vicinity of the spin-Peierls transition for the $(TMTTF)_2PF_6$ were examined and compared with those for the typical spin-Peierls materials, MEM(TCNQ)$_2$. The temperature dependence of the electron-spin relaxation rate, T_1^{-1} and T_2^{-1}, in the vicinity of the spin-Peierls transition was measured by pulsed-ESR spectroscopy. The FID signal was successfully detected and the relaxation rate for the condensed matter could be estimated. In the typical spin-Peierls system, MEM(TCNQ)$_2$, decrease of the spin-lattice relaxation and increase of the spin-spin relaxation were observed below the T_{sP}. On the other hand, an anomaly of the spin-spin relaxation rate was observed for the $(TMTTF)_2PF_6$ below the T_{sP}, which suggests the re-orientation of the charge. This behavior is not shown in typical spin-Peierls materials, and is peculiar to the spin dynamics of spin-Peierls materials with a charge ordering phase. This result is the first example of direct experimental estimation of the electron spin dynamics of the spin-Peierls transition.

5. ESR Investigation for Competed Electronic Phases in $(TMTTF)_2X$

A Quasi-one-dimensional conductors based on TMT*C*F (*C* = S, Se) are some of the most extensively studied materials among organic conductors. They possess various ground states including the spin-Peierls (sP), antiferromagnetic state (AF), incommensurate spin density wave (IC-SDW) and superconductivity (SC), with applied pressures or counter anions, *X*. Findings of charge-ordering (CO) and related phenomena in $(TMTTF)_2X$ have attracted significant recent attention. We have also investigated the completed ground states and CO phenomena observed in the intermediated temperature region from the viewpoint of magnetic resonance.

Based on recent systematic transport measurements for $(TMTTF)_2X$ salts under ultra-high pressures, a possible modified generalized Pressure-Temperature phase diagram was proposed. However, this phase diagram is based on the preconceived idea that the spin-gap (spin-Peierls) phase, which is a quantum one-dimensional phase, is sandwiched between two antiferromagnetic phases. In a general sense, for conventional systems, antiferromagnetic phases are stabilized with finite inter-chain interactions with the application of pressure.

Therefore, in order to understand the whole phase diagram of the TMT*C*F-family salts, we prepared several TMTTF-family salts, such as $(TMTTF)_2TaF_6$ and $(TMTTF)_2I$, and carried out ESR measurements. Both salts undergo antiferromagnetic states, but the temperature dependences of the ESR properties are quite different. We discussed the competed electronic phases in $(TMTTF)_2X$ from a view of microscopic.

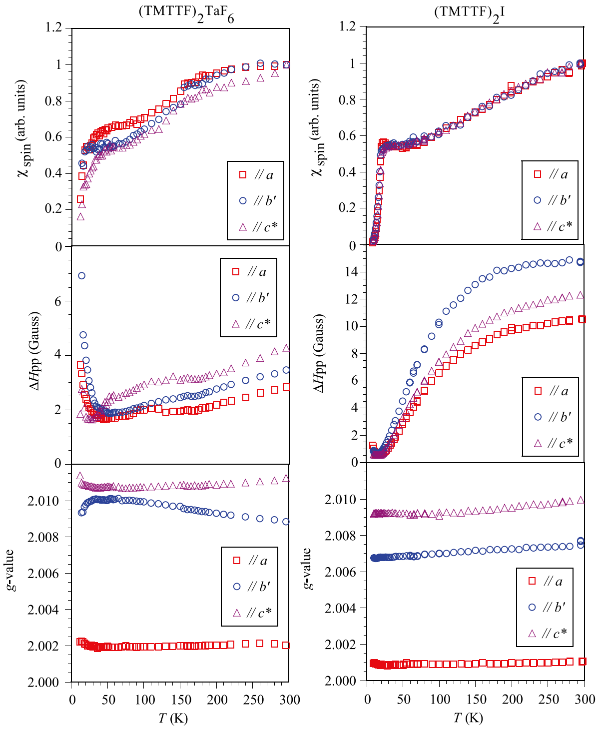

Figure 2. Temperature dependence of the ESR parameters, χ_{spin}, ΔH_{pp} and *g*-values, for $(TMTTF)_2TaF_6$ and $(TMTTF)_2I$.

References

1) F. Iwase, K. Sugiura, K. Furukawa and T. Nakamura, *J. Phys.: Conf. Series* **132**, 012015 (4 pages) (2008).

2) T. Nakamura, F. Iwase, H. Satsukawa, K. Furukawa and T. Takahashi, *J. Phys.: Conf. Series* **150**, 042137 (4 pages) (2009).

3) K. Furukawa, T. Hara and T. Nakamura, *J. Phys. Soc. Jpn.* **78**, 104713 (6 pages) (2009).

4) F. Iwase, K. Furukawa and T. Nakamura, *J. Phys.: Conf. Series* in press.

Topological Design of Sheet-Shaped Macromolecules and Organic Framewarks

Department of Materials Molecular Science
Division of Molecular Functions

JIANG, Donglin	Associate Professor
ISHIZUKA, Tomoya	Assistant Professor
GUO, Jia	JSPS Post-Doctral Fellow
KOU, Yan	Post-Doctoral Fellow
MAITARAD, Phornphimon	Post-Doctoral Fellow
CHENG, Sit-Feng	Post-Doctoral Fellow
WAN, Shun	Graduate Student
CHEN, Long	Graduate Student
ODA, Masafumi	Graduate Student
YUSA, Masaaki	Graduate Student
FENG, Xiao	Graduate Student*
ISONO, Yukiko	Technical Fellow
SUZUKI, Hiroko	Secretary

Covalent organic frameworks (COFs) are porous and crystalline materials with pre-designable 2D and 3D polymer structures. Due to covalent linkage between components together with an elaborate control on structure parameters including porosity and composition, COFs are promising for the design of tailor-made porous materials for gas storages. Recently, co-condensation of triphenylene and pyrene monomers has been reported, to create a π-electronic COF that is semiconducting (TP-COF). The well-defined crystalline structure of COFs would have a high probability of forming conduction path that transports charge carriers across the framework. Inspired by this finding, we are interested in the synthesis of photofunctional COFs, especially photoconductive COF that requires photoinduced carrier generation and carrier transportation in the framework. Crystal engineering has demonstrated that high quality single crystals of certain π-conjugated arenes are photoconductive as the result of exciton migration over lattice followed by charge separation at molecule-electrode interface. To fulfill this prerequisite, we turned to the exploration of arene-based COF, which should retain crystal-lattice-like highly ordered arene arrangement, can absorb photons of visible region, and is robust under irradiation. Herein, we report the first example of photoconductive COF, bearing eclipsed molecular order of arene building blocks in the framework (Figure 1, PPy-COF).

1. Toward Photoconductive Sheet-Shaped Macromolecules and COFs

We employed self-condensation of pyrene diboronic acid (Figure 1a, PDBA) for polymerization that would topologically integrate pyrene unit on edges and boronic ester ring at vertices (Figure 1), to assume uniform and single aromatic component of the framework. We found that under solvothermal condition it successfully leads to the desirable eclipsed alignment of 2D polypyrene sheets in the micrometer-scale cubes (Figure 1b). Such an ultimately superimposed stack together with uniform composition in sheet structure significantly facilitates exciton migration and carrier transportation. We highlight that PPy-COF harvests visible light and triggers photocurrent generation with a quick response to visible light irradiation, allows

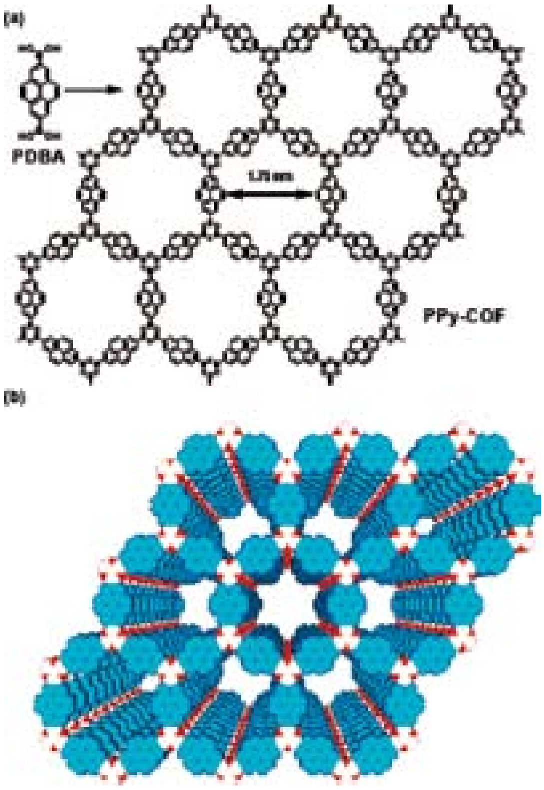

Figure 1. Schematic representations of (a) the synthesis and (b) the framework of PPy-COF (Structure is based on quantum calculation and crystal lattice parameters; Red: B, White: O, Blue: Pyrene; H atoms are omitted for clarity).

repetitive switching of photocurrent without deterioration, and displays a large on-off ratio over 8.0×10^4.

FE SEM shows that PPy-COF adopts cubic shape, while no any other morphologies such as belt, fiber, sphere, or rod are present. Close checks at high magnification confirm that the cubes are in micrometer scale with similar dimension. HR TEM reveals the aligned 2D polymer sheets with face-to-face distance of about 3.4 Å, which is reasonable for π-π stack. These observations indicate that self-condensation of PDBA leads to the formation of quite uniform cube-shaped COF with well-aligned polypyrene sheets.

To fully understand the structure of PPy-COF, we carried out PXRD analysis, quantum simulation and gas sorption experiments. PXRD measurement of PPy-COF displays a main peak at 4.6° due to 100 diffraction together with minor peaks at 9.3, 12.2 and 26.2° due to 200, 210, 001 diffractions, respectively. To elucidate the lattice packing, we first carried out quantum chemical calculation with Gaussian 03. Rev. C01 at PM3 level to optimize the geometry of pore unit structure and then performed molecular modeling and Pawley refinement by using Reflex, a software package for crystal structure determination from the PXRD pattern, implemented in Materials Studio modeling version 4.2. Simulation using $P6/mmm$ space group with $a = b = 22.16295$ Å and $c = 3.42066$ Å results in a PXRD pattern that is in good agreement with the experimentally observed one. Therefore, the 2D polypyrene sheets stack along c axis in a perfectly eclipsed fashion, with all vertices and edges superimposed on those from neighbouring sheet, thus leaving aligned tubular channels with a pore diameter of 1.73 nm. Gas sorption measurement with N_2 at 77 K displays typical type-I sorption profile, suggesting a microporous character. The BET surface area was evaluated to be 923 m^2g^{-1} and the pore width was 1.88 nm calculated by NLDFT method. These results indicate that PPy-COF is supermicroporous crystalline macromolecule with eclipsed alignment of polypyrene sheets.

Upon excitation at 414 nm, PPy-COF emits at 484 nm. In contrast, the simple solid of PDBA gives an emission at 421 nm. Therefore, the fluorescence of PPy-COF most likely originates from excimer, as a result of close packing of pyrene building blocks. Along this line, we further investigated the fluorescence anisotropy upon excitation with a polarized light. When a chromophore with a restricted Brownian motion is excited by a polarized light, it emits a polarized fluorescence. However, the fluorescence should be depolarized when the excitation energy migrates within the lifetime of the excited state. PDBA shows an anisotropy (p) value of 0.020. In contrast, PPy-COF under identical conditions exhibited a significantly depolarized fluorescence with an extremely low p value of 0.001. This value is much smaller than that of previously reported TP-COF (0.017). Unlike TP-COF that contains two alternatively linked components with difference in energy gaps, the exciton migration in the single component PPy-COF is facilitated, since it can flow “borderlessly” not only over the sheet plane but across the stacked layers as well.

The well-defined sheet structure together with superimposed layer alignment of PPy-COF would also benefit the flow of carriers. To verify this, we measured the electrical conductivity by using a two-probe method across a 10-µm-width Pt gap. PPy-COF displays an almost linear *I–V* profile in air at 25 °C, while the gap itself is silent, irrespective of voltage bias. In contrast, PDBA shows a low current under otherwise identical conditions. The electric current of PPy-COF can be on–off switched for many times. The relatively high electrical conductivity is clearly resulted from the highly aligned molecular order. Upon doping with iodine to induce hole generation, the electric current increased, suggesting that PPy-COF is a hole transporting material.

We investigated the photoconductivity of PPy-COF by casting a thin film of PPy-COF on Al electrode and vapor depositing 30-nm thick Au on the top of the film to fabricate sandwich-type electrodes. Indeed, on irradiation from Au side with visible light (> 400 nm) of a xenon lamp, PPy-COF is highly responsive and shows sharp rise in photocurrent generation to give a linear *I–V* profile. Moreover, the photocurrent can be repetitively switched for many times without deterioration at an on-off ratio over 8.0×10^4. Such a quick response together with a large on-off ratio is most likely related to the facilitated exciton migration and carrier transportation in PPy-COF. In sharp contrast, PDBA hardly shows response to light irradiation under otherwise identical conditions. On the other hand, TP-COF consisting of co-condensed triphenylene and pyrene network shows a low photocurrent with significantly decreased on-off ratio, which is only one-forth that of PPy-COF. Although 1,4-benzene diboronic acid forms a crystalline COF, which, however, eventually adopts staggered structure and hardly absorbs any photons in the visible region.

In summary, we demonstrate the first example of photoconductive COF, newly synthesized by self-condensation of pyrene diboronic acid under solvothermal condition. The ultimate alignment of 2D polypyrene sheets in perfectly eclipsed fashion leads to the formation of micrometer-scale cubes that favor exciton migration and carrier flow over the framework. PPy-COF harvests visible photons and triggers prominent photocurrent generation, displays quick response to light irradiation, and is capable of repetitive on–off photocurrent switching with large on–off ratio. These unique properties are unprecedented and thus constitute an important step to the utility of COFs in optoelectronics and photovoltaics.

Reference

1) S. Wan, J. Guo, J. Kim, H. Ihee and D. Jiang, *Angew. Chem., Int. Ed.* **48**, 5439–5442 (2009).
2) L. Chen, L. Wang, X. Guo, S. Nagase, Y. Honsho, A. Saeki, S. Seki and D. Jiang, *Chem. Commun.* 3119–3121 (2009).
3) L. Chen, J. Kim, T. Ishizuka, Y. Honsho, A. Saeki, S. Seki, H. Ihee and D. Jiang, *J. Am. Chem. Soc.* **131**, 7287–7292 (2009).

---

* from Beijing Institute of Technology

Developments of New Techniques and Magnetically Aligned Lipid Bilayer System for Structural Biology Based on Solid State NMR Spectroscopy

Department of Materials Molecular Science
Division of Molecular Functions

NISHIMURA, Katsuyuki	Associate Professor
IIJIMA, Takahiro	Assistant Professor
UEKAMA, Naoko	IMS Fellow

Solid state NMR is one of the useful tools to characterize dynamics and structures of molecules on amorphous condition without specific limitations. We are working on methodology developments of solid state NMR for structural biology and material science. Especially, we are focusing on elucidation of functions and dynamic structure of peripheral membrane protein bound to lipid bilayer surface based on solid state NMR. In the following, we show the newly developed solid state NMR techniques to enhance spectral sensitivity for aligned sample, and new lipid sample system enabling magnetically aligned planer lipid bilayers useful for structural characterization of peripheral membrane proteins. In addition, a study of molybdenum compounds was reported.

1. ^{1}H-^{13}C Heteronuclear Polarization Transfer for Aligned Solid1)

Analysis of anisotropic interactions such as dipolar interaction and chemicals shift anisotropy in aligned sample give information of local molecular structure straightforwardly. Thus membrane proteins embedded in magnetically aligned lipid bilayer samples have been studied so far. In such experiment, heteronuclear polarization transfer from ^{1}H to rare nuclei such as ^{13}C and ^{15}N plays important role to enhance spectral sensitivities of rare nuclei. Recently, Jayanthi et al developed DAPT which is the INEPT type dipolar based heteronuclear polarization transfer technique to be used in aligned sample. However due to the lack of refocusing mechanism of ^{1}H carrier frequency offset in DAPT, performance of DAPT is quite poor.

In this study, we show improved version of DAPT, which is insensitive to ^{1}H carrier frequency offset. We refer developed technique to as refocused DAPT (REDAPT), which refocuses ^{1}H carrier frequency offset based on refocused multiple pulse technique which author developed. The performance of REDAPT was assessed using liquid crystalline molecule of 5CB as shown in Figure 1 (a). The practically obtained polarization transfer profile was shown in Figure 1 (b). Because of refocusing of ^{1}H carrier frequency offset in REDAPT, signal intensities were gradually decreased respect to the ^{1}H carrier frequency offset.

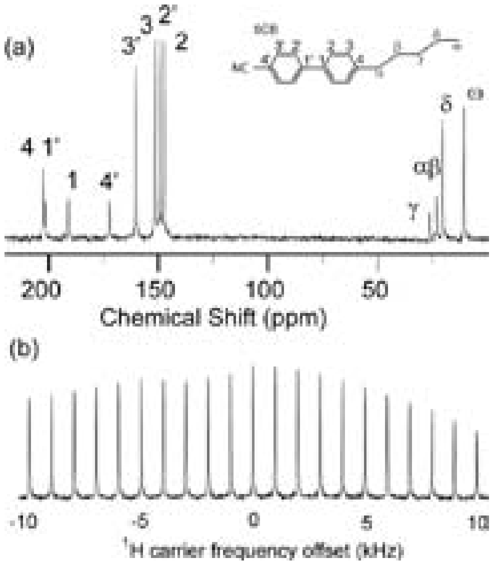

Figure 1. (a) REDAPT enhanced ^{13}C-NMR spectrum of 5CB liquid crystal at 20 °C. Plot of site 3 signals in 5CB obtained from REDAPT at mixing time of 264 μs for various ^{1}H carrier frequency offsets.

2. A Bicelle Magnetically Aligned Planner Lipid Bilayers at Room Temperature for Structural Characterization of Membrane Bound Proteins by Solid State NMR2)

The properly hydrated mixture of saturated lipids possessing short and long acyl-chains at proper composition forms planer lipid bilayer so called bicelle which can be magnetically aligned under static magnetic field at temperature from 30 to 40 °C. Bicelle is widely used in solid state NMR for structural characterization of membrane associated proteins. Triba *et al.*, proposed a bicelle prepared by mixture of saturated lipid 1,2-dimyristoyl-sn-glycero-3-phosphocholine (DMPC) and unsaturated lipid 1-palmitoyl-2-oleoyl-sn-glycero-3-phosphocholine (POPC) for long acyl chain, and 1,2-dihexanoyl-sn-glycero-3-phosphocholine (DHPC) for short acyl chain lipid, respectively in order to achieve magnetic alignment at temperature lower than that of conventional bicelle. In the following we refer above bicelle to as POPC/DMPC/DHPC-bicelle.

In this study, we developed a new bicelle enabling better magnetic alignment at room temperature over POPC/DMPC/DHPC-bicelle. Our developed bicelle consists of phosphatidylinositol 4, 5-bisphosphate (PIP_2) in addition to above lipids at proper molar ratio. Orientational property of developed bicelle was compared to those for POPC/DMPC/DHPC-bicelle based on ^{31}P-NMR. As shown in Figure 2, (b) newly developed bicelle exhibited better magnetic alignment over (c) POPC/DMPC/DHPC-bicelle. Furthermore, temperature range for magnetic alignment for developed bicelle was twice wider than that of POPC/DMPC/DHPC-bicelle. We have successfully developed new bicelle magnetically aligned at room temperature stably. New bicelle may be useful especially for structural characterization of membrane proteins which are sensitive to fluctuation depending on the sample temperature such as peripheral membrane proteins.

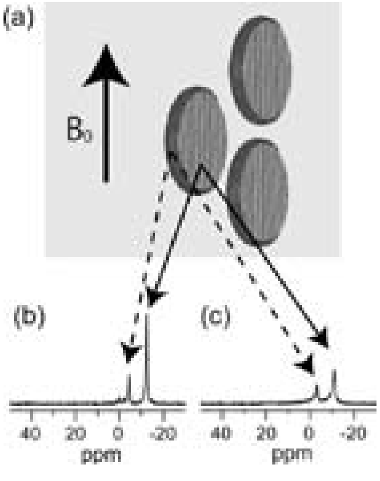

Figure 2. (a) Schematic representation of bicelle. Dark and light gray colored areas indicate polar heads of short and long acyl chain lipids, respectively. (b) ^{31}P-NMR spectra of magnetically aligned POPC/ DMPC/ PIP_2/DHPC-bicelle and (c) POPC/ DMPC/ PIP_2/DHPC-bicelle at 16 °C , respectively.

3. ^{95}Mo NMR of Mixed Valence Polyoxomolybdates (V, VI)[3]

Solid state NMR of half integer quadrupole nuclei benefits from recent development of high field magnets for high-resolution NMR, because a higher field brings higher sensitivity and resolution by decrease in second-order quadrupole coupling and increase in equilibrium magnetization. Structural researches utilizing high-field NMR for quadrupolar nuclei such as ^{95}Mo have been recently reported. Studies of ^{95}Mo NMR can be classified by the oxidation number of molybdenum taking from Mo^0 to Mo^{VI}. While solution ^{95}Mo NMR has accessed all species with the integer oxidation number, ^{95}Mo solid state NMR studies are limited to Mo^0, Mo^{IV} and Mo^{VI}. Although the Mo^V or $Mo^{V,VI}$ species frequently appear in polyoxomolybdates such as ε-Keggin anion and nanosized oxides with ring-, tube- and ball-structure, only several ^{95}Mo solution NMR spectra have been measured for Mo^V. In this study, we investigated high-field solid-state ^{95}Mo NMR of Mo^V, $Mo^{V,VI}$ and Mo^{VI} species in mixed valence polyoxomolybdates(V, VI).

Compounds used here are $[Me_3NH]_6[H_2Mo^V{}_{12}O_{28}(OH)_{12}(Mo^{VI}O_3)_4]2H_2O$ (**1**) and $[NMe_4]_2[NH_4]_8[(Mo^{VI}{}_6Mo^VO_{23})_2]8H_2O$ (**2**) which have localized or delocalized d^1 electrons, respectively. As show in Figure 3, ^{95}Mo MAS NMR spectra were measured under moderate (9.4 T) and ultrahigh magnetic fields (21.8 T). By simulating the acquired NMR spectra and density functional theory (DFT) calculation for isolated anions, NMR parameters for each of molybdenum sites within the crystals were obtained. Despite different state of the d^1 electrons, a similar trend that exhibits large chemical shifts for Mo^V in **1** and $Mo^{V,VI}$ in **2** was found. Highest-energy occupied molecular orbital(s) of the anions was mainly consisting of 4d atomic orbitals of Mo^V or $Mo^{V,VI}$. Then the large shift was ascribed to a paramagnetic deshielding term by magnetic-dipole allowed mixing of the occupied and virtual orbitals containing the 4d orbitals of these species.

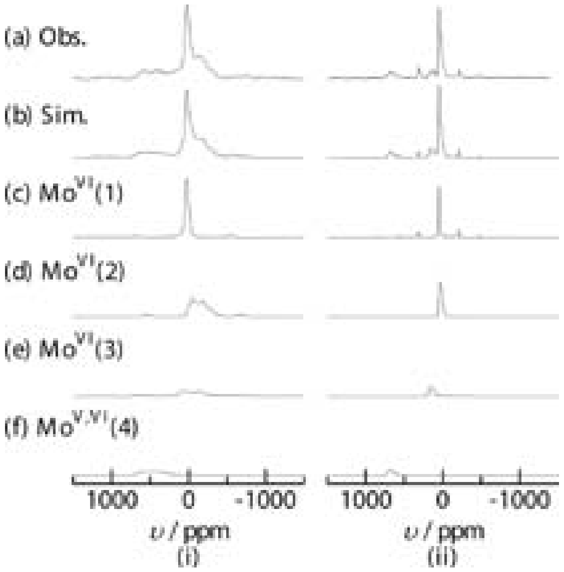

Figure 3. ^{95}Mo MAS NMR spectra of $[NMe_4]_2[NH_4]_8[(Mo^{VI}{}_6Mo^VO_{23})_2]8H_2O$ under (i) 9.4 and (ii) 21.8 T. (a) and (b) show the observed and simulated spectra, respectively. (c–f) denote spectral components consisting of the spectrum (b).

References

1) To be submitted.
2) To be submitted.
3) To be submitted.

Organic Solar Cells

Research Center for Molecular Scale Nanoscience
Division of Molecular Nanoscience

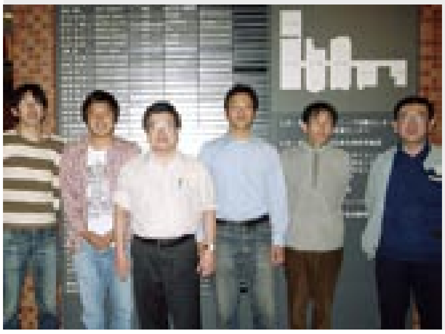

HIRAMOTO, Masahiro	Professor
KAJI, Toshihiko	Assistant Professor
IKETAKI, Kai	IMS Fellow
NAKAO, Satoru	Post-Doctoral Fellow
NAKAYAMA, Takahiro	Post-Doctoral Fellow*
KITADA, Keitaro	Graduate Student†
AULSIRISAWAD, Nithi	Graduate Student‡
ANNEN, Sayuri	Secretary

Organic solar cell is recognized as a future 3rd generation solar cell. Our group accomplished the world record conversion efficiency of 5.3% by ultra-high purification and nanostructure design.[1,2] Moreover, a new organic solar cell having the sensitivity of near-infrared (NIR) region to 1050 nm like Si cell is successfully fabricated.

1. Efficient Organic *p-i-n* Solar Cells Having NIR Sensitivity by Using J-Aggregate of Pb Phthalocyanine

In 1991, we proposed *p-i-n* organic solar cells in which the *i*-interlayer is a codeposited film composed of *p*- and *n*-type organic semiconductors.[3,4] *i*-interlayer acts as an efficient photocarrier generation layer.

Unfortunately, organic solar cells did not have sensitivity to near infrared (NIR) so far. Since there is a lot of NIR photon in the solar spectrum, they should be utilized in order to obtain photocurrent density reaching 30 mA/cm^2 like Si solar cells.

In order to solve this problem, we incorporated Pb phthalocyanine (PbPc) having shuttle-cock type molecular structure in *p-i-n* cell (Figure 1). *p*-type layer of ZnPc, codeposited *i*-interlayer composed of C_{60} and PbPc, and *n*-type layer of C_{60} were successively deposited by vacuum evaporation on ITO glass substrate.

Figure 2(a) shows the spectral dependence external quantum efficiency (EQE) of short-circuit photocurrent. The present cell showed the NIR sensitivity to 1050 nm. Maximum EQE reached 43%, which is the largest value of NIR sensitivity observed so far. Conversion efficiency by NIR light irradiation reached 2.3% (Figure 2(b)).

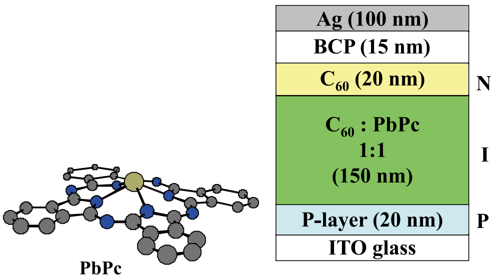

Figure 1. Structure of organic *p-i-n* cell incorporating PbPc:C_{60} *i*-interlayer.

Codeposited *i*-interlayer was revealed to have nanostructure composed of 3 phases, *i.e.*, amorphous C_{60}, H-aggregate of PbPc, and J-aggregate of PbPc (Figure 3). This nanostructure has the efficient carrier generation ability due to 3-separated functions, *i.e.*, electron transport, hole transport, and photocarrier generation by NIR, respectively.

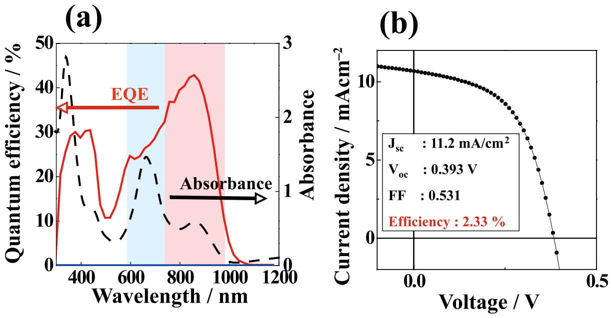

Figure 2. (a) Spectral dependence external quantum efficiency of short-circuit photocurrent. Absorption spectrum of PbPc:C_{60} *i*-interlayer is also shown. Absorption peaks at 650 nm and 860 nm are attributed to H- and J-aggregates of PbPc. (b) Photourrent-voltage characteristic for *p-i-n* cell.

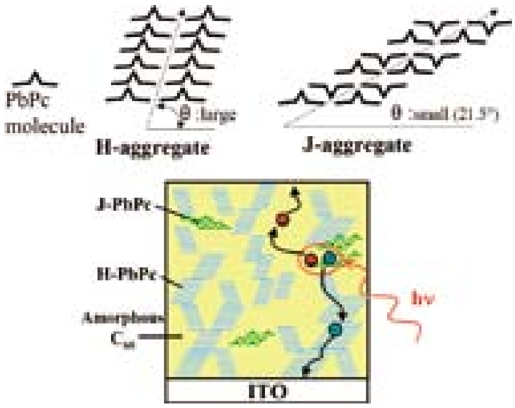

Figure 3. 3-function separated nanostructure consists of amorphous C_{60}, H-PbPc, and J-PbPc, which act as electron transport, hole transport, and photocarrier generation by NIR, respectively. Molecular stackings of H- and J-aggregates are also shown.

2. Hole-Transport Highway in Phthalocyanine:C_{60} *i*-interlayer Showing Conversion Efficiency of 5.3%

Our group accomplished the world record conversion efficiency of 5.3% by *p*-*i*-*n* cell having *i*-interlayer composed of metal-free phthalocyanine (H_2Pc) and seven-nine (7N, 99.99999%) purified C_{60} (Figure 4).[1,2] Utilization of entire visible light of solar spectrum without decreasing fill factor by incorporating 1 μm-thick C_{60}:H_2Pc *i*-interlayer is essential to obtain large J_{sc} value of 20 $mAcm^{-2}$ and efficiency of 5.3%.

Figure 5 shows the TEM image of 1 μm-thick H_2Pc:C_{60} codeposited *i*-interlayer. H_2Pc whisker structures having diameter of around 20 nm were clearly observed. Carrier is photogenerated at H_2Pc whisker/C_{60} interface and photogenerated holes are efficiently transported *via* this H_2Pc whisker to electrode. This observation suggests that H_2Pc hole-transport highway is formed in H_2Pc:C_{60} *i*-interlayer.

We also investigated the nanostructure of 1 μm-thick ZnPc:C_{60} *i*-interlayer which showed essentially the same results to H_2Pc:C_{60} system. Figure 6 shows the schematic illustration of a ZnPc nanocrystal (a) and nanocrystals-connected nanostructure clarified by cross sectional SEM and XRD observations. (i) ZnPc nanocrystals having diameter of around 20 nm surrounded by amorphous C_{60} (Figure 6(a)). (ii) ZnPc:C_{60} thickness < 300 nm; π-stacking direction is parallel to the substrate electrode (Figure 6(a)(b)). (iii) 300 nm < ZnPc:C_{60} thickness < 1 μm; π-stacking direction is changed to be vertical to the electrodes (Figure 6(b)). Since photogenerated holes are transported *via* π-stacking, the present observation suggests the formation of hole-transport highway between two metal electrodes. Note that the H_2Pc whisker structure in Figure 5 resembles to this hole-transport highway. Formation of such hole-transport highway is one of the reasons of 5.3% high efficiency of *p*-*i*-*n* cells.

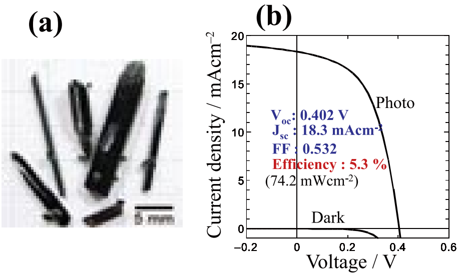

Figure 4. (a) Photograph of 7N(99.99999%)-C_{60} single crystals. (b) Current-voltage characteristics for *p*-*i*-*n* cell having 1 μm-thick H_2Pc:C_{60} *i*-interlayer.

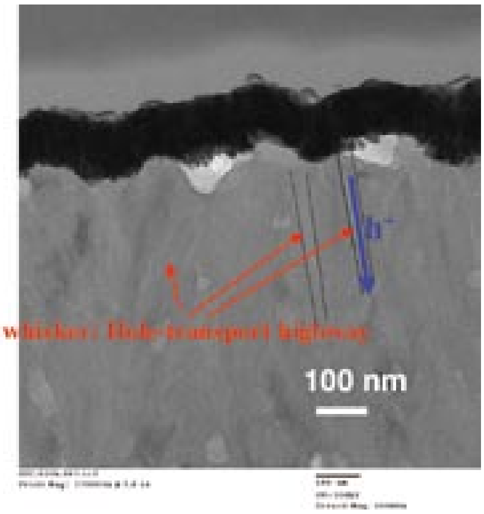

Figure 5. TEM image of 1 μm-thick H_2Pc:C_{60} codeposited *i*-interlayer.

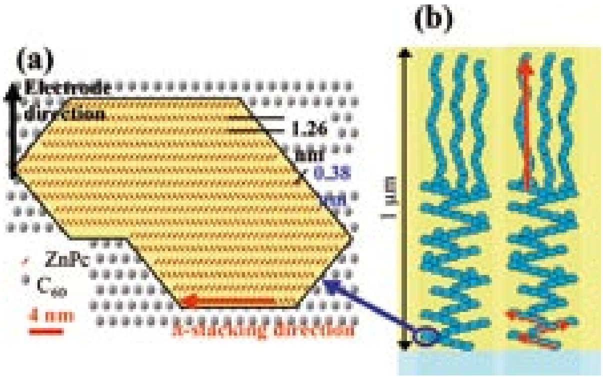

Figure 6. (a) Schematic illustration of a ZnPc nanocrystal surrounded by C_{60}. (b) Schematic illustration of 1 μm-thick ZnPc:C_{60} *i*-interlayer. Red arrows represent the direction of π-stacking, *i.e.*, hole transport direction. Hole-transport highway between electrodes is formed.

References

1) M. Hiramoto, *Proc. SPIE Vol. 7052, Organic photovoltaics IX* pp. 70520H-1–6, San Diego, CA, 12-14 Aug. (2008).

2) K. Sakai and M. Hiramoto, *Mol. Cryst. Liq. Cryst.* **491**, 284–289 (2008).

3) M. Hiramoto, H. Fujiwara and M. Yokoyama, *J. Appl. Phys.* **72**, 3781 (1992).

4) M. Hiramoto, H. Fujiwara and M. Yokoyama, *Appl. Phys. Lett.* **58**, 1062 (1991).

5) M. Hiramoto, T. Yamaga, M. Danno, K. Suemori, Y. Matsumura and M. Yokoyama, *Appl. Phys. Lett.* **88**, 213105 (2006).

* from Hitachi

† carrying out graduate research on Cooperative Education Program of IMS with Osaka University

‡ carrying out graduate research on Cooperative Education Program of IMS with Kyoto University

Development of Organic Semiconductors for Molecular Thin-Film Devices

Research Center for Molecular Scale Nanoscience
Division of Molecular Nanoscience

SUZUKI, Toshiyasu	Associate Professor
SAKAMOTO, Youichi	Assistant Professor
WATANABE, Yoko	Secretary

Organic light-emitting diodes (OLEDs) and organic field-effect transistors (OFETs) based on π-conjugated oligomers have been extensively studied as molecular thin-film devices. Organic semiconductors with low injection barriers and high mobilities are required for highly efficient OLEDs and OFETs. Radical cations or anions of an organic semiconductor have to be generated easily at the interface with an electrode (or a dielectric), and holes or electrons must move fast in the semiconducting layer. Compared with organic p-type semiconductors, organic n-type semiconductors for practical use are few and rather difficult to develop. Recently, we found that perfluorinated aromatic compounds are efficient n-type semiconductors for OLEDs and OFETs.

1. High-Mobility Bottom-Contact Thin-Film Transistor Based on Anthracene Oligomer[1)]

The mobility in top- and bottom-contact thin-film transistors (TFTs) based on 2,2-bianthryl (**2A**) was improved. The mobility of the top-contact **2A**-TFT was improved from 0.25 to 1.0 cm^2/Vs by octyltrichlorosilane (OTS) treatment of the SiO_2 gate-insulator surface. Large grains and clear step structures corresponding to the molecular length of **2A** were observed in the AFM image of a **2A** film deposited on the OTS-treated SiO_2. The bottom-contact **2A**-TFT with typical source–drain (S–D) electrodes of Cr/Au showed a non-linear rise in the output characteristics due to the large injection barrier between the work function of Au and the HOMO level of **2A**. The non-linear rise in the output characteristics was successfully improved by employing MoO_x as the carrier injection layer for the S–D electrodes. Consequently, the mobility of the bottom-contact **2A**-TFT with a MoO_x/Au electrode was improved to 1.0 cm2/Vs, which is comparable to that in the top-contact **2A**-TFT.

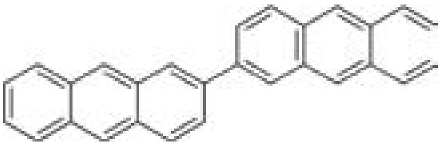

Figure 1. Structure of 2,2-bianthryl (**2A**).

2. Structure, Morphology, and Growth Dynamics of Perfluoropentacene Thin Films[2)]

We report high structural order in thin films of the organic semiconductor perfluoropentacene (PFP), which is a candidate material for n-type applications, deposited by vacuum sublimation on oxidized silicon wafers. Bragg reflections up to high order in both specular and grazing incidence geometries and a mosaicity of less than 0.01° demonstrate the well defined structure. The thin film entirely consists of crystallites with a structure close to the bulk phase without any contamination with a second phase. Real-time X-ray measurements show that

PFP grows in a Stranski–Krastanov growth mode with the first monolayer wetting the substrate before 3d-growth sets in during growth of the second monolayer. Implications for its use are discussed.

3. Impact of Perfluorination on the Charge-Transport Parameters of Oligoacene Crystals3)

The charge-transport parameters of the perfluoropentacene and perfluorotetracene crystals are studied with a joint experimental and theoretical approach that combines gas-phase ultraviolet photoelectron spectroscopy and density functional theory. To gain a better understanding of the role of perfluorination, the results for perfluoropentacene and perfluorotetracene are compared to those for their parent oligoacenes, that is, pentacene and tetracene. Perfluorination is calculated to increase the ionization potentials and electron affinities by ~1 eV, which is expected to reduce significantly the injection barrier for electrons in organic electronics devices. Perfluorination also leads to significant changes in the crystalline packing, which greatly affects the electronic properties of the crystals and their charge-transport characteristics. The calculations predict large conduction and valence bandwidths and low hole and electron effective masses in the perfluoroacene crystals, with the largest mobilities expected along the π-stacks. Perfluorination impacts as well both local and nonlocal vibrational couplings, whose strengths increase by a factor of about 2 with respect to the parent compounds.

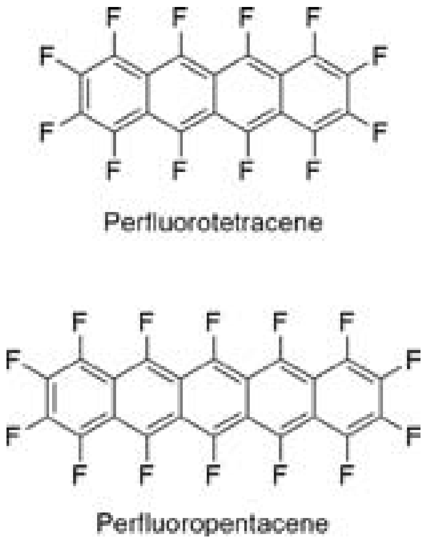

Figure 2. Structures of perfluorotetracene and perfluoropentacene.

References

1) D. Kumaki, T. Umeda, T. Suzuki and S. Tokito, *Org. Electron.* **9**, 921–924 (2008).
2) S. Kowarik, A. Gerlach, A. Hinderhofer, S. Milita, F. Borgatti, F. Zontone, T. Suzuki, F. Biscarini and F. Schreiber, *Phys. Status Solidi RRL* **2**, 120–122 (2008).
3) M. C. R. Delgado, K. R. Pigg, D. A. da Silva Filho, N. E. Gruhn, Y. Sakamoto, T. Suzuki, R. M. Osuna, J. Casado, V. Hernández, J. T. L. Navarrete, N. G. Martinelli, J. Cornil, R. S. Sánchez-Carrera, V. Coropceanu and J. L. Brédas, *J. Am. Chem. Soc.* **131**, 1502–1512 (2009).

Building Photosynthesis by Artificial Molecules

Research Center for Molecular Scale Nanoscience
Division of Molecular Nanoscience

NAGATA, Toshi	Associate Professor
KON, Hiroki	IMS Fellow
KAWAO, Masahiro	IMS Fellow
MIURA, Takahiro	Graduate Student
TANEMURA, Hiroyo	Technical Fellow
WANATABE, Yoko	Secretary

The purpose of this project is to build nanomolecular machinery for photosynthesis by use of artificial molecules. The world's most successful molecular machinery for photosynthesis is that of green plants—the two photosystems and related protein complexes. These are composed almost exclusively from organic molecules, plus a small amount of metal elements playing important roles. Inspired by these natural systems, we are trying to build up multimolecular systems that are capable of light-to-chemical energy conversion. At present, our interest is mainly focused on constructing necessary molecular parts.

1. Synthesis of A New, Ternary TEMPO-Porphyrin-Quinone Pool Molecule[1)]

Plant photosynthesis is one of the most important biological activities on this planet. It is of interest, both academic and industrial, to mimic this process by artificial chemical systems. To achieve this goal, it is useful for chemists to mimic individual processes of photosynthesis by use of artificial molecules. Although many aspects of natural photosynthesis have been modeled by use of artificial molecules, there are still many important features of photosynthesis that are yet unexplored by model chemists.

Among these disregarded features in photosynthesis, we have been focusing on the quinone pools. The quinone pools in biological systems consist of a collection of quinones embedded in special membranes, and they work as buffers between the redox enzymes embedded in the same membranes. Previously we reported our research on building a "single-molecular" quinone pool by use of synthetic dendrimer molecules; in these molecules, the quinones were converted to quinols by irradiation in the presence of reducing agent (thiols).

Our "first-generation" quinone pool, however, lacked one important aspect. After giving an electron to the quinone, the oxidized porphyrin must receive an electron from the electron donor directly (Figure 1a). This is not always easy, because one-electron oxidation of a closed-shell molecule often requires high overpotential. To overcome this difficulty, it is desirable that the porphyrin has a neighboring catalytic site that oxidizes the substrate (electron donor) with low overpotential and supply electrons to the porphyrin (Figure 1b).

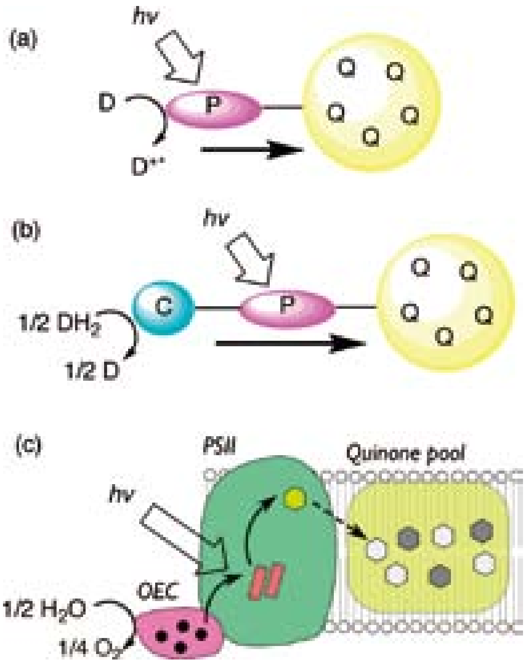

Figure 1. Pictorial representation of the quinone pools. P, Q, D, C denote pigment (porphyrin), quinone, electron donor, and catalytic site, respectively. The bold arrows indicate the flow of electrons. (a) A simple quinone-pool molecule, (b) a "ternary" quinone-pool molecule with a electrocatalytic site, (c) a schematic view of the oxidizing end of plant photosynthesis. OEC: oxygen evolving complex, PSII: photosystem II.

In this work, we present the first preparation of "ternary" quinone-pool molecules (Figure 2). As the electrocatalytic site, we featured TEMPO (2,2,6,6-tetramethylpiperidinyloxy free radical), which is known to catalyze oxidation of various organic substrates including alcohols, thiols, and alkenes. The choice of TEMPO was based on our previous finding that the TEMPO/porphyrin/quinone ternary system was effective for photochemical oxidation of alcohol.[2)]

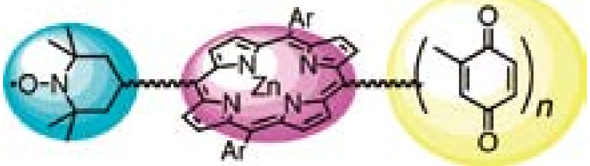

Figure 2. The "ternary" quionone-pool molecule in this work.

2. Syntheses of the Terpyridine-Bipyridine Linked Binary Ligands, and Structural, Redox Properties of Their Cobalt Complexes[3)]

One of the necessary components for photosynthetic chemical conversion is the redox catalysts that generate useful chemicals from abundant source via electrochemical reactions. Transition metal complexes are especially important in this respect, because they are capable of facile single-electron transfer. Among the various transition metals, the 3d metals are particularly important because of their wide availability. However, the 3d metals are generally more substitution labile than the 4d and 5d congeners, so that a certain artifice is necessary in the ligand part to make useful complexes of 3d metals. It is noteworthy that many metalloenzymes use 3d metals in their active centers, where appropriate arrangement of donor atoms are provided by the amino acids embedded in the protein backbone.

We are currently studying "binary" ligands, in which the two different ligands are arranged closely so that the construction of mixed-ligand complexes are made easy and, at the same time, the connection is flexible enough for the complex to accommodate to the change of the chemical environments. We are particularly interested in cobalt complexes among the 3d metals, and previously we synthesized the terpyridine-catechol-Co(III) complexes and discussed their structural and redox properties. However, we would also like to work with Co(II) and Co(I) complexes, because Co(II) and Co(I) complexes exhibit various interesting chemistry, such as hydrogen production and formation of metal-carbon bonds, which should be useful in development of photosynthetic chemical conversion. On the other hand, the Co(II) and Co(I) complexes pose a greater synthetic challenge than the Co(III) complexes, because these ions are more labile towards ligands substitution than Co(III).

In this work, we report the syntheses of new terpyridine-based binary ligands, **1a-1d** and their Co(II) complexes, **2a-2d** and **2a'-2d'**. By using the bipyridine and terpyridine, the ligands act as the penta-dentate ligands and, one coordination site will be vacant. We found that the redox properties were greatly affected by ligand exchange at this "vacant" site, as well as by the length of the intervening methylene chains.

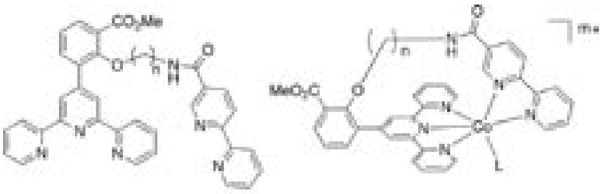

1a-d **2a-d, 2a'-d'**

Figure 3. (a) The binary ligands **1a-d** (*n* = 3–6). (b) The cobalt(II) complexes **2a-d** (L = Cl, *m* = 1) and **2a'-d'** (L = H_2O, *m* = 2).

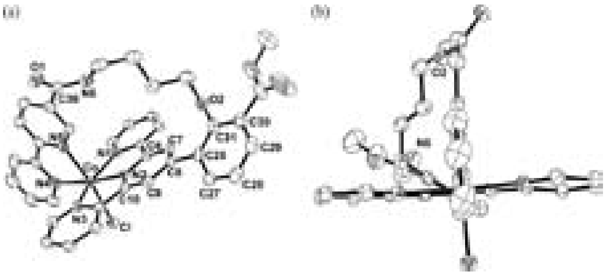

Figure 4. The ORTEP drawing of the complex cation of **2b**. [Reprinted with permission from ref. 3, Copyright (2009) American Chemical Society.]

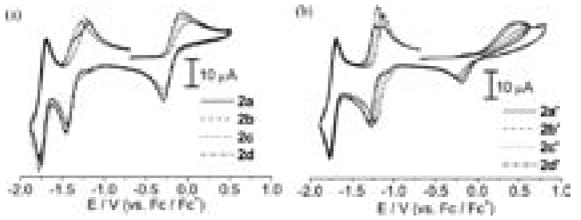

Figure 5. The cyclic voltammograms of the cobalt complexes **2a-d** and **2a'-d'**. [Reprinted with permission from ref. 3, Copyright (2009) American Chemical Society.]

References

1) T. Nagata, Y. Kikuzawa, T. Nagasawa and S. I. Allakhverdiev, *Trans. Mater. Res. Soc. Jpn.* in press.

2) T. Nagasawa, S. I. Allakhverdiev, Y. Kimura and T. Nagata, *Photochem. Photobiol. Sci.* **8**, 174–180 (2009).

3) H. Kon and T. Nagata, *Inorg. Chem.* in press (DOI: 10.1021/ic900932j).

Chemistry of Bowl-Shaped Aromatic Compounds and Metal Nanocluster Catalysts

Research Center for Molecular Scale Nanoscience
Division of Molecular Nanoscience

SAKURAI, Hidehiro	Associate Professor
HIGASHIBAYASHI, Shuhei	Assistant Professor
TSURUOKA, Ryoji	IMS Fellow
MURUGADOSS, Arumugam	Post-Doctoral Fellow
VARIPARAMBIL, Sajisha Sanjayan	Post-Doctoral Fellow
YARASI, Soujanya	Visiting Scientist
SCHMIDT, Bernd	Visiting Scientist
TOPOLINSKI, Berit	Visiting Scientist
CHAKRABORTTY, Sabyasachi	Visiting Scientist
CHIEN, Tran Van	Visiting Scientist
PREEDASURIYACHAI, Patcharee	Visiting Scientist
NGUYEN, Duc Vinh	Visiting Scientist
CHEN, Hsiao Wei	Visiting Scientist
REZA, A. F. G. Masud	Graduate Student
KITAHARA, Hiroaki	Graduate Student
ONOGI, Satoru	Graduate Student
KATAOKA, Keita	Graduate Student
NAKANO, Sachiko	Technical Fellow
KAI, Noriko	Technical Fellow
SASAKI, Tokiyo	Secretary
YURIKUSA, Tomoko	Secretary

Bowl-shaped π-conjugated compounds including partial structures of the fullerenes, which are called “buckybowls,” are of importance not only as model compounds of fullerenes but also as their own chemical and physical properties. Heteroatom-containing buckybowls (heterobuckybowls) have also been expected to exhibit unique physical characters. For example, in solution they show the characteristic dynamic behavior such as bowl-to-bowl inversion. On the other hand, they sometimes favor stacking structure in a concave-convex fashion in the solid state, giving excellent electron conductivity. Furthermore, some buckybowls are conceivable to possess the bowl-chirality if the racemization process, as equal as bowl-to-bowl inversion, is slow enough to be isolated. However, very few buckybowls/heterobuckybowls has been achieved for preparation mainly due to their strained structure, and no report on the preparation of chiralbowls has appeared. In the present project, we develop the rational route to the various kinds of buckybowls/heterobuckybowls with perfect chirality control using the organic synthesis approach.

We also investigate to develop novel catalytic properties of metal nanoclusters. We focus on the following projects: Preparation of size-selective gold nanoclusters supported by hydrophilic polymers and its application to aerobic oxidation catalysts: Synthetic application using metal nanocluster catalyst: Development of designer metal nanocluster catalyst using the highly- functionalized protective polymers: Catalytic activity of metal nanoclusters under the laser-irradiated conditions.

1. Preparation of C_3 Symmetric Homochiral *syn*-Trisnorbornabenzenes through Regio-Selective Cyclotrimerization of Enantiopure Iodonorbornenes[1)]

C_3 symmetric homochiral (-)-*syn*-trisoxonorbornabenzene **1** possessing a rigid cup-shaped structure was synthesized through a novel regio-selective cyclotrimerization of enantiopure iodonorbornenes catalyzed by palladium nanoclusters. The yield of the cyclotrimerization was dependent on the stability of the palladium clusters, which was ascertained from the appearance and TEM images of the reaction mixtures. The efficient preparation of (-)-*syn*-**1** was established in short steps including the newly developed cyclotrimerization reaction.

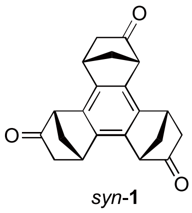

syn-**1**

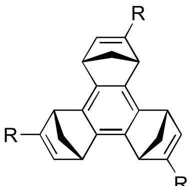

syn-**2**

The thus-prepared homochiral (-)-*syn*-**1** can serve as a key intermediate for the synthesis of C_3 symmetric homochiral cup-shaped molecules with a helical arrangement of substituents. Introduction of several types of substituents was well demonstrated through palladium-catalyzed coupling reactions with the corresponding phosphate and triflate of (-)-*syn*-**1**.

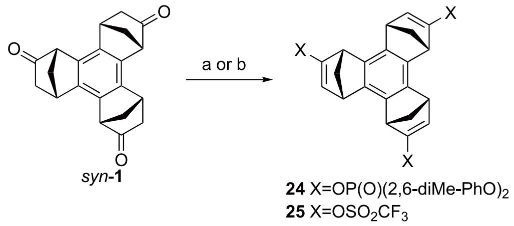

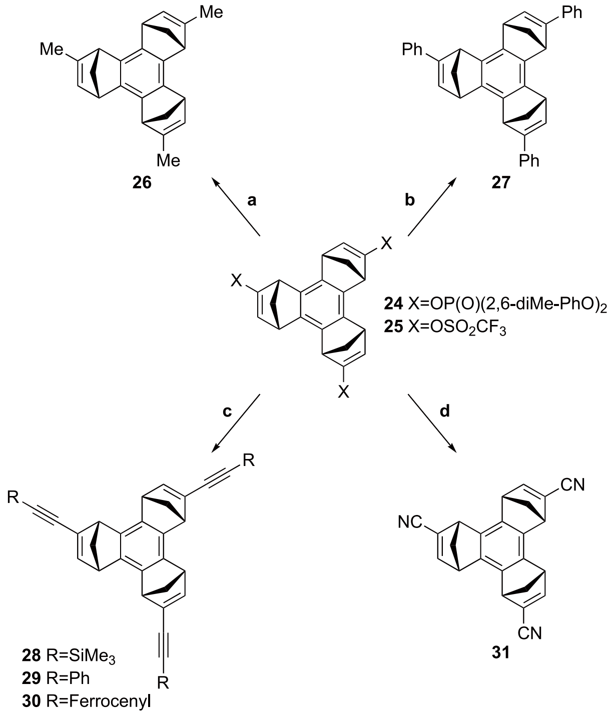

2. Effect of Electronic Structures of Au Clusters Stabilized by Poly (*N*-vinyl -2-pyrrolidone) on Aerobic Oxidation Catalysis[2)]

Au clusters smaller than 1.5 nm and stabilized by poly (*N*-vinyl-2-pyrrolidone) (PVP) showed higher activity for aerobic oxidation of alcohol than those of larger size or stabilized by poly(allylamine) (PAA). X-ray photoelectron spectroscopy, Fourier transform infrared spectroscopy of adsorbed CO, and X-ray absorption near edge structure measurements revealed that the catalytically active Au clusters are negatively charged by electron donation from PVP, and the catalytic activity is enhanced with increasing electron density on the Au core. Based on similar observations of Au cluster anions in the gas phase, we propose that electron transfer from the anionic Au cores of Au:PVP into the LUMO (π*) of O_2 generates superoxo or peroxo-like species, which plays a key role in the oxidation of alcohol. On the basis of these results, a simple principle is presented for the synthesis of Au oxidation catalysts stabilized by organic molecules.

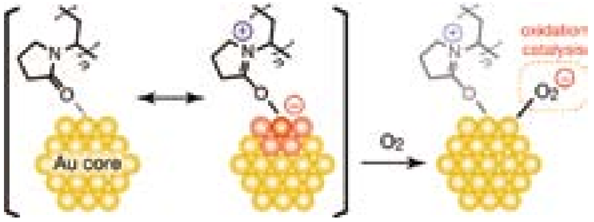

3. Aerobic Oxygenetion of Benzylic Ketones Promoted by Gold Nanocluster Catalyst[3)]

Au:PVP promoted the oxidation of benzylic ketones, including auto-oxidation-type bond cleavage reactions and α-hydroxylation, under ambient conditions. The catalyst accelerates the formation of an α-peroxide intermediate, from which bond cleavage spontaneously proceeds in aqueous solvent to give the auto-oxidation products. In contrast, the α-hydroxylation product is obtained predominantly in DMSO solvent.

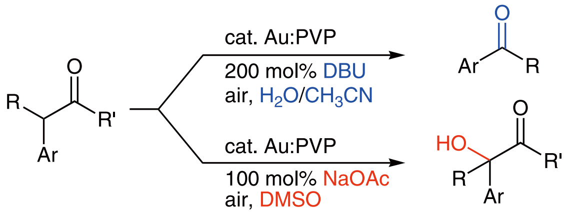

4. Intramolecular Addition of Toluene-Sulfonamide to Unactivated Alkenes Catalyzed by Gold Nanoclusters under Aerobic Conditions[4)]

Au:PVP catalyzed the intramolecular addition of tosyl amides to unactivated alkenes in EtOH under aerobic conditions.

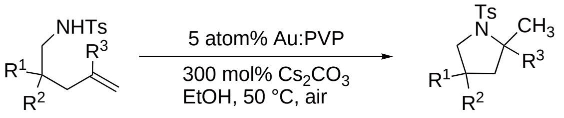

References

1) A. F. G. M. Reza, S. Higashibayashi and H. Sakurai, *Chem. –Asian J.* **4**, 1329–1337 (2009).
2) H. Tsunoyama, N. Ichikuni, H. Sakurai and T. Tsukuda, *J. Am. Chem. Soc.* **131**, 7086–7093 (2009).
3) H. Sakurai, I. Kamiya, H. Kitahara, H. Tsunoyama and T. Tsukuda, *Synlett* 245–248 (2009).
4) H. Kitahara, I. Kamiya and H. Sakurai, *Chem. Lett.* **38**, 908–909 (2009).

Multifunction Integrated Macromolecules for Molecular-Scale Electronics

Research Center for Molecular Scale Nanoscience
Division of Molecular Nanoscience

TANAKA, Shoji — Assistant Professor

We have been developing step-wise synthetic protocols for integrating molecule-based quantum device elements (quantum dots, wells, and tunnel junctions) within a single planar macromolecule. Our strategy is based on "modular architecture" using a library of versatile molecular building blocks. The flexible functionality of our building blocks is derived from the 3,4-diaminothiophene component, which can be easily modified to tune the structural and electronic properties of the main π-conjugated chain.

1. Step-Wise Synthesis of Molecular Wire Modules of Over 100 nm Lengths

We have finished the step-wise synthesis of precisely defined molecular wires of over 100 nm lengths (**1-2**). Now we have a series of wire modules of 1–166 nm lengths. These are not a final product, but a starting material for our next target system, that is, 2-dimension macromolecules of 100 × 100 nm size. As a first step, we have synthesized multi-terminal modules (**3-6**), and set out to build up molecular ladder structures.

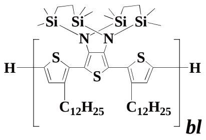

1 (*bl* = 96) [288T, *l* = 110 nm, $C_{4608}H_{8066}N_{192}S_{288}Si_{384}$, MW = 86,185]

2 (*bl* = 144) [432T, *l* = 166 nm, $C_{6912}H_{12098}N_{288}S_{432}Si_{576}$, MW = 129,276]

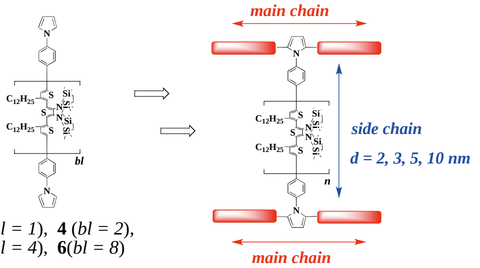

3 (*bl* = 1), **4** (*bl* = 2),
5 (*bl* = 4), **6**(*bl* = 8)

Figure 1. Structures of building blocks (**1-6**).

2. Isomeric Discriminating and Indiscriminating Assembly of Adsorbed Oligothiophenes on Ag(110)1)

Selective discriminating and indiscriminating assembly of isomeric oligothiophene derivatives is performed on a Ag(110) surface. The self-assembled structures are directly analyzed by using scanning tunneling microscopy. We demonstrate that the phase separation and phase mixing of s-*cis*- and s-*trans*-oligothiophenes can be controlled by "shape complementary intermolecular interactions" associated with the overall molecular shapes. The overall shapes of the s-*cis*- and s-*trans*-oligothiophenes are tuned by the length of alkyl side chains.

3. Electrical Resistance of Long Oligothiophene Molecules2)

The electrical resistance of single oligothiophene molecular wires with lengths ranging from 2.2 nm (5-mer) to 9 nm (23-mer) was measured by the break junction method. A linear relationship between the molecular length and resistance was found for molecules longer than 11 mer, whereas an exponential increase in the resistance was observed for molecules shorter than 11-mer. These results indicate that the carrier transport mechanism changes from tunneling to hopping at around 11–14-mer (5.6 nm).

References

1) T. Yokoyama, S. Kurata and S. Tanaka, *J. Phys. Chem. C* **112**, 12590–12593 (2008).
2) R. Yamada, H. Kumazawa, S. Tanaka and H. Tada, *Appl. Phys. Express* **2**, 025002 (3 pages) (2009).

Development of Novel Heterocyclic Compounds and Their Molecular Assemblies for Advanced Materials

Safety Office

TOMURA, Masaaki Assistant Professor

Heterocycles containing sulfur and/or nitrogen atoms are useful as components of functional organic materials since heteroatoms in their rings are helpful to stabilize ions or ion-radical species. In addition, intermolecular interactions caused by heteroatom contacts can be expected to form unique molecular assemblies. In this project, novel functional organic materials based on various heterocycles were synthesized and their physical and structural properties were investigated.

1. A Linear Chain of Water Molecules Accommodated in a Macrocyclic Nanotube Channel[1)]

A macrocyclic tetramer of 2-phenyl-1,3,4-oxadiazole was synthesized, and its self-assembly was investigated. The macrocycle was stacked to form a one-dimensional (1D) columnar structure containing water molecules. The nanotube self-assembled into a bundle, which grew into a molecular wire. The association of the water molecules in the tubular cavity resulted in shielding of the 1D chain of water molecules by the nanotube; these macrocyclic nanotube channels are promising candidates for nanotechnological applications.

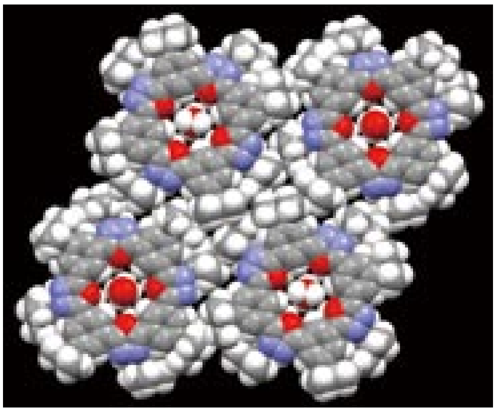

Figure 1. Bundle structure of the microcyclic nanotube.

2. Theoretical Study of Noncovalent Interactions Between Triple Bonds and Chlorine Atoms in Complexes of Acetylene and Some Chloromethanes[2)]

The intermolecular potential surfaces of the acetylene–chloromethane complexes containing C–Cl···π (triple bond) interaction were calculated by the HF and MP2 methods with cc-pVXZ (X = D, T, Q) basis sets. At the minimum, the intermolecular distances between the triple bond and chlorine atom range from 3.3 to 3.5 Å. The CCSD(T) method predicted that the binding energies of the acetylene complexes with CH_3Cl, CH_2Cl_2, $CHCl_3$ and CCl_4 are –0.49, –0.77, –1.05 and –1.34 kcal/mol at the basis set limit, respectively.

3. Theoretical Study for a Complex of 1,2,5-Thiadiazole with Formic Acid[3)]

Ab initio and DFT calculations have been performed on a complex of 1,2,5-thiadiazole with formic acid. Fifteen local minima of the complex are found using the MP2/6-31G method. The three stable structures with the lowest total energies are examined at the HF, MP2 and B3LYP/6-311++G(2d,2p) levels. The first and second stable structures contain intermolecular O–H···N/C–H···O and S···O/O–H···N interactions, respectively. Their binding energies by MP2 corrected BSSE and ZPE are –7.0 and –7.2 kcal/mol, which indicate a great stabilization of the complex.

References

1) K. Ono, K. Tsukamoto, R. Hosokawa, M. Kato, M. Suganuma, M. Tomura, K. Sako, K. Taga and K. Saito, *Nano Lett.* **9**, 122–125 (2009).
2) M. Tomura, *Chem. Phys.* **359**, 126–131 (2009).
3) M. Tomura, *THEOCHEM* **868**, 1–5 (2008).

Visiting Professors

Visiting Professor

AWAGA, Kunio *(from Nagoya University)*

Research on Organic Radical Materials

Organic radicals are key materials in both solid-state and solution redox processes. Organic radical solids always exhibit semiconductive behavior, due to electrostatic repulsion between unpaired electrons and/or electron-lattice interactions. This strongly suggests a potential application of organic radicals to organic electronics. We are performing fundamental research on electrical and magnetic properties of organic radical solids and application research on photo- and current-induced phenomena. We are also working on solid-state electrochemistry of insoluble self-assembled organic thin-films and transition metal complex clusters, targeting rechargeable batteries, functional electrodes, and electrochromic devices.

Visiting Professor

NAKAZAWA, Yasuhiro *(from Osaka University)*

Construction of a Low-Temperature Calorimeter Equipped with a Dilution Refrigerator

Organic conductors, Organic magnets, and metal complexes are fascinating materials which give various interesting electronic phases at low temperatures. The electron-phonon interactions, electron correlations in low-dimensional lattices have been widely investigated in them. With a purpose of studying these subjects and finding novel electronic behaviors, we are developing a new thermal-relaxation calorimeter for measuring heat capacity at extremely low-temperature region. The dilution refrigerator available under magnetic fields up to 16 T in the instrument center of IMS is utilized to get low-temperatures condition. The minimum temperature reached without sample cell was 21 mK and the cooling power at 100 mK was confirmed as 400 µW. A chip-type resistance containing ruthenium-oxide thick film was calibrated against standard thermometer and it was mounted on the Ag-based calorimetry cell. The heat capacity of tiny single crystals with typical weight of 50–300 µg can be measured with absolute precision in this temperature region. The microchip calorimetry devices obtained by the micro-fabrication technique will be installed in the dilution refrigerator in order to study µg class single crystal samples with high resolution.

Visiting Professor

SEKIYA, Hiroshi *(from Kyushu University)*

Spectroscopic Study on Intermolecular Interactions and Dynamics in Hydrogen-Bonded Clusters and Coordination and Solvation Structures of Transition Metal Ions

We investigate structures, intermolecular interactions, and multiple-proton/hydrogen transfer reactions in hydrogen-bonded clusters such as 7-azaindole(alcohol)$_n$/(water)$_n$ (n = 1–3) in the gas phase to clarify multi-dimensional potentials and the tunneling effect by combining electronic and IR spectroscopy with high-level quantum chemistry calculations. These studies provide specific features of multiple-proton/hydrogen transfer reactions that are different from single- and double-proton trasfer reactions. We also investigate the coordination and solvation structures of transition-metal ions. $Ag^+(NH_3)_n$ and $Ni^+(NH_3)_n$ are studied by infrared spectroscopy and quantum chemical calculations. Ag^+ and Ni^+ adopt tetrahedral and square-planar coordination, respectively. The results demonstrate a close relationship between the d-electron configurations of the metals and the geometric structures of the solvated complexes.

RESEARCH ACTIVITIES

Life and Coordination-Complex Molecular Science

Department of Life and Coordination-Complex Molecular Science is composed of four divisions of Biomolecular science, two divisions of Coordination molecular science and two adjunct divisions. Biomolecular science divisions cover the studies on the elucidation of functions and mechanisms for various types of sensor proteins, protein folding, molecular chaperone, and metal proteins. Coordination complex divisions aim to develop molecular catalysts for the transformation of organic molecules, activation small inorganic molecules, and reversible conversion between chemical and electrical energies. Interdisciplinary alliances in the Department aim to create new basic concepts for the molecular and energy conversion through the fundamental science conducted at each division.

Bioinorganic Chemistry of Novel Hemeproteins

Department of Life and Coordination-Complex Molecular Science
Division of Biomolecular Functions

AONO, Shigetoshi	Professor
YOSHIOKA, Shiro	Assistant Professor
ISHIKAWA, Haruto	IMS Research Assistant Professor
SAWAI, Hitomi	JSPS Post-Doctoral Fellow
TANIZAWA, Misako	Secretary

Hemeproteins are a typical metalloprotein, which show a variety of functions including oxygen storage/transport, electron transfer, redox catalysis with various substrates. Besides these traditional functions of hemeproteins, several new functions of hemeproteins have been found recently. Heme-based sensor proteins show a novel function of the heme prosthetic group, in which the heme acts as the active site for sensing the external signal such as diatomic gas molecules and redox change. Aldoxime dehydratase is another novel hemeprotein, in which the heme prosthetic group tethers the substrate for its dehydration reaction. Our research interests are focused on the elucidation of the structure-function relationships of these novel hemeproteins.

1. Structure and Function of Aldoxime Dehydratase Containing a Heme as the Active Site for Dehydration Reaction

Aldoxime dehydratase (Oxd) is a new heme-containing enzyme that works as a hydro-lyase. The enzymatic activity of Oxd is dependent on the oxidation state of the heme iron, though the reaction catalyzed by Oxd is not a redox reaction. Ferrous Oxd containing a Fe^{2+}-heme shows the enzymatic activity, but ferric Oxd containing a Fe^{3+}-heme does not. Previous spectroscopic analyses reveal a novel mechanism, where the change in the coordination mode of the substrate plays a crucial role for the regulation of the enzymatic activity. While the oxygen atom of aldoxime is coordinated to the ferric heme, the nitrogen atom of aldoxime is coordinated to the ferrous heme. The dehydration reaction proceeds only via N-coordinated substrate in the ferrous heme. The organic substrate is directly coordinated to the heme iron in dehydration of aldoxime, which is a unique example among heme enzymes though the coordination of O_2 or H_2O_2 to the heme is well known in the heme-containing oxygenases, catalases, and peroxidases. It is proposed that the dehydration reaction of the heme-bound aldoxime proceeds in a general acid-base catalysis with a histidine working as a catalytic residue in the distal heme pocket. However, the detail reaction mechanisms remained to be elucidated mainly because the structural information of Oxd was lacking.

We have determined the crystal structures of Oxd from *Rhodococcus* sp. N-771 (OxdRE) in the substrate-free and substrate-bound forms. OxdRE formed a homodimer with non-crystallographic two-fold symmetry, consistent with previous gel filtration analyses results. Each monomer contained one heme molecule. The α10 helix of one monomer interacted with the α10 helix of the other to create the dimer interface, which was stabilized by hydrogen bonds and electrostatic interactions.

We could determine the crystal structure of the Michaelis complex of OxdRE by means of the unique property of OxdRE for the substrate binding. As the reaction spontaneously proceeds when mixing ferrous Oxd and the substrate, the crystallization of the substrate-bound OxdRE in the ferrous form (the Michaelis complex of OxdRE) is not possible by usual methods. However, we could prepare the crystal of the Michaelis complex of OxdRE by the reduction of the crystal of the substrate-ferric Oxd complex using X-ray irradiation under cryogenic temperature. The structures of the resting state and the Michaelis complex provide the structural insights into the mechanisms of substrate recognition and the catalysis of OxdRE.

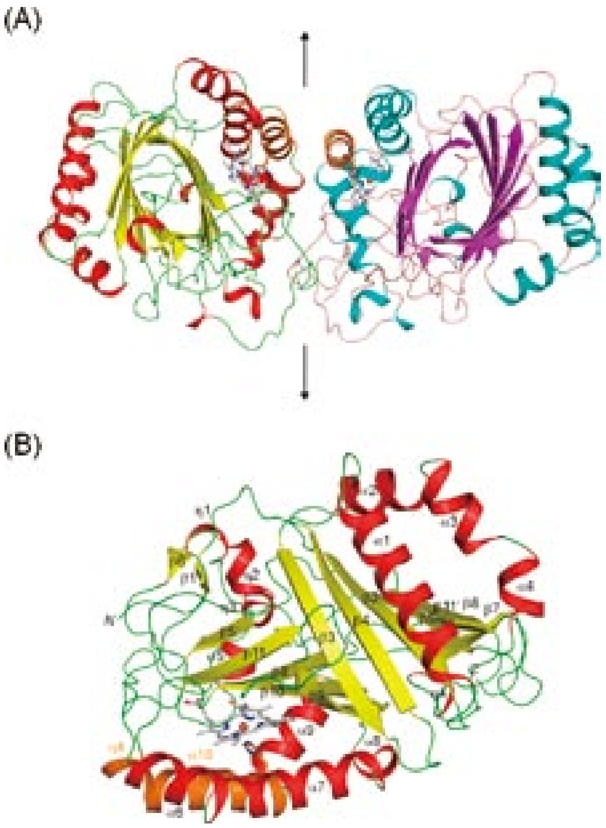

Figure 1. Crystal Structure of OxdRE in substrate-free form. The structures are colored based on the secondary structural elements. The heme is represented by a silver-colored stick model. The heme proximal helix (α10), the subsequent 3_{10} helix (η4), and the axial His299 are colored in orange. (A) Structure of the OxdRE dimer. Two subunits are related by non-crystallographic two-fold symmetry. (B) Closed-up view of the monomer.

2. Regulation of Enzymatic Activity of a Heme-containing Diguanylate Cyclase (HemDGC) by O_2 Binding to the Heme in the Sensor Domain

Bis-(3’,5’)-cyclic dimeric guanosine monophosphate (c-di-GMP) is a ubiquitous bacterial second messenger involved in the regulation of cell motility, differentiation, development, virulence, and biofilm formation. This second messenger generally regulates transitions between the free-living, motile lifestyle and the sessile life style. Low concentrations of c-di-GMP promote motile growth, while high concentrations promote sessile growth with biofilm formation. The intracellular concentrations of c-di-GMP are controlled by the balance between synthesis and hydrolysis of c-di-GMP, which are catalyzed by the enzymes, diguanylate cyclases (DGCs) and phosophodiesterases (PDEs), respectively.

DGCs contain the GGDEF domain, named from the conserved sequence motif (Gly-Gly-Asp-Glu-Phe) that constitutes part of the active site of the enzymes. The GGDEF domain is typically found coupled to a variety of other sensor and/or regulator domains within multidomain proteins.

We have studied the structural and enzymatic properties of a diguanylate cyclase from an obligatory anaerobic bacterium *Desulfotalea psychrophila*, which consists of the N-terminal sensor domain and the C-terminal diguanylate cyclase domain. The sensor domain shows an amino acid sequence homology and spectroscopic properties similar to those of the sensor domains of the globin-coupled sensor proteins containing a protoheme. This heme-containing diguanylate cyclase catalyzes the formation of cyclic di-GMP from GTP only when the heme in the sensor domain binds molecular oxygen. When the heme is in the ferric, deoxy, CO-bound, and NO-bound forms, no enzymatic activity is observed. Resonance Raman spectroscopy reveals that Tyr55 forms a hydrogen bond with the heme-bound O_2, but not with CO. Instead, Gln81 interacts with the heme-bound CO. These differences of hydrogen bonding network will play a crucial role for the selective O_2 sensing responsible for the regulation of the enzymatic activity.

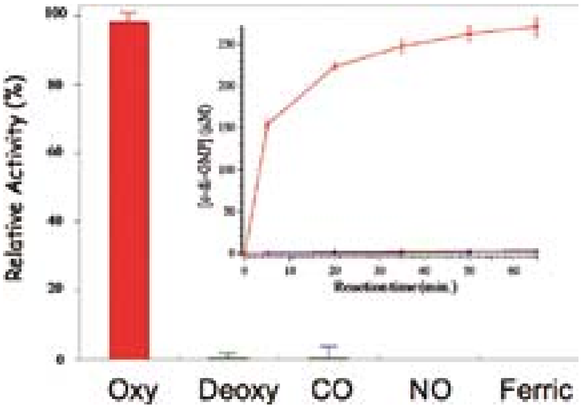

Figure 2. The enzymatic activity of HemDGC is regulated by the coordination state of the heme in its sensor domain. Only when O_2 is bound to the heme, HemDGC shows the activity for the formation of cyclic di-GMP from GTP. Inset: the time-course of the formation of cyclic di-GMP.

Elucidation of the Molecular Mechanisms of Protein Folding

Department of Life and Coordination-Complex Molecular Science
Division of Biomolecular Functions

KUWAJIMA, Kunihiro	Professor
MAKABE, Koki	Assistant Professor
MUKAIYAMA, Atsushi	IMS Fellow
NAKAMURA, Takashi	Post-Doctoral Fellow
CHEN, Jin	Post-Doctoral Fellow
TAKAHASHI, Kazunobu	Graduate Student*
MIZUKI, Hiroko	Technical Fellow
TANAKA, Kei	Secretary

Kuwajima group is studying mechanisms of *in vitro* protein folding and mechanisms of molecular chaperone function. Our goals are to elucidate the physical principles by which a protein organizes its specific native structure from the amino acid sequence. In this year, we studied the folding/unfolding of goat α-lactalbumin, the single-molecule unfolding of staphylococcal nuclease, and the comparative analysis of folding reactions of tear lipocalin and β-lactoglobulin.

1. Experimental and Simulation Studies of the Folding/Unfolding of Goat α-Lactalbumin[1)]

We studied (1) the unfolding behavior of the authentic and recombinant forms of goat α-lactalbumin and (2) the structure of the transition state of folding/unfolding of the protein, both experimentally and by simulation of the molecular dynamics. Experimentally, the recombinant protein exhibited remarkable destabilization and unfolding-rate acceleration as compared to those of the authentic protein; these differences were caused by the presence of an extra N-terminal methionine residue in the recombinant form. We also characterized the transitionstate structure by mutational Φ-value analysis, based on which the structure was localized in a region containing the C-helix and the Ca^{2+}-binding site of the protein. Simulation of the molecular dynamics of unfolding at high temperatures (398 and 498 K) yielded good reproduction of the experimental observations and gave atomically detailed descriptions of the unfolding behavior and the transition-state structure of folding/unfolding. The present series thus demonstrated the power of combination of experiments and simulations for studying the problems of protein folding.

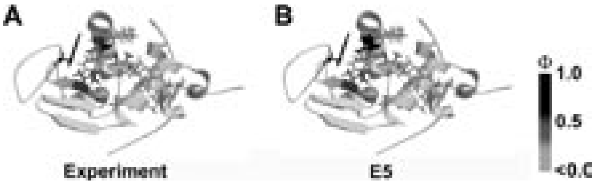

Figure 1. The Φ-values ((a) experimental Φ-values, and (b) Φ_{MD} obtained from molecular dynamics trajectories) mapped onto the three-dimensional structure of goat α-lactalbumin.

2. Probing Force-Induced Unfolding Intermediates of a Single Staphylococcal Nuclease Molecule and the Effect of Ligand Binding[2)]

Single-molecule manipulation techniques have given experimental access to unfolding intermediates of proteins that are inaccessible in conventional experiments. A detailed characterization of the intermediates is a challenging problem that provides new possibilities for directly probing the energy landscape of proteins. We investigated single-molecule mechanical unfolding of a small globular protein, staphylococcal nuclease (SNase), using atomic force microscopy. The unfolding trajectories of the protein displayed sub-molecular and stochastic behavior with typical lengths corresponding to the size of the unfolded substructures. Our results support the view that the single protein unfolds along multiple pathways as suggested in recent theoretical studies. Moreover, we found the drastic change, caused by the ligand and inhibitor bindings, in the mechanical unfolding dynamics.

3. Non-Native α-Helix Formation Is Not Necessary for Folding of Lipocalin: Comparison of Burst-Phase Folding between Tear Lipocalin and β-Lactoglobulin[3)]

Tear lipocalin and β-lactoglobulin are members of the lipocalin superfamily. They have similar tertiary structures but unusually low overall sequence similarity. Non-native helical structures are formed during the early stage of β-lactoglobulin folding. To address whether the non-native helix formation is found in the folding of other lipocalin superfamily proteins, the folding kinetics of a tear lipocalin variant were investigated by stopped-flow methods measuring the time-dependent changes in circular dichroism (CD) spectrum and small-angle X-ray scattering (SAXS). CD spectrum showed that extensive secondary structures are not formed during a burst-phase (within a measurement dead time). The SAXS data showed that the radius of gyration becomes much smaller than in the unfolded state during the burst-phase, indicating that the molecule is collapsed during an early stage of folding. Therefore, non-native helix formation is not general for folding of all lipocalin family members. The non-native helix content in the burst-phase folding appears to depend on helical propensities of the amino acid sequence.

References

1) K. Kuwajima, T. Oroguchi, T. Nakamura, M. Ikeguchi and A. Kidera, in *Water and Biomolecules–Physical Chemistry of Life Phenomena*, K. Kuwajima, Y. Goto, F. Hirata, M. Kataoka and M. Terazima, Eds., Springer-Verlag; Berlin Heiderberg, pp. 13–35 (2009).
2) T. Ishii, Y. Murayama, A. Katano, K. Maki, K. Kuwajima and M. Sano, *Biochem. Biophys. Res. Commun.* **375**, 586–591 (2008).
3) S. Tsukamoto, T. Yamashita, Y. Yamada, K. Fujiwara, K. Maki, K. Kuwajima, Y. Matsumura, H. Kihara, H. Tsuge and M. Ikeguchi, *Proteins* **76**, 226–236 (2009).

Award

MAKABE, Koki; The Protein Science Society of Japan (PSSJ) Incentive Award for Young Investigators (9th PSSJ Annual Meeting, Kumamoto, May, 2009).

---

* carrying out graduate research on Cooperative Education Program of IMS with the University of Tokyo

Elucidation of Dynamical Structures of Biomolecules toward Understanding the Mechanisms Underlying Their Functions

Department of Life and Coordination-Complex Molecular Science
Division of Biomolecular Functions

KATO, Koichi	Professor
YAMAGUCHI, Takumi	Assistant Professor
KAMIYA, Yukiko	IMS Research Assistant Professor
SERVE, Olivier	Post-Doctoral Fellow
SUGIHARA, Takahiro	Research Fellow
CHETTERJEE, B. P.	Visiting Scientist*
YAGI-UTSUMI, Maho	Graduate Student[†]
YOSHIKAWA, Sumi	Graduate Student[†]
NISHIO, Miho	Graduate Student[†]
YAMAMOTO, Masahiro	Graduate Student[†]
BUNKO, Yuji	Graduate Student[†]
SUZUKI, Mariko	Technical Fellow
ISONO, Yukiko	Technical Fellow
TANAKA, Kei	Secretary

Our biomolecular studies are based on detailed analyses of structures and dynamics of various biological macromolecules and their complexes at atomic level, primarily using nuclear magnetic resonance (NMR) spectroscopy. In particular, we conducted studies aimed at elucidating dynamic structures of glycoconjugates and proteins for integrative understanding of the mechanisms underlying their biological functions. For this purpose, we use multidisciplinary approaches integrating the methodologies of molecular and cellular biology and nanoscience along with molecular spectroscopy.

1. Molecular Basis for Glycoprotein-Fate Determination in Cells1–3)

Accumulating evidence indicates that a variety of lectins are involved in folding, transport and degradation of glycoproteins in cells. These intracellular lectins are supposed to recognize the *N*-linked oligosaccharides when they act as molecular chaperones, cargo receptors, or ER-associated degradation factors in the quality control system of glycoproteins. To understand the details of the structural and molecular basis of the mechanisms underlying quality control of glycoproteins, we characterize the sugar-binding specificities of the intracellular lectins with a series of intermediates of high-mannose-type oligosaccharides, which are generated through the actions of specific glycosidases in the endoplasmic reticulum. Our frontal affinity chromatographic analyses revealed that molecular chaperone CRT, cargo receptor VIPL, and ER-associated degradation factor OS-9 exhibit distinct sugar-binding specificities (Figure 1). On the basis of these data, we conclude that intracellular lectins recognize distinct 'glycotopes' located on the different site of the high-mannose-type oligosaccharides.

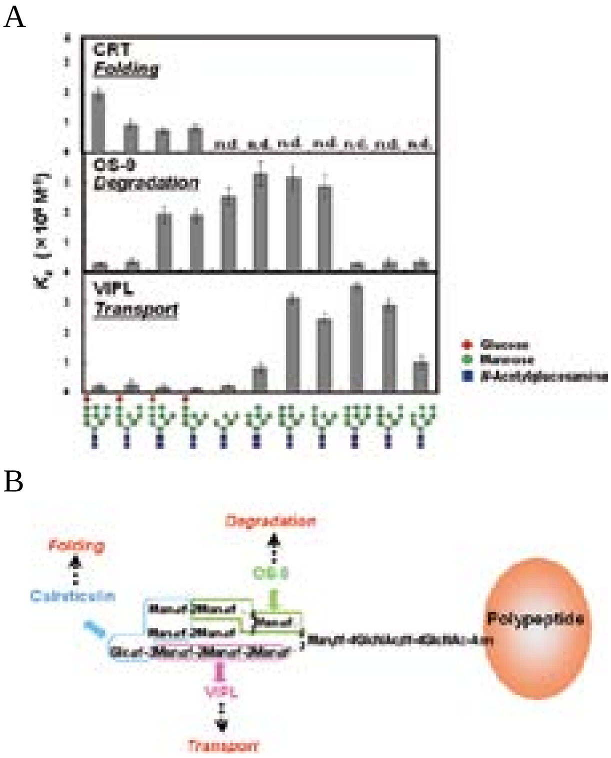

Figure 1. (A) K_a values for CRT, VIPL, and OS-9 determined by the frontal affinity chromatographic analyses. While CRT specifically interacts with monoglucosylated oligosaccharide, VIPL has higher affinity for deglucosylated oligosaccarides. On the other hand, Mannose-trimmed glycans are specifically recognized by OS-9. (B) Schematic representation of a glycoprotein indicating the glycotopes recognized by the intracellular lectins.

2. ^{13}C-Detection NMR Approach for Large Glycoproteins[4)]

NMR spectroscopy has great potential to provide us with information on structure and dynamics at atomic resolution of glycoproteins in solution. In larger glycoproteins, however, the detrimental fast ^{1}H transverse relaxation renders the conventional ^{1}H-detected NMR experiments difficult. ^{13}C direct detection potentially offers a valuable alternative to ^{1}H detection to overcome the fast T_2 relaxation. Furthermore, ^{13}C-detected experiments are expected to have several advantages for the NMR spectral assignments of the carbohydrate peaks of glycoproteins. In general, the ^{1}H signals of glycans except for those originating from the anomeric position are severely overlapped in a narrow spectral region (3–4 ppm) while most ^{13}C signals are dispersed in a wide range (50–110 ppm). Secondly, the information of ^{13}C–^{13}C shift correlation obtained from the ^{13}C-detected experiments can be helpful in classifying the carbohydrate signals simply by comparing with the reported ^{13}C chemical shift values (Figure 2A). This is due to the fact that ^{13}C chemical shift values of a sugar residue primarily depend on the covalent structures but are not largely affected by the glycosidic linkages conformations and any other environmental factors in contrast to the ^{1}H chemical shifts, which are influenced, for example, by the interactions with the polypeptide chains. We applied ^{13}C-detected NMR methods to observe the NMR signals of ^{13}C-labeled glycans attached to Fc fragment of immunoglobulin G with a molecular mass of 56 kDa. We successfully demonstrated that ^{13}C-detected ^{13}C–^{13}C NOESY experiment is highly useful for spectral assignments of the glycans of large glycoproteins because ^{13}C–^{13}C magnetization transfer is efficiently achieved through dipolar-dipolar interaction in a large glycoprotein due to slower molecular tumbling (Figure 2B). This approach would be in part complementary to ^{13}C–^{13}C TOCSY and ^{1}H-detection experiments.

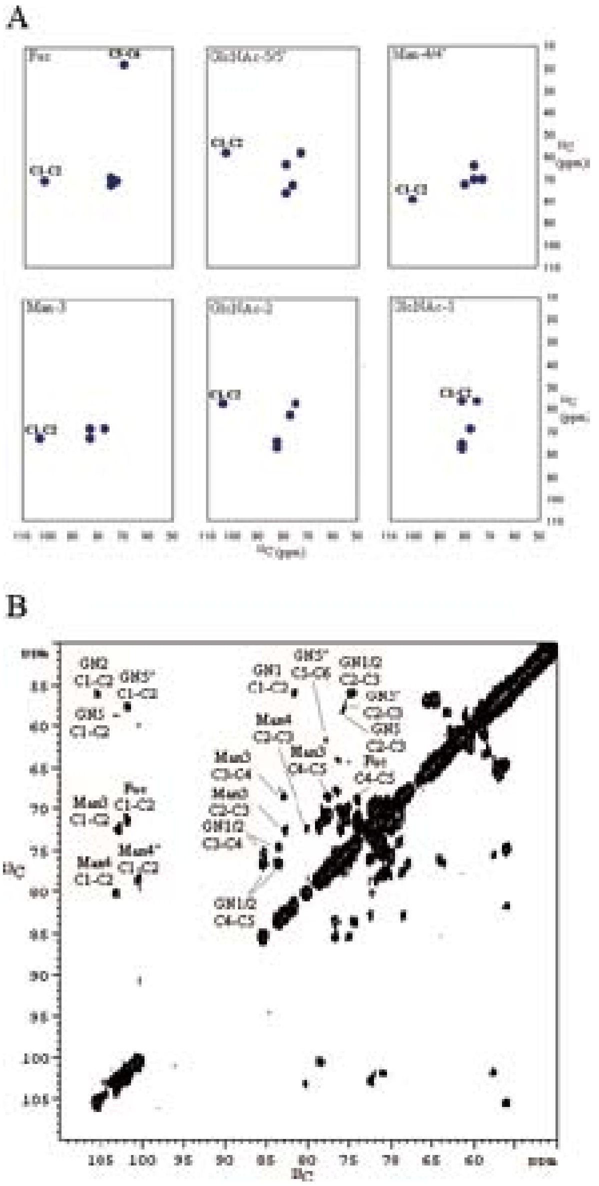

Figure 2. Use of two-dimensional ^{13}C–^{13}C NOESY spectrum for the assignment of IgG-Fc glycans. (A) Two-dimensional ^{13}C–^{13}C NOESY patterns expected for the sugar residues, Fuc, GlcNAc-5/5', Man-4/4', Man-3, GlcNAc-2 and GlcNAc-1, in a bianntenary complex type oligosaccharide based on the ^{13}C chemical shift values of the sugar residues in glycopeptides derived from ^{13}C-labeled IgG-Fc. (B) Two-dimensional ^{13}C–^{13}C NOESY spectrum of ^{13}C-labeled IgG-Fc.

References

1) E. M. Quan, Y. Kamiya, D. Kamiya, V. Denic, J. Weibezahn, K. Kato and J. S. Weissman, *Mol. Cell* **32**, 870–877 (2008).
2) N. Hosokawa, Y. Kamiya, D. Kamiya, K. Kato and K. Nagata, *J. Biol. Chem.* **284**, 17061–17068 (2009).
3) Y. Kamiya, D. Kamiya, R. Urade, T. Suzuki and K. Kato, *Glycobiology Research Trends*, G. Powell and O. McCabe, Eds., NOVA Science Publishers; New York, pp. 27–40 (2009).
4) Y. Yamaguchi, M. Wälchli, M. Nagano and K. Kato, *Carbohydr. Res.* **344**, 535–538 (2009).

Award

KAMIYA, Yukiko; Poster Presentation Award, Annual meeting in Protein Community-organization and maintenance of protein functions (2008).

---

* Present Address;Department of Natural Science, Humanities & Management, West Bengal University of Technology, Kolkata 700-064, India
† carrying out graduate research on Cooperative Education Program of IMS with Nagoya City University

Structure-Function Relationship of Metalloproteins

Department of Life and Coordination-Complex Molecular Science
Division of Biomolecular Functions

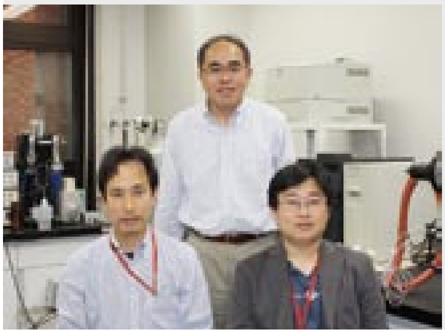

FUJII, Hiroshi	Associate Professor
KURAHASHI, Takuya	Assistant Professor
NONAKA, Daisuke	IMS Fellow*
CONG, Zhiqi	IMS Fellow
TAKAHASHI, Akihiro	Graduate Student†
TANIZAWA, Misako	Secretary

Metalloproteins are a class of biologically important macromolecules, which have various functions such as oxygen transport, electron transfer, oxidation, and oxygenation. These diverse functions of metalloproteins have been thought to depend on the ligands from amino acid, coordination structures, and protein structures in immediate vicinity of metal ions. In this project, we are studying the relationship between the electronic structures of the metal active sites and reactivity of metalloproteins.

1. Critical Role of External Axial Ligands in Chirality Amplification of *trans*-Cyclohexane-1,2-diamine in Salen Complexes1)

A series of Mn^{IV}(salen)(L)$_2$ complexes bearing different external axial ligands (L = Cl, NO_3, N_3 and OCH_2CF_3) from chiral salen ligands with *trans*-cyclohexane-1,2-diamine as a chiral scaffold are synthesized, in order to gain insight into conformational properties of metal salen complexes. X-ray crystal structures show that Mn^{IV}(salen)(OCH_2CF_3)$_2$ and Mn^{IV}(salen)(N_3)$_2$ adopt a stepped conformation with one of two salicylidene rings pointing upward and the other pointing downward due to the bias from the *trans*-cyclohexane-1,2-diamine moiety, which is in clear contrast to a relatively planar solid-state conformation for Mn^{IV}(salen)(Cl)$_2$. The CH_2Cl_2 solution of Mn^{IV}(salen)(L)$_2$ shows circular dichroism of increasing intensity in the order of L = Cl < NO_3 « N_3 < OCH_2CF_3, which indicates Mn^{IV}(salen)(L)$_2$ adopts a solution conformation of an increasing chiral distortion in this order. Quantum-chemical calculations with symmetry adapted cluster–configuration interaction method indicate that a stepped conformation exhibits more intense circular dichroism than a planar conformation. The present study clarifies an unexpected new finding that the external axial ligands (L) play a critical role in amplifying the chirality in *trans*-cyclohexane-1,2-diamine in Mn^{IV}(salen)(L)$_2$ to facilitate the formation of a chirally-distorted conformation, possibly a stepped conformation.

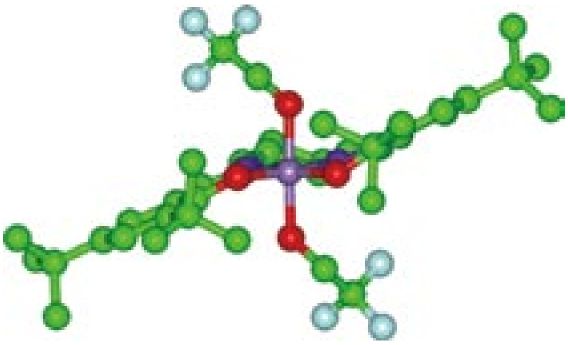

Figure 1. Chiral stepped conformation of Mn^{IV}(salen)(OCH_2CF_3)$_2$.

2. Catalytic Reactivity of a *Meso*-N-Substituted Corrole and Evidence for a High-Valent Iron–Oxo Species2)

It is shown that an iron(III) *meso*-N-substituted corrole (TBP_8Cz)Fe^{III} (**1**) (TBP_8Cz) octakis(4-*tert*-butylphenyl)corrolazinato), is a potent catalyst for the oxidation of alkenes in the presence of pentaflouroiodosylbenzene (C_6F_5IO) as oxidant. In the case of cyclohexene, complex **1** performs on a par with one of the best porphyrin catalysts (($TPPF_{20}$)FeCl), exhibiting rapid turnover and a high selectivity for epoxide ($CzFe^{III}$/C_6F_5IO/cyclohexene (1:100:1000) in CH_2Cl_2/CH_3OH (3:1 v:v) gives 33 turnovers of epoxide in <2 min). Reaction rates for **1** are greatly enhanced compared to other Fe or Mn corroles under similar catalytic conditions, consistent with an increase in the electrophilicity of a high-valent iron–oxo intermediate induced by *meso*-N substitution. Reaction of dark-green **1** (λ_{max}) 440, 611, 747 nm) under single-turnoverlike conditions at –78 °C leads to the formation of a new dark-brown species (**2**) (λ_{max}) 396, 732, 843 nm). The Fe^{III} complex **1** is restored upon the addition of 2 equiv of ferrocene to **2**, or by the addition of 1 equiv of PPh_3, which concomitantly yields $OPPh_3$. In addition, complex **2** reacts with excess cyclohexene at –42 °C to give **1**. Complex **2** was also characterized by EPR spectroscopy, and all of the data are consistent with **2** being an antiferromagnetically coupled iron(IV)-oxo π-cation-radical complex. Rapidmixing stopped-flow UV–vis studies show that the low-temperature complex **2** is generated as a shortlived intermediate at room temperature.

3. Effect of Imidazole and Phenolate Axial Ligands on the Electronic Structure and Reactivity of Oxoiron(IV) Porphyrin π-Cation Radical Complexes: Drastic Increase in Oxo-Transfer and Hydrogen Abstraction Reactivities[3]

To study the effect of axial ligands on the electronic structure and reactivity of compound I of peroxidases and catalases, oxoiron(IV) porphyrin π-cation radical complexes with imidazole, 2-methylimidazole, 4(5)-methylimidazole, and 3-fluoro-4-nitrophenolate as the axial ligands were prepared by ozone oxidation of iron(III) complexes of 5, 10, 15, 20-tetramesitylporphyrin (TMP) and 2, 7, 12, 17-tetramethyl-3, 8, 13, 18-tetramesitylporphyrin (TMTMP). These complexes were fully characterized by absorption, ^{1}H, ^{2}H, and ^{19}F NMR, EPR, and ESI-MS spectroscopy. The characteristic absorption peak of compound I at approximately 650 nm was found to be a good marker for estimation of the electron donor effect from the axial ligand. The axial ligand effect did not change the porphyrin π-cation radical state, the a_{2u} state of the TMP complexes, or the a_{1u} radical state of both the TMTMP complexes and compound I. The ferryl iron and porphyrin π-cation radical spins were effectively transferred into the axial ligands for the a_{2u} complexes, but not for the a_{1u} complexes. Most importantly, the reactivity of the oxoiron(IV) porphyrin π-cation radical complex was drastically increased by the imidazole and phenolate axial ligands. The reaction rate for cyclooctene epoxidation was increased 100 ~ 400-fold with axial coordination of imidazoles and phenolate. A similar increase was also observed for oxidation of 1,4-cyclohexadiene, *N,N*-dimethyl-*p*-nitroaniline, and hydrogen peroxide. These results suggest extreme enhancement of the reactivity of compound I by the axial ligand in heme enzymes. The functional role of axial ligands on the compound I in heme enzymes is discussed.

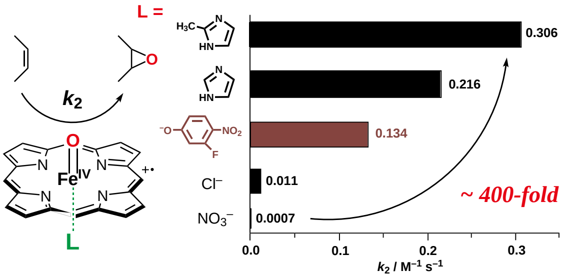

Figure 2. Axial ligand effect on the epoxidation reactivity.

4. Paramagnetic ^{13}C and ^{15}N NMR Analyses of Cyanide ($^{13}C^{15}N$)-Ligated Ferric Peroxidases: The Push-Effect, not Pull-Effect, Modulates the Compound I Formation Rate[4]

Paramagnetic ^{13}C and ^{15}N NMR spectroscopy of heme-bound cyanide ($^{13}C^{15}N$) was utilized to quantitatively distinguish the electron donor effect (the push-effect) from the proximal histidine and hydrogen bonding effect (the pull-effect) from the distal amino acid residues in cytochrome *c* peroxidase (CcP), ascorbate peroxidase (APX), lignin peroxidase (LiP) and manganese peroxidase (MnP). Paramagnetic ^{13}C NMR signals of heme-bound $^{13}C^{15}N$ of these peroxidases were observed in a wide range: –3501 ppm (CcP), –3563 ppm (APX), –3823 ppm (MnP), and –3826 ppm (LiP), while paramagnetic ^{15}N NMR signals of those were detected in a narrow range: 574 ppm (ARP), 605 ppm (CcP), 626 ppm (LiP), and 654 ppm (MnP). Detailed analysis, combined with the previous results for horseradish peroxidase and *Arthromyces ramosus* peroxidase, indicated that the push-effect is quite different among these peroxidases while the pull-effect is similar. More importantly, a strong correlation between the ^{13}C NMR shift (the push-effect) and the compound I formation rate was observed, indicating that the push-effect causes a variation in the compound I formation rate. Comparison of the ^{13}C and ^{15}N NMR results of these peroxidases with their crystal structures suggests that the orientation of the proximal imidazole plane to the heme N–Fe–N axis controls the push-effect and the compound I formation rate of peroxidase.

References

1) T. Kurahashi, M, Hada and H, Fujii, *J. Am. Chem. Soc.* in press.
2) A. J. Mcgrown, W. D. Kerber, H. Fujii and D. P. Goldberg, *J. Am. Chem. Soc.* **131**, 8040–8048 (2009).
3) A. Takahashi, T. Kurahashi and H. Fujii, *Inorg. Chem.* **48**, 2614–2625 (2009).
4) D. Nonaka, H. Wariishi and H. Fujii, *Biochemistry* **48**, 898–905 (2009).

---

* Present Address; Osaka University, Suita, Osaka 565-0871

† Present Address; Sumika Chemical Analysis Service, Ltd. Osaka 541-0043

Fabrication of Silicon-Based Planar Ion-Channel Biosensors and Integration of Functional Cell Membrane Model Systems on Solid Substrates

Department of Life and Coordination-Complex Molecular Science
Division of Biomolecular Sensing

URISU, Tsuneo	Professor
YANG, Dah-Yen	Visiting Professor
TERO, Ryugo	Assistant Professor
ASANO, Toshifumi	IMS Fellow
NAGAHIRO Takeshi	Research Fellow
UNO, Hidetaka	Graduate Student
NAKAI, Naohito	Graduate Student
SHANG, Zhi-Guo	Graduate Student
FUJIWARA, Kuniyo	Graduate Student
SAYED, Abu	Graduate Student
HE, Tingchao	Graduate Student*
SHIMIZU, Atsuko	Secretary

We are interested in the investigation of cell membrane surface reactions and the pathogen mechanism of the neurodegenerative diseases, based on the molecular science. We are advancing two subjects, aiming the creation and development of new molecular science field, “medical molecular science.” One is the development of ion channel biosensor and its application to the neural network analyzer device. The other is the fundamental understanding of bilayer membrane properties using the artificial lipid bilayers on solid substrates, which is called supported bilayers, by means of atomic force microscope and fluorescence microscope-based techniques.

1. Development of Cell-Culture-Type Planar Ion Channel Biosensor[1)]

We have developed a new planar-type ion channel biosensor with a silicon-on-insulator (SOI) substrate and a cell culture function. Fibronectin is coated on the substrate surface to promote cell growth in this sensor. A transient receptor potential vanilloid type 1 (TRPV1) channel-expressing HEK293 cell is positioned on the micropore of the SOI sensor chip and incubated. Although the seal resistance was quite small, 10–20 MΩ, compared with that of the conventional pipette patch-clamp method, the signal-to-noise level was sufficiently high. However, a much lower noise level is required for observing the opening and closing of fewer than 30 channels.

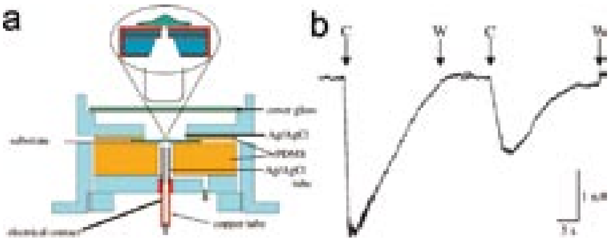

Figure 1. (a) Schematic drawing of the incubation-type planar ion channel biosensor. The sensor chip is fabricated using Si-SOI substrates (7×7 mm^2) with micropores at the center. (b) Whole-cell channel current recording of TRPV1-transfected HEK-293; current was activated by repeated capsaicin stimulation (c) and wash-out (w) cycles.

2. Noise Properties of Incubation-Type Planar Ion Channel Biosensor[2)]

Noise properties are the most important issues in the planar-type ion channel biosensors, as well as in the pipette patch-clamp and black membrane biosensors. Therefore the current noise and its power spectrum appearing in the incubation-type planar ion channel biosensor (Figure 1) were

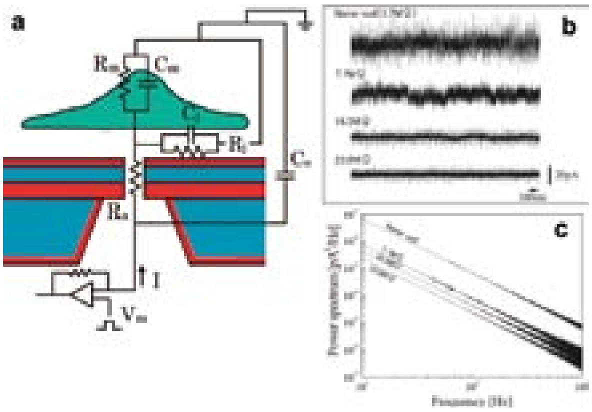

Figure 2. (a) Equivalent circuit of the incubation-type planar ion channel biosensor. The oxide layer of SOI and the ~1-µm-thick surface oxide layer are important for reducing substrate capacitance C_s. (b, c) Observed noise properties of the incubation -type planar ion channel biosensor: (b) noise current and (c) its spectral density for various cleft resistances (R_j).

measured and analyzed in detail to detect the main origin of the noise. The dominant noise sources are classified into (i) current noise induced by head stage preamplifier input voltage noise, (ii) thermal noise, and (iii) excess noise. The spectral density and variance of these noises are formulated in the general form using an equivalent circuit shown in Figure 2a. The baseline currents at various cleft resistance (R_j in Figure 2a) were measured (Figure 2b) and their power spectra were calculated (Figure 2c). We concluded that the main source of the noise in the device is the excess noise, which depends on $1/f$ and originates primarily from the current passing through the cleft between the cell membrane and the substrate surface. The measured noise level ($1.0–2.4 \times 10^{-11}$ A) corresponds to channel current through 5–10 membrane proteins, thus sufficiently small to measure the signal of whole-cell current ($\sim 10^{-9}$ A) (Figure 1b).

3. Synchrotron-Radiation-Stimulated Etching of Polydimethylsiloxane (PDMS) Using XeF_2 as a Reaction Gas[3)]

The synchrotron radiation (SR) stimulated etching of silicon elastomer polydimethylsiloxane (PDMS) using XeF_2 as an etching gas has been demonstrated. The etching system with differential pumps and two parabolic focussing mirrors was constructed to perform the etching. The PDMS was found to be effectively etched by the SR irradiation under the XeF_2 gas flow, and the etching process was area-selective and anisotropic. Extremely high etching rate of 40–50 µm was easily obtained at the XeF_2 gas pressure of 0.2–0.4 Torr. This suggests that SR etching using XeF_2 gas provides a new microfabrication technology for thick PDMS membranes, which can open new applications such as the formation of three dimensional microfluidic circuits.

4. Surface-Induced Phase Separation of Sphingomyelin/Cholesterol/Ganglioside GM1-Planar Bilayer on Mica Surfaces and Molecular Conformation that Accelerates Aβ Oligomerization

Lipid bilayers containing ganglioside GM1 (GM1) are used in the development of new therapies for Alzheimer's disease (AD), because GM1 mediates the amyloid beta (Aβ) aggregation that is the hallmark of AD. To investigate how ganglioside-containing lipid bilayers interact with Aβ, we examined the interaction between Aβ40 and supported planar lipid bilayers (SPLBs) on mica and SiO_2 substrates using atomic force microscopy, fluorescence microscopy, and molecular dynamics computer simulations. These SPLBs contained several compositions of sphingomyelin, cholesterol, and GM1 which covers compositions commonly seen in eukaryotic biomembranes and were treated at physiological salt concentrations. Surprisingly high speed Aβ aggregations of fibril formation were induced for all GM1 concentrations examined on the mica surface, but only globular agglomerates are formed slowly on the SiO_2 surfaces. Especially for the 20 mol% GM1 concentration on the mica surface, unique triangular domains were formed and the high speed Aβ aggregations were observed only outside of the triangular domains. The speed of Aβ40 aggregation and the shape of the agglomerates depend on the molecular conformation of GM1, which varies depending on the substrate materials.

5. Shape Transformation of Adsorbed Vesicles on Oxide Surfaces: Effect of Substrate Material and Photo-Irradiation[4)]

Shape transformation of phospholipid vesicles on oxide surfaces was investigated by a fluorescence microscope. The transformation of spherical vesicles to a planar lipid bilayer membrane spontaneously proceeded on mica and glass, while the intact vesicular layer formed on TiO_2. Interaction energy between the substrate and the bilayer, which was evaluated using the rigorously calculated Hamaker constant, was ~10 times larger on TiO_2 than on mica and SiO_2. The results seems inconsistent with the conventionally proposed adhesion induced tension model, in which stronger adsorption leads to easier planar membrane formation from vesicles, thus indicate that the shape transformation from vesicles to a planar membrane is dominated by the kinetic processes and the dynamics of the vesicles, rather than the adsorption state of individual vesicle. Area-selective SPLB formation of adsorbed vesicles was induced by the irradiation of strong excitation light, which was assisted by the photo-induced expansion of SPLB containing dye-labeled lipid molecules.

References

1) T. Asano, H. Uno, K. Shibasaki, M. Tominaga and T. Urisu, *Trans. Mater. Res. Soc. Jpn.* **33**, 767–770 (2008).
2) T. Asano, T. Nakamura, A. Wakahara and T. Urisu, *Jpn. J. Appl. Phys.* **48**, 027001 (4 pages) (2009).
3) T. -Y. Chiang, T. Makimura, T. He, S. Torii, R. Tero, C. Wand and T. Urisu, *Rev. Sci. Instrum.* **17**, 69–74 (2010).
4) R. Tero, T. Ujihara and T. Urisu, *Trans. Mater. Res. Soc. Jpn.* **34**, 183–188 (2009).

Awards

ASANO, Toshifumi; The best poster award in 2nd International Symposium on Nanomedicine.
TERO, Ryugo; The best poster award in 61th Divisional Meeting on Colloid and Interface Chemistry, CSJ.

---

* from Shanghai Jiao Tong University

Investigation of Molecular Mechanisms of Transporters and Receptors in Membrane by Using Stimulus-Induced Difference FT-IR Spectroscopy

Department of Life and Coordination-Complex Molecular Science
Division of Biomolecular Sensing

FURUTANI, Yuji	Associate Professor
SHIMIZU, Atsuko	Secretary

The cell, the elementary unit of life, uptakes nutrient and exhausts waste. Its ion balance between inside and outside of cell membrane is adjusted strictly. These works are performed by membrane proteins such as channels and transporters. There are some other membrane proteins such as cell sensor proteins which detect various environmental changes. A main goal of my group is to clarify molecular mechanisms of transporters and receptors in cell membrane mainly by using stimulus-induced difference infrared spectroscopy which is sensitive to structural and environmental changes of protein molecules.

I have moved to IMS in this March and have been setting up my lab. In this review article, I'd like to present my recent studies done in my previous work place, Nagoya Institute of Technology, and progress in a recent research by using a new FT-IR spectrometer installed in IMS.

1. Time-Resolved FT-IR Spectroscopy Detecting O–H and O–D Stretching Vibrations of Internal Water Molecules in a Light-Driven Proton Pump Protein, Bacteriorhodopsin

Bacteriorhodopsin (bR) is one of well known light-driven proton pump protein, which has an all-*trans* retinal covalently linked to Lys216 via a protonated Schiff base (SB). Upon light absorption, photo-isomerization occurs from the all-*trans* to 13-*cis* form in less than one picosecond, followed by a cyclic reaction that comprises a series of intermediates, called as the K, L, M, N, and O states, back to the bR ground state (BR). During the bR photocycle the first proton transfer reaction takes place in the L to M transition. A proton is transferred from the protonated SB to Asp85, together with the apparently simultaneous release of a proton from the so-called proton release group (PRG), which is composed of water molecules, Glu194 and Glu204, to the extracellular side. Further proton transfers take place in the later intermediates (accompanied by other protein and retinal structural changes), leading to a net proton transport from the cytoplasmic to the extracellular side, and the recovery of the bR ground state.

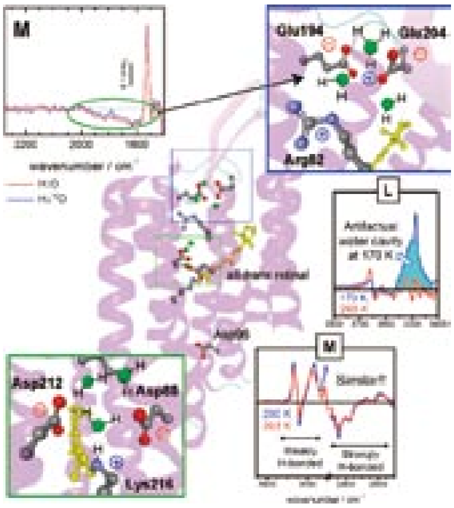

Figure 1. X-ray crystal structure of bacteriorhodopsin and O–H stretching vibrations observed in its photocycle. Several water molecules exist in the protein cavities and play an important roll for pumping protons.

By use of time-resolved FT-IR spectroscopy with bR film samples moderately hydrated with water, H_2O, or isotope labeled water, $H_2{}^{18}O$, infrared difference spectra in O–H stretching region were successfully collected and some of the bands were assigned to the internal water molecules (Figure 1). Especially, we firstly gave experimental evidence that the continuum band in the 2000–1800 cm^{-1} region was originated from the protonated water cluster which probably locates in the extracellular side.$^{1)}$ It was also elucidated that water structure formed in the L intermediate at room temperature is different from that trapped in low temperature.

Now, I try to extend observable spectral range to the region around peak of water absorption, 3400 cm^{-1} in H_2O and 2400 cm^{-1} in D_2O. By use of D_2O and optimizing hydration level, accurate light-induced difference spectra were collected (Figure 2). In the X–H and X–D stretching region, structural changes in the hydrophobic and hydrophilic part were separately observed, respectively. By analyzing these spectral changes, real-time hydrogen-bonding changes of the internal water molecules and protein moiety of bR will be elucidated, leading to better understand of the light-driven proton pumping mechanism of bR.

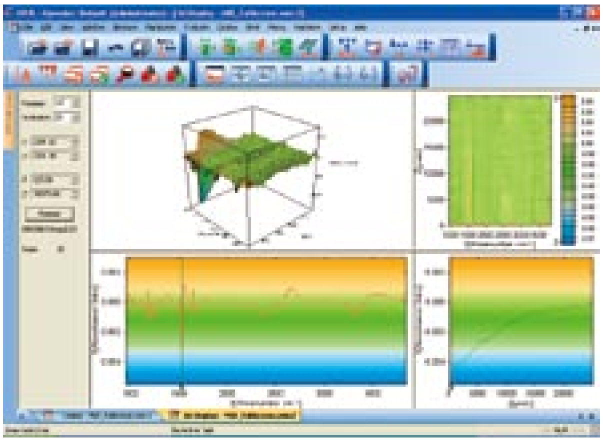

Figure 2. Time-resolved FT-IR spectra of bacteriorhodopsin in the whole mid-infrared region. By use of D_2O and optimizing hydration level, plausible spectral changes were observed.

2. Perfusion-Induced Difference FT-IR Spectroscopy Investigating Ion Binding Sites of Membrane Proteins

Membrane proteins are important for homeostasis of living cells, which work as ion channel, ion pump, various types of chemical and biophysical sensors, *etc*. These proteins are considered as one of important targets for biophysical studies. However, their molecular mechanisms have not been studied well, because X-ray crystallography and NMR spectroscopy are hard to access them in general. Recently, it has been demonstrated that stimulus-induced attenuated total reflection (ATR) FTIR spectroscopy is another promising technique for investigating molecular mechanism of membrane proteins.

In 2009 before coming to IMS, I have demonstrated molecular mechanism of the proton releasing group (PRG) in *pharaonis* phoborhodopsin (*p*pR) by means of Cl$^-$-induced and light-induced difference ATR-FTIR spectroscopy in aqueous condition.$^{2)}$ *Pharaonis* phoborhodopsin (*p*pR, also called *pharaonis* sensory rhodopsin II; *p*SRII) is a photoreceptor for negative phototaxis in *Natronomonas pharaonis*, and in the absence of transducer protein, *p*HtrII, *p*pR can pump protons like BR. Fast, BR-like proton release was observed during the lifetime of the M intermediate (ppR_M) at acidic pH, but it was diminished in the absence of Cl$^-$. It was suggested that Cl$^-$ binding controls the pKa of PRG in *p*pR and ppR_M.

As shown in Figure 3, Cl$^-$-induced difference ATR-FTIR spectra clearly demonstrated that Cl$^-$-binding to *p*pR accompanies protonation of a carboxylic acid (C=O stretch at 1724 cm^{-1}). The amino acid was identified as Asp193, because the corresponding band is shifted to 1705 cm^{-1} in the D193E mutant protein. It means that the PRG of *p*pR includes Asp193, whose pKa change is partly controlled by Cl$^-$.

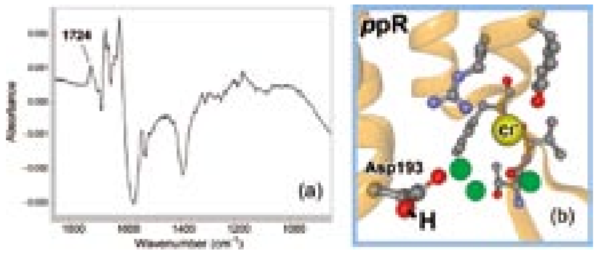

Figure 3. (a) Chloride-ion binding induced difference infrared spectra of a membrane protein (*pharaonis* phoborhodopsin; light sensor in an archaebacterium). The 1724-cm^{-1} band was assigned to the protonated carboxylate group of Asp193. (b) The existence of hydrogen at Asp193, which has not been detected by X-ray crystallography, was revealed by infrared spectroscopy.

Application of ATR-FTIR to other membrane proteins, such as an ion channel (KcsA) and a transporter protein (V-ATPase), started before coming to IMS. It has been succeeded to measure the difference infrared spectra between the conditions of several types of ions and pH. Based on these spectra, the molecular mechanism of recognition and transportation of ions will be discussed in the near future.

At IMS, I will develop new methods of stimulus-induced ATR-FTIR spectroscopy by constructing stopped-flow system or using caged compounds for improving time-resolution. Reduction of buffer waste is also important for using isotope labeled water or expensive reagents, which will be achieved by designing a micro-flow chamber.

References

1) V. A. Lórenz-Fonfría, Y. Furutani and H. Kandori, *Biochemistry* **47**, 4071–4081 (2008).

2) Y. Kitade, Y. Furutani, N. Kamo and H. Kandori, *Biochemistry* **48**, 1596–1603 (2009).

Heterogeneous Catalytic Systems for Organic Chemical Transformations in Water

Department of Life and Coordination-Complex Molecular Science
Division of Complex Catalysis

UOZUMI, Yasuhiro	Professor
OSAKO, Takao	Assistant Professor
HAMASAKA, Go	Post-Doctoral Fellow
MATSUURA, Yutaka	Post-Doctoral Fellow
YAMAMOTO, Yoshikazu	Post-Doctoral Fellow
HIRAI, Yoshinori	Research Fellow
BEPPU, Tomohiko	Graduate Student
WATANABE, Toshihiro	Graduate Student
KOBAYASHI, Noboru	Graduate Student
MUTO, Tsubasa	Graduate Student
TORII, Kaoru	Technical Fellow
SASAKI, Tokiyo	Secretary
TANIWAKE, Mayuko	Secretary
FUKUSHIMA, Tomoko	Secretary

Various organic molecular transformations catalyzed by transition metals were achieved under heterogeneous aqueous conditions by use of amphiphilic resin-supported metal complexes or convoluted polymeric metal catalysts which were designed and prepared by this research group. In particular, asymmetric Suzuki-Miyaura coupling and oxidative cyclization of alkenols and alkenoic acids, both of which were performed in water under heterogeneous conditions with high recyclability of the polymeric catalysts, are highlights among the achievements of the 2008–2009 period to approach what may be considered ideal chemical processes of next generation. Representative results are summarized hereunder.

1. Synthesis of [2,6-Bis(2-oxazolinyl)phenyl]palladium Complexes via the Ligand Introduction Route[1)]

A series of [2,6-bis(2-oxazolinyl)phenyl]palladium (Phebox-Pd) complexes were synthesized via the ligand introduction route. *trans*-Bromo(2,6-dicarboxyphenyl)bis(triphenyl phosphine)palladium was prepared by the reaction of 2-bromoisophthalic acid with $Pd(PPh_3)_4$ in 93% yield, and the carboxy groups of the palladium complex were converted into the oxazolinyl groups to give the Phebox-Pd complexes in 44–57% yield (Scheme 1).

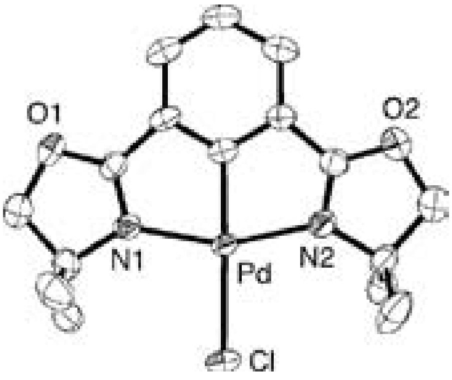

Figure 1. ORTEP drawing of Phebox-Pd complex.

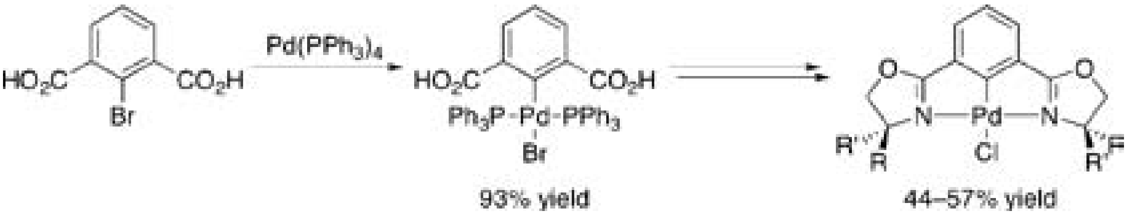

Scheme 1. Ligand Introduction Route for the Synthesis of [2,6-Bis(2-oxazolinyl)phenyl]palladium Complexes.

2. Development of Tightly Convoluted Polymeric Phosphotungstate Catalysts and Their Application to an Oxidative Cyclization of Alkenols and Alkenoic Acids[2)]

Tightly convoluted polymeric phosphotungstate catalysts were prepared via ionic-assembly of $H_3PW_{12}O_{40}$ and poly(alkylpyridinium)s. An oxidative cyclization of various alkenols and alkenoic acids was efficiently promoted by the polymeric phosphotungstate catalyst in *aq*. H_2O_2 in the absence of organic solvents to afford the corresponding cyclic ethers and lactones in high yield. The catalyst was reused four times without loss of catalytic activity. The polymeric phosphotungstate was unambiguously characterized by spectro- and microscopic studies (MAS $^{31}P\{^1H\}$ NMR, IR spectroscopy, elemental analysis, TEM, SEM, and EDS).

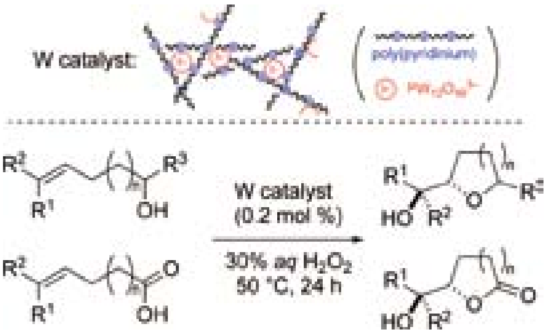

Scheme 2. Oxidative Cyclization of Alkenyl Alcohols and Alkenoic Acids with a Convoluted Polymeric Phosphotungstate.

3. Asymmetric Suzuki-Miyaura Coupling in Water with an Amphiphilic Resin-Supported Chiral Palladium Catalyst[3)]

Asymmetric Suzuki-Miyaura coupling of aryl halides (Cl, Br, I) and aryl boronic acids was achieved in water with wide functional group tolerance by use of a readily-recyclable amphiphilic polymer (PS-PEG) resin-supported chiral imidazoindolephosphine-palladium complex to give a variety of biaryls with up to 94 % ee.

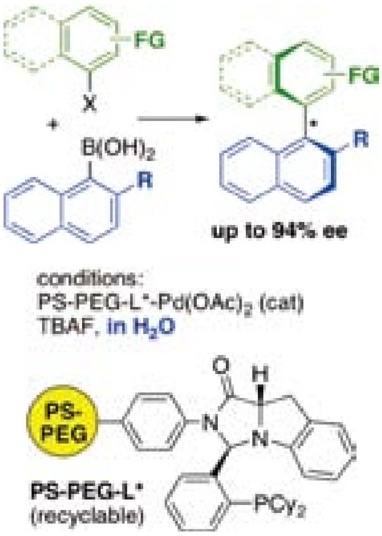

Scheme 3. Asymmetric Suzuki-Miyaura Coupling in Water with an Amphiphilic Resin-Supported Chiral Palladium Complex.

References

1) T. Kimura and Y. Uozumi, *Organometallics* **27**, 5159–5162 (2008).

2) Y. M. A. Yamada, H. Guo and Y. Uozumi, *Heterocycles* **76**, 645–655 (2008).

3) Y. Uozumi, Y. Matuura, T. Arakawa and Y. M. A. Yamada, *Angew. Chem., Int. Ed.* **48**, 2708–2710 (2009).

Synthesis of Metal Complexes Aiming at Reversible Conversion between Chemical Energy and Electrical One

Department of Life and Coordination-Complex Molecular Science
Division of Functional Coordination Chemistry

TANAKA, Koji	Professor
WADA, Tohru	Assistant Professor
OHTSU, Hideki	IMS Research Assistant Professor
FUKUSHIMA, Takashi	Post-Doctoral Fellow
SUMANTA, Kumar	Post-Doctoral Fellow
BAI, Zhengshuai	Post-Doctoral Fellow
MIYAJI, Mariko	Post-Doctoral Fellow
TSUKAHARA, Yuhei	Graduate Student
YAMAGUCHI, Yumiko	Secretary
NAKAGAKI, Shizuka	Secretary

Metal ions involved in various metal proteins play key roles to generate metabolic energies through redox reactions of bio-organic molecules. Metal complexes that have an ability to oxidize organic molecules at potentials more negative than reduction of dioxygen are feasible molecular energy converters from chemical energy to electrical one. High valent Ru=O complexes are prepared by sequential proton and electron loss of the correspondent aqua-Ru complexes. Although some of them are active for the oxidation of organic molecules, the oxidation potentials required to convert from Ru-OH_2 to high valent Ru=O species are generally too positive for the purpose of the use as the energy converters. On the other hand, unusual Ru–oxyl radical complexes spontaneously are formed by deprotonation of aqua-Ru-dioxolene complexes due to intramolecular charge transfer from the negatively charged deprotonated aqua ligand to dioxolene (eq 1). Oxyl radical complexes formed in eq 1 are expected to have an ability to abstract hydrogen atom of C–H bonds of organic molecules, which would play the key role in the energy conversion from chemical energy to electrical one.

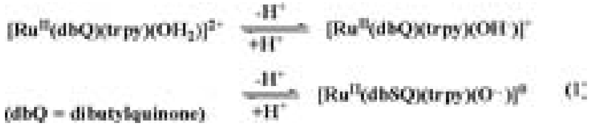

The difficulty in photochemical activation of small inorganic molecules such as N_2, O_2, CO_2, and H_2O results from the undesirable formation of high energy intermediates that are produced by stepwise one-electron transfer to the reaction centers. Recently, we showed that a mononuclear $[Ru^{II}(pbn)(bpy)_2]^{2+}$ (bpy = 2,2'-bipyridine, pbn = 2-(2-pyridyl)benzo[*b*]-1,5-naphthyridine) ($[\mathbf{1}]^{2+}$) is smoothly reduced to $[Ru(pbnH_2)(bpy)_2]^{2+}$ ($[\mathbf{1}H_2]^{2+}$) under visible light irradiation in the presence of sacrificial electron donors (eq 2). Furthermore, oxidation of $[\mathbf{1}H_2]^{2+}$ by appropriate oxidants smoothly regenerates $[\mathbf{1}]^{2+}$. Thus, the $[\mathbf{1}H_2]^{2+}/[\mathbf{1}]^{2+}$ redox couple is the first functional model of the nicotinamide adenine dinucleotide NAD^+/NADH redox reaction that works as a reservoir/source of two electrons and one proton in various biological energy transfer systems.

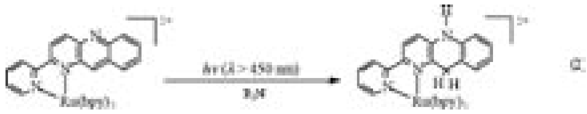

1. Synthesis and Electrochemical Reduction of Novel Ruthenium Complex Having *N*,*N*-Bis(benzo[*b*]-1,5-naphthyridin-2-ylmethyl)propane-2-amine Ligand as NAD^+/NADH Type Redox Site

Hydrogenation is one of the most important reactions in chemical transformations of a wide range of materials. A variety of metal-hydrides have been used in catalytic hydrogenation reactions under hydrogen gas, but those compounds are generally sensitive to water because of their high reactivity. Alternatively, electrocatalytic reduction without using hydrogen gas has several advantages such as clean, simple, safe, and easy regulation of reactivity of catalysts by choosing applied potentials. On the other hand, the nicotinamide adenine dinucleotide redox couple (NAD^+/NADH) functions as a reservoir/source of two electrons and one proton in various biological redox reactions. To mimic the efficiency and versatility of the NAD^+/NADH redox couple, a variety of model reactions have been conducted by using NADH model compounds. However, the reactions reported so far have been limited to stoichiometric ones. We, therefore, prepared $[Ru(bpy)_2(pbn)](PF_6)_2$ as a molecular electrocatalyst to simulate the function of the NAD^+/NADH redox couple. As mentioned above, the $[Ru(bpy)_2(pbn)]^{2+}/[Ru(bpy)_2(pbnH_2)]^{2+}$ redox couple well simulates the NAD^+/NADH couple. To improve the ability of

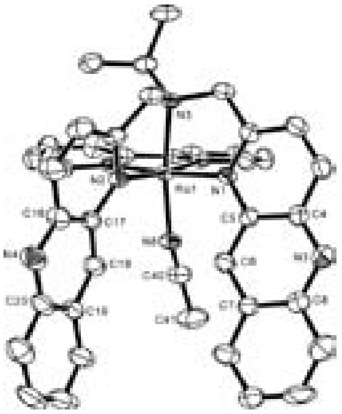

Figure 1. Crystal structure of [Ru(bbnma)(CH_3CN)]$^{2+}$.

multi-electron redox reaction of pbn, a new type of tridentate ligand, *N*,*N*-bis(benzo[*b*]-1,5-naphthyridin-2-ylmethyl) propane-2-amine (denoted as bbnma) possessing two benzo[*b*]-1,5-naphthyridines tethered to tertiary amine was designed and its ruthenium complex, [Ru(bbnma)(bpy)L](PF_6)$_2$, was synthesized. The conception of bbnma is to make a space not only to introduce substrates (*e.g.* ketones, imines, and related substrates) into the ruthenium center by a substitution reaction but also to place them forcibly at the vicinity of the two NADH type hydride sources generating on bbnam coordinated in a facial fashion (Figure 1). In fact, [Ru(bbnma)(bpy)(CO)]$^{2+}$ smoothly underwent four-electron reduction under the electrolysis at –0.95 V in the presence of pivalic acid, and [Ru (bbnmaH_4)(bpy)(CO)]$^{2+}$ was obtained in a high yield.

(1)

2. Photoinduced Four-, and Six-Electron Reduction of Mononuclear Ruthenium Complexes Bearing NAD$^+$ Analogous Ligands

The development of artificial photosynthetic processes aiming to generate high-energy molecules from low-energy ones (*e.g.* reduction of carbon dioxide or water splitting) is the top research priority to regulate consumption of non-renewable fossil fuels against the strong pressure of the energy demand that keeps increasing. Multi-electron reactions through stepwise one-electron transfer inevitably generate high-energy free radical intermaeiates, which often yield undesired products. Therefore construction of artificial photosynthetic systems that are able to mediate multi-electron transfer from photosensitizers to the reaction sites without accompanying high energy intermediates would open new era to achieve light-driven multi-electron carbon dioxide reduction and water splitting. Despite the large efforts devoted to the development of complex supramolecular assemblies for light harvesting and directional charge separation, photosynthetic systems designd for light-induced multi-electron transfer rarely generate reducing equivalents. As mentioned above, we have succeeded photochemical two-electron reduction of [Ru(bpy)$_2$(pbn)]$^{2+}$ ([**1**]$^{2+}$) affording [Ru(bpy)$_2$(pbnH_2)]$^{2+}$ in the presence of N(CH_2CH_2OH)$_3$ (eq 2). Photochemical two-electron reduction of [Ru(bpy)$_2$(pbn)]$^{2+}$ proceeds via (i) reductive quenching of photo-exited [Ru(bpy)$_2$(pbn)]$^{2+*}$ by N(CH_2CH_2OH)$_3$, (ii) subsequent protonation of free nitrogen of the anion radical pbn ligand of [Ru(bpy)$_2$(pbn$^{-\bullet}$)]$^+$, (iii) inter-molecular π–π adduct formation between two neutral pbnH$^\bullet$ of the resultant [Ru(bpy)$_2$(pbnH$^\bullet$)]$^+$, and (iv) disproportionation of {[Ru(bpy)$_2$ (pbnH$^\bullet$)]$^+$}$_2$ affording an equimolar mixture of [Ru(bpy)$_2$ (pbnHH)]$^{2+}$ and [Ru(bpy)$_2$(pbn)]$^{2+}$. The finding of the path for the two-electron reduction driven us to repeat the two-electron reduction of pbn of [Ru(bpy)(pbn)$_2$](PF_6)$_2$ ([**2**] (PF_6)$_2$) and [Ru(pbn)$_3$](PF_6)$_2$ ([**3**](PF_6)$_2$) to achieve the first photochemical four- and six-electron reductions of monomeric metal complexes.

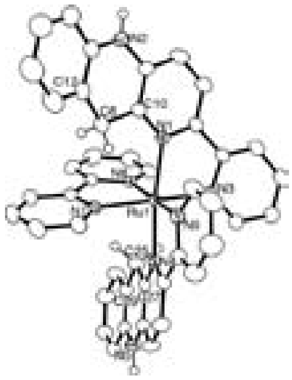

Figure 2. Crystal structure of [Ru(bpy)(pbnH_2)]$^{2+}$.

The molecular structure of [**2**](PF_6)$_2$ (Figure 2) has a C_2 symmetry. Although many attempts to grow single crystal of [**3**](PF_6)$_2$ for X-ray diffraction study were not succeeded, an appearance of 33 proton signals in the aromatic region in the ^{1}H NMR spectrum implied the formation of a single stereo isomer of [**3**]$^{2+}$. Low enrgy level of π* orbiatal of pbn of [**1**]$^{2+}$, [**2**]$^{2+}$ and, [**3**]$^{2+}$ reflects their redox potentilas; they showed one (–1.07 V vs Ag/AgNO$_3$), two (–1.01 and –1.14 V), and three (–0.94, –1.11, and –1.31 V) pbn localized reversible (pbn/ pbn$^{-\bullet}$) redox couples in the cyclic voltammogram. Irradiation of visible light to [**2**](PF_6)$_2$ and [**3**](PF_6)$_2$ in CH_3CN/N(CH_2CH_2OH)$_3$ (4 : 1, v/v) smoothly produced [**2**·H_4]$^{2+}$ and [**3**·H_6]$^{2+}$ with time.

References

1) K. Kimura and K. Tanaka, *Angew. Chem., Int. Ed.* **47**, 9768–9771 (2008).
2) D. Polansky, D. Cabelli, J. Muckerman, T. Fukushima, K. Tanaka and E. Fujita, *Inorg. Chem.* **47**, 3958–3968 (2008).

Visiting Professors

Visiting Professor
ITOH, Shinobu *(from Osaka University)*

Dioxygen Activation Mechanism by Copper Proteins and Models

The structure and reactivity of copper/active-oxygen complexes have attracted much interest during the past decades because of their potential relevance to biological systems and numerous copper-catalyzed oxidation reactions. In our laboratory, we have been studying the reactivity of several types of copper/active-oxygen species such as mononuclear copper(II)-superoxo and copper(II)-hydroperoxo complexes as well as dinuclear copper(II)-peroxo and bis(μ-oxo)dicopper(III) complexes in order to evaluate the catalytic mechanism of copper oxygenases and to develop efficient oxidation catalysts for organic synthesis.

Visiting Professor
TAKAHASHI, Satoshi *(from Tohoku University)*

Dynamics of Protein Folding by Single Molecule and Ensemble Techniques

Protein is a linear macromolecule that has a unique property to fold to a specific three-dimensional structure from fully unfolded conformations. We are interested in the physical principles that connect the unfolded and the folded conformations of proteins. To detect fast kinetic processes involved in protein folding, we use rapid mixing device for the time resolved observation of average protein structures. To observe heterogeneity and dynamic fluctuations, we use single molecule observation systems. Based on the ensemble measurements on several proteins using small angle X-ray scattering and circular dichroism spectroscopy, we proposed “collapse and search” mechanism of protein folding. The recent application of single molecule fluorescence measurements clarified a relatively slow conformational dynamics in the unfolded state. We are hoping to obtain important information required for the protein structure prediction and design through the further examination of protein folding dynamics.

Visiting Associate Professor
HASEGAWA, Miki *(from Aoyama Gakuin University)*

Development of the Polarized Emission System of Lanthanide Complexes in the Nano-Thickness Molecular Films

The nano-thickness molecular films containing lanthanide ions induce the polarized emission. The phenomenon is not generally observed from both a fluorescent organic compound and a lanthanide ion. However, we firstly succeeded to construct functional multilayers by the Langmuir-Blodgett (LB) method. The film containing the Pr(III) layer showed the polarized ππ* emission of the inserted aromatic molecule, which was slightly affected by the interaction with metals. On the other hand, the Eu(III) layer within the film led to the polarized ff-emissions of metal ion itself. The principle should be clarified from the viewpoint of molecular science. We are in progress to reveal the relation between the structure around metals and the photo-phenomena of the lanthanides’ LB film.

RESEARCH FACILITIES

The Institute includes five research facilities. This section describes their latest equipment and activities. For further information please refer to previous IMS Annual Review issues (1978–2008).

UVSOR Facility

KOSUGI, Nobuhiro	Director
KATOH, Masahiro	Professor
SHIGEMASA, Eiji	Associate Professor
KIMURA, Shin-ichi	Associate Professor
HIKOSAKA, Yasumasa	Assistant Professor
ITO, Takahiro	Assistant Professor*
ADACHI, Masahiro	Assistant Professor
ZEN, Heishun	Assistant Professor
HORIGOME, Toshio	Technical Associate
NAKAMURA, Eiken	Technical Associate
YAMAZAKI, Jun-ichiro	Technical Associate
HASUMOTO, Masami	Technical Associate
SAKAI, Masahiro	Technical Associate
HAYASHI, Kenji	Technical Associate
KONDO, Naonori	Technical Associate
TOKUSHI, Tetsunari	Technical Fellow
HAGIWARA, Hisayo	Secretary

Outline of UVSOR

The UVSOR accelerator complex consists of a 15 MeV injector linac, a 600 MeV booster synchrotron, and a 750 MeV storage ring. The magnet lattice of the storage ring is the so-called double-bend achromat. The double RF system is routinely operated for the user beam time, and the lifetime of the electron beam has been improved to around 6 hours at 200 mA. The storage ring is normally operated under multi-bunch mode with partial filling. The single bunch operation is also conducted about two weeks per year, which provides pulsed synchrotron radiation (SR) for time-resolved experiments. Initial beam currents stored under multi-bunch and single-bunch modes are 350 mA and 70 mA, respectively.

Eight bending magnets and three insertion devices are available for utilizing SR. The bending magnet with its radius of 2.2 m provides SR, whose critical energy is 425 eV. After completing the upgrade project, there are 14 beamlines available in total (13 operational, and 1 under construction) at UVSOR, which can be classified into two categories. 9 of them are the so-called "Open beamlines," which are open to scientists of universities and research institutes belonging to the government, public organizations, private enterprises and those of foreign countries. The rest of the 5 beamlines are the so-called "In-house beamlines," which are dedicated to the use of the research groups within IMS. We have 1 soft X-rays (SX) station equipped with a double-crystal monochromator, 8 EUV and SX stations with a grazing incidence monochromator, 3 VUV stations with a normal incidence monochromator, 1 (far) infrared station equipped with FT interferometers, 1 station with a multi-layer monochromator.

Figure 1. Overview of the UVSOR storage ring room.

Collaborations at UVSOR

Variety of investigations related to molecular/material science is carried out at UVSOR by IMS researchers. In addition, many researchers outside IMS visit UVSOR to conduct their own research work. The number of visiting researchers per year tops about 800, whose affiliations extend to 60 different institutes. International collaboration is also pursued actively and the number of visiting foreign researchers reaches over 80, across 10 countries. UVSOR invites new/continuing proposals for research conducted at the open beamlines twice a year. The proposals from academic and public research organizations (charge-free) and from enterprises (charged) are acceptable. The fruit of the research activities using SR at UVSOR is published as a UVSOR ACTIVITY REPORT annually. The refereed publications per year count more than 60 since 1996. In recent five years, the number of beamlines has been reduced from 22 to 14. The upgrade project of the UVSOR storage ring, in which the creation of four new straight sections and the achievement of much smaller emittance (27 nm-rad) were planned in 2002–2003, has been accomplished on schedule. The upgraded storage ring is named UVSOR-II. The numbers of users and related publications have shown an upward tendency, since 2004.

Highlights of Users' Researches 2008

1) Modification of Gallium Oxide Photocatalyst with Mg Ions

K. Shimura, T. Yoshida, H. Yoshida *(Nagoya Univ.)*

The development of a hydrogen production method from renewable resources and natural energy would be important to realize a sustainable society. Photocatalytic steam reforming of methane (PSRM; $CH_4 + 2H_2O \rightarrow 4H_2 + CO_2$) is an attractive reaction because it has a potential to produce hydrogen from water and biomethane by using solar energy. We applied the Ga_2O_3 photocatalyst for PSRM and examined the loading effect of Mg ions on the structure and the activity of Ga_2O_3.

Mg K-edge XANES spectrum of MgO shows some peaks and Ga L_I-edge XANES of Ga_2O_3 was broad spectrum although both absorption edges are known to appear at 1307 eV (Figure 2 (a) and (f)). The spectra of Mg^{2+}-loaded Ga_2O_3 samples calcined at various temperatures were much different from each other (Figure 2 (b)–(d)). For the sample calcined at 773 K, the spectrum was similar to that of MgO. When the calcination temperature was higher than 1073 K, the spectra were the same as that of $MgGa_2O_4$ spinel. It was suggested that Mg ions would form $MgGa_2O_4$ spinel-like local structure by substituting for Ga ions at tetrahedral site when the calcination temperature was higher than 1073 K. The Mg ions in the bulk would improve the property of the Ga_2O_3 photocatalyst.

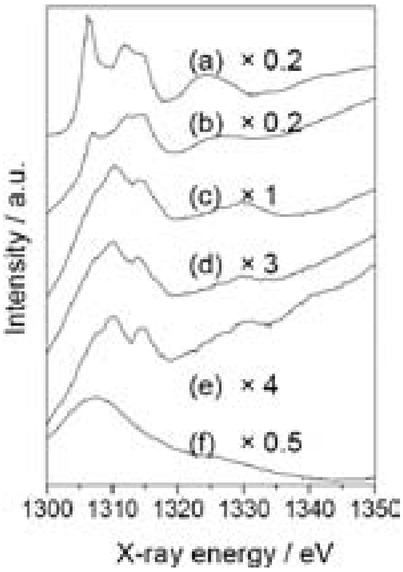

Figure 2. X-ray absorption spectra of (a) MgO, (b)–(d) Mg^{2+}-loaded Ga_2O_3 samples, (e) $MgGa_2O_4$ and (f) Ga_2O_3. Loading amount was 2 mol%. The calcination temperature was (b) 773 K, (c) 1073 K and (d) 1273 K, respectively.

2) Magneto-Optical Kerr Effect in $Nd_2(Mo_{1-x}Nb_x)_2O_7$

S. Iguchi, S. Kumakura, Y. Onose, Y. Tokura *(Univ. of Tokyo)*

The origin of the anomalous Hall effect (AHE) has long been discussed since 1960's in terms of the band effect by Karplus-Luttinger, the spin fluctuation, and the side jump, *etc*. Recent theoretical studies on the AHE due to the Berry phase or the spin-chirality mechanism are the quantum theoretical extension from the traditional perturbative treatment by Karplus-Luttinger, and have revealed the significance of the resonant effect at a small gap in band structure due to some kind of interaction, such as the spin–orbit interaction or the spin chirality. Magneto-optical Kerr effect (MOKE) is an extension of AHE with respect to the energy range. The MOKE measurements for $Nd_2Mo_2O_7$ with spin chirality and $Gd_2Mo_2O_7$ without it have revealed that there is an enhancement in the mid-IR region of the off-diagonal optical conductivity $\sigma_{xy}(\omega)$ originated from the spin chirality.

Figure 3 shows the spectra of the optical conductivity, the real and imaginary components of $\sigma_{xy}(\omega)$ in NMNO at 10 K. The $\sigma_{xx}(\omega)$ shows the correspondent change with the dc conductivity (metallic to insulating with increasing x) without remarkable anomaly such as a peak. In contrast, the characteristic peak structure was observed in the mid-IR range in the $\sigma_{xy}(\omega)$ as well as the continuity to the dc value. Especially, some of the peak-top values are larger than dc ones meaning the resonance effect is intrinsic for the off diagonal conductivity. The shift of the peak to higher energy is considered as the increase in the chemical potential by Nd doping.

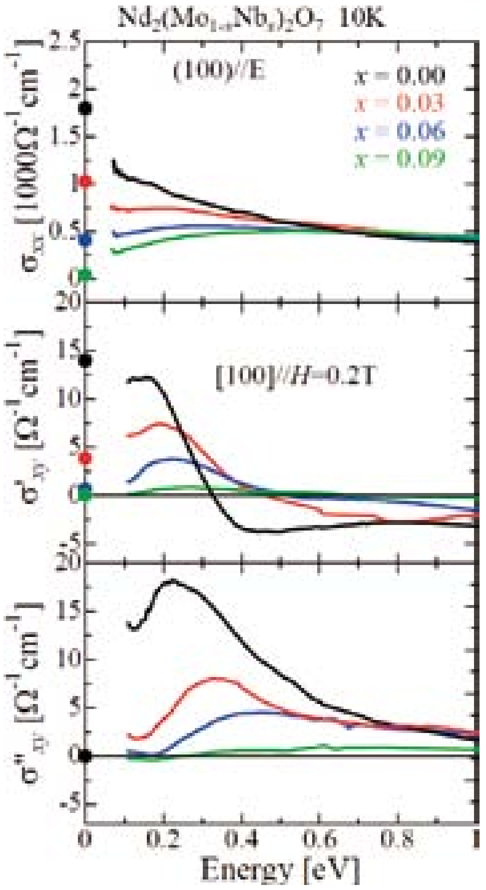

Figure 3. (a) The optical conductivity, (b) the real and (c) the imaginary part of off-diagonal optical conductivity in NMNO at 10 K.

---

* Present Address; Nagoya University , Furo-cho, Chikusa-ku, Nagoya 464-8601

Research Center for Molecular Scale Nanoscience

YOKOYAMA, Toshihiko	Director, Professor
HIRAMOTO, Masahiro	Professor
NISHI, Nobuyuki	Professor
OKAMOTO, Hiromi	Professor
NAGAYAMA, Kuniaki	Professor (OIIB)
KATO, Koichi	Professor (OIIB)
UOZUMI, Yasuhiro	Professor
NAGASE, Shigeru	Professor
OGAWA, Takuji	Professor
SUZUKI, Toshiyasu	Associate Professor
NAGATA, Toshi	Associate Professor
SAKURAI, Hidehiro	Associate Professor
NISHIMURA, Katsuyuki	Associate Professor
TADA, Mizuki	Associate Professor
TANAKA, Shoji	Assistant Professor
SAKAMOTO, Yoichi	Assistant Professor
HIGASHIBAYASHI, Shuhei	Assistant Professor
KAJI, Toshihiko	Assistant Professor
NAKAO, Satoru	Post-Doctoral Fellow (NanoNet project)
SUGIHARA, Takahiro	Research Fellow*
NOTO, Madomi	Secretary
SUZUKI, Hiroko	Secretary
WATANABE, Yoko	Secretary
FUNAKI, Yumiko	Secretary
ITO, Yumi	Secretary (Nanonet project)

Research Center for Molecular Scale Nanoscience was established in 2002 with the mission of undertaking comprehensive studies of “Molecular Scale Nanoscience.” The Center consists of one division staffed by full-time researchers (Division of Molecular Nanoscience), two divisions staffed by adjunctive researchers (Divisions of Instrumental Nanoscience and Structural Nanoscience), one division staffed by visiting researchers (Division of Advanced Molecular Science). Their mandates are

1) Fabrication of new nanostructures based on molecules
2) Systematic studies of unique chemical reactions
3) Systematic studies of physical properties of these nanostructures.

The Center administers offers public usage of the advanced ultrahigh magnetic field NMR (Nuclear Magnetic Resonance, 920 MHz) spectrometer not only for solution specimens but for solid samples. Since 2004 a number of collaborating researches with the 920 MHz NMR measurements have been examined. Figure shows the apparatus, together with a typical example of the NMR spectra, where one can easily find much better resolving power than that of a standard 500 MHz NMR spectrometer. (1) dynamic structures of biological macromolecules, (2) structure of bioactive natural products, (3) characterization of metal ion complexes and so forth. We will continuously call for the collaborating research applications using the 920MHz NMR spectrometer with a view to use the NMR of a wide scientific tolerance (*e.g.* structural biology, organic chemistry, catalyst chemistry, *etc*.).

Since 2005, Nanoforum has been organized, which supports small international/domestic meetings and seminars related to nanoscience. The Center also conducts the Nanotechnology Network Project of the Ministry of Education, Culture, Sports, Science and Technology (MEXT) as a core organization, and provides various kinds of nanotechnology public support programs to Japanese and foreign researchers. This project will be described in the other section in this book.

Figure 1. 920 MHz NMR spectrometer and an example measured using 920 and 500 MHz spectrometers. Much higher resolution in 920 MHz can be clearly seen.

---

* from JEOL Datum

Laser Research Center for Molecular Science

OHMORI, Kenji	Director, Professor
KATOH, Masahiro	Professor
OKAMOTO, Hiromi	Professor
OHSHIMA, Yasuhiro	Professor
MATSUMOTO, Yoshiyasu	Professor
TAIRA, Takunori	Associate Professor
HISHIKAWA, Akiyoshi	Associate Professor
ISHIZUKI, Hideki	Assistant Professor
CHIBA, Hisashi	Technical Associate
MASUDA, Michiko	Secretary

The center aims to develop new experimental apparatus and methods to open groundbreaking research fields in molecular science, in collaboration with the Department of Photo-Molecular Science. Those new apparatus and methods will be served as key resources in advanced collaborations with the researchers from the community of molecular science. The main targets are (1) advanced photon sources covering wide energy ranges from terahertz to soft X-day regions; (2) novel quantum-control schemes based on intense and ultrafast lasers; and (3) high-resolution optical imaging and nanometric microscopy. The center also serves as the core of the joint research project “Extreme Photonics” between IMS and RIKEN.

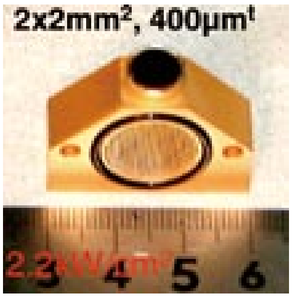

Figure 1. Microchip laser developed at the center.

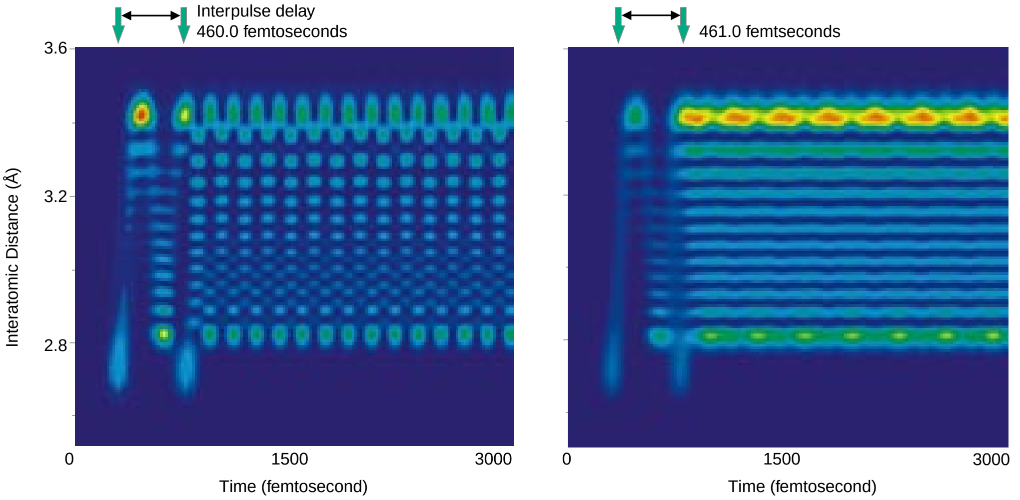

Figure 2. Theoretical simulation of quantum interferometric images generated in a single molecule with a pair of two laser pulses whose timing is controlled on the attosecond (10^{-18} sec) timescale.

Instrument Center

YAKUSHI, Kyuya	Director
YAMANAKA, Takaya	Technical Associate
TAKAYAMA, Takashi	Technical Associate
FUJIWARA, Motoyasu	Technical Associate
OKANO, Yoshinori	Technical Associate
MIZUKAWA, Tetsunori	Technical Associate
MAKITA, Seiji	Technical Associate
NAKANO, Michiko	Technical Associate
SAITO, Midori	Technical Associate
UEDA, Tadashi	Technical Associate
OTA, Akiyo	Secretary
NAKAGAWA, Nobuyo	Secretary

Instrument Center was organized in April of 2007 by integrating the general-purpose facilities of research center for molecular-scale nanoscience and laser research center for molecular science. The mission of Instrument Center is to support the in-house and external researchers in the field of molecular science, who are conducting their researches with the aid of general-purpose instruments such as ESR, x-ray diffractometer, fluorescence spectrometer, *etc*. The staffs of Instrument Center maintain the best condition of the machines, and provide consultation for how to use them. The main instruments are NMR (JEOL JNM-LA500, JEOL JNM-LA400), mass spectrometer (Voyager DE-STR), powder x-ray diffractometer (Rigaku RINT-Ultima III), and circular dichroic spectrometer (JASCO JW-720WI) in Yamate campus and ESR (Bruker E680, E500, EMX Plus), SQUID (Quantum Design MPMS-7, MPMS-XL7minTK), powder (MAC Science MXP3) and single-crystal (Rigaku Mercury CCD, RAXIS IV, 4176F07) diffractometers, thermal analysis instrument (TA TGA2950, DSC2920, SDT2960), fluorescence spectrophotometer (SPEX Fluorogll), UV-VIS-NIR (Hitachi U-3500) spectrophotometer, excimer+dye laser system (LPX105i+LPD3002), Nd-YAG+ OPO laser (GCR-250), and excimer laser (Complex 110F) in Myodaiji campus. Instrument Center provides liquid nitrogen and liquid helium using helium liquefiers. The staffs of Instrument Center provide consultation for how to treat liquid helium, and provide various parts necessary for low-temperature experiments. Instrument Center supports also the network sharing system of the chemistry-oriented instruments, which started in the April of 2007.

In the fiscal year of 2008 (April 2008 to March 2009), Instrument Center introduced new equipments shown below: Differential scanning calorimeter (VP-DSC) [Yamate campus], Isothermal titration calorimeter (iTC200) [Yamate campus], X-ray fluorescence spectrometer (JEOL JSX-3400RII) [Myodaiji campus]. The excimer laser of Excimer+dye laser system (Lambda physics LPX 105i + LPD3002) [Myodaiji] was renewed, and Picosecond tunable laser system (TSUNAMI-TITAN-TOPAS) [Myodaiji campus] was transferred from the research group of Professor Nishi. Instrument Center accepted 61 applications from 29 institutions outside of IMS. The users mainly used SQUID (22), ESR (20), x-ray diffractometer (24), circular dichroism spectrometer (6), thermal analysis instrument (5), mass spectrometer (4), NMR (2), and Excimer-dye laser (3), where the numbers in parenthesis shows the number of use by external users. Instrument Center provided 54,716 ℓ of liquid helium, 71,964 ℓ of liquid nitrogen, and 1,406 m^3 of nitrogen gas.

Figure 1. Differential scanning calorimeter (VP-DSC).

Figure 2. Isothermal titration calorimeter (iTC200).

Figure 3. X-ray fluorescence spectrometer (JEOL JSX-3400RII).

Figure 4. Picosecond tunable laser system (TSUNAMI-TITAN-TOPAS System).

Figure 5. Excimer+dye laser (Lambda physics LPX 105i + LPD3002)

Equipment Development Center

URISU, Tsuneo	Director
MIZUTANI, Nobuo	Technical Associate
AOYAMA, Masaki	Technical Associate
YANO, Takayuki	Technical Associate
KONDOU, Takuhiko	Technical Associate
YOSHIDA, Hisashi	Technical Associate
UTCHIYAMA, Kouichi	Technical Associate
TOYODA, Tomonori	Technical Associate
NAGATA, Masaaki	Technical Associate
TAKADA, Noriko	Technical Associate
MIYASHITA, Harumi	Technical Fellow
TAKAMATSU, Yoshiteru	Technical Fellow
URANO, Hiroko	Secretary

Design and fabrication including the research and developments of the new instruments demanded for the molecular science are the mission of this center, which consists of the mechanical, electronics and glass work sections. We expanded our service to the researchers of other universities and research institutes since 2005. The main aims of this new attempt are to contribute to the molecular science community and to improve the technology level of the center staffs.

The technical staff of the Equipment Development Center is engaged in planning, researching, designing and constructing high technology experimental instruments in collaboration with the scientific staff. And these experimental instruments are manufactured by incorporating with new technologies and new mechanical ideas. A part of our activity in the current fiscal year is described below.

Development of Universal Data Logger with USB 2.0 Interface for NMR Spectroscopy

This project was proposed by Associate Prof. Kawamoto (Faculty of Science, Hokkaido University). Since FID (Free Induction Decay) signal of NMR spectroscopy decays fast and amplitude of the signal is very small, the high speed and high resolution A/D system is required. However, commercially available products are expensive and some of them are obsolete. Although USB is the most popular interface between A/D devices and computer, it is difficult to make an original interface circuit board for transmitting A/D data to a personal computer. Then, we developed the universal data logger with USB connection for high speed and high resolution A/D converter evaluation board.

We assumed the evaluation board of AD9248BCPZ-40, 14bit, dual inputs, 40MSPS A/D converter (Figure 1, left) as the target A/D device. The data from A/D converter are stored to 4Mbits SRAM controlled with CPLD XC95144XL-10TQ144 with the hardware description language, VHDL, and transmitted to computer via USB by CY7C68013A-56, high speed USB 2.0 microcontroller. The system (Figure 1, right) can be constructed with commercially available components and some customized codes.

The transfer rate of this equipment is about 13.08 msec for transmitting 4 Mbits data (4 Mbit/13.08 msec) 305.8 Mbps). This rate is sufficient for NMR Spectroscopy and most of transient measurements. Our system can be easily upgraded to up to date A/D device with minimal modifications of the source code.

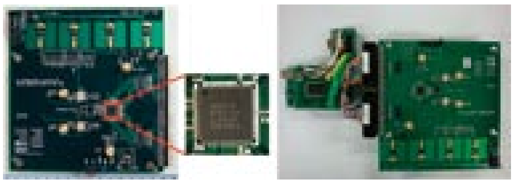

Figure 1. A/D converter and evaluation board (left) and constructed data logger (right).

Fabrication of Acrylic Substrate for 4x4 Points Type Ion Channel Biosensor

For fabrication of 4×4 points type ion channel biosensor which is currently under development in Urisu group, it is required to precisely form the 4×4 electrode inserting parts in the acrylic thin-plate (Figure 2, left). The most important point in this device is the control of thickness X in Figure 2 less than 10 µm in the acrylic substrate homogeneously at the 4×4 electrode points. In order to form this structure, we are trying hot embossing method: a heated metal mold is pressed against the acrylic substrate (cooperated by National Institute of Advanced Industrial Science and Technology (AIST)). To date, we have formed 17µm-thick thin-film in acrylic substrate. SEM image of acrylic substrate after hot embossing is shown in Figures 2 (right).

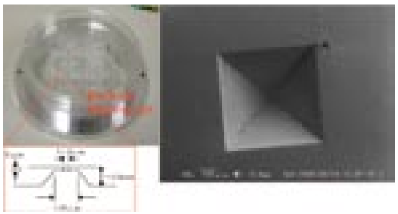

Figure 2. Multipoint type ion channel biosensor (left) and SEM image of acrylic substrate at the electrode inserting part after the hot embossing using a pyramidal mold (right).

Development of LD Pumped Passively Q-Switched Micro-Laser

We developed this equipment requested by Dr. Masaki TSUNEKANE, a member of Advanced Laser Development Division TAIRA Group, in Laser Research Center for Molecular Science. The research and study of a LD-pumped passively Q-switched micro-laser aim for laser ignition of vehicle engines taking the place of a spark plug. The developed passively Q-switched micro-laser module and a commercial spark plug are shown in Figure 3.

We have tested the various designs of micro-lasers at TAIRA Group and have improved the design for high-power, stabilization, and miniaturization. Since we achieved the energy conservation, effective ignition compared to a conventional spark plug and stable ignition for lean mixtures of gasoline and air by using the micro-laser, we have confirmed the practicality and domination of this equipment as the light source for laser ignition of engines. Now we are optimizing the design for further miniaturization comparable to a spark plug and durability to heating and vibration.

Figure 3. Compact micro-laser module.

Motorized XYZ Stages for Inverted Microscopes

This project was proposed by Prof. Urisu, who is developing an *in vitro* neural network device as a new methodology for the study of biomolecular sensing molecular science. The instrument was designed to place the PDMS stamp on the micro-pore position of the Si chip precisely (Figure 4). The specification of this stage system is shown in Table 1. It is carefully designed to provide high performance for routine applications.

Figure 4. Inverted microscope equipped on the motorized XYZ stage.

Table 1. Specification of the motorized XYZ stage.

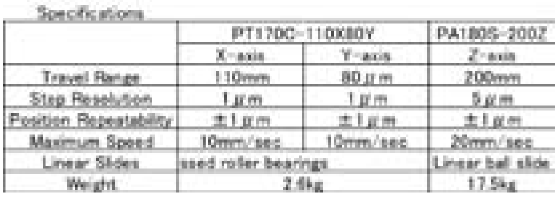

Specifications

	PT170C-110X80Y		PA180S-200Z
	X-axis	Y-axis	Z-axis
Travel Range	110mm	80 μm	200mm
Step Resolution	1 μm	1 μm	5 μm
Position Repeatability	±1 μm	±1 μm	±1 μm
Maximum Speed	10mm/sec	10mm/sec	20mm/sec
Linear Slides	ssed roller bearings		Linear ball slide
Weight	2.4kg		17.5kg

Fabrication of a 3D Microfluidic Circuit for Compartmentalized Culture

3D micro-fluidic circuit for compartmentalized cell culture with a 25 μm hole in diameter cross-shape micro channels with 5 μm height was fabricated by injecting PDMS into a specially designed mold composing of two parts. The mold was achieved using a precise CNC milling machine, collaborating with the company supplying these molds.

Support for Outside Researchers

Table 2 shows the list of the titles which we accepted during July 2008 to June 2009. No. 1 is a design and fabrication of the apparatus to analyze the surface condition of TiO_2 photocatalyst by measuring the water contact angle without exposing to the air after cleaning of the TiO_2 surface. The photograph of the apparatus is shown in Figure 5, left. Number 5 is the fabrication of the high luminance reflection spheroid mirror. The mirror with high profile accuracy and the low surface-roughness was produced by the NC lathe followed by the hand polish processing (Figure 5, right). The number of applications to this study support from the outside researcher was about seven per year as average since 2005. More users are welcome to this system.

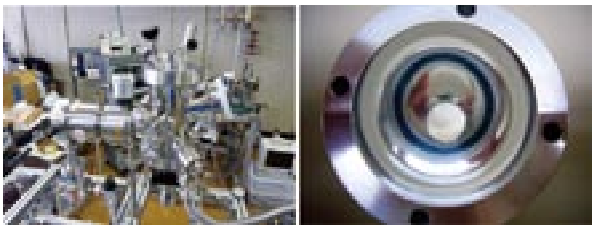

Figure 5. Apparatus for developed for the title No.1 in Table (left), and high luminance reflection spheroid mirror for No. 5.

Table 2. List of orders from outside researchers.

1	Construction of apparatus for analysis of the TiO_2 photoinduced super hydrophilicity mechanisms (HASHIMOTO, Kazuhito/The Univ. Tokyo)
2	Development of the four times reflection type X-rays telescope (TAWARA, Yuzuru/Nagoya Univ.)
3	Fabrication of the high luminance reflection mirror (BABA, Masaaki/Kyoto Univ.)
4	Development of a projection optical system and alignment stage, for ultraviolet radiation and projection exposure system (MEKARU, Harutaka/AIST)
5	Fabrication of the high luminance reflection spheroid mirror (BABA, Masaaki/Kyoto Univ.)
6	Fabrication of the Ga-compression type infrared detector (SUZUKI, Kazushi/Nagoya Univ.)
7	A compact mechanical velocity selector holder of use to analyze molecular alignment (KASAI, Toshio/Osaka Univ.)

Research Center for Computational Science

HIRATA, Fumio	Director, Professor
SAITO, Shinji	Professor
EHARA, Masahiro	Professor
OKUMURA, Hisashi	Associate Professor
OONO, Hitoshi	Assistant Professor
ISHIDA, Tateki	Assistant Professor
KIM, Kang	Assistant Professor
FUKUDA, Ryoichi	Assistant Professor
MIZUTANI, Fumiyasu	Technical Associate
TESHIMA, Fumitsuna	Technical Associate
NAITO, Shigeki	Technical Associate
SAWA, Masataka	Technical Associate
IWAHASHI, Kensuke	Technical Associate
MATSUO, Jun-ichi	Technical Associate
NAGAYA, Takakazu	Technical Associate
TOYA, Akiko	Secretary
ISHIHARA, Mayumi	Secretary

Research Center for Computational Science, Okazaki Research Facilities, National Institutes of Natural Sciences, provides state-of-the-art computational resources and software to academic researchers in molecular science and related fields. The Center currently has over 600 users in 145 project groups from a wide range of molecular science, *i.e.* quantum chemistry, molecular simulation, chemical reaction dynamics and solid state physics. In order to meet a wide variety of users' demands, the computer systems consist of Fujitsu PRIMEQUEST, SGI Altix4700, and Hitachi SR-16000. These systems are linked to Internet through Science Information Network (SINET3).

The Center provides a number of state-of-the-art application programs, including Gaussian 03, GAMESS, Molpro, AMBER, NAMD, *etc*, which are installed to the computer systems and kept updated for immediate use of the users. The Center also maintains and offers the Quantum Chemistry Literature Database (QCLDB, http://qcldb2.ims.ac.jp/), which has been developed by the Quantum Chemistry Database Group in collaboration with staff members of the Center. The latest release, QCLDB II Release 2007, contains 97,718 data of quantum chemical studies. Detailed information on the hardware and software at the Center is available on the web site (http://ccinfo.ims.ac.jp/).

In addition to offering computer resources to molecular scientists, another vital aspect of the Center is to perform leading computational researches with massive computations. In 2003, the Center joined the National Research Grid Initiative (NAREGI) project, a three-year national project by National Institute of Informatics (NII) and IMS. This joint project aimed at developing grid computing system (NII) and thereby realizing extremely large-scale computational studies in the frontier of nanoscience (IMS). For these purposes, two supercomputer systems, Hitachi SR11000 and HA8000, were introduced to the Center in 2004, with combined performance exceeding 10 TFlops. In 2006, the NAREGI project was reformed to join a new national project Development and Application of Advanced High-Performance Supercomputer Project by RIKEN, where IMS plays an important role in the application of the PFlops-scale supercomputer to nanoscience. Further information on next-generation supercomputer project and computer systems at the Center is found on the web site (http://ims.ac.jp/nanogrid/).

Figure 1. Super-High-Performance Molecular Simulator.

Award

MIZUTANI, Fumiyasu; The CSJ Award for Technical Achievements.

Okazaki Institute for Integrative Bioscience

AONO, Shigetoshi	Professor
KUWAJIMA, Kunihiro	Professor
KATO, Koichi	Professor
FUJII, Hiroshi	Associate Professor
KURAHASHI, Takuya	Assistant Professor
YOSHIOKA, Shiro	Assistant Professor
MAKABE, Koki	Assistant Professor
YAMAGUCHI, Takumi	Assistant Professor
ISHIKAWA, Haruto	IMS Research Assistant Professor
KAMIYA, Yukiko	IMS Research Assistant Professor
TANIZAWA, Misako	Secretary
TANAKA, Kei	Secretary

The main purpose of Okazaki Institute for Integrative Bioscience (OIIB) is to conduct interdisciplinary, molecular research on various biological phenomena such as signal transduction, differentiation and environmental response. OIIB, founded in April 2000, introduces cutting edge methodology from the physical and chemical disciplines to foster new trends in bioscience research. OIIB is a center shared by and benefited from all three institutes in Okazaki, thus encouraging innovative researches adequately in advance of academic and social demands. The research groups of three full professors and one associate professor who have the position in IMS join OIIB. The research activities of these groups are as follows.

Aono group is studying the bioinorganic chemistry of hemeproteins that show a novel function. They elucidated the structure and function relationships of the heme-based sensor proteins in which a heme was the active site for sensing gas molecules such as CO and O_2. They also reported the structure and function relationships of aldoxime dehydratase, which is a novel heme-containing dehydrase enzyme. Kato group is studying structure, dynamics, and interactions of biological macromolecules primarily using ultra-high field nuclear magnetic resonance (NMR) spectroscopy. In particular, they conducted studies aimed at elucidating the dynamic structures of glycoconjugates and proteins for integrative understanding of the mechanisms underlying their biological functions. Kuwajima group is studying mechanisms of *in vitro* protein folding and mechanisms of molecular chaperone function. Their goals are to elucidate the physical principles by which a protein organizes its specific native structure from the amino acid sequence. In this year, they studied folding pathways of homologous proteins, goat α-lactalbumin and canine milk lysozyme, by experimental and computational analysis. Fujii group is studying molecular mechanisms of metalloenzymes, which are a class of biologically important macromolecules having various functions such as oxygen transport, electron transfer, oxygenation, and signal transduction, with synthetic model complexes for the active site of the metalloenzymes. In this year, they studied molecular mechanisms of metalloenzymes relating to monooxygenation reactions and denitification processes.

OIIB is conducting the cooperation research program, “Frontiers of Membrane Protein Research,” with Institute for Protein Research, Osaka University from 2005. In this program, the following projects have being carried out to elucidate the role of membrane proteins in life: (i) the development of expression systems, purification methods, and chemical synthesis of membrane proteins, (ii) the development of new methods for analyzing the structure and function of membrane proteins. As a part of this cooperation program, the 7th OIIB Symposium was held in Okazaki on November 12 and 13, 2008.

Safety Office

TANAKA, Koji	Director
TOMURA, Masaaki	Assistant Professor
TANAKA, Shoji	Assistant Professor
SUZUI, Mitsukazu	Technical Associate
YOSHIDA Hisashi	Technical Associate
NAGATA, Masaaki	Technical Associate
YAMANAKA, Takaya	Technical Associate
UEDA, Tadashi	Technical Associate
TAKAYAMA, Takashi	Technical Associate
HAYASHI, Kenji	Technical Associate
MAKITA, Seiji	Technical Associate
ONITAKE, Naoko	Secretary
TSURUTA, Yumiko	Secretary

The Safety Office was established in April 2004. The mission of the Office is to play a principal role in the institute to secure the safety and health of the staffs by achieving a comfortable workplace environment, and improvement of the working conditions. In concrete terms, it carries out planning, work instructions, fact-findings, and other services for safety and health in the institute. The Office is comprised of the following staffs: The Director of the Office, Safety-and-Health Administrators, Safety Office Personnel, Operational Chiefs and other staff members appointed by the Director General. The Safety-and-Health Administrators patrol the laboratories in the institute once every week, and check whether the laboratory condition is kept sufficiently safe and comfortable to conduct researches. The Office also edits the safety manuals and gives safety training courses, for Japanese and foreign researchers.

SUPPORTING STAFF

Public Affairs Office

HIRATA, Fumio	Head
OHSHIMA, Yasuhiro	Vice-Head
HARADA, Miyuki	Technical Associate
NAKAMURA, Rie	Technical Fellow

Archives

YAKUSHI, Kyuya	Head
MINAMINO, Satoshi	Technical Associate
KIMURA, Katsumi	Professor Emeritus
SUZUKI, Satomi	Secretary

Archives of Institute for Molecular Science (IMS Archives) collect the documents, audios, photos, and videos which are related to the foundation of Institute for Molecular Science. IMS Archives have collected and arranged the documents which were provided by Prof. Saburo Nagakura (second Director-General), Prof. Hiroo Inokuchi (third Director-General), and related parties. The prehistory of IMS written by Prof. Nagakura was published in *IMS letters* **Vol. 57**, 8 (2008). IMS Archives plans to publish the selected documents in a standard archive format EAD.

Technical Division

SUZUI, Mitsukazu	Head
OMARU, Tadakazu	Technical Fellow

Secretary for Director-General

NOGAWA, Kyoko	Secretary

Information Office

OHHARA, Kyoko	Secretary
SUGIYAMA, Kayoko	Secretary
TSURUTA, Yumiko	Secretary
KAMO, Kyoko	Secretary

The Technical Division is an organization of the technical staff which supports research facilities of IMS. The technical staffs are assigned to support the research by using their professional skills of mechanical engineering, electrical engineering, instrumental analysis, optical technology, computer engineering, cryogenic technology, and the SOR technology, *etc*.

In addition, the Technical Division supports IMS facilities by managing Safety Office, Research groups, Public Affairs Office, Archives and Information Office.

The annual meeting for technical staff of research Institute and Universities was organized in 1975 and since then the meeting has been regularly held every year. We aim toward a higher technology and exchange discussion concerning the various technical problems related to our technology.

Special Research Projects

IMS has special research projects supported by national funds. Five projects in progress are:

(a) Next Generation Integrated Nanoscience Simulation Software
Development & Application of Advanced High-Performance Supercomputer Project
(b) Formation of Interdisciplinary and International Bases for Natural Sciences, NINS
"Development of New Computational Methods for Large-Scale Systems and Establishment of Advanced Simulation Center for Molecules and Materials"
(c) Extreme Photonics
(d) MEXT Nanotechnology Network
Nanotechnology Support Project in Central Japan: Synthesis, Nanoprocessing and Advanced Instrumental Analysis
(e) Inter-University Network for Efficient Utilization of Chemical Research Equipments

These five projects are being carried out with close collaboration between research divisions and facilities. Collaborations from outside also make important contributions. Research fellows join these projects.

(a) Next Generation Integrated Nanoscience Simulation Software Development & Application of Advanced High-Performance Supercomputer Project

A national project entitled, "Next Generation Integrated Nanoscience Simulation Software" was initiated on April 1, 2006 at Institute for Molecular Science (IMS). The project is a part of the "Development & Application of Advanced High-Performance Supercomputer Project" of MEXT, which aims to develop a next generation supercomputer and application software to meet the need in the computational science nation-wide.

The primary mission of our project is to resolve following three fundamental problems in the field of nanoscience, all of which are crucial to support society's future scientific and technological demands: (1) "Next Generation Energy" (*e.g.*, effective utilization of the solar energy), (2) "Next Generation Nano Biomolecules" (*e.g.*, scientific contributions toward overcoming obstinate diseases), and (3), "Next Generation Nano Information Function and Materials" (*e.g.*, molecular devices). In these fields, new computational methodologies and programs are to be developed to clarify the properties of nanoscale substances such as catalysts (enzymes), biomaterials, molecular devises, and so forth, by making the best use of the next generation supercomputer.

Among many application programs developed in the project, we have selected six programs, three from the molecular science and three from the solid state physics, as "core applications" in the nano-science, and concentrating our effort to tune those programs to the next generation machine. The programs in molecular science are concerned with the MD simulation, the quantum chemistry, and the statistical mechanics of liquids.

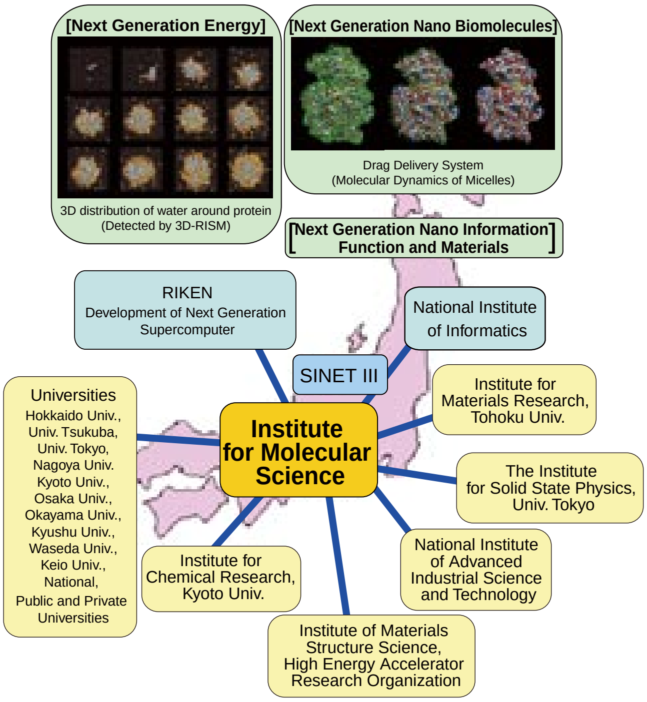

(b) Formation of Interdisciplinary and International Bases for Natural Sciences, NINS "Development of New Computational Methods for Large-Scale Systems and Establishment of Advanced Simulation Center for Molecules and Materials"

This project aims to establish a core computational science center for molecular and material systems and to develop advanced methodologies for large-scale calculations. We are trying to create a new interdisciplinary field by integrating the different views and methodologies in each field that belongs to a different hierarchy of natural sciences. Structures and dynamics of large-scale complex systems, *e.g.* nanomaterials and biological systems, are investigated with a variety of sophisticated computational methods based on theories of quantum and statistical mechanics, and so on. Seminars and workshops for the advanced calculations and for the development of human resources are also conducted by this project.

The project is organized by five institutes of the National Institutes of Natural Sciences, *i.e.* Institute for Molecular Science, National Astronomical Observatory of Japan, National Institute for Fusion Science, National Institute for Basic Biology, and National Institute for Physiological Sciences, and other universities and research institutes. The followings are the research titles of groups participating from IMS:

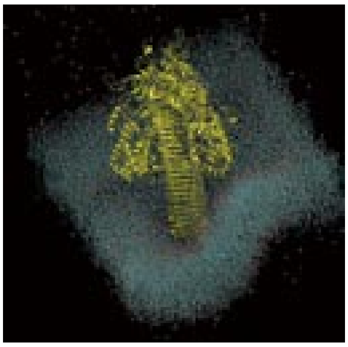

Massive molecular dynamics to simulate puncture of lipid bilayer by gp5.

EHARA, Masahiro	Theoretical Studies of Molecular Excited States and Chemical Reactions
HIRATA, Fumio	Theoretical Study of Molecular Recognition Based on the 3D-RISM Theory
NAGASE, Shigeru	Quantum Chemistry Calculations of Nanomolecules
NOBUSADA, Katsuyuki	Theoretical Calculations for Electron Dynamics Strongly Coupled to the Electromagnetic Field
OKUMURA, Hisashi	Development of New Algorithms for Molecular Dynamics Simulation and its Application to Biomolecular Systems
SAITO, Shinji	Theoretical Studies of Condensed Phase Dynamics by Using Molecular Simulation
YONEMITSU, Kenji	Theory for Nonequilibrium Control of Collective Dynamics in Quantum-Classical Hybrid Many-Particle Systems
YANAI, Takeshi	Theory Development for Multireference Electronic Structures with *ab initio* Quantum Chemical Methods

(c) Extreme Photonics

Institute for Molecular Science has a long-standing tradition of promoting spectroscopy and dynamics of molecules and molecular assemblies. Accordingly, photo-molecular science is one of major disciplines in molecular science. This field is not confined in the traditional spectroscopy, but makes solid basis for other disciplines including nanoscience and bioscience, *etc*. Therefore, continuing developments in spectroscopy and microscopy are vital to enhance our abilities to elucidate more complex systems in time and spatial domains. In order to achieve full developments of photo-molecular science, we need to pursue three branches in developing: (1) new light source, (2) new spatio-temporally resolved spectroscopy, and (3) new methods to control atomic and molecular dynamics. Since 2005, we have started the program of "Extreme Photonics" in collaboration with the RIKEN institute. Currently 6 groups in IMS are involved in this program, and the specific research titles are as follows:

(1) Development of new light sources

TAIRA, Takunori	Micro Solid-State Photonics

(2) Development of new spatio-temporally resolved spectroscopy

OKAMOTO, Hiromi	Development of Extreme Time-Resolved Near-Field Spectroscopy
MATSUMOTO, Yoshiyasu	Development of Spatio-Temporally Resolved Spectroscopy for Surfaces and Interfaces

(3) Development of new methods to control atomic and molecular dynamics

OHMORI, Kenji	Development of Attosecond Coherent Control and Its Applications
HISHIKAWA, Akiyoshi	Reaction Imaging and Control with Extremely Short Laser Pulses
OHSHIMA, Yasuhiro	Quantum-State Manipulation of Molecular Motions by Intense Coherent Laser Pulses

(d) MEXT Nanotechnology Network Nanotechnology Support Project in Central Japan: Synthesis, Nanoprocessing and Advanced Instrumental Analysis

The Ministry of Education, Culture, Sports, Science and Technology (MEXT), Japan started the Nanotechnology Network Project in April 2007 in order to support Japanese nanotechnology researches not only for university and government researchers but also for private company researchers. IMS participates in this project as a core organization (project leader: YOKOYAMA, Toshihiko, Prof. & Director of Research Center for Molecular Scale Nanoscience) with Nagoya University (representative: BABA, Yoshinobu, Prof.), Nagoya Institute of Technology (representative: HIHARA, Takehiko, Prof.) and Toyota Technological Institute (representative: SAKAKI, Hiroyuki, Prof. & Vice President of TTI), and establishes a nanotechnology support center in central Japan area for these five years. We will support

1) Public usage of various advanced nanotechnology instruments such as ultrahigh magnetic field NMR (920 MHz), advanced transmission electron microscopes, and so forth
2) Design, synthesis and characterization of organic, inorganic and biological molecules and materials,
3) Semiconductor nanoprocessing using advanced facilities and technologies.

We will promote applications not only to each supporting element, but to combined usage of several supporting elements such as a nanobiotechnology field that is highly efficient in this joint project. In 2008 Apr.–2009 Mar., the number of accepted projects applied to IMS amounted 127 (the total number of days is 897).

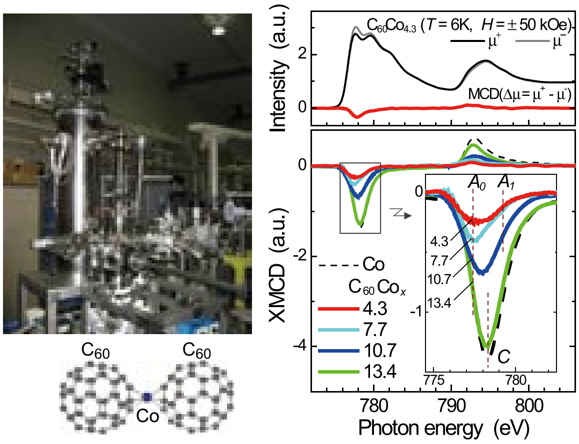

(left) Measurement system of high magnetic field (±7 T) and low temperature (5 K) X-ray magnetic circular dichroism installed at UVSOR-II and (right) examples of the recorded XMCD data by Drs. Y. Matsumoto and S. Sakai in JAERI, published in *Chem. Phys. Lett.* **470**, 244–248 (2009).

List of Supports in IMS

Person in Charge	Support Element
OKAMOTO, Hiromi	Space- and Time-Resolved Near-Field Microspectroscopy
YOKOYAMA, Toshihiko	Magneto-Optical Characterization of Surface Nanomagnetism
YOKOYAMA, Toshihiko	Electron Spectroscopy for Chemical Analysis
NISHI, Nobuyuki	Tunable Picosecond Raman Spectroscopy
HIRAMOTO, Masahiro	Fabrication and Characterization of Organic Semiconductor Devices
NISHI, Nobuyuki	300kV Transmission Analytical Electron Microscopy
YOKOYAMA, Toshihiko	Focus Ion Beam Processing & Field Emission Scanning Electron Microscopy
NAGAYAMA, Kuniaki	Phase Contrast Transmission Electron Microscopy for Nanobiological Materials
TADA, Mizuki	Design and Structural Analysis of Molecular Catalysts
YOKOYAMA, Toshihiko; KATO, Koichi	920 MHz NMR Spectrometer
NAGASE, Shigeru	Quantum Chemical Calculation for Molecular Design
SUZUKI, Toshiyasu; NAGATA, Toshi; SAKURAI, Hidehiro	Synthesis & Design of Functional Organic Nanomaterials

(e) Inter-University Network for Efficient Utilization of Chemical Research Equipments

Academic and industrial activities in Chemistry in Japan have been world-leading over the past 30 years. Needless to say, it is highly important to improve the supporting environment for research and education in science and engineering. In particular, research equipments are advancing all the time to more intelligent and expensive ones, making measurement time shorter with higher reliability. It would be economic and efficient for the researchers and students of all national universities to share such equipments for performing high level research and education.

From 2007, we started the 5 year project "Functioning of Inter-University Network for Efficient Utilization of Chemical Research Equipments." This network is operated through an internet machine-time reservation and charging system by the help of equipment managers and accounting sections in each university. All the universities are grouped into 12 regions and in each region the hub university organizes the regional committee for the operation of regional network system. There is no barrier for every user to access to any universities beyond his/her regional group.

Although the financial condition of the government is now extremely hard, the government decided to start this project in the end of 2006. In 2007, some starting budget was appropriated for preparing the new system and we started a trial network operation with 119 equipments offered by 55 universities and IMS. In 2008 and 2009, the budget increased more than ten times and has been used for preparing a full-scale operation system of machine reservation/charging, and for repairing/upgrading of 19 and 25 instruments, respectively. In June, the number of user registrants amounts to 4563 in 72 universities and IMS covering 1299 laboratories in Japan. Now the registered equipment increases to 206. With the supplementary budget in 2009, the government decided to introduce the 36 advanced instruments, such as transmission electron microscopes, high-resolution mass-spectrometers, nuclear magnetic resonance imaging systems, a surface Plasmon resonance spectrometer, high resolution nuclear magnetic resonance spectrometers for solid samples, a highly sensitive high-resolution electron spin resonance spectrometer, a highly sensitive small angle X-ray diffraction spectrometer, *et al.* into the network. These most advanced instruments can encourage the users in outer universities.

We believe that this innovative system can motivate and stimulate researchers and students to carry out new researches, and make chemistry research in Japan far more successful and active.

Okazaki Conference

The 68th Okazaki Conference
From Aromatic Molecules to Graphene; Chemistry, Physics and Device Applications

Organizers: T. Enoki (*Tokyo Tech.*), T. Yokoyama (*IMS*), K. Tsukagoshi (*NIMS*), T. Kubo (*Osaka Univ.*), K. Kusakaba (*Osaka Univ.*)

Invited Overseas Speakers: PW. de Heer (*Georgia Tech.*), P. Esquinazi (*Univ. Leipzig*), F. Guinea (*Inst. Ciencia de Mater., Madrid*), R. Haddon (*Univ. California, Riverside*), S. G. Louie (*Univ. California, Berkeley*), A. F. Morpurgo (*Univ. Geneva*), K. Novosedlov (*Univ. Manchester*), A. Sood (*Indian Inst. Sci., Bangalore*)

The 68th Okazaki Conference was held on Jan. 21–23, 2009 in Okazaki Conference Center, in which we had about 90 of attendees including 38 invited speakers. The discovery of single sheet of graphite, which is called graphene, has triggered intensive studies on graphene and related materials. The electronic structure of graphene is described in terms of massless Dirac fermion, which makes it distinguished from traditional electronic systems. The interesting unconventional electronic feature of graphene is stimulating also in building electronic/spintronics device applications. Nanosized graphene called nanographene provides another intriguing issue due to the presence of edges. Indeed the electronic structure of nanographene is strongly dependent on the shape of the edges. The creating of nonbonding π-electron state (edge state) around the zigzag edges brings about unconventional nanoscopic magnetism and chemical reactivities. This situation is relevant to the issue of non-Kekulé structure with neutral radical state in aromatic hydrocarbon molecules in organic chemistry.

In this conference we were aiming at enriching the aspects of the issues on graphene by discussing comprehensively the physics, chemistry and device applications of graphene, nanographene and aromatic hydrocarbon molecules on the common basis. It was devoted to develop a new interdisciplinary area of graphene-related research by bridging between physics, chemistry and device applications.

Joint Studies Programs

As one of the important functions of an inter-university research institute, IMS facilitates joint studies programs for which funds are available to cover the costs of research expenses as well as the travel and accommodation expenses of individuals. Proposals from domestic scientists are reviewed and selected by an interuniversity committee.

(1) Special Projects

A. New Developments in Spin Science Using Pulsed and High-Frequency ESR

KATO, Tatsuhisa *(Josai Univ.)*
MIZOGUCHI, Kenji *(Tokyo Metropolitan Univ.)*
SAKAMOTO, Hirokazu *(Tokyo Metropolitan Univ.)*
NAKAMURA, Toshikazu *(IMS)*
FURUKAWA, Ko *(IMS)*

In order to develop advanced ESR (electron spin resonance) spectroscopy for materials science, we performed functional materials studies, both on isolated molecules and on molecular assemblies. The following two topics were investigated: 1) We investigated the electron-spin coupled states composed of Cu(II) ions in the square-planar coordination with the ligands. 2) We carried out an analysis of spin dynamics for functional molecular assemblies, including2) metal ions inserted in M-DNA and3) dye-sensitized solar cell. We searched for cooperative phenomena involved in intra-molecule freedom, and new functional physical-properties originating in molecular assemblies.

A-1 Spin Coupled State Composed of Cu(II) Ions in Square-Planar Ligand Field

The arrays of spin active metal ions are expected to lead to the coupled spin states. Herein we show two unique approaches to form copper ions' arrays, which exhibited the coupled high spin states. As the first approach, Fujita *et al*. reported a discrete homo Cu(II)–Cu(II)–Cu(II) metal array, as shown in Figure 1., through the intercalation of Cu-aza-porphines into an organic pillared coordination box, which is self assembled from two panels, three pillars and six Pd(II) hinges.1) We clarified by using an ESR spectrometer that the homo Cu–Cu–Cu array shows unique spin interaction, which is clearly reproduced by a computer simulation as a quartet spin state.2)

The other approach is owing to the efficient self-assembly properties of DNA. Shionoya *et al.* showed that upon replacement of hydrogen-bonded base pairing by metal-mediated base pairing in DNA, it is possible to align metal ions within the double helical DNA scaffold.3) They reported the alignment of up to five Cu(II) ions within the DNA scaffold by using a hydroxypyridone-metal base pair, H-MBP in Figure 2. Electron spin transient nutation (ESTN) measurement as well as cw-ESR observation exhibited that the Cu(II) centers were ferro-magnetically coupled to one another, with each Cu(II) center being in a distorted square-planar geometry.4) On the other hand Clever and Carell reported the alignment up to ten Cu(II) ions within the DNA double helix using a salicylic aldehyde metal base pair in the presence of an ethylenediamine, salen ligands metal base pair (S-MBP) in Figure 2. However, no magnetic measurements were reported for the S-MBPs.5) Recently Ono *et al*. synthesized the thymidine dimer linked DNA with N4-carboxymethylcytosine metal base pair, CA-MBP in Figure 2, having the alignment up to five Cu(II) ions. The EPR spectrum exhibited the spectra due to the coupled spin state with much smaller dipole interaction than the case of Shionoya's metal-DNA. The comparison among the cases shows that the magnetic interactions in the metal-DNA structures are strongly dependent on the conformation characteristics of the metal base pair. The formation of an extended network in the stacked array of H-MBP favors ferro-magnetic coupling, whereas the ordered pairwise-stacked arrangement of S-MBP suppresses magnetic coupling. In the case of CA-MBP, the Cu(II) array exhibits the small magnetic dipole interaction, indicating the long distance between neighboring Cu(II) ions.

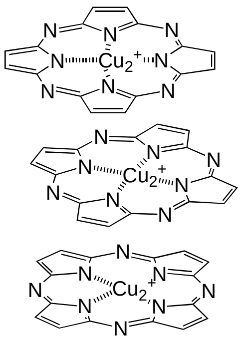

Figure 1. Stacked array of Cu-aza-porphines.

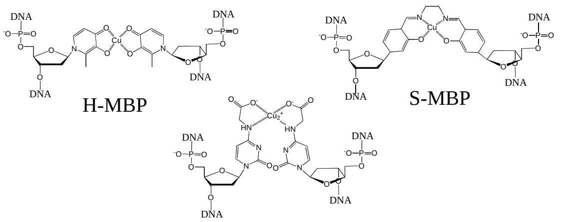

Figure 2. Three metal base pairs, hydroxypyridone MBP (H-MBP), salicylic aldehyde MBP with ethylenediamine (S-MBP), and N4-carboxymethylcytosine MBP (CA-MBP).

A-2 ESR Study of Metal Ions Inserted in M-DNA

In the view point of materials science, DNA shows several interesting properties such as self-organizing nature based on the complementarity of base pairs, arbitrariness of sequence design, and the possibility of π-electron stacking between adjacent bases. However, it has been confirmed that natural

DNA is a semiconductor with a large energy gap more than 5 eV. To introduce charge carriers into the DNA, there are several possibilities: Composite with divalent metal ions, chemical doping, and electric field induction. Here, we report an ESR study on the divalent metal ions of M-DNA.

It has been confirmed that several alkaline earth and transition metal ions, such as Mg, Ca, Mn, Fe, Co, Ni, and Zn, could form composites with DNA, locating in between the bases of a base pair. The magnetic transition metal ions are useful as a probe to investigate the electronic states of metal ions in the M-DNAs. Especially, Mn^{2+} ions are the ideal magnetic probe with $S = 5/2$ which gives ESR signal around the free electron g-value, $g \sim 2$. Analysis of ESR spectra in M^{2+}-DNA has led us to the conclusion that the charge transfer from the metal ions to the DNA base pairs did not occur, keeping DNA semiconducting after M^{2+} introduction. Only the exception has been found in Fe-DNA, where Fe^{2+} ion introduced into DNA base pairs changed to Fe^{3+}, as confirmed by its color and ESR g-value just near $g \sim 2$, corresponding to $S = 5/2$ expected for a high-spin state of Fe^{3+}, as demonstrated in Figure 3. Thus, one could conclude that one electron should transfer to DNA in Fe-DNA. Fe-DNA also shows another curious behaviors in magnetization and ESR spectra, which suggest a mixture of high-spin state, $S = 5/2$ and low-spin state, $S = 1/2$ of Fe^{3+}, especially as a function of Fe concentration.

On the location of metal ions are suggested to be in between the bases of a base pair from several experimental facts. However, the bonding state of the metal ion is still open question. We have succeeded to study the bonding state of Mn in Mn-DNA from the analysis of six hyperfine split spectra of $Mn_{0.01}Ca_{0.99}$-DNA taken at Q-band in Figure 2. It is known that the separation of the central two spectra represents the bonding nature of metal ion. Isolated Mn^{2+} ion in the ionic crystal CaF_2 shows the separation of more than 100 G, but in the crystal, ZnS made of mainly covalent bond indicates the separation of around 70 G. From the separation of 96 G in $Mn_{0.01}Ca_{0.99}$-DNA in Figure 4, we can clearly conclude that the bonding of Mn ion with surrounding bases in Mn-DNA is ionic in character. The present observation of the bonding nature of metal ions in M-DNA strongly supports further investigation and understanding of M-DNA, experimentally and theoretically.

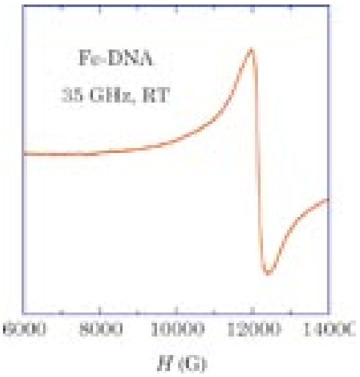

Figure 3. (left) ESR spectrum of Fe-DNA located at about $g = 2$, suggesting that $S = 5/2$ for Fe^{3+}.

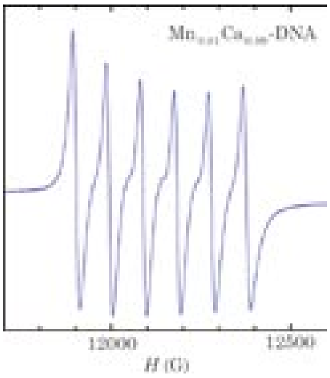

Figure 4. (right) ESR spectra of Mn ion in $Mn_{0.01}Ca_{0.99}$-DNA show the six hyperfine peaks. The separation of the center two spectra could be a measure of bonding nature, ionic or covalent.

A-3 ESR Study of Spin Dynamics for Dye-Sensitized Solar Cell

In dye-sensitized solar cells (DSSC), dye molecules are excited from the ground state S to the excited state S* by photo energy. The electron transfer from the excited dye molecules to the electrode plays an important role of the photoelectric transfer characteristic in DSSC. A various type of dye molecules were investigated. Time-resolved ESR measurements give us to detailed information of the photoelectric transfer characteristic. The aim of the present study is to reveal the relationship between the photoelectric transfer characteristic and the spin dynamics of electron in DSSC. The spin dynamics of the various organic dye molecules such as the eosin-Y was investigated by time-resolved ESR spectroscopy with laser photolysis (Nd:YAG 2nd harmonics, 532 nm). We discuss the spin dynamics of the various organic dye molecules with TiO_2.

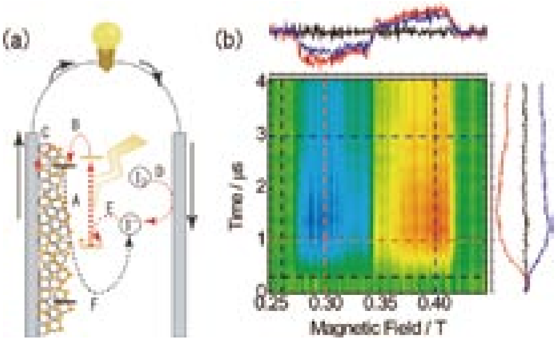

Figure 5. (a)Schematic image of the DSSC and (b)TR-ESR spectra for eosin-Y.

References

1) K. Ono, M. Yoshizawa, T. Kato and M. Fujita, *Angew. Chem., Int. Ed.* **46**, 1803–1806 (2007).
2) K. Ono, M. Yoshizawa, T. Kato and M. Fujita, *Chem. Commun.* 2328–2330 *(*2008).
3) K. Tanaka, Y. Yamada and M. Shionoya, *J. Am. Chem. Soc.* **124**, 8802–8803 (2002).
4) K. Tanaka, A. Tengeiji, T. Kato and M. Shionoya, *Science* **299**, 1212–1213 (2003).
5) G. H. Clever and T. Carell, *Angew. Chem., Int. Ed.* **46**, 250–253 (2007).

B. Construction of the Research Methodology for Biomolecular Sensing System

URISU, Tsuneo *(IMS)*
TERO, Ryugo *(IMS)*
ASANO, Toshifumi *(IMS)*
UNO, Hidetaka *(SOKENDAI)*
SHIBASAKI, Koji *(OIIB)*
TOMINAGA, Makoto *(OIIB)*
SHIGEMOTO, Ryuichi *(NIPS)*
FUKAZAWA, Yugo *(NIPS)*
YAWO, Hiromu *(Tohoku Univ.)*
ISHIZUKA, Toru *(Tohoku Univ.)*

The neurodegenerative diseases are intractable diseases for which neither of the cause and the treatment method is clarified. Statistically, 20% of more than 85 years old persons get dementia. Thus developments of treatment method and clarification of the cause are the urgent problem of human beings. Concerning this point, it is one of the problems to be solved that there is no suitable screening device of neural systems. In this program, we have started the research to develop a screening device which have the function of in vitro neural network analysis.

B-1 Development of Cell Culture Type Planar Ion Channel Biosensor for Nerve Cell Signaling Analysis

Cells growing on SOI substrates with and without the FN coating are compared. The FN coating clearly promoted cell growth. Although we did not control the cell positions, a cell was often positioned on the micropore.

The sequence of steps in the incubation mode recording is as follows. The culture mediums in the upper and lower chambers were exchanged to the extracellular and intracellular solutions, respectively, for the ion channel current measurements. Perforated patch mode recordings were formed by nystatin (100–200 μg/ml). The increase of capacitance (5–10 pF) of the cell membrane was observed 5–10 min after addition of the nystatin solution.

The whole-cell current of the TRPV1 activated by capsaicin stimulation was recorded. The first capsaicin application induced a large current increase, and the current increase induced by the second application was weaker than the first one. The decrease in the sensitivity unique to the capsaicin stimulation of TRPV1 with a Ca^{2+}-containing solution was observed.

B-2 Fabrication of Light Gated Ion Channel Biosensor

In the investigation of the electrically excitable cells, photo-stimulation provides a versatile alternative to electrode stimulation. Channel of the excitable cell by the photo-stimulation is especially useful in constructing the neural network analysis device. In the present work, we have expressed Chlamydomonas reinhardii channelrhodopsin 2 (ChR2) on the cell membrane of a kind of excitable cell C2C12, and measured the basic characteristics of the photo-response. ChR2 has a light absorbance peak at 460 nm and forms a non-selective cation channel, the gating of which is triggered by the photo-isomerization of the all-trans retinal to 13-cis configuration. To investigate the photo-response characteristics of ChR2-expressed C2C12 cell, we have constructed the planer-type ion channel biosensor by putting a single C2C12 cell on the micropore of the Si substrate and successfully observed the light-gated whole cell channel current. We are now measuring the basic characteristics of this system such as, effects of cell-cell interaction and coupling of the cell's own characteristics and the chamber's electric characteristics on the time dependence of the whole cell current.

(2) Research Symposia

(From Oct. 2008 to Sep. 2009)

Dates	Theme	Chair
Jan. 22–23, 2009	Plasmonic Materials for Molecular Science	**UENO, Kosei** **IMURA, Kohei**
Mar. 5– 6, 2009	Workshop on Biradical Chemistry and Its Future Perspect	**ABE, Manabu** **SAKURAI, Hidehiro**
Jul. 23, 2009	Preparatory Meeting for Molecular Science Summer School	**TANAKA, Midori** **HISHIKAWA, Akiyoshi**

(3) Numbers of Joint Studies Programs

Categories		Oct. 2008–Mar. 2009	Apr. 2009–Sep. 2009	Total
Special Projects		0	1	1
Research Symposia		2	0	2
Research Symposia for Young Researchers		0	1	1
Cooperative Research		44	60	104
Use of Facility	Instrument Center	36	18	54
	Equipment Development Center	4	9	13
Use of UVSOR Facility		85	70	155
Use of Facility Program of the Computer Center				147*

* from April 2008 to March 2009

Collaboration Programs

(a) IMS International Program

IMS has accepted many foreign scientists and hosted numerous international conferences since its establishment and is now universally recognized as an institute that is open to foreign countries. In 2004, IMS initiated a program to further promote international collaborations. As a part of this program, IMS faculty members can (1) nominate senior foreign scientists for short-term visits, (2) invite young scientists for long-term stays, and (3) undertake visits overseas to conduct international collaborations.

Leader	Title	Partner
SHIGEMASA, Eiji	Deexcitation Dynamics of Core Excited Molecules Studied by Electron Spectroscopy	France: Dr. SIMON, Marc and group members
KATOH, Masahiro	Generation of Coherent Radiation by Using Laser and Electron Beam	France: Dr. COUPRIE, Marie Emmanuelle Dr. BIELAWSKI, Serge and their group members
KIMURA, Shin-ichi	Optical and Photoelectrical Studies on the Local to Itinerant Electronic Structure of Strongly Correlated Electron Systems	Korea: Prof. KWON, Yong-Seung and group members Germany: Dr. SICHELSHMIDT, Jorg
KOSUGI, Nobuhiro	Study of Weak Intermolecular Interaction by Resonant Soft X-Ray Photoelectron Spectroscopy	Germany: Prof. RUEHL, Eckart Dr. WINTER, Bernd and their group members Sweden: Prof. PETTERSSON, Lars G. M. Prof. GEL'MUKANOV, Faris and their group members France: Dr. MIRON, Catalin and group members
UOZUMI, Yasuhiro	Development of Novel Asymmetric Catalysis with Chiral Pincer Complexes	China: Prof. WANG, Hongxing
SAKURAI, Hidehiro	Development of Novel Gold Cluster Catalyst Supported by Polymers	Thailand: Prof. CHAVASIRI, Warinthorn and group members
JIANG, Donglin	Study on the Synthesis of Magnetic Particles with Light-Harvesting Antenna	China: Prof. WANG, Changchun and group members
TAIRA, Takunori	Q-Switched Nd-Microchip Lasers with COB Doubler	France: Prof. AKA, Gerard Philippe Prof. LOISEAU, Pascal and their group members
YOKOYAMA, Toshihiko	Two Photon-Photoemission Magnetic Circular Dichroism in Co Ultrathin Film on Pt(111)	Germany: Prof. SCHONHENSE, Gerd and group members
YOKOYAMA, Toshihiko	A Competition between Magnetic Anisotropy and Interlayer Coupling in the Multilayer Systems of Alternating In-Plane and Perpendicular Anisotropy	Germany: Prof. PRSYBYLSKI, Marek and group members

URISU, Tsuneo	Construction of Neural Cell Molecular Signal Transmission System and Development of Molecular Science New Field	China: Prof. WANG, Chang-Shun Mr. HE, Tingchao
OHMORI, Kenji	Coherent Control of Ultracold Atoms and Molecules	Canada: Prof. SHAPIRO, Moshe and group members

(b) Asian Core Program "Frontiers of Material, Photo- and Theoretical Molecular Sciences"

Asian Core Program is a multilateral international collaboration program carried our by JSPS (Japan Society for the Promotion of Science). It is designed to create world-class research hubs in selected fields within the Asian region, while fostering the next generation of leading researchers. The program is based on a principle of equal partnership among core institutions in Japan and other Asian countries, so that each institution is expected to secure its own matching fund. Institute for Molecular Science has launched a collaboration project "material, photo- and theoretical molecular sciences" (2006–2011) within the framework of this Asian Core Program with three key institutes in east Asian countries: Institute of Chemistry, Chinese Academy of Science (China); The College of Natural Science, Korea Advanced Institute of Science and Technology (Korea); and Institute of Atomic and Molecular Sciences, Academia Sinica (Taiwan). At present, nine joint researches are in progress, and six joint seminars are planned within JFY 2009.

(c) Exchange Program for East Asian Young Researchers "Improvement of Fundamental Research Base for Environmental and Energy Problems"

At the Second East Asia Summit (EAS), held in January 2007, Mr. Shinzo Abe, Prime Minister of Japan, announced a plan to implement a ¥35-billion youth exchange program, inviting about 6,000 young people to Japan mainly from the EAS member states every year for the next five years. Based on this plan, the Government of Japan has launched the Japan-East Asia Network of Exchange for Students and Youths (JENESYS) Programme, under which it is conducting a variety of exchange activities. As a part of the JENESYS Programme, the Japan Society for the Promotion of Science (JSPS) has launched the "Exchange Program for East Asian Young Researchers." Aimed at promoting researcher exchanges with East Asian countries, this program supports initiatives by Japanese universities and research institutions to invite young researchers (*e.g.*, master's and doctoral students and post-doctoral researchers) from those countries. By supporting exchange programs implemented by Japanese universities and research institutions, the "Exchange Program for East Asian Young Researchers" works to establish and expand networks with researchers mainly from Asian countries. It also helps to develop high-caliber human resources and to create a regional science and technology community. IMS is a center of the basic research of physical/chemistry fields in Japan and has a role for the center of both domestic and international collaboration. From 2008, IMS has organized the JENESYS program for chemistry/physics fields. IMS provides the opportunity for young researchers from Asian countries to stay in the laboratories related to the basic research for environmental and energy problem for 14–60 days. Through the experience, we encourage them to continue the basic research in their own countries as well as to build up the future collaboration. IMS welcomed totally 24 young researchers (11 in 2008 autumn and 13 in 2009 spring) from Thailand, Singapore, Malaysia, Indonesia, Vietnam, and India.

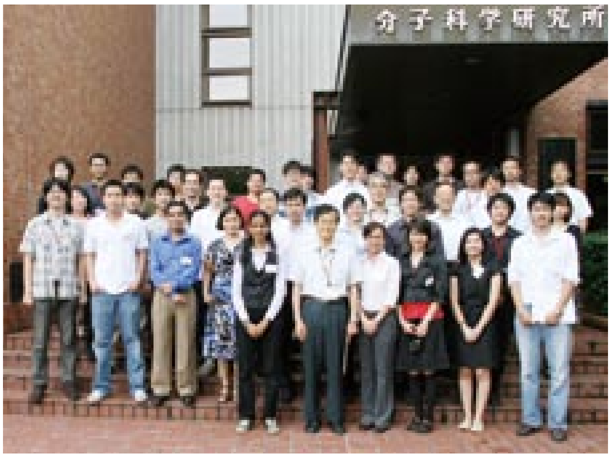

AWARDS

TANAKA, Koji Life and Coordination-Complex Molecular Science	Award of Japan Society of Coordination Chemistry in 2008 “Design and Synthesis of Metal Complex Catalysts towards Inter-Conversion between Chemical Energy and Electric One”
YANAI, Takeshi Theoretical and Computational Molecular Science	The Wiley-International Journal of Quantum Chemistry Young Investigator Award “Canonical Transformation and Renormalization Group for an Efficient Multireference Electronic Structure Method”
TAIRA, Takunori Laser Research Center for Molecular Science	The 24th Kenjiro Sakurai Memorial Prize, Optoelectronic Industry and Technology Development Association “Pioneering Research in Micro Solid-State Photonics”
TADA, Mizuki Materials Molecular Science	The 13th JSSRR Scientific Awards “Innovation in Catalytic Chemistry by In-Situ Time-Resolved XAFS” The 1st Inoue Science Research Award “Advanced Design of Surface Molecular-Imprinted Metal-Complex Catalysts with Molecular Recognition Property” The 11th Morita Fellowship Award “Surface-Mediated Catalyst Design and Time-Resolved Characterization for Selective Catalysis”
CHONG, Song-ho Theoretical and Computational Molecular Science	Young Scientist Award of the Physical Society of Japan “Development of a New Theory for Glass Transition and Its Verification from Computer Simulation”
YAMASHITA, Yasufumi Theoretical and Computational Molecular Science	Young Scientist Award of the Physical Society of Japan “Spin-Driven Jahn-Teller Mechanism in Geometrically Frustrated Spin Systems”
KATSUKI, Hiroyuki Photo-Molecular Science	PCCP Prize for Outstanding Achievement of Young Scientists in Physical Chemistry and Chemical Physics “Wave Packet Interferometry with Attosecond Precision and Picometric Structure”
NAGASAKA, Masanari Photo-Molecular Science	The 25th Inoue Research Aid for Young Scientists “Mechanisms for Catalytic Reactions on Metal Surfaces Studied by X-Ray Absorption Spectroscopy and Dynamic Monte Carlo Method”
MAKABE, Koki Life and Coordination-Complex Molecular Science	The Protein Science Society of Japan Incentive Award for Young Investigators “Role of the Main-Chain Hydrogen Bonding in β-Sheet Register”
MIZUTANI, Fumiyasu Research Center for Computational Science	The CSJ Award for Technical Achievements “Development of Large-Scale Computer Management Technology and Advanced Computer Use Technology for Computational Molecular Science Research”

LIST OF VISITING FOREIGN SCHOLARS

Visitors from abroad are always welcome at IMS and they have always played an important role in the research activities of the Institute. The foreign scientists who visited IMS during the past year (September 2008–August 2009) are listed below.

(1) MONKASHO (Ministry of Education, Culture, Sports, Science and Technoogy, Japan) or JSPS (Japan Society for the Promotion of Science) Invited Fellow

Dr. Lu Yunpeng	Nanyang Tech. Univ.	Singapore	Feb. ’09–Mar. ’09
Dr. Maitarad Phornphimon	Kasetsart Univ.	Thailand	Feb. ’09–Apr. ’09
Dr. Poolmee Potjaman	Kasetsart Univ	Thailand	Mar. ’09
Dr. Cheng Sit Foon	Univ. of Malaya	Malaysia	Jun. ’09–Aug. ’09
Dr. Pal Subhankar	Natl. Inst. of Tech. Rourkela	India	Jun. ’09–Aug. ’09
Mr. Vinh Ngyuen Doc	Inst. of Chem. Vietnam Acad. of Sci.and Tech.	Vietnam	Jun. ’09–Aug. ’09
Dr. Maitarad Phornphimon	Kasetsart Univ.	Thailand	Jun. ’09
Mr. Vongachariya Arthit	Chulalongkorn Univ.	Thailand	Jul. ’09–Sep. ’09
Ms. Chen Shiao	Natl. Univ. of Singapore	Singapore	Jul. ’09–Sep. ’09
Dr. Wacharashindhu Sumrit	Chulalongkorn Univ.	Thailand	Jul. ’09–Aug. ’09
Dr. Maitarad Phornphimon	Kasetsart Univ.	Thailand	Jul. ’09–Aug. ’09
Ms. Rujee Lorpitthaya	Nanyang Tech. Univ.	Singapore	Aug. ’09–Sep. ’09

(2) IMS Councillor

Prof. Miller William H.	Univ. of California, Barkeley	U.S.A.	Feb. ’09
Prof. Laubereau Alfred	Tech. Univ. Munchen	Germany	Mar. ’09

(3) IMS Visiting Professor or Associate Professor from Abroad (period of stay from 3 to 12 months)

Prof. Sankar Das	Jawaharlal Nehru Univ.	India	Feb. ’09
Dr. Yang Dah-Yen	Inst. of Atomic and Mol. Sci.	Taiwan	Feb. ’09–Jan. ’10
Dr. Pavel Nicolaie	Natl. Inst. for Laser, Plasma and Radiation Phys.	Rumania	Feb. ’09–Mar. ’09
Prof. Bishnu Pada Chatterjee	West Bengal Univ. of Tech.	India	May ’09–Aug. ’10
Prof. Gadre Shridhar	Univ. of Pune	India	May ’09–Aug. ’09
Prof. Peng Shie-Ming	Natl.Taiwan Univ.	Taiwan	Sep. ’08–Dec. ’08

(4) JSPS Post-Doctoral or Ronpaku Fellow

Dr. Veshapidze Giorgi	JSPS	Japan	Nov. ’08
Dr. Alni Anita	Nanyang Tech. Univ.	Philippines	Feb. ’09–Mar. ’09
Mr. Chien Tran, Van	Jenesys Program	Vietnam	Feb. ’09–Mar. ’09
Mr. Sabyasachi Ohakraborty	Natl. Univ. of Singapore	Singapore	Feb. ’09–Mar. ’09
Dr. Sajisha Valiparambil Snjayan	Natl. Inst. for Interdisciplinary Sci. and Tech.	India	Feb. ’09–Mar. ’09
Dr. Krishnan Yamuna	Natl. Center for Biology Sci.	India	Feb. ’09
Prof. Lee Yoon-Sik	Seoul Natl. Univ.	Korea	Feb. ’09
Prof. Wan Li-Jun	CAS, China	China	Feb. ’09
Prof. Chen Chung Hsuan Winston	Acad. Sinica	Taiwan	Feb. ’09
Dr. Sichelschmidt Joerg	Max-Planck-Inst. for Chem. -Phys. of Solids	Germany	Mar. ’09
Dr. Yarasi Soujanya	Indian Inst. of Chem. Tech.	India	Apr. ’09–May ’09
Dr. Patcharee Preedasuriyacha	Indian Inst. of Chem. Tech.	Thailand	May ’09–Aug. ’09
Dr. Ibrahim Heide	JSPS	Japan	May ’09
Mr. Sarker Goutam Kumar	Beximco Pharmaceuticals Ltd.	India	Aug. ’09–Sep. ’09

(5) IMS Visiting Scientist

Dr. Serdaroglu Ertugrul	Free Univ. of Berlin	Germany	Sep. ’08–Oct. ’08
Dr. Flesch Roman	Free Univ. of Berlin	Germany	Sep. ’08–Oct. ’08
Ms. Li Junjun	Fudan Univ.	China	Sep. ’08–Feb. ’09
Prof. Przybylski Marek	Max-Planck-Inst. für Mikrostruktur Phys.	Germanay	Sep. ’08
Associate Prof. Won Jongok	Sejong Univ.	Korea	Oct. ’08–Apr. ’09
Dr. Watson Mark Adrian	Univ. Tokyo	Japan	Oct. ’08
Prof. Ruehl Eckart	Free Univ. of Berlin	Germany	Oct. ’08
Prof. Sutcliffe Brian Terence	Univ. Libre de Bruxelles	Belgium	Oct. ’08
Prof. Puspendu Kumar Das	Indian Inst. of Sci.	India	Oct. ’08
Prof. Sutcliffe Brian Terence	Univ. Libre de Bruxelles	Belgium	Nov. ’08

LIST OF VISITING FOREIGN SCHOLARS

Prof. Gel'mukhanov Faris	Royal Inst. of Tech.	Sweden	Nov. '08
Mr. Velkov Yasen	Royal Inst. of Tech.	Sweden	Nov. '08
Dr. Serve Olivier	Universite Paris XI	France	Nov. '08
Dr. Choudhury Aref	Alcatel Lucent	U.S.A.	Dec. '08–Jan. '09
Prof. Bielawski Serge	Univ. of Lill	France	Dec. '08
Prof. Szwaj Christophe	Univ. of Lill	France	Dec. '08
Mr. Evain Clement	Univ. of Lill	France	Dec. '08
Mr. Serdaroglu Ertugrul	Free Univ. of Berlin	Germany	Jan. '09–Feb. '09
Prof. Kwon Yong Seung	Sungkyunkwann Univ.	Korea	Jan. '09
Prof. Oh Hyunjin	Masan College	Korea	Jan. '09
Prof. Song Yun Young	Te-Ju Tourism College	Korea	Jan. '09
Mr. Hong Jeong Beom	Sungkyunkwan Univ.	Korea	Jan. '09
Mr. Kang Se-Hun	Yonsei Univ.	Korea	Jan. '09
Prof. Aka Gerard	Ecole Natl. Suprieure de Chimie de Paris/Univ. Pierre & Marie Curie	France	Jan. '09
Ms. Vailikhit Veeramol	Kasetsart Univ.	Thailand	Feb. '09–Mar. '09
Prof. Pulay Peter	Univ. of Arkansas	U.S.A.	Feb. '09–Mar. '09
Dr. Thanyada Rungrotmongkol	Chulalongkorn Univ.	Thailand	Feb. '09–Apr. '09
Prof. Cammi Roberto	Univ. di Parna	Italy	Feb. '09
Associate Prof. Jeong Dea Hong	Seoul Natl. Univ.	Korea	Feb. '09
Dr. Flesch Roman	Free Univ. of Berlin	Germany	Feb. '09
Ms. Promkatkeaw Malinee	Kasetsart Univ.	Thailand	Apr. '09–May '09
Prof. Aka Gerard	Ecole Natl. Suprieure de Chimie de Paris	France	Apr. '09
Associate Prof. Loiseau Pascal	Ecole Natl. Suprieure de Chimie de Paris	France	Apr. '09
Ms. Xu Yanhong	Northeast Normal Univ.	China	May '09
Mr. Adulsirisawad Nithi	Kyoto Univ.	Japan	May '09
Dr. Chen Jin	Tech. Univ. of Munich	China	May '09
Prof. Muhkerjee Debashis	Raman Center for Atomic	India	May '09
Mr. Herzog Alexander	Max Planck Inst.	Germany	May '09
Ms. Rahalkar Anuja	Univ. of Pune	India	Jun. '09–Aug. '09
Prof. Ng Cheuk-Yiu	Univ. of California	U.S.A.	Jun. '09
Dr. Pooarporn Yingyot	SLRI	Thailand	Jul. '09–Sep. '09
Mr. Yingyot Pooarporn	Jenesys	Thailand	Jul. '09–Sep. '09
Prof. Sanderson Joseph	Univ. of Waterloo	Canada	Jul. '09
Mr. Feng Xiao	Beijing Inst. of Tech.	China	Aug. '09–Oct. '09
Mr. Chiang Hsin-Lin	Natl. Tsing Hua Univ.	Taiwan	Aug. '09

(6) Visitor to IMS

Prof. Oleksandr Kobryn	Natl. Inst. for Nanotechnology	Canada	Sep. '08–Oct. '08
Mr. Kinahan Niall	CRANN and School of Chemistry, Trinity College Dublin	Ireland	Nov. '08
Prof. Doyle John	Harvard Univ.	U.S.A.	Nov. '08
Prof. Shapiro Moshe	Univ. of British Columbia	Canada	Nov. '08
Dr. Ni Kang-Kuen	JILA	U.S.A.	Nov. '08
Prof. Fejer Martin	Stanford Univ.	U.S.A.	Nov. '08
Prof. Baumert Thomas	Univ. of Kassel	Germany	Dec. '08
Ms. BashyalKang Homan	Seoul Natl. Univ.	Korea	Feb. '09
Ms. Cho Hong-Jun	Seoul Natl. Univ.	Korea	Feb. '09
Dr. Mitsi Maria	ETH Zurich	Swiss	Feb. '09
Prof. Boxer Steven G.	Stanford Univ.	U.S.A.	Feb. '09
Prof. Neusser Hans (Jurgen)	Tech. Univ. München	Germany	Mar. '09
Prof. Chen Jinhua	SINAP	China	Mar. '09
Prof. Xu Zhongmin	SINAP	China	Mar. '09
Prof. Guo Zhi	SINAP	China	Mar. '09
Associate Prof. Xu Zhongmin	Shanghai Synchrotron Radiation Facility	China	Mar. '09
Associate Prof. Chen Jinhua	Shanghai Synchrotron Radiation Facility	China	Mar. '09
Associate Prof. Guo Zhi	Shanghai Synchrotron Radiation Facility	China	Mar. '09
Associate Prof. Dawes Judith	Macquarie Univ.	Australia	May '09
Dr. Annika Bande	Inst. of Quantum Sci.	Japan	May '09
Prof. Weidemuller Matthias	Ruprecht-Karl Univ. Heidelberg	Germanay	Jun. '09
Prof. Leo Karl	Tohoku Univ.	Japan	Jun. '09

Prof. Rossky Peter	Univ. of Texas at Austin	U.S.A.	Jul. ’09
Prof. Alexander Wei	Purdue Univ.	U.S.A.	Jul. ’09
Prof. DePaola Brett	Kanssas State Univ.	U.S.A.	Jul. ’09
Mr. Chandak Mahesh	MGM Medical College, MGM Univ. of Health Sci.	India	Aug. ’09–Sep. ’09
Prof. Cailleau Herve	Inst. de Phys. de Rennes	France	Aug. ’09

Scientists who would like to visit IMS under programs (1) and (2) are invited to make contact with IMS staff in their relevant field.

Theoretical and Computational Molecular Science

Y. MAEDA, Y. TAKANO, A. SAGARA, M. HASHIMOTO, M. KANDA, S. -I. KIMURA, Y. LIAN, T. NAKAHODO, T. TSUCHIYA, T. WAKAHARA, T. AKASAKA, T. HASEGAWA, S. KAZAOUI, N. MINAMI, J. LU and S. NAGASE, "Simple Purification and Selective Enrichment of Metallic SWCNTs Produced Using the Arc-Discharge Method," *Carbon* **46**, 1563–1569 (2008).

Z. SLANINA, F. UHLIK, S. -L. LEE, L. ADAMOWICZ and S. NAGASE, "Computations on Three Isomers of La@C_{74}," *Int. J. Quantum Chem.* **106**, 2636–2640 (2008).

Y. MAEDA, M. HASHIMOTO, S. KANEKO, M. KANDA, T. HASEGAWA, T. TSUCHIYA, T. AKASAKA, Y. NAITOH, T. SHIMIZU, H. TOKUMOTO, J. LU and S. NAGASE, "Preparation of Transparent and Conductive Thin Films of Metallic Single-Walled Carbon Nanotubes," *J. Mater. Chem.* **18**, 4189–4192 (2008).

Z. SLANINA, F. UHLIK, S. -L. LEE, L. ADAMOWICZ and S. NAGASE, "MPWB1K Calculations of Stepwise Encapsulations: Li_XC_{60}," *Chem. Phys. Lett.* **463**, 121–123 (2008).

Y. YAMAZAKI, K. NAKAJIMA, T. WAKAHARA, T. TSUCHIYA, M. O. ISHITSUKA, Y. MAEDA, T. AKASAKA, M. WAELCHLI, N. MIZOROGI and S. NAGASE, "Observation of ^{13}C NMR Chemical Shifts of Metal Carbides Encapsulated in Fullerenes: Sc_2C_2@C_{82}, Sc_2C_2@C_{84} and Sc_3C_2@C_{80}," *Angew. Chem., Int. Ed.* **47**, 7905–7908 (2008).

Y. OHTSUKA and S. NAGASE, "Projector Monte Carlo Method Based on Configuration State Functions. Test Applications to the H_4 System and Dissociation of LiH," *Chem. Phys. Lett.* **463**, 431–434 (2008).

T. AKASAKA, T. KONO, Y. TAKEMATSU, H. NIKAWA, T. NAKAHODO, T. WAKAHARA, M. O. ISHITSUKA, T. TSUCHIYA, Y. MAEDA, M. T. H. LIU, K. YOZA, T. KATO, K. YAMAMOTO, N. MIZOROGI, Z. SLANINA and S. NAGASE, "Does Gd@C_{82} Have an Anomalous Endohedral Structure? Synthesis and Single Crystal X-Ray Structure of the Carbene Adduct," *J. Am. Chem. Soc.* **130**, 12840–12841 (2008).

D. WANG, J. LU, J. ZHOU, L. LAI, L. WANG, G. LUO, Z. GAO, G. LI, W. N. MEI, S. NAGASE, Y. MAEDA, T. AKASAKA and Y. ZHOU, "Selective Adsorption of Cations on Single-Walled Carbon Nanotubes: A Density Functional Theory Study," *Comput. Mater. Sci.* **43**, 886–891 (2008).

T. SASAMORI, K. HIRONAKA, Y. SUGIYAMA, N. TAKAGI, S. NAGASE, Y. HOSOI, Y. FURUKAWA and N. TOKITOH, "Synthesis and Reactions of a Stable 1,2-Diaryl-1,2- Dibromodisilene: A Precursor for Substituted Disilenes and a 1,2-Diaryldisilyne," *J. Am. Chem. Soc.* **130**, 13856–13857 (2008).

F. UHLIK, Z. SLANINA and S. NAGASE, "Computational Treatment of Alkaline Earth Encapsulations in C_{74}: Relative Thermodynamic Production Abundances," *Fullerenes, Nanotubes, Carbon Nanostruct.* **16**, 507–516 (2008).

X. LU, H. NIKAWA, T. TSUCHIYA, Y. MAEDA, M. O. ISHITSUKA, T. AKASAKA, M. TOKI, H. SAWA, Z. SLANINA, N. MIZOROGI and S. NAGASE, "Bis-Carbene Adducts of Non-IPR La_2@C_{72}: Localization of High Reactivity around Fused Pentagons and Electrochemical Properties," *Angew. Chem., Int. Ed.* **47**, 8642–8645 (2008).

Z. SLANINA, F. UHLIK, S. -L. LEE, L. ADAMOWICZ and S. NAGASE, "Li_xC_{60}: Calculations of the Encapsulation Energetics and Thermodynamics," *Int. J. Mol. Sci.* **9**, 1841–1850 (2008).

Y. TAKANO, A. YOMOGIDA, H. NIKAWA, M. YAMADA, T. WAKAHARA, T. TSUCHIYA, M. O. ISHITSUKA, Y. MAEDA, T. AKASAKA, T. KATO, Z. SLANINA, N. MIZOROGI and S. NAGASE, "Radical Coupling Reaction of Paramagnetic Endohedral Metallofullerene La@C_{82}," *J. Am. Chem. Soc.* **130**, 16224–16230 (2008).

N. TAJIMA, M. IKEDA, M. SAITO, K. ISHIMURA and S. NAGASE, "Synthesis, Structure and Reactions of a Trianion Equivalent, Trilithiostannane," *Chem. Commun.* 6495–6497 (2008).

Y. MAEDA, T. KATO, J. HIGO, T. HASEGAWA, T. KITANO, T. TSUCHIYA, T. AKASAKA, T. OKAZAKI, J. LU and S. NAGASE, "$C_{60}(OH)_n$-Assisted Dispersion of Single-Walled Carbon Nanotubes," *NANO* **3**, 455–459 (2008).

J. ZHOU, Y. MAEDA, J. LU, A. TASHIRO, T. HASEGAWA, G. LUO, L. WANG, L. LAI, T. AKASAKA, S. NAGASE, Z. GAO, R. QIN, W. N. MEI, G. LI and D. YU, "Electronic-Type- and Diameter-Dependent Reduction of Single-Walled Carbon Nanotubes Induced by Adsorption of Electron-Donor Molecules," *Small* **5**, 244–255 (2009).

T. TSUCHIYA, T. AKASAKA and S. NAGASE, "Construction of Supramolecular Systems Based on Endohedral Metallofullerenes," *Bull. Chem. Soc. Jpn. (Accounts)* **82**, 171–181 (2009).

A. H. HAN, T. WAKAHARA, Y. MAEDA, T. AKASAKA, M. FUJITSUKA, O. ITO, K. YAMAMOTO, M. KATO, K. KOBAYASHI and S. NAGASE, "A New Method for Separating the D_3 and C_{2v} Isomers of C_{78}," *New J. Chem.* **33**, 497–500 (2009).

Y. MAEDA, A. SAGARA, M. HASHIMOTO, Y. HIRASHIMA, K. SODE, T. HASEGAEA, M. KANDA, M. O. ISHITSUKA, T. TSUCHIYA, T. AKASAKA, T. OKAZAKI, H. KATAURA, J. LU, S. NAGASE and S. TAKEUCHI, "Tuning of Electronic Properties of Single-Walled Carbon Nanotubes under Homogenous Conditions," *ChemPhysChem* **10**, 926–930 (2009).

X. GAO, K. ISHIMURA, S. NAGASE and Z. CHEN, "Dichlorocarbene Addition onto C_{60} from the Trichloromethyl Anion: Carbene Mechanism or Bingel Mechanism?" *J. Phys. Chem. A* **113**, 3673–3676 (2009).

M. KATOUDA and S. NAGASE, "Efficient Parallel Algorithm of Second-Order Møller Plesset Perturbation Theory with Resolution-of-Identity Approximation (RI-MP2)," *Int. J. Quantum Chem.* **109**, 2121–2130 (2009).

K. TAKEUCHI, M. ICHINOHE, A. SEKIGUCHI, J. -D. GUO and S. NAGASE, "Reactivity of the Disilyne RSi≡SiR (R = $Si^iPr[CH(SiMe_3)_2]_2$) toward Nitriles: Unexpected Formation of Triazo-1,4-disilabicyclo[2.2.2]octa-2,5,7-triene Derivatives," *Organometallics* **28**, 2658–2660 (2009).

T. ASADA, S. NAGASE, K. NISHIMOTO and S. KOSEKI, "Simulation Study of Interactions and Reactivities between NADH Cytochrome b5 Reductase and Cytochrome b5," *J. Mol. Liq.* **147**, 139–144 (2009).

K. E. WHITENER, R. J. CROSS, M. SAUNDERS, S. -I. IWAMATSU, S. MURATA, N. MIZOROGI and S. NAGASE, "Methane in an Open-Cage [60]Fullerene," *J. Am. Chem. Soc.* **131**, 6338–6339 (2009).

Z. ZHU, R. C. FISCHER, B. D. ELLIS, E. RIVARD, W. A. MERRILL, M. M. OLMSTEAD, P. P. POWER, J. -D. GUO, S. NAGASE and L. PU, "Synthesis, Characterization and Real Molecule DFT Calculations for Neutral Organogallium (I) Aryl Dimers and Monomers: Weakness of Gallium–Gallium Bonds in Digallenes and Digallynes," *Chem. –Eur. J.* **15**, 5263–5272 (2009).

L. CHEN, L. WANG, X. GAO, S. NAGASE, Y. HONSHO, A. SAEKI, S. SEKI and D. JIANG, "The Non-Covalent Assembly of Benzene-Bridged Metallosalphen Dimers: Photoconductive Tapes with Large Carrier Mobility and Spatially Distinctive Conduction Anisotropy," *Chem. Commun.* 3119–3121 (2009).

T. NAKAHODO, K. TAKAHASHI, M. O. ISHITSUKA, T. TSUCHIYA, Y. MAEDA, H. FUJIHARA, S. NAGASE and T. AKASAKA, "Preparation, Characterization, and Electrochemical Properties of Selenylfullerenes," *Phosphorus, Sulfur Silicon Relat. Elem.* **184**, 1523–1540 (2009).

Y. TAKANO, M. AOYAGI, M. YAMADA, H. NIKAWA, Z. SLANINA, N. MIZOROGI, M. O. ISHITSUKA, T. TSUCHIYA, Y. MAEDA, T. AKASAKA, T. KATO and S. NAGASE, "Anisotropic Magnetic Behavior of Anionic Ce@C_{82} Carbene Derivatives," *J. Am. Chem. Soc.* **131**, 9340–9346 (2009).

X. GAO, L. WANG, Y. OHTSUKA, D. -E. JIANG, Y. ZHAO, S. NAGASE and Z. CHEN, "Oxidation Unzipping of Stable Nanographenes into Joint Spin-Rich Fragments," *J. Am. Chem. Soc.* **131**, 9663–9669 (2009).

H. NIKAWA, T. YAMADA, B. GAO, N. MIZOROGI, Z. SLANINA, T. TSUCHIYA, T. AKASAKA, K. YOZA and S. NAGASE, "Missing Metallofullerene with C_{80} Cage," *J. Am. Chem. Soc.* **131**, 10950–10954 (2009).

D. -E. JIANG, K. NOBUSADA, W. LUO and R. L. WHETTEN, "Thiolated Gold Nanowires: Metallic versus Semiconducting," *ACS NANO* **3**, 2351–2357 (2009).

T. YASUIKE and K. NOBUSADA, "Photoinduced Coherent Adsorbate Dynamics on a Metal Surface: Nuclear Wave-Packet Simulation with Quasi-Diabatic Potential Energy Curves Using an Open-Boundary Cluster Model Approach," *Phys. Rev. B* **80**, 035430 (8 pages) (2009).

K. SHIRATORI and K. NOBUSADA, "Development of a Finite-Temperature Density Functional Approach to Electrochemical Reactions," *J. Phys, Chem. A* **112**, 10681–10688 (2008).

Y. KUBOTA and K. NOBUSADA, "Exciton Transfer in Quantum Dot Arrays: Comparison of Eigenbasis and Site Basis Representations," *J. Chem. Phys.* **129**, 094704 (7 pages) (2008).

T. YANAI, Y. KURASHIGE, D. GHOSH and G. K-L. CHAN, "Accelerating Convergence in Iterative Solution for Large-Scale Complete Active Space Self-Consistent-Field Calculations," *Int. J. Quantum Chem.* **109**, 2178–2190 (2009).

E. NEUSCAMMAN, T. YANAI and G. K-L. CHAN, "Quadratic Canonical Transformation Theory and Higher Order Density Matrices," *J. Chem. Phys.* **130**, 124102 (12 pages) (2009).

Y. KURASHIGE and T. YANAI, "High-Performance Ab Initio Density Matrix Renormalization Group Method: Applicability to Large-Scale Multireference Problems for Metal Compounds," *J. Chem. Phys.* **130**, 234114 (21 pages) (2009).

B. KIM, S. -H. CHONG, R. ISHIZUKA and F. HIRATA, "An Attempt toward the Generalized Langevin Dynamics Simulation," *Cond. Matt. Phys.* **11**, 179–190 (2008).

Y. IKUTA, S. KARITA, Y. KITAGO, N. WATANABE and F. HIRATA, "Detecting Reaction Intermediate in Enzymatic Reaction of Cel44A, GH Family 44 Endoglucanase with 3D-RISM Theory," *Chem. Phys. Lett.* **465**, 279–284 (2008).

K. NISHIYAMA, T. YAMAGUCHI and F. HIRATA, "Solvation Dynamics in Polar Solvents Studied by Means of RISM/Mode-Coupling Theory," *J. Phys. Chem. B* **113**, 2800–2804 (2009).

Y. KIYOTA, R. HIRAOKA, N. YOSHIDA, Y. MARUYAMA, T. IMAI and F. HIRATA, "Theoretical Study of CO Escaping Pathway in Myoglobin with the 3D-RISM Theory," *J. Am. Chem. Soc. (Communication)* **131**, 3852–3853 (2009).

S. PHONGPHONPHANEE, N. YOSHIDA and F. HIRATA, "The Potential of Mean Force of Water and Ions in Aquaporin Channels Investigated by the 3D-RISM Method," *J. Mol. Liq.* **147**, 107–111 (2009).

T. IMAI, A. KOVALENKO, F. HIRATA and A. KIDERA, "Molecular Thermodynamics of Trifluoroethanol-Induced Helix Formation: Analysis of the Solvation Structure and Free Energy by the 3D-RISM Theory," *Interdiscip. Sci. Comput. Life Sic.* **1**, 156–160 (2009).

S. -H. CHONG and B. KIM, "Nonequilibrium Mode-Coupling Theory for Uniformly Sheared Systems," *Phys. Rev. E* **79**, 021203 (2009).

S. -H. CHONG and W. KOB, "Coupling and Decoupling between Translational and Rotational Dynamics in a Supercooled Molecular Liquid," *Phys. Rev. Lett.* **102**, 025702 (2009).

S. -H. CHONG, "Connections of Activated Hopping Processes with the Breakdown of the Stokes-Einstein Relation and with Aspects of Dynamical Heterogeneities," *Phys. Rev. E* **78**, 041501 (2008).

S. MIYASHITA and K. YONEMITSU, "Spin and Charge Fluctuations and Lattice Effects on Charge Ordering in α-(BEDT-TTF)$_2$I$_3$,'' *J. Phys. Soc. Jpn.* **77**, 094712 (6 pages) (2008).

Y. YAMASHITA and K. YONEMITSU, "Modified Barrett Formula near the Neutral–Ionic Quantum Phase Transition,'' *J. Phys.: Conf. Series* **132**, 012019 (5 pages) (2008).

K. YONEMITSU, "Enhanced Coherent Dynamics near a Transition between Neutral Quantum-Paraelectric and Ionic Ferroelectric Phases in the Quantum Blume-Emery-Griffiths Model,'' *Phys. Rev. B* **78**, 205102 (5 pages) (2008).

K. YONEMITSU and N. MAESHIMA, "Energy Transfer to Phonons after Photoexcitation in One-Dimensional Correlated Electron–Phonon Systems,'' *Phys. Status Solidi C* **6**, 240–243 (2009).

N. MAESHIMA, K. YONEMITSU and K. HINO, "Photogenerated Polaronic State in a One-Dimensional Dimerized Mott Insulator K-TCNQ,'' *J. Phys.: Conf. Series* **148**, 012005 (4 pages) (2009).

S. MIYASHITA and K. YONEMITSU, "Effects of Spin Fluctuations, Charge Fluctuations and Lattice Distortions on Charge Orders in θ- and α-Type BEDT-TTF Salts,'' *J. Phys.: Conf. Series* **148**, 012006 (3 pages) (2009).

K. YONEMITSU, N. MAESHIMA, Y. TANAKA and S. MIYASHITA, "Photoinduced Melting and Charge Order in Quarter-Filled Organic Conductors: Itinerant Electron Systems with Competing Interactions,'' *J. Phys.: Conf. Series* **148**, 012054 (5 pages) (2009).

Y. TANAKA and K. YONEMITSU, "Photoinduced Melting of Charge Order in Quasi-Two-Dimensional Organic Conductors,'' *J. Phys.: Conf. Series* **148**, 012063 (3 pages) (2009).

K. YONEMITSU and N. MAESHIMA, "Coupling-Dependent Rates of Energy Transfers from Photoexcited Mott Insulators to Lattice Vibrations,'' *Phys. Rev. B* **79**, 125118 (6 pages) (2009).

S. MIYASHITA, Y. YAMASHITA, K. YONEMITSU, A. KOGA and N. KAWAKAMI, "Mott Insulating State in a Quarter-Filled Two-Orbital Hubbard Chain with Different Bandwidths,'' *J. Phys.: Conf. Series* **150**, 042128 (4 pages) (2009).

Y. TANAKA and K. YONEMITSU, "Role of Electron–Lattice Couplings on Charge Order in Quasi-Two-Dimensional Organic Conductors,'' *J. Phys.: Conf. Series* **150**, 042204 (4 pages) (2009).

K. YONEMITSU, "Nonequilibrium Green's-Function Approach to the Suppression of Rectification at Metal–Mott-Insulator Interfaces,'' *J. Phys. Soc. Jpn.* **78**, 054705 (8 pages) (2009).

A. FURUKAWA, K. KIM, S. SAITO and H. TANAKA, "Anisotropic Cooperative Structural Rearrangements in Sheared Supercooled Liquids," *Phys. Rev. Lett.* **102**, 016001 (4 pages) (2009).

K. KIM and S. SAITO, "Multiple Time Scales Hidden in Heterogeneous Dynamics of Glass-Forming Liquids," *Phys. Rev. E* **79**, 060501(R) (4 pages) (2009).

M. EHARA, J.R. GOUR and P. PIECUCH, "Low-Lying Valence Excited States of Open-Shell Triatomic Molecules Studied Using the Electron-Attached and Ionized Symmetry-Adapted Cluster-Configuration Interaction and Equation-of-Motion Coupled Cluster Methodologies," *Mol. Phys.*, **107**, 871–880 (2009).

K. UEDA, R. PUTTNER, N. A. CHEREPKOV, F. GEL'MUKHANOV and M. EHARA, "High Resolution X-Ray Photoelectron Spectroscopy on Nitrogen Molecules," *Eur. Phys. J.* **169**, 95–107 (2009).

T. WATANABE, M. EHARA, K. KURAMOTO and H. NAKATSUJI, "Possible Reaction Pathway in Methanol Dehydrogenation on Pt and Ag Surfaces/Clusters Starting from OH Scission: Dipped Adcluster Model Study," *Surf. Sci.* **603**, 641–646 (2009).

M. EHARA, K. KURAMOTO and H. NAKATSUJI, "Relativistic Effect in the K-Shell Ionizations: SAC-CI General-R Study Based on DK2 Hamiltonian," *Chem. Phys.* **356**, 195–198 (2009).

M. EHARA and H. NAKATSUJI, "Theoretical Spectroscopy of Inner-Shell Electronic Processes and Photochemistry of Fluorescent Molecules," *Progress in Theoretical Chemistry and Physics, The Proceedings of the 13th International Workshop on Quantum Systems in Chemistry and Physics (QSCP-XIII)*, 79–101 (2009).

S. ARULMOZHIRAJA, M. EHARA and H. NAKATSUJI, "Electronic Transitions in *cis*- and *trans*- Dichloroethylenes and in Tetrachloroethylene," *J. Chem. Phys.* **129**, 174506 (8 pages) (2008).

M. EHARA and H. NAKATSUJI, "Geometry Relaxation after Inner-Shell Electronic Excitations and Ionizations," *Collect. Czech. Chem. Commun.* **73**, 771–785 (2008).

Y. ABE, K. KURAMOTO, M. EHARA, H. NAKATSUJI, M. SUGINOME, M. MURAKAMI and Y. ITO, "Mechanism of the Palladium-Catalyzed Regioselective Silaboration of Allene: Theoretical Study," *Organometallics* **27**, 1736–1742 (2008).

T. TANAKA, M. HOSHINO, H. KATO, M. EHARA, N. YAMADA, R. FUKUDA, H. NAKATSUJI, Y. TAMENORI, J. R. HARRIES, G. PRUEMPER, H. TANAKA and K. UEDA, "Vibration-Induced Suppression of Valence-Rydberg Mixing in the O 1s → nsσ Rydberg Series in N_2O," *Phys. Rev. A* **77**, 012709 (4 pages) (2008).

R. FUKUDA and H. NAKATSUJI, "Formulation and Implementation of Direct Algorithm for the Symmetry Adapted Cluster and Symmetry Adapted Cluster-Configuration Interaction Method," *J. Chem. Phys.* **128**, 094105 (14 pages) (2008).

M. TASHIRO, "Electron Scattering from Gas-Phase Glycine Molecules," *J. Chem. Phys.* **129**, 164308 (2008).

M. TASHIRO, "Electron Impact Excitations of S_2 Molecules," *Chem. Phys. Lett.* **453**, 145 (2008).

M. TASHIRO, "Exchange Effects in Elastic Collisions of Spin-Polarized Electrons with Open-Shell Molecules with $^3\Sigma_g^-$ Symmetry," *Phys. Rev. A* **77**, 012723 (2008).

T. ISHIDA, "Solvent Motions and Solvation Processes in a Short-Time Regime: Effects on Excited-State Intramolecular Processes in Solution," *J. Phys. Chem. B* **113**, 9255–9264 (2009).

H. SHIROTA, K. NISHIKAWA and T. ISHIDA, "Atom Substitution Effects of $[XF_6]^-$ in Ionic Liquids. 1. Experimental Study," *J. Phys. Chem. B* **113**, 9831–9839 (2009).

T. ISHIDA, K. NISHIKAWA and H. SHIROTA, "Atom Substitution Effects of $[XF_6]^-$ in Ionic Liquids. 2. Theoretical Study," *J. Phys. Chem. B* **113**, 9840–9851 (2009).

Photo-Molecular Science

N. N. HORIMOTO, K. IMURA and H. OKAMOTO, “Dye-Fluorescence Enhancement and Quenching by Gold Nanoparticles: Direct Near-Field Microscopic Observation of Shape Dependence,” *Chem. Phys. Lett.* **467**, 105–109 (2008).

Y. JIANG, N. N. HORIMOTO, K. IMURA, H. OKAMOTO, K. MATSUI and R. SHIGEMOTO, “Bio-Imaging with Two-Photon Induced Luminescence from Triangular Nanoplates and Nanoparticle Aggregates of Gold,” *Adv. Mater.* **21**, 2309–2313 (2009).

K. IMURA and H. OKAMOTO, “Properties of Photoluminescence from Single Gold Nanorods Induced by Near-Field Two-Photon Excitation,” *J. Phys. Chem. C* **113**, 11756–11759 (2009).

K. IMURA, Y. C. KIM, S. KIM, D. H. JEONG and H. OKAMOTO, “Two-Photon Imaging of Localized Optical Fields in the Vicinity of Silver Nanowires Using a Scanning Near-Field Optical Microscope,” *Phys. Chem. Chem. Phys.* **11**, 5876–5881 (2009).

H. HASEGAWA and Y. OHSHIMA, “Coherent Rotational Dynamics of Molecules in Intense Laser Field,” *Proc. SPIE-Int. Soc. Opt. Eng.* **7027**, 70271F-1–10 (2008).

H. KATSUKI, H. CHIBA, C. MEIER, B. GIRARD and K. OHMORI, “Actively Tailored Spatiotemporal Images of Quantum Interference on the Picometer and Femtosecond Scales,” *Phys. Rev. Lett.* **102**, 103602 (4 pages) (2009).

I. L. BRADEANU, N. KOSUGI, R. FLESCH and E. RÜHL, “Site-Dependent Spectral Shifts in Core-to-π^* Excitations of Pyridine Clusters,” *J. Phys. Chem. A* **112**, 9192–9199 (2008).

M. NAGASAKA, T. HATSUI and N. KOSUGI, “Exchange Interaction in Kr 3d Excitations of Small Krypton Clusters,” *J. Electron Spectrosc.* **166–167**, 16–20 (2008).

Y. VELKOV, V. KIMBERG, N. KOSUGI, P. SAŁEK and F. GEL’MUKHANOV, “Origin of Fine Structures on the Dissociative 1s–σ^* Resonance in X-Ray Absorption Spectra of O_2,” *Chem. Phys. Lett.* **476**, 147–150 (2009).

V. KIMBERG, N. KOSUGI and F. GEL’MUKHANOV, “Theoretical Studies of Angle-Resolved Ion Yield Spectra of Core-to-Valence Transitions of Acetylene,” *J. Chem. Phys.* **130**, 114302 (10 pages) (2009).

M. NAGASAKA, H. KONDOH, K. AMEMIYA, T. OHTA and Y. IWASAWA, “Proton Transfer in Water-Hydroxyl Mixed Overlayers on Pt(111): Combined Approach of Laser Desorption and Spatially-Resolved X-Ray Photoelectron Spectroscopy,” *Surf. Sci.* **603**, 1690–1695 (2009).

I. NAKAI, H. KONDOH, T. SHIMADA, M. NAGASAKA, R. YOKOTA, T. KATAYAMA, K. AMEMIYA, H. ORITA and T. OHTA, “Mechanism of N + NO Reaction on Rh(111) Surfaces: A Precursor-Mediated Reaction,” *J. Phys. Chem. C* **113**, 13257–13265 (2009).

S. KERA, H. YAMANE and N. UENO, “First Principles Measurements of Charge Mobility in Organic Semiconductors: Valence Hole-Vibration Coupling in Organic Ultrathin Films,” *Prog. Surf. Sci.* **84**, 135–154 (2009).

H. YAGI, K. NAKAJIMA, K. R. KOSWATTAGE, K. NAKAGAWA, C. HUANG, MD. S. I. PRODHAN, B. P. KAFLE, H. KATAYANAGI and K. MITSUKE, “Photoabsorption Cross Section of C_{60} Thin Films from the Visible to Vacuum Ultraviolet,” *Carbon* **47**, 1152–1157 (2009).

MD. S. I. PRODHAN, H. KATAYANAGI, C. HUANG, H. YAGI, B. P. KAFLE and K. MITSUKE, “Velocity Map Imaging Apparatus Applicable to a Study of Multiple Photofragmentation of C_{60},” *Chem. Phys. Lett.* **469**, 19–25 (2009).

H. YAGI, K. NAKAJIMA, K. R. KOSWATTAGE, K. NAKAGAWA, H. KATAYANAGI and K. MITSUKE, “Photoabsorption Cross Section of C_{70} Thin Films from Visible to Vacuum Ultraviolet,” *J. Chem. Phys.* **130**, 234510 (5 pages) (2009).

A. MATSUDA, M. FUSHITANI and A. HISHIKAWA, “Electron–Ion Coincidence Momentum Imaging of Molecular Dissociative Ionization in Intense Laser Fields: Application to CS_2,” *J. Electron Spectrosc. Relat. Phenom.* **169**, 97–101(2009).

A. MATSUDA, M. FUSHITANI, R. D. THOMAS, V. ZHAUNERCHYK and A. HISHIKAWA, “Multiple Explosion Pathways of the Deuterated Benzene Trication in 9-fs Intense Laser Fields,” *J. Phys. Chem. A* **113**, 2254–2260 (2009).

M. LABAT, M. HOSAKA, M. SHIMADA, M. KATOH and M. E. COUPRIE, “Optimization of a Seeded Free-Electron Laser with Helical Undulators,” *Phys. Rev. Lett.* **101**, 164803 (2008).

M. LABAT, M. HOSAKA, M. SHIMADA, N. YAMAMOTO, M. KATOH and M. E. COUPRIE, “Observation of Synchrotron Sidebands in a Storage-Ring-Based Seeded Free-Electron Laser,” *Phys. Rev. Lett.* **102**, 014801 (2009).

J. TAKAHASHI, H. SHINOJIMA, M. SEYAMA, Y. UENO, T. KANEKO, K. KOBAYASHI, H. MITA, M. ADACHI, M. HOSAKA and M. KATOH, “Chirality Emergence in Thin Solid Films of Amino Acids by Polarized Light from Synchrotron Radiation and Free Electron Laser,” *Int. J. Mol. Sci.* **10**, 3044–3064 (2009).

S. KIMURA, T. ITO, H. MIYAZAKI, T. MIZUNO, T. IIZUKA and T. TAKAHASHI, “Electronic Inhomogeneity EuO: Possibility of Magnetic Polaron States,” *Phys. Rev. B* **78**, 052409 (4 pages) (2008).

K. E. LEE, C. I. LEE, H. J. OH, M. A. JUNG, B. H. MIN, H. J. IM, T. IIZUKA, Y. S. LEE, S. KIMURA and Y. S. KWON, “Optical Properties of the Charge-Density-Wave Compound $CeTe_2$,” *Phys. Rev. B* **78**, 134408 (5 pages) (2008).

T. MIZUNO, T. IIZUKA, S. KIMURA, K. MATSUBAYASHI, K. IMURA, H. S. SUZUKI and N. K. SATO, “Excitonic Instability in the Transition from the Black Phase to the Golden Phase of SmS under Pressure Investigated by Infrared Spectroscopy,” *J. Phys. Soc. Jpn.* **77**, 113704 (4 pages) (2008).

J. ONOE, T. ITO and S. KIMURA, “Time Dependence of the Electronic Structure of an Electron-Beam-Irradiated C_{60} Film,” *J. Appl. Phys.* **104**, 103706 (3 pages) (2008).

S. KIMURA, T. IIZUKA and Y. S. KWON, “Origin of Middle-Infrared Peaks in Cerium Compounds,” *J. Phys. Soc. Jpn.* **78**, 013710 (4 pages) (2009).

LIST OF PUBLICATIONS

A. A. POPOV, V. M. SENYAVIN, V. I. KOREPANOV, I. V. GOLDT, A. M. LEBEDEV, V. G. STANKEVICH, K. A. MENSHIKOV, N. YU. SVECHNIKOV, O. V. BOLTALINA, I. E. KAREEV, S. KIMURA, O. SIDOROVA, K. KANNO and I. AKIMOTO, "Vibrational, Electronic, and Vibronic Excitations of Polar $C_{60}F_{18}$ Molecules: Experimental and Theoretical Study," *Phys. Rev. B* **79**, 045413 (11 pages) (2009).

H. MIYAZAKI, T. ITO, H. J. IM, K. TERASHIMA, S. YAGI, M. KATO, K. SODA and S. KIMURA, "Single Crystalline Growth and Magnetic, Optical and Photoelectrical Properties of EuO Thin Films," *Jpn. J. Appl. Phys.* **48**, 055504 (4 pages) (2009).

H. J. IM, T. ITO, S. KIMURA, H. -D. KIM, J. B. HONG and Y. S. KWON, "Crystalline Electric Field Effects in Ce 3d Core-Level Spectra of Heavy-Fermion Systems: Hard X-Ray Photoemission Spectroscopy on $CeNi_{1-x}Co_xGe_2$," *Phys. Rev. B* **79**, 193105 (4 pages) (2009).

H. MIYAZAKI, T. ITO, H. J. IM, S. YAGI, M. KATO, K. SODA and S. KIMURA, "Direct Observation of Momentum-Dependent Exchange Interaction in a Heisenberg Ferromagnet," *Phys. Rev. Lett.* **102**, 227203 (4 pages) (2009).

S. KIMURA, "Origin of Infrared Peaks in the Optical Conductivity of Ytterbium Compounds," *Phys. Rev. B* **80**, 073103 (4 pages) (2009).

Y. HIKOSAKA, P. LABLANQUIE, E. SHIGEMASA, T. AOTO and K. ITO, "Sub-Natural Linewidth Spectroscopy on Core-Valence Doubly Ionized States of OCS," *J. Phys. B* **41**, 025103 (4 pages) (2008).

T. KANEYASU, Y. HIKOSAKA, E. SHIGEMASA, P. LABLANQUIE, F. PENENT and K. ITO, "Auger Decays of 1s Shake-up and Shake-off States in N_2 Molecules," *J. Phys. B* **41**, 135101 (6 pages) (2008).

Y. HIKOSAKA, Y. VELKOV, E. SHIGEMASA, T. KANEYASU, Y. TAMENORI, J. LIU and F. GEL'MUKHANOV, "X-Ray Absorption Measured in the Resonant Auger Scattering Mode," *Phys. Rev. Lett.* **101**, 073001 (4 pages) (2008).

Y. VELKOV, Y. HIKOSAKA, E. SHIGEMASA, S. GAVRILYUK and F. GEL'MUKHANOV, "X-Ray Absorption Spectroscopy Measured in Resonant X-Ray Scattering Mode: How Unnatural Is the Resolution beyond the Natural Width?" *Chem. Phys. Lett.* **465**, 153–156 (2008).

T. KANEYASU, Y. HIKOSAKA, P. LABLANQUIE, F. PENENT, L. ANDRIC, G. GAMBLIN, J. H. D. ELAND, Y. TAMENORI, T. MATSUSHITA and E. SHIGEMASA, "Mechanisms of Spontaneous Two-Electron Emission from Core-Excited States of Molecular CO," *Phys. Rev. Lett.* **101**, 183003 (4 pages) (2008).

Y. HIKOSAKA, T. KANEYASU and E. SHIGEMASA, "Formation of Metastable Fragments around the Cl 2p Ionization Thresholds of HCl," *J. Korean Phys. Soc.* **53**, 3798–3801 (2008).

T. KANEYASU, M. ITO, Y. HIKOSAKA and E. SHIGEMASA, "Stability and Fragmentation of OCS^{2+} Studied by Using Auger-Electron-Ion Coincidence Measurement," *J. Korean Phys. Soc.* **54**, 371–375 (2009).

Y. HIKOSAKA, P. LABLANQUIE, F. PENENT, T. KANEYASU, E. SHIGEMASA, R. FEIFEL, J. H. D. ELAND and K. ITO, "Energy Correlation among Three Electrons Emitted in Triple Photoionization of Ar," *Phys. Rev. Lett.* **102**, 013002 (4 pages) (2009).

Y. VELKOV, Y. HIKOSAKA, E. SHIGEMASA, T. KANEYASU, Y. TAMENORI, J. -C. LIU and F. GEL'MUKHANOV, "X-Ray Absorption Spectroscopy beyond the Natural Width Measured in Partial Auger Yield Mode," *Phys. Rev. A* **79**, 022508 (11 pages) (2009).

H. ISHIZUKI and T. TAIRA, "Mg-Doped Congruent $LiTaO_3$ Crystal for Large-Aperture Quasi-Phase Matching Device," *Opt. Express* **16**, 16963–16970 (2008).

K. XU, P. LOISEAU, G. AKA, R. MAILLARD, A. MAILLARD and T. TAIRA, "Nonlinear Optical Properties of $Ca_5(BO_3)_3F$ Crystal," *Opt. Express* **16**, 17735–17744 (2008).

H. SAKAI, H. KAN and T. TAIRA, ">1 MW Peak Power Single-Mode High-Brightness Passively Q-Switched Nd^{3+}:YAG Microchip Laser," *Opt. Express* **16**, 19891–19899 (2008).

Y. SATO, H. ISHIZUKI and T. TAIRA, "Novel Model of Thermal Conductivity for Optical Materials," *Rev. Laser Eng. Supplemental* **2008**, 1081–1084 (2008).

X. GU, G. MARCUS, Y. DENG, T. METZGER, C. TEISSET, N. ISHII, T. FUJI, A. BALTUSKA, R. BUTKUS, V. PERVAK, H. ISHIZUKI, T. TAIRA, T. KOBAYASHI, R. KIENBERGER and F. KRAUSZ, "Generation of Carrier-Envelope-Phase-Stable 2-Cycle 740-μJ Pulses at 2.1-μm Carrier Wavelength," *Opt. Express* **17**, 62–69 (2009).

Y. SATO, J. AKIYAMA and T. TAIRA, "Effects of Rare-Earth Doping on Thermal Conductivity in $Y_3Al_5O_{12}$ Crystals," *Opt. Mater.* **31**, 720–724 (2009).

S. HAYASHI, T. SHIBUYA, H. SAKAI, T. TAIRA, C. OTANI, Y. OGAWA and K. KAWASE, "Tunability Enhancement of a Terahertz-Wave Parametric Generator Pumped by a Microchip Nd:YAG Laser," *Appl. Opt.* **48**, 2899–2902 (2009).

S. HAYASHI, T. SHIBUYA, H. SAKAI, T. YASUI, T. TAIRA, Y. OGAWA, C. OTANI and K. KAWASE, "Portable and Tunable Terahertz-Wave Parametric Generator Pumped by Microchip Nd:YAG Laser," *Rev. Laser Eng.* **37** (Special Issue on Micro Solid-State Photonics), 278–282 (2009).

M. TSUNEKANE, T. INOHARA, A. ANDO, N. KIDO, K. KANEHARA and T. TAIRA, "Micro-Lasers for Ignition Engines," *Rev. Laser Eng.* **37** (Special Issue on Micro Solid-State Photonics), 283–289 (2009).

Y. IDO, K. WATANABE, N. ISHIGAKI, A. KADOYA, K. TOKUDA, K. TOJO and T. TAIRA, "Development of Microchip Laser/Periodically Poled Stoichiometric $LiTaO_3$ (PPSLT) for the Light Source of MALDI," *Rev. Laser Eng.* **37** (Special Issue on Micro Solid-State Photonics), 290–295 (2009).

M. MIYAZAKI, J. SAIKAWA, M. FUJII, H. ISHIZUKI and T. TAIRA, "Development of a High-Energy, Broadly Tunable and Narrow Band-Width Mid-Infrared Light Source and Its Application to Infrared-Ultraviolet Double Resonance Spectroscopy," *Rev. Laser Eng.* **37** (Special Issue on Micro Solid-State Photonics), 296–303 (2009).

I. NAKAI, Y. MATSUMOTO, N. TAKAGI and S. OKAZAKI, “Structure and Thermal Fluctuation of One-Dimensional AgO Chains on Ag(110) Surfaces Studied with Density Functional Theory and Monte Carlo Simulations,” *J. Chem. Phys.* **129**, 154709 (8 pages) (2008).
M. NAGAO, K. WATANABE and Y. MATSUMOTO, “Ultrafast Vibrational Energy Transfer in the Layers of D_2O and CO on Pt(111) Studied with Time-Resolved Sum-Frequency-Generation Spectroscopy,” *J. Phys. Chem. C* **113**, 11712–11719 (2009).
T. NAKAGAWA, I. YAMAMOTO, Y. TAKAGI, K. WATANABE, Y. MATSUMOTO and T. YOKOYAMA, “Two-Photon Photoemission Magnetic Circular Dichroism and Its Energy Dependence,” *Phys. Rev. B* **79**, 172404 (4 pages) (2009).
T. NAKAGAWA, K. WATANABE, Y. MATSUMOTO and T. YOKOYAMA, “Magnetic Circular Dichroism Photoemission Electron Microscopy Using Laser and Threshold Photoemission,” *J. Phys.: Condens. Matter* **21**, 314010 (6 gages) (2009).
K. WATANABE, K. INOUE, I. F. NAKAI, M. FUYUKI and Y. MATSUMOTO, “Ultrafast Electron and Lattice Dynamics at Potassium-Covered Cu(111) Surfaces,” *Phys. Rev. B* **80**, 075404 (10 gages) (2009).

P. DUTTA and K. TOMINAGA, “Terahertz Time-Domain Spectroscopic Study of the Low-Frequency Spectra of Nitrobenzene in Alkanes,” *J. Mol. Liq.* **147**, 45–51 (2009).
C. S. PONSECA Jr., O. KAMBARA, S. KAWAGUCHI and K. TOMINAGA, “Terahertz Absorption Measurements of Amino Acids and Peptides,” *PISIKA (the Journal of the Physics Society of the Philippines)* **2**, 27–29 (2008).
P. DUTTA and K. TOMINAGA, “Obtaining Low Frequency Spectra of Acetone Dissolved in Cyclohexane by Terahertz Time-Domain Spectroscopy,” *J. Phys. Chem. A* **113**, 8235–8242 (2009).

M. NAGASAKA, H. KONDOH, K. AMEMIYA, T. OHTA and Y. IWASAWA, “Proton Transfer in Water-Hydroxyl Mixed Overlayers on Pt(111): Combined Approach of Laser Desorption and Spatially-Resolved X-Ray Photoelectron Spectroscopy,” *Surf. Sci.* **603**, 1690 (2009).
I. NAKAI, H. KONDOH, T. SHIMADA, M. NAGASAKA, R. YOKOTA, T. KATAYAMA, K. AMEMIYA, H. ORITA and T. OHTA, “Mechanism of N+NO Reaction on Rh(111) Surfaces: A Precursor-Mediated Reaction,” *J. Phys. Chem. C* **113**, 13257 (2009).

Materials Molecular Science

K. HINO, R. SHINGAI, T. MORITA, K. TOKU, T. HIRANO, H. YOSHIKAWA, H. NAKANO and N. NISHI, “Size Distribution of Gold Nanoparticles Covered with Thiol-Terminated Cyanobiphenyltype Liquid Crystal Molecules Studied with Small-Angle X-Ray Scattering and TEM,” *Chem. Phys. Lett.* **460**, 173–177(2008).
K. INOUE, K. OHASHI, T. IINO, J. SASAKI, K. JUDAI, N. NISHI and H. SEKIYA, “Coordination Structures of the Silver Ion: Infrared Photodissociation Spectroscopy of $Ag^+(NH_3)_n$ (n = 3–8),” *Phys. Chem. Chem. Phys.* **10**, 3052–3062, (2008) Cover article.
K. JUDAI, S. NUMAO, A. FURUYA, J. NISHIJO and N. NISHI, “Increased Electric Conductance through Physisorbed Oxygen on Copper Nanocables Sheathed in Carbon,” *J. Am. Chem. Soc.* **130**, 1142–1143 (2008).
S. NUMAO, K. JUDAI, J. NISHIJO, K. MIZUUCHI and N. NISHI, “Synthesis and Characterization of Mesoporous Carbon Nano-Dendrites with Graphitic Ultra-Thin Walls and Their Application to Supercapacitor Electrodes,” *Carbon* **47**, 306–312 (2009).
J. NISHIJO, S. NUMAO, K. JUDAI and N. NISHI, “Ferromagnetic Interaction between $[Ni(bdt)_2]^-$ Anions in $[Mn_2(Saloph)_2(\mu\text{-OH})][Ni(bdt)_2](CH_3CN)_2$,” *Polyhedron* **28**, 1664–1667(2009).
S. TAKAYAMA, K. KAKURAI, M. TAKEDA, A. MATSUBARA, Y. NISHIHARA, J. NISHIJO, S. SANO, N. NISHI and M. SATO, “Investigation of Crystal Structure Formation under Microwave Heating,” *Nucl. Instrum. Methods Phys. Res., Sect. A* **600**, 246–249 (2009).
J. SASAKI, K. OHASHI, K. INOUE, T. IMAMURA, K. JUDAI, N. NISHI and H. SEKIYA, “Infrared Photodissociation Spectroscopy of $V^+(H_2O)_n$ (n = 2–8): Coordinative Saturation of V^+ with Four H_2O Molecules,” *Chem. Phys. Lett.* **474**, 36–40 (2009).

Y. ITO, A. MIYAZAKI, K. FUKUI, S. V. VEETTIL, T. YOKOYAMA and T. ENOKI, “Pd Nanoparticle Embedded with Only One Co Atom Behaves as a Single-Particle Magnet,” *J. Phys. Soc. Jpn.* **77**, 103701 (4 pages) (2008).
X. -D. MA, T. NAKAGAWA, Y. TAKAGI, M. PRZYBYLSKI, F. M. LEIBSLE and T. YOKOYAMA, “Magnetic Properties of Self-Assembled Co Nanorods Grown on Cu(110)-(2×3)N,” *Phys. Rev. B* **78**, 104420 (9 pages) (2008).
Y. MATSUMOTO, S. SAKAI, Y. TAKAGI, T. NAKAGAWA, T. YOKOYAMA, T. SHIMADA, S. MITANI and K. TAKANASHI, “X-Ray Absorption Spectroscopy and Magnetic Circular Dichroism in Codeposited C_{60}-Co Films with Giant Tunnel Magnetoresistance,” *Chem. Phys. Lett*. **470**, 244–248 (2009).
T. NAKAGAWA, I. YAMAMOTO, Y. TAKAGI, K. WATANABE, Y. MATSUMOTO and T. YOKOYAMA, “Two-Photon Photoemission Magnetic Circular Dichroism and Its Energy Dependence,” *Phys. Rev. B* **79**, 172404 (4 pages) (2009).
X. -D. MA, D. I. BAZHANOV, O. FRUCHART, F. YILDIZ, T. YOKOYAMA, M. PRZYBYLSKI, V. S. STEPANYUK, W. HERGERT and J. KIRSCHNER, “Strain Relief Guided Novel Growth of Atomic Nanowires in Cu_3N-Cu(110) Molecular Network,” *Phys. Rev. Lett.* **102**, 205503 (4 pages) (2009).
H. IRIE, K. KAMIYA, T. SHIBANUMA, S. MIURA, D. TRYK, T. YOKOYAMA and K. HASHIMOTO, “Visible Light-Sensitive Cu(II)-Grafted TiO_2 Photocatalysts: Activities and XAFS Analyses,” *J. Phys. Chem. C* **113**, 10761–10766 (2009).
M. INAGAWA, H. YOSHIKAWA, T. YOKOYAMA and K. AWAGA, “Electrochemical Structural Transformation and Reversible Doping/Dedoping of Lithium Phthalocyanine Thin Films,” *Chem. Comm.* 3389–3991 (2009).
T. NAKAGAWA, K. WATANABE, Y. MATSUMOTO and T. YOKOYAMA, “Magnetic Circular Dichroism Photoemission Electron Microscopy Using Laser and Threshold Photoemission,” *J. Phys.: Condens. Matter* **21**, 314010 (2009).

LIST OF PUBLICATIONS

T. SASAKI, M. TADA, C. ZHONG, T. KUME and Y. IWASAWA, “Immobilized Metal Ion-Containing Ionic Liquids: Preparation, Structure and Catalytic Performances in Kharasch Addition Reaction and Suzuki Cross-Coupling Reactions,” *J. Mol. Catal. A: Chem.* **279**, 200–209 (2008).

K. MOTOKURA, M. TOMITA, M. TADA and Y. IWASAWA, “Acid-Base Bifunctional Catalysis of Silica-Alumina-Supported Organic Amines for Carbon–Carbon Bond-Forming Reactions,” *Chem. –Eur. J.* **14**, 4017–4027 (2008).

M. TADA, K. MOTOKURA and Y. IWASAWA, “Conceptual Integration of Homogeneous and Heterogeneous Catalyses,” *Top. Catal.* **48**, 32–40 (2008).

M. L. KANTAM, U. PAL, B. SREEDHAR, S. BHARGAVA, Y. IWASAWA, M. TADA and B. M. CHOUDARY, “Aerobic Alcohol Oxidation by Ruthenium Species Stabilized on Nanocrystalline Magnesium Oxide by Basic Ionic Liquids,” *Adv. Synth. Catal.* **350**, 1225–1229 (2008).

K. MOTOKURA, M. TADA and Y. IWASAWA, “Acid-Base Bifunctional Catalytic Surfaces for Nucleophilic Addition Reactions,” *Chem. –Asian J.* **3**, 1230–1236 (2008).

K. MOTOKURA, M. TADA and Y. IWASAWA, “Cooperative Catalysis of Primary and Tertiary Amines Immobilized on Oxide Surface for One-Pot C–C Bond Forming Reactions,” *Angew. Chem., Int. Ed.* **47**, 9230–9235 (2008).

M. TADA, Y. AKATSUKA, Y. YANG, T. SASAKI, M. KINOSHITA, K. MOTOKURA and Y. IWASAWA, “Photoinduced Reversible Structural Transformation and Selective Oxidation Catalysis of Unsaturated Ruthenium Complexes Supported on SiO$_2$,” *Angew. Chem., Int. Ed.* **47**, 9252–9255 (2008).

K. MOTOKURA, M. TOMITA, M. TADA and Y. IWASAWA, “Michael Reactions Catalyzed by Basic Alkylamines and Dialkylaminopyridine Immobilized on Acidic Silica–Alumina Surfaces,” *Top. Catal.* **52**, 579–585 (2009).

T. SASAKI, M. TADA and Y. IWASAWA, “Density Functional Theory Study on the Re Cluster/HZSM-5 Catalysis for Direct Phenol Synthesis from Benzene and Molecular Oxygen: Active Re Structure and Reaction Mechanism,” *Top. Catal.* **52**, 880–887 (2009).

K. MOTOKURA, M. TADA and Y. IWASAWA, “Layered Materials with Coexisting Acidic and Basic Sites for Catalytic One-Pot Reaction Sequences,” *J. Am. Chem. Soc.* **131**, 7944–7945 (2009).

T. MURATA, G. SAITO, Y. ENOMOTO, G. HONDA, Y. SHIMIZU, S. MATSUI, M. SAKATA, O. DROZDOVA and K. YAKUSHI, “Complex Formation between a Nucleobase and Tetracyanoquinodimethane Derivatives: Crystal Structures and Transport Properties of Charge-Transfer Solids of Cytosine,” *Bull. Chem. Soc. Jpn.* **81**, 331–344 (2008).

K. KUBO, A. NAKAO, Y. ISHII, T. YAMAMOTO, M. TAMURA, R. KATO, K. YAKUSHI and G. MATSUBAYASHI, “Electrical Properties and Electronic States of Molecular Conductors Based on Unsymmetrical Organometallic-Dithiolene Gold(III) Complexes,” *Inorg. Chem.* **47**, 5495–5502 (2008).

X. SHAO, Y. NAKAO, M. SAKATA, H. YAMOCHI, Y. YOSHIDA, M. MAESATO, M. URUICHI, K. YAKUSHI, T. MURATA, A. OTSUKA, G. SAITO, S. KOSHIHARA and K. TANAKA, “Room Temperature First-Order Phase Transition in a Molecular Conductor (MeEDO-TTF)$_2$PF$_6$,” *Chem. Mater.* **20**, 7551–7562 (2008).

Y. YUE, C. NAKANAO, K. YAMAMOTO, M. URUICHI, R. WOJCIECHOWSKI, M. INOKUCHI and K. YAKUSHI, “Charge Order–Disorder Phase Transition in α’-(BEDT-TTF)$_2$IBr$_2$,” *J. Phys. Soc. Jpn.* **78**, 044701 (10 pages) (2009).

A. SHIMIZU, M. URUICHI, K. YAKUSHI, H. MATSUZAKI, H. OKAMOTO, M. NAKANO, Y. HIRAO, K. MATSUMOTO, H. KURATA and T. KUBO, “Resonance Balance Shift in Stacks of Delocalized Singlet Biradicals,” *Angew. Chem., Int. Ed.* **48**, 5482–5486 (2009).

Y. NAKANO, H. YAMOCHI, G. SAITO, M. URUICHI and K. YAKUSHI, “Isotope Effect on Metal–Insulator Transition of (EDO-TTF)$_2$XF$_6$ (X = P, As) with Multi-Instability of Metallic State,” *Solid State Sci.* **10**, 1780–1785 (2008).

Y. YUE, C. NAKANO, K. YAMAMOTO, M. URUICHI, K. YAKUSHI and A. KAWAMOTO, “Charge-Ordering Phase Transition in α’-(BEDT-TTF)$_2$IBr$_2$,” *J. Phys.: Conf. Series* **132**, 012007 (7 pages) (2008).

A. A. KOWALSKA, K. YAMAMOTO and K. YAKUSHI, “Ferroelectric Polarization in α-(ET)$_2$I$_2$Br Studied by Second-Harmonic Generation Microscopy,” *J. Phys.: Conf. Series* **132**, 012006 (5 pages) (2008).

Y. NAKANO, H. YAMOCHI, G. SAITO, M. URUICHI and K. YAKUSHI, “Anion Size and Isotope Effects in (EDO-TTF)$_2$XF$_6$,” *J. Phys.: Conf. Series* **148**, 012007 (4 pages) (2009).

M. MAESATO, Y. NAKANO, X. SHAO, Y. YOSHIDA, H. YAMOCHI, G. SAITO, A. MOREAC, J. -C. AMELINE, E. COLLET, M. URUICHI and K. YAKUSHI, “Control of Metal–Insulator Transition in (EDO-TTF)$_2$SbF$_6$,” *J. Phys.: Conf. Series* **148**, 012004 (4 pages) (2009).

H. NAKAYA, Y. TAKAHASHI, S. IWAI, K. YAMAMOTO, K. YAKUSHI and S. SAITO, “Ultrafast THz Response of Photo-Induced Insulator to Metal Transition in Charge Ordered Organic Conductor α-(BEDT-TTF)$_2$I$_3$,” *J. Phys.: Conf. Series* **148**, 012039 (4 pages) (2009).

F. IWASE, K. SUGIURA, K. FURUKAWA and T. NAKAMURA, “^{13}C NMR Study of the Chemical Pressure Effect in (TMTTF)$_2$ [(AsF$_6$)$_x$(SbF$_6$)$_{1-x}$] ($x \sim 0.5$),” *J. Phys.: Conf. Series* **132**, 012015 (4 pages) (2008).

T. NAKAMURA, F. IWASE, H. SATSUKAWA, K. FURUKAWA and T. TAKAHASHI, “^{13}C NMR Investigation of Re-Entrant Antiferromagnetic States of (TMTTF)$_2$SbF$_6$,” *J. Phys.: Conf. Series* **150**, 042137 (4 pages) (2009).

S. OKUBO, H. YAMAMOTO, M. FUJISAWA, H. OHTA, T. NAKAMURA and H. KIKUCHI, “High Field ESR Measurements of Quantum Triple Chain System Cu$_3$(OH)$_4$SO$_4$,” *J. Phys.: Conf. Series* **150**, 042156 (4 pages) (2009).

T. TAKENO, K. KOBAYASHI, Y. NISHIO, K. KAJITA, H. MORI and T. NAKAMURA, “Mysterious Charge Ordering on θ-(BEDT-TTF)$_2$RbZn(SCN)$_4$,” *J. Phys.: Conf. Series* **150**, 042201 (4 pages) (2009).

N. GUSKOS, H. OHTA, G. ZOLNIERKIEWICZ, S. OKUBO, W. ZHANG, J. TYPEK, C. RUDOWICZ, R. SZYMCZAK, M. BOSACKA and T. NAKAMURA, “Magnetic Interactions in Frustrated Mn$_3$Fe$_4$(VO$_4$)$_6$,” *J. Non-Crys. Solids* **355**, 1419–1426 (2009).

S. WAN, J. GUO, J. KIM, H. IHEE and D. JIANG, "A Photoconductive Covalent Organic Framework: Self-Condensed Arene Cubes with Eclipsed 2D Polypyrene Sheets for Photocurrent Generation," *Angew. Chem., Int. Ed.* **48**, 5439–5442 (2009).
L. CHEN, L. WANG, X. GUO, S. NAGASE, Y. HONSHO, A. SAEKI, S. SEKI and D. JIANG, "The Non-Covalent Assembly of Benzene-Bridged Metallosalphen Dimers: Photoconductive Tapes with Large Carrier Mobility and Spatially Distinctive Conduction Anisotropy," *Chem. Commun.* 3119–3121 (2009).
L. CHEN, J. KIM, T. ISHIZUKA, Y. HONSHO, A. SAEKI, S. SEKI, H. IHEE and D. JIANG, "Noncovalently Netted, Photoconductive Sheets with Extremely High Carrier Mobility and Conduction Anisotropy from Triphenylene-Fused Metal Trigon Conjugates," *J. Am. Chem. Soc.* **131**, 7287–7292 (2009).

M. HIRAMOTO, "Efficient Organic *p-i-n* Solar Cells Having Very Thick Codeposited *i*-Layer Composed of Highly Purified Organic Semiconductors," *Proceedings of SPIE Vol. 7052, Organic photovoltaics IX*, pp 70520H-1-6, San Diego, CA, USA, 12-14 Augst (2008).
K. SAKAI and M. HIRAMOTO, "Efficient Organic *p-i-n* Solar Cells Having Very Thick Codeposited *i*-Layer Consisting of Highly Purified Organic Semiconductors," *Mol. Cryst. Liq. Cryst.* **491**, 284–289 (2008).
H. SHIOKAWA and M. HIRAMOTO, "Nanostructure Control by Interlaminated Fullerene/Phthalocyanine Ultrathin Films in *p-i-n* Organic Solar Cells," *Mol. Cryst. Liq. Cryst.* **491**, 277–283 (2008).

D. KUMAKI, T. UMEDA, T. SUZUKI and S. TOKITO, "High-Mobility Bottom-Contact Thin-Film Transistor Based on Anthracene Oligomer," *Org. Electron.* **9**, 921–924 (2008).
S. KOWARIK, A. GERLACH, A. HINDERHOFER, S. MILITA, F. BORGATTI, F. ZONTONE, T. SUZUKI, F. BISCARINI and F. SCHREIBER, "Structure, Morphology, and Growth Dynamics of Perfluoro-Pentacene Thin Films," *Phys. Status Solidi-RRL* **2**, 120–122 (2008).
M. C. R. DELGADO, K. R. PIGG, D. A. DA SILVA FILHO, N. E. GRUHN, Y. SAKAMOTO, T. SUZUKI, R. M. OSUNA, J. CASADO, V. HERNÁNDEZ, J. T. L. NAVARRETE, N. G. MARTINELLI, J. CORNIL, R. S. SÁNCHEZ-CARRERA, V. COROPCEANU and J. L. BRÉDAS, "Impact of Perfluorination on the Charge-Transport Parameters of Oligoacene Crystals," *J. Am. Chem. Soc.* **131**, 1502–1512 (2009).

T. NAGATA, S. K. ZHARMUKHAMEDOV, A. A. KHOROBRYKH, V. V. KLIMOV and S. I. ALLAKHVERDIEV, "Reconstitution of the Water-Oxidizing Complex in Manganese-Depleted Photosystem II Preparations Using Synthetic Mn Complexes: A Fluorine-19 NMR Study of the Reconstitution Process," *Photosynth. Res.* **98**, 277–284 (2008).
T. NAGASAWA, S. I. ALLAKHVERDIEV, Y. KIMURA and T. NAGATA, "Photooxidation of Alcohols by a Porphyrin/Quinone/TEMPO System," *Photochem. Photobiol. Sci.* **8**, 174–180 (2009).
H. YAMAZAKI, T. NAGATA and M. YAGI, "Non-Catalytic O_2 Evolution by $[(OH_2)(\text{Clterpy})Mn(\mu\text{-}O)_2Mn(\text{Clterpy})(OH_2)]^{3+}$ (Clterpy = 4'-chloro-2,2':6',2"-terpyridine) Adsorbed on Mica with Ce^{IV} Oxidant," *Photochem. Photobiol. Sci.* **8**, 204–209 (2009).
V. N. KURASHOV, S. I. ALLAKHVERDIEV, S. K. ZHARMUKHAMEDOV, T. NAGATA, V. V. KLIMOV, A. Y. SEMENOVA and M. D. MAMEDOV, "Electrogenic Reactions on the Donor Side of Mn-Depleted Photosystem II Core Particles in the Presence of $MnCl_2$ and Synthetic Trinuclear Mn-Complexes," *Photochem. Photobiol. Sci.* **8**, 162–166 (2009).

H. SAKURAI, I. KAMIYA, H. KITAHARA, H. TSUNOYAMA and T. TSUKUDA, "Aerobic Oxygenation of Benzylic Ketones Promoted by Gold Nanocluster Catalyst," *Synlett* 245–248 (2009).
H. TSUNOYAMA, N. ICHIKUNI, H. SAKURAI and T. TSUKUDA, "Effect of Electronic Structures of Au Clusters Stabilized by Poly(N-vinyl-2-pyrrolidone) on Aerobic Oxidation Catalysis," *J. Am. Chem. Soc.* **131**, 7086–7093 (2009).
A. F. G. M. REZA, S. HIGASHIBAYASHI and H. SAKURAI, "Preparation of C_3 Symmetric Homochiral *syn*-Trisnorbornabenzenes through Regio-Selective Cyclotrimerization of Enantiopure Iodonorbornenes," *Chem. –Asian J.* **4**, 1329–1337 (2009).
H. KITAHARA, I. KAMIYA and H. SAKURAI, "Intramolecular Addition of Toluenesulfonamide to Unactivated Alkenes Catalyzed by Gold Nanoclusters under Aerobic Conditions," *Chem. Lett.* **38**, 908–909 (2009).

T. YOKOYAMA, S. KURATA and S. TANAKA, "Isomeric Discriminating and Indiscriminating Assembly of Adsorbed Oligothiophenes on Ag(110)," *J. Phys. Chem. C* **112**, 12590–12593 (2008).
R. YAMADA, H. KUMAZAWA, S. TANAKA and H. TADA, "Electrical Resistance of Long Oligothiophene Molecules," *Appl. Phys. Express* **2**, 025002 (3 pages) (2009).

K. ONO, H. ITO, A. NAKASHIMA, M. UEMOTO, M. TOMURA and K. SAITO, "Synthesis and Properties of Naphthalene Trimers Linked by 1,3,4-Oxadiazole Spacers," *Tetrahedron Lett.* **49**, 5816–5819 (2008).
K. ONO, T. HIEI, M. TAJIKA, M. TOMURA, K. SAITO, J. NISHIDA and Y. YAMASHITA, "Synthesis of 6,13-Dithienylpentacenes by Photolysis of Their Endoperoxides," *Lett. Org. Chem.* **5**, 522–526 (2008).
M. TOMURA, "Theoretical Study for a Complex of 1,2,5-Thiadiazole with Formic Acid," *THEOCHEM* **868**, 1–5 (2008).
K. ONO, M. TOMURA and K. SAITO, "5,5-Bis(4-methoxyphenyl)-2,8-bis[3-(trifluoromethyl)phenyl]-5*H*-cyclopenta[2,1-*b*:3,4-*b*']dipyridine," *Acta Crystallogr., Sect. E: Struct. Rep. Online* **64**, o2183–o2183 (2008).
M. TOMURA, K. ONO and Y. YAMASHITA, "Crystallographic and Theoretical Studies of 4,4'-Dimethyl-7,7'-bi([1,2,5]thia-diazolo[3,4-*b*]pyridylidene)–Chloranilic Acid (1/1) with Intermolecular O–H···N Hydrogen Bonds and S···O Heteroatom Interactions," *Struct. Chem.* **19**, 967–974 (2008).
K. ONO, K. TSUKAMOTO, R. HOSOKAWA, M. KATO, M. SUGANUMA, M. TOMURA, K. SAKO, K. TAGA and K. SAITO, "A Linear Chain of Water Molecules Accommodated in a Macrocyclic Nanotube Channel," *Nano Lett.* **9**, 122–125 (2009).
K. ONO, K. NAKAGAWA and M. TOMURA, "1,4-Bis[(3,5-dimethoxyphenyl)ethynyl]benzene," *Acta Crystallogr., Sect. E: Struct. Rep. Online* **65**, o346–o346 (2009).

M. TOMURA and Y. YAMASHITA, "5-Isopropylidene-1,3-dithiolo[4,5-*d*][1,3]dithiole-2-thione," *Acta Crystallogr., Sect. E: Struct. Rep. Online* **65**, o1050–o1050 (2009).

M. TOMURA and Y. YAMASHITA, "5-(1,3-Dithiolo[4,5-*d*][1,3]dithiol-2-ylidene)-1,3-dithiolo[4,5-*c*][1,2,5]thiadiazole: An Unsymmetrical Tetrathiafulvalene with Fused 1,2,5-Thiadiazole and 1,3-Dithiole Rings," *Acta Crystallogr., Sect. E: Struct. Rep. Online* **65**, o1082–o1082 (2009).

M. TOMURA, "Theoretical Study of Noncovalent Interactions between Triple Bonds and Chlorine Atoms in Complexes of Acetylene and Some Chloromethanes," *Chem. Phys.* **359**, 126–131 (2009).

K. ONO, K. TSUKAMOTO and M. TOMURA, "5,5'-Di-4-pyridyl-2,2'-(5-*tert*-butyl-*m*-phenylene)bis(1,3,4-oxadiazole)," *Acta Crystallogr., Sect. E: Struct. Rep. Online* **65**, o1873–o1873 (2009).

M. INAGAWA, H. YOSHIKAWA, T. YOKOYAMA and K. AWAGA, "Electrochemical Structural Transformation and Reversible Doping/Dedoping of Lithium Phthalocyanine Thin Films," *Chem. Commun.* 3389–3391 (2009).

A. IWASAKI, L. HU, R. SUIZU, K. NOMURA, H. YOSHIKAWA, K. AWAGA, Y. NODA, K. KANAI, Y. OUCHI, K. SEKI and H. ITO, "Photoconductive Organic Radical Thin Films: Interactive Radical Dimers for Photofunctions," *Angew. Chem., Int. Ed.* **48**, 4022–4024 (2009).

Q. -L. YE, H. YSHIKAWA, S. BANDOW and K. AWAGA, "Green Magnetite (Fe_3O_4): Unusual Optical Mie Scattering and Magnetic Isotropy of Submicron-Size Hollow Spheres," *Appl. Phys. Lett.* **94**, 063114 (2009).

M. KEPENEKIEN, B. LE GUENNIC, K. AWAGA and V. ROBERT, "Ligands Bonded to Metal Ion or Through-Metal Interacting Ligands? Analysis of Unusual Bonds Formation in the $(BDTA)_2[Co(mnt)_2]$ Material," *Phys. Chem. Chem. Phys.* **11**, 6066–6071 (2009).

Y. SHUKU, R. SUIZU, K. AWAGA and O. SATO, "Fe(II) Spincrossover Complex of [1,2,5]Thiadiazolo[3,4-f][1,10]phenanthroline," *CrystEngComm* **11**, 2065–2068 (2009).

T. FUJIMOTO, M. M. MATSUSHITA, H. YOSHIKAWA and K. AWAGA, "Electrochemical and Electrochromic Properties of Octathio[8]circulene Thin Films in Ionic Liquids," *J. Am. Chem. Soc.* **130**, 15790–15791 (2008).

K. INOUE, K. OHASHI, T. IINO, J. SASAKI, K. JUDAI, N. NISHI and H. SEKIYA, "Coordination Sructures of Silver Ion: Infrared Photodissociation Spectroscopy of $Ag^+(NH_3)_n$ (n = 3–8)," *Phys. Chem. Chem. Phys.* **10**, 3052–3062 (2008).

K. OHASHI, K. INOUE, T. IINO, J. SASAKI, K. JUDAI, N. NISHI and H. SEKIYA, "A Molecular Picture of Metal Ions Solvation: Infrared Spectroscopy of $Cu^+(NH_3)_n$ and $Ag^+(NH_3)_n$ in the Gas Phase," *J. Mol. Liq.* **147**, 71–76 (2009).

J. SASAKI, K. OHASHI, K. INOUE, T. IMAMURA, K. JUDAI, N. NISHI and H. SEKIYA, "Infrared Photodissociation Spectroscopy of $V^+(H_2O)_n$ (n = 2–8): Coordinative Saturation of V^+ with Four H_2O Molecules," *Chem. Phys. Lett.* **474**, 36–40 (2009).

Life and Coordination-Complex Molecular Science

T. ISHII, Y. MURAYAMA, A. KATANO, K. MAKI, K. KUWAJIMA and M. SANO, "Probing Force-Induced Unfolding Intermediates of a Single Staphylococcal Nuclease Molecule and the Effect of Ligand Binding," *Biochem. Biophys. Res. Commun.* **375**, 586–591 (2008).

T. KANZAKI, R. IIZUKA, K. TAKAHASHI, K. MAKI, R. MASUDA, M. SAHLAN, H. YÉBENES, J. M. VALPUESTA, T. OKA, M. FURUTANI, N. ISHII, K. KUWAJIMA and M. YOHDA, "Sequential Action of ATP-Dependent Subunit Conformational Change and Interaction between Helical Protrusions in the Closure of the Built-in Lid of Group II Chaperonins," *J. Biol. Chem.* **283**, 34773–34784 (2008).

S. TSUKAMOTO, T. YAMASHITA, Y. YAMADA, K. FUJIWARA, K. MAKI, K. KUWAJIMA, Y. MATSUMURA, H. KIHARA, H. TSUGE and M. IKEGUCHI, "Non-Native α-Helix Formation Is Not Necessary for Folding of Lipocalin: Comparison of Burst-Phase Folding between Tear Lipocalin and β-Lactoglobulin," *Proteins* **76**, 226–236 (2009).

M. TAKEDA, N. SUGIMORI, T. TORIZAWA, T. TERAUCHI, A. M. ONO, H. YAGI, Y. YAMAGUCHI, K. KATO, T. IKEYA, J. G. JEE, P. GÜNTERT, D. J. ACETI, J. L. MARKLEY and M. KAINOSHO, "Structure of the Putative 32 kDa Myrosinase-Binding Protein from *Arabidopsis* (At3g16450.1) Determined by SAIL-NMR," *FEBS J.* **275**, 5873–5884 (2008).

E. M. QUAN, Y. KAMIYA, D. KAMIYA, V. DENIC, J. WEIBEZAHN, K. KATO and J. S. WEISSMAN, "Defining the Glycan Destruction Signal for Endoplasmic Reticulum-Associated Degradation," *Mol. Cell* **32**, 870–877 (2008).

E. Y. PARK, M. ISHIKIRIYAMA, T. NISHINA, T. KATO, H. YAGI, K. KATO and H. UEDA, "Human IgG1 Expression in Silkworm Larval Hemolymph Using BmNPV Bacmids and Its *N*-Linked Glycan Structure," *J. Biotechnol.* **139**, 108–114 (2009).

M. SHIBATA-KOYAMA, S. IIDA, A. OKAZAKI, K. MORI, K. KITAJIMA-MIYAMA, S. SAITOU, S. KAKITA, Y. KANDA, K. SHITARA, K. KATO and M. SATOH, "The *N*-Linked Oligosaccharide at FcγRIIIa Asn-45: An Inhibitory Element for High FcγRIIIa Binding Affinity to IgG Glycoforms Lacking Core Fucosylation," *Glycobiology* **19**, 126–134 (2009).

M. SUGIYAMA, K. HAMADA, K. KATO, E. KURIMOTO, K. OKAMOTO, Y. MORIMOTO, S. IKEDA, S. NAITO, M. FURUSAKA, K. ITOH, K. MORI and T. FUKUNAGA, "SANS Simulation of Aggregated Protein in Aqueous Solution," *Nucl. Instrum. Methods Phys. Res., Sect. A* **600**, 272–274 (2009).

Y. YAMAGUCHI, M. WÄLCHLI, M. NAGANO and K. KATO, "A ^{13}C-Detection NMR Approach for Large Glycoproteins," *Carbohydr. Res.* **344**, 535–538 (2009).

N. SRIWILAIJAROEN, S. KONDO, H. YAGI, P. WILAIRAT, H. HIRAMATSU, M. ITO, Y. ITO, K. KATO and Y. SUZUKI, "Analysis of *N*-Glycans in Embryonated Chicken Egg Chorioallantoic and Amniotic Cells Responsible for Binding and Adaptation of Human and Avian influenza Viruses," *Glycoconjugate J.* **26**, 433–443 (2009).

N. HOSOKAWA, Y. KAMIYA, D. KAMIYA, K. KATO and K. NAGATA, "Human OS-9, a Lectin Required for Glycoprotein Endoplasmic Reticulum-Associated Degradation, Recognizes Mannose-Trimmed *N*-Glycans," *J. Biol. Chem.* **284**, 17061–17068 (2009).

M. OGATA, M. NAKAJIMA, T. KATO, T. OBARA, H. YAGI, K. KATO, T. USUI and E. Y. PARK, “Synthesis of Sialoglycopolypeptide for Potentially Blocking Influenza Virus Infection Using a Rat α2,6-Sialyltransferase Expressed in BmNPV Bacmid-Injected Silkworm Larvae,” *BMC Biotechnol.* **9**:54 (2009).

T. DOJIMA, T. NISHINA, T. KATO, T. UNO, H. YAGI, K. KATO and E. Y. PARK, “Comparison of the *N*-Linked Glycosylation of Human β1,3-*N*-Acetylglucosaminyltransferase 2 Expressed in Insect Cells and Silkworm Larvae,” *J. Biotechnol.* **143**, 27–33 (2009).

S. THONGRATSAKUL, T. SONGSERM, C. POOLKHET, S. KONDO, H. YAGI, H. HIRAMATSU, M. TASHIRO, H. OKADA, K. KATO and Y. SUZUKI, “Determination of *N*-Linked Sialyl-Sugar Chains in the Lungs of Domestic Cats and Dogs in Thailand Susceptible to the Highly Pathogenic Avian Influenza Virus (H5N1),” *Open Glycoscience* **2**, 28–36 (2009).

K. SASAKI, M. KAJIKAWA, K. KUROKI, T. MOTOHASHI, T. SHIMOJIMA, E. Y. PARK, S. KONDO, H. YAGI, K. KATO and K. MAENAKA, “Silkworm Expression and Sugar Profiling of Human Immune Cell Surface Receptor, KIR2DL1,” *Biochem. Biophys. Res. Commun.* **387**, 575–580 (2009).

A. J. MCGOWN, W. D. KERBER, H. FUJII and D. P. GOLDBERG, “Catalytic Reactivity of a Meso-N-Substituted Corrole and Evidence for a High-Valent Iron-Oxo Species,” *J. Am. Chem. Soc.* **131**, 8040–8048 (2009).

A. TAKAHASHI, T. KURAHASHI and H. FUJII, “Effect of Imidazole and Phenolate Axial Ligands on the Electronic Structure and Reactivity of Oxoiron(IV) Porphyrin π-Cation Radical Complexes: Drastic Increase in Oxo-Transfer and Hydrogen Abstraction Reactivities,” *Inorg. Chem.* **48**, 2614–2625 (2009).

D. NONAKA, H. WARIISHI and H. FUJII, “Paramagnetic ^{13}C and ^{15}N NMR Analyses of Cyanide(^{13}C^{15}N)-Ligated Ferric Peroxidases: The Push-Effect, not Pull-Effect, Modulates the Compound I Formation Rate,” *Biochemistry* **48**, 898–905 (2009).

T. SATO, S. NOZAWA, K. ICHIYANAGI, A. TOMITA, M. CHOLLET, H. ICHIKAWA, H. FUJII, S. ADACHI and S. KOSHIHARA, “Capturing Molecular Structural Dynamics by 100 ps Time-Resolved X-Ray Absorption Spectroscopy,” *J. Synchrotron Radiat.* **16**, 110–115 (2009).

A. TAKAHASHI, Y. OHBA, S. YAMAUCHI and H. FUJII, “ENDOR Study of Oxoiron(IV) Porphyrin π-Cation Radical Complexes as Models for Compound I of Heme Enzymes,” *Chem. Lett.* **38**, 68–69 (2009).

T. ASANO, H. UNO, K. SHIBASAKI, M. TOMINAGA and T. URISU, “A Cell-Culture-Type Planar Ion Channel Biosensor,” *Trans. Mater. Res. Soc. Jpn.* **33**, 767–770 (2008).

M. A. SAYED, H. UNO, K. HARADA, K. TANAKA, Y. -H. KIM, Y. NAKAOKI, K. OKUMURA, R. TERO and T. URISU, “New Infrared Reflection Absorption Spectroscopy (IRRAS) System for Observation of Solid-Solution Interface Biomaterials,” *Chem. Phys. Lett.* **466**, 235–239 (2008).

R. TERO, T. UJIHARA and T. URISU, “Lipid Bilayer Membrane with Atomic Step Structure: Supported Bilayer on Step-and-Terrace TiO_2(100) Surface,” *Langmuir* **24**, 11567–11576 (2008).

T. UJIHARA, S. SUZUKI, Y. YAMAUCHI, R. TERO and Y. TAKEDA, “Local Concentration of Gel Phase Domains in Supported Lipid Bilayers under Light Irradiation in Binary Mixture of Phospholipids Doped with Dyes for Photoinduced Activation,” *Langmuir* **24**, 10974–10980 (2008).

T. ASANO, T. NAKAMURA, A. WAKAHARA and T. URISU, “Noise Properties of Incubation-Type Planar Ion Channel Biosensor,” *Jpn. J. Appl. Phys.* **48**, 027001 (4 pages) (2009).

T. OKAZAKI, T. INABA, Y. TATSU, R. TERO, T. URISU and K. MORIGAKI, “Polymerized Lipid Bilayers on a Solid Substrate: Morphologies and Obstruction of Lateral Diffusion,” *Langmuir* **25**, 345–351 (2009).

R. TERO, T. UJIHARA and T. URISU, “Shape Transformation of Adsorbed Vesicles on Oxide Surfaces: Effect of Substrate Material and Photo-Irradiation,” *Trans. Mater. Res. Soc. Jpn.* **34**, 183–188 (2009).

T. UJIHARA, S. SUZUKI, Y. YAMAUCHI, R. TERO and Y. TAKEDA, “Local Condensation of Artificial Raft Domains under Light Irradiation in Supported Lipid Bilayer of PSM-DOPC-Cholesterol System,” *Trans. Mater. Res. Soc. Jpn.* **34**, 179–182 (2009).

Y. M. A. YAMADA, H. GUO and Y. UOZUMI, “Development of Tightly Convoluted Polymeric Phosphotungstate Catalysts and Their Application to an Axidative Cyclization of Alkenols and Alkenoic Acids,” *Heterocycles* **76**, 645–655 (2008).

T. KIMURA and Y. UOZUMI, “Synthesis of [2,6-Bis(2-oxazolinyl)-phenyl]palladium Complexes via the Ligand Introduction Route,” *Organometallics* **27**, 5159–5162 (2008).

Y. UOZUMI, “Heterogeneous Asymmetric Catalysis in Water with Amphiphilic Polymer-Supported Homochiral Palladium Complexes,” *Bull. Chem. Soc. Jpn.* **81**, 1183–1195 (2008).

Y. UOZUMI, Y. MATSUURA, T. ARAKAWA and Y. M. A. YAMADA, “Asymmetric Suzuki-Miyaura Coupling in Water with a Chiral Palladium Catalyst Supported on an Amphiphilic Resin,” *Angew. Chem., Int. Ed.* **48**, 2708–2710 (2009).

Y. M. A. YAMADA, T. ARAKAWA, H. HOCKE and Y. UOZUMI, “An Amphiphilic Resin-Dispersion of Nanoparticles of Platinum (ARP-Pt): A Highly Active and Recyclable Catalyst for the Aerobic Oxidation of a Variety of Alcohols in Water,” *Chem. –Asian J.* **4**, 1092–1098 (2009).

Y. M. A. YAMADA, K. TORII and Y. UOZUMI, “Oxidative Cyclization of Alkenols with Oxone Using a Miniflow Reactor,” *Beilstein J. Org. Chem.* **5**, 1–5 (2009).

J. MUCKERMAN, D. POLANSKY, T. WADA, K. TANAKA and E. FUJITA, “Water Oxidation by a Ruthenium Complex with Non-Innocent Quinone Ligands: Possible Formation of an O–O Bond at a Low Oxidation State of the Metal,” *Inorg. Chem.* **47**, 1787–1802 (2008).

D. POLANSKY, D. CABELLI, J. MUCKERMAN, T. FUKUSHIMA, K. TANAKA and E. FUJITA, “Mechanism of Hydride Donor Generation Using a Ru(II) Complex Containing an NAD$^+$ Model Ligand: Pulse and Steady-State Radiolysis Studies,” *Inorg. Chem.* **47**, 3958–3968 (2008).

K. TANAKA, T. WADA, E. FUJITA and J. MUCKERMAN, "Reversible Conversion between Chemical and Electrical Energies Catalyzed by Ru Complexes Aimed to Construct a Sustainable Society," *Reprints of Symposia, Division of Fuel Chemistry, American Chemical Society*, **53**, 236–237 (2008).

K. KIMURA and K. TANAKA, "Synthesis and Electrochemical Reduction of a Ruthenium Complex Bearing an N,N-bis[(benzo[g][1,5]naphthyridin-2-yl)methyl]propane-2-amine Ligand as an NAD^+/NADH-Type Redox Site," *Angew. Chem., Int. Ed.* **47**, 9768–9771 (2008).

M-K. TSAI, J. ROCHFORD, D. POLYANSKY, T. WADA, K. TANAKA, E. FUJITA and J. MUCKERMAN, "Chracterization of Redox Sites of $[Ru(OH_2)(Q)(tpy)]^{2+}$ (Q = 3,5-di-*tert*-butyl-1,2-benzoquinone, tpy = 2,2':6',2"-terpyridine) and Related Species through Experiment and Theoretical Studies," *Inorg. Chem.* **48**, 4372–4383 (2009).

K. TANAKA, "Design and Synthesis of Metal Complex Catalysts towards Inter-Conversion between Chemical Energy and Electric One," *Bull. Jpn. Soc. Coord. Chem.* **53**, 3–16 (2009).

K. TANAKA, "Metal-Catalyzed Reversible Conversion between Chemical and Electrical Energy Designed towards a Sustainable Society," *Chem. Rec.* **9**, 169–186 (2009).

A. KUNISHITA, J. D. SCANLON, H. ISHIMARU, K. HONDA, T. OGURA, M. SUZUKI, C. J. CRAMER and S. ITOH, "Reactions of Copper(II)–H_2O_2 Adducts Supported by Tridentate Bis(2-pyridylmethyl)amine Ligands: Sensitivity to Solvent and Variations in Ligand Substitution," *Inorg. Chem.* **47**, 8222–8232 (2008).

M. INOSAKO, A. KUNISHITA, C. SHIMOKAWA, J. TERAOKA, M. KUBO, T. OGURA, H. SUGIMOTO and S. ITOH, "Reaction of β-Diketiminate Copper(II) Complexes and Na_2S_2," *Dalton Trans.* 6250–6256 (2008).

A. KUNISHITA, M. KUBO, H. ISHIMARU, T. OGURA, H. SUGIMOTO and S. ITOH, "H_2O_2-Reactivity of Copper(II) Complexes Supported by TPA Ligands with 6-Phenyl Substituents," *Inorg. Chem.* **47**, 12032–12039 (2008).

A. KUNISHITA, M. KUBO, H. SUGIMOTO, T. OGURA, K. SATO, T. TAKUI and S. ITOH, "Mononuclear Copper(II)-Superoxo Complex that Mimics the Structure and Reactivity of the Active Centers of PHM and DβH," *J. Am. Chem. Soc.* **131**, 2788–2789 (2009).

A. KUNISHITA, Y. DOI, T. OGURA, H. SUGIMOTO and S. ITOH, "Ni(II)/H_2O_2 Reactivity in Bis[(pyridin-2-yl)methyl]amine Tridentate Ligand Sysetm. Aromatic Hydroxylation Reaction by Bis(μ-oxo)dinickel(III) Complex," *Inorg. Chem.* **48**, 4997–5004 (2009).

T. UZAWA, C. NISHIMURA, S. AKIYAMA, K. ISHIMORI, S. TAKAHASHI, H. J. DYSON and P. E. WRIGHT, "Hierarchical Folding Mechanism of Apomyoglobin Revealed by Ultra-Fast H/D Exchange Coupled with 2D NMR," *Proc. Natl. Acad. Sci. U.S.A.* **105**, 13859–13864 (2008).

T. KIMURA, A. MAEDA, S. NISHIGUCHI, K. ISHIMORI, I. MORISHIMA T. KONNO, Y. GOTO and S. TAKAHASHI, "Dehydration of Mainchain Amides in the Final Folding Step of Single Chain Monellin Revealed by Time-Resolved Infrared Spectroscopy," *Proc. Natl. Acad. Sci. U.S.A.* **105**, 13391–13396 (2008).

Theoretical and Computational Molecular Science

T. TSUCHIYA, Y. MAEDA, T. AKASAKA and S. NAGASE, "Basic Study of Endohedral Metallofullerenes and Carbon Nanotubes for Functional Materials," *Catalysts & Catalysis* (in Japanese) **51**, 20–25 (2009).
Y. MAEDA, T. HASEGAWA, T. AKASAKA and S. NAGASE, "Isolation and Purification of Metallic Single-Walled Carbon Nanotubes," *CONVERTECH* (in Japanese) **37**, 127–131 (2009).

G. K-L. CHAN, J. J. DORANDO, D. GHOSH, J. HACHMANN, E. NEUSCAMMAN, H. WANG and T. YANAI, "An Introduction to the Density Matrix Renormalization Group Ansatz in Quantum Chemistry," in *Frontiers in Quantum Systems in Chemistry and Physics, Series: Progress in Theoretical Chemistry and Physics*, S. Wilson *et al.*, Eds., Springer, **Vol. 18**, pp. 49–64 (2008).

N. YOSHIDA, T. IMAI, S. PHONGPHANPHANEE, A. KOVALENKO and F. HIRATA, "Molecular Recognition in Biomolecules Studied by Statistical-Mechanical Integral-Equation Theory of Liquids," *J. Phys. Chem. B (Feature Article)* **113**, 873–886 (2009).
T. IMAI, N. YOSHIDA, A. KOVALENKO and F. HIRATA, "A Statistical Mechanics of Molecular Recognition," in *Water and Biomolecules*, K. Kuwajima, Y. Goto, F. Hirata, M. Kataoka and M. Terazima, Eds., Springer (2009).

K. YONEMITSU, "Photoinduced Phase Transitions Clarified by Theory,'' *Chemistry & Chemical Industry* (in Japanese) **62**, 892–894 (2009).

N. NISHI, T. TSUKUDA, S. SAITO and T. YAGASAKI, *Cluster Science : Creation of Functional Nanostructures* (in Japanese), Yoneda Pub. Co.; Chiba, Japan, ISBN978-4-946553-38-7 C3403 (2009).

M. EHARA and H. NAKATSUJI, "Photochemistry of Biological Chemosensors, Organic Light-Emitting Diodes, and Inner-Shell Electronic Processes," *AIP Conf. Proc., Proceedings of the Workshop on Nuclei and Mesoscopic Physics (WNMP07)*, Melville, New York, **995**, pp. 145–151 (2008).
M. EHARA, "Development and Applications of Highly Accurate Electronic Structure Theory for Molecular Excited States," *Chemistry & Chemical Industry* (in Japanese) **61**, pp. 576–578 (2008).

Photo-Molecular Science

H. OKAMOTO and K. IMURA, "Near-Field Optical Imaging of Enhanced Electric Fields and Plasmon Waves in Metal Nanostructures," *Prog. Surf. Sci.* **84**, 199–229 (2009).
H. OKAMOTO, "Imaging of Plasmons," in *Latest Trends in Plasmonic Nanomaterials* (in Japanese), S. Yamada, Ed., CMC Publishing Co., Ltd.; Tokyo, pp. 105–115 (2009).

K. OHMORI, "Wave-Packet and Coherent Control Dynamics," *Annu. Rev. Phys. Chem.* **60**, 487–511 (2009).

A. HISHIKAWA, A. MATSUDA, M. FUSHITANI and E. J. TAKAHASHI, "Real-Time Visualization of Intramolecular Hydrogen Migration Reaction by Coulomb Explosion Imaging," *J. Japanese Laser Processing Society* (in Japanese) **15**, 16–49 (2008).

E. SHIGEMASA and M. YABASHI, "Chapter 5: Selecton of Photon Energy (Basic Concept)," in *Introduction to beamline optics technology for synchrotron radiation: —for beginner users of synchrotron radiation—*, H. OHASHI and K. HIRANO, Eds., The Japanese Society for Synchrotron Radiation Research (2008).

M. TSUNEKANE, Y. OISHI and T. TAIRA, "High-Power Continuous-Wave, Yb-Doped Solid-State Lasers," *KOGAKU* (in Japanese), Optical Society of Japan, **38**, 17–24 (2009).
T. TAIRA, "Micro Solid-State Photonics —Review—," *Rev. Laser Eng. (Special Isuue on Micro Solid-State Photonics)* (in Japanese), The Laser Society of Japan, **37**, 227–234 (2009).
Y. SATO and T. TAIRA, "Micro Solid-State Photonics Materials —Properties of Lasers Materials—," *Rev. Laser Eng. (Special Isuue on Micro Solid-State Photonics)* (in Japaneses), The Laser Society of Japan, **37**, 242–247 (2009).
T. TAIRA and M. TSUNEKANE, "High Brightness Micro-Laser for Engine Ignition," *OPTRONICS* (in Japaneses), Optronics Co., Ltd., **28**, 124–130 (2009).
T. TAIRA, "6.3 Microchip Laser," in *MEMS device souron* (in Japanese), Science & technology Co., Ltd., pp. 251–269 (2009).

K. AMEMIYA, "Prospects of the Thin Film Study by Means of a Three-Dimensional XAFS Technique," *J. Surf. Sci. Soc. Jpn.* (in Japanese) **30**, 11 (2009).
K. AMEMIYA and S. KIMURA, "Chapter 7: Selecton of photon energy (VUV and SX)," in *Introduction to beamline optics technology for synchrotron radiation: —for beginner users of synchrotron radiation—*, The Japanese Society for Synchrotron Radiation Research (2008).

LIST OF REVIEW ARTICLES AND TEXTBOOKS

Materials Molecular Science

N. NISHI, T. TSUKUDA, S. SAITO and T. YAGASAKI, *Cluster Science : Creation of Functional Nanostructures* (in Japanese), Yoneda Pub. Co.; Chiba, Japan, ISBN978-4-946553-38-7 C3403 (2009).

T. YOKOYAMA, “Novel Characterization Techniques for Surface Magnetism Based on New Principles and Phenomena (Preface),” *J. Surf. Sci. Soc. Jpn.* (in Japanese) **30**, 311–311 (2009).

T. NAKAGAWA and T. YOKOYAMA, “Photoemission Electron Microscopy Using Magnetic Circular Dichroism with Laser,” *J. Surf. Sci. Soc. Jpn.* (in Japanese) **30**, 332–338 (2009).

M. TADA, “Preparation of Supported Metal Catalysts,” in *Handbook of Catalysts*, Kodansha Scientific, pp. 287–290 (2008).

M. TADA and Y. IWASAWA, “3D Design of Active Structures and Catalysis by Metal Complexes at Surfaces,” *Hyomen* (in Japanese) **33**, pp. 267–283 (2008).

M. TADA and Y. IWASAWA, “Molecular Imprinting of Supported Metal Complexes at Surfaces toward Chemical Design of Artificial Enzymatic Catalysts,” *Catalysts & Catalysis* (in Japanese) **50**, pp. 319-325 (2008).

M. TADA, “Size- and Shape-Controlled Synthesis of Platinum Nanoparticles for Fuel Cell Catalysts,” *Kagaku* (in Japanese) **63**, pp. 63–64 (2008).

T. E. MULLER, K.HULTZSCH, M. YU, F. FOUBELO and M. TADA, “Hydroamination: Direct Addition of Amines to Alkenes and Alkynes,” *Chem. Rev.* **108**, 3795–3892 (2008).

M. TADA, “Structural Kinetics of Catalyst Surfaces Studied by Time-Resolved XAFS,” *Surf. Sci. (Hyomen Kagaku)* (in Japanese) **30**, pp. 75–83 (2009).

M. TADA, ”In-Situ Time-Resolved XAFS for Catalytic Chemistry,” *J. Jpn. Soc. Synchrotron Radiation Res.* **22**, pp. 106–109 (2009).

M. TADA and Y. IWASAWA, “Nanofabrication of Catalyst Surface,” in *Third Edition Modern Interface Colloid Chemistry*, Maruzen, pp. 185–192 (2009).

M. TADA and Y. IWASAWA, “X-Ray Absorption Fine Structures,” in *Third Edition Modern Interface Colloid Chemistry*, Maruzen, pp. 413–417 (2009).

K. YAKUSHI, “Charge-Ordered State in Organic Conductors Studied by Infrared and Raman Spectroscopy,” *Hyomen* (in Japanese) **47**, 45–56 (2009).

K. YAMAMOTO, “Ferroelectricity Induced by Crystallization Conduction Electrons; the Nonlinear and Ultrafast Responses,” *Kotai Butsuri* (in Japanese) **44**, 117–125 (2009).

T. NAKAMURA, K. FURUKAWA and F. IWASE, “Various Competing Electronic Phases in Organic Conductors and Molecular Solids — Physical Properties Investigation by Multi-Frequency and Pulsed Magnetic Resonance—,” *Magnetics Japan* (in Japanese) **4**, 224–228 (2009).

M. HIRAMOTO, “Organic Solar Cells,” in *New Technologies of Printable Organic Electronics* (in Japanese), CMC Publishing, pp. 220–230 (2008).

M. HIRAMOTO, “Technology Trend of Organic Thin-Film Solar Cells for Practical Application,” *Display* (in Japanese) **14**, 34–38 (2008).

M. HIRAMOTO, “Development of Small-Molecular-Type Organic Solid-State Solar Cells,” *Kagakukogyo* (in Japanese) **59**, 776–781 (2008).

M. HIRAMOTO, “Application of Organic Thin-Film Solar Cells,” in *Practical Thin Film Process—Function Creation and Development* (in Japanese), F. Saito and Y. Taga, Eds., NTS Publishing, pp. 355–366 (2008).

M. HIRAMOTO, “Efficient Solar Cells by the High Purification of Organic Semiconductors and 1000 Hours Operation Test,” in *Development of Efficiency and Durability of Organic Thin-Film Solar Cells* (in Japanese), Science&Technology Co. Ltd., pp. 97–104 (2009).

M. HIRAMOTO, “Now and Future of Organic Thin-Film Solar Cells,” *Mirai Zairyo* (in Japanese) **8**, pp. 25–30 (2008).

M. HIRAMOTO, “Fundamentals and Recent Progress of Small-Molecular-Type Organic Solar Cells—High Purification of Organic Semiconductors and Long-Term Operation Test,” in *Frontier Technology of Organic Thin-Film Solar Cells (II)* (in Japanese), CMC Publishing, pp. 79–86 (2008).

M. HIRAMOTO, “Efficient Organic Thin-Film Solar Cells by High Purification of Organic Semiconductors,” *Molecular Electronics and Bioelectronics* (in Japanese) **19**, 221–230 (2008).

M. HIRAMOTO, “Organic Solar Cells,” in *Knowledge Basement* (in Japanese), Electronic Information and Communication Society (2009).

M. HIRAMOTO, “Efficient Organic Solar Cells and Durability Evaluation” in *New Concept Solar Cells and Fabrication Process* (in Japanese), T. Miyasaka Ed., CMC Publishing, pp. 123–130 (2009).

M. HIRAMOTO, “Organic Thin-Film Solar Cells Having ZnO Protection Layer,” *Material Stage* (in Japanese) **9**, pp. 96–99 (2009).

M. HIRAMOTO, “Potential of 10% Conversion Efficiency—Development of Organic Thin-Film Solar Cells—Accomplishment of 5.3% Efficiency,” in *Semiconductor FPD World (Technology Plus)* (in Japanese), Press Journal, pp. 48–49, June (2009).

M. HIRAMOTO, “Evaluation of Electron Injection Barrier of Organic Devices by Ballistic Electron Emission Microscopy,” in *Interface Control Technology for Organic Device* (in Japanese), CMC Publishing, pp. 111–117, August (2009).

S. I. ALLAKHVERDIEV, V. D. KRESLAVSKI, V. THAVASI, V. V. KLIMOV, T. NAGATA, H. NISHIHARA, B. ANDERSSON and S. RAMAKRISHNA, “Hydrogen Photoproduction by Use of Photosynthetic Organisms and Biomimetic Systems,” *Photochem. Photobiol. Sci.* **8**, 148–156 (2009).

H. SAKURAI, “A Novel Carbon Compound Connects Inorganic and Organic Chemistry,” *Kinou Zairyo* (in Japanese) **29**, 46–51 (2009).
S. HIGASHIBAYASHI, “Synthesis of Bowl-Shaped Aromatic Hydrocarbons,” *Yuki Gosei Kagaku Kyokaishi* (in Japanese) **67**, 40–52 (2009).
H. SAKURAI and T. TSUKUDA, “Catalytic Activity of Gold Nanocluster Catalyst Protected by Poly(*N*-vinyl-2-pyrrolidone),” *Yuki Gosei Kagaku Kyokaishi* (in Japanese) **67**, 517–528 (2009).
H. SAKURAI, “Metal Cluster Catalyst in Organic Synthesis,” *Kagaku Kogyo* (in Japanese) **60**, 553–558 (2009).

Life and Coordination-Complex Molecular Science

K. KUWAJIMA, T. OROGUCHI, T. NAKAMURA, M. IKEGUCHI and A. KIDERA, “Experimental and Simulation Studies of the Folding/Unfolding of Goat α-Lactalbumin,” in *Water and Biomolecules—Physical Chemistry of Life Phenomena*, K. Kuwajima, Y. Goto, F. Hirata, M. Kataoka and M. Terazima, Eds., Springer-Verlag; Berlin Heiderberg, pp. 13–35 (2009).

K. KATO, “Structural Glycobiology and Glycodrug Discovery : Overview,” *Tanpakushitsu Kakusan Koso* (in Japanese) **53**, 1661 (2008).
Y. KAMIYA and K. KATO, “Structural Basis for Trafficking and Quality Control of Glycoproteins by Intracellular Lectins,” *Tanpakushitsu Kakusan Koso* (in Japanese) **53**, 1662–1669 (2008).
Y. KAMIYA and K. KATO, “Structural and Molecular Basis for Intracellular Glycoprotein-Fate Determination through Sugar Recognition,” *Seibutsu Butsuri* (in Japanese) **49**, 62–69 (2009).
M. YAGI-UTSUMI and K. KATO, “A Systematic Approach to Structural Glycobiology by Using Ultra-high Field NMR Spectroscopy and Multi-dimensional HPLC,” *Kagaku to Seibutsu* (in Japanese) **47**, 261–268 (2009).
Y. KAMIYA, D. KAMIYA, R. URADE, T. SUZUKI and K. KATO, “Sophisticated Modes of Sugar Recognition by Intracellular Lectins Involved in Quality Control of Glycoproteins,” in *Glycobiology Research Trends*, G. Powell and O. McCabe, Eds., NOVA Science Publishers; New York, pp. 27–40 (2009).
H. YAGI and K. KATO, “Multidimensional HPLC Mapping Method for the Structural Analysis of Anionic *N*-Glycans,” *Trends Glycosci. Glycotech.* **21**, 95–104 (2009).

Y. SHIRO and H. FUJII, “Structures and Electronic Structures of Reaction Intermediates of Metalloenzymes,” *Solid State Physics* (in Japanese) **43**, 699–710 (2008).

R. TERO, “Formation and Structural Observation of Artificial Cell Membranes Supported on Oxide Surfaces,” *Colloid & Interface Communication* (in Japanese) **34**, 19–22 (2009).
K. FURUKAWA, H. NABIKA, K. MURAKOSHI, K. MORIGAKI and R. TERO, “Supported Lipid Bilayer,” *Hyomen Kagaku* (in Japanese) **30**, 207–218 (2009).

Y. UOZUMI, “Heterogeneous Asymmetric Catalysis in Aqueous Media,” in *Handbook of Asymmetric Heterogeneous Catalysis*, Wiley-VCH; Weinheim, Germany, pp. 209–232 (2008).
Z. WANG, K. DING and Y. UOZUMI, “An Overview of Heterogeneous Asymmetric Catalysis,” in *Handbook of Asymmetric Heterogeneous Catalysis*, Wiley-VCH; Weinheim, Germany (2008).
Y. UOZUMI, “Green Catalysts,” *Kagaku* (in Japanese) **63**, 44–46 (2008).

INDEX

to “Research Activities”

MAPS

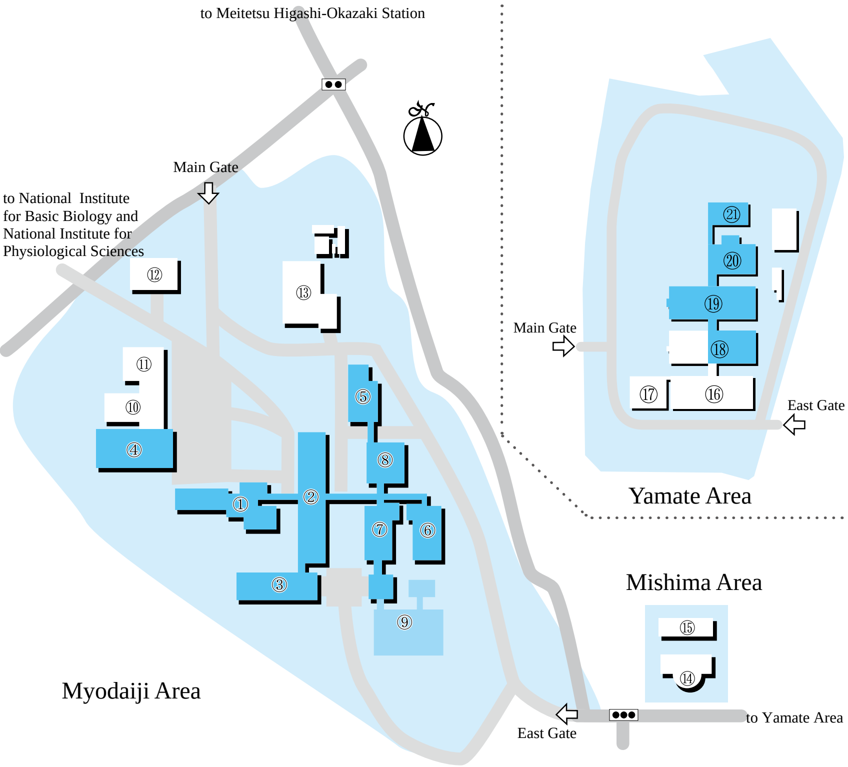

1. Research Office Building
2. Main Laboratory Building
3. South Laboratory Building
4. Research Center for Computational Science
5. Low-Temperature Facilities Building
6. Instrument Center
7. Laser Research Center for Molecular Science
8. Equipment Development Center
9. UVSOR Facility
10. Central Administration
11. Library
12. Faculty Club
13. Power Station
14. Okazaki Conference Center
15. Mishima Lodge
16. Yamate Bldg. 1A
17. Yamate Bldg. 1B
18. Yamate Bldg. 2
19. Yamate Bldg. 3
20. Yamate Bldg. 4
21. Yamate Bldg. 5

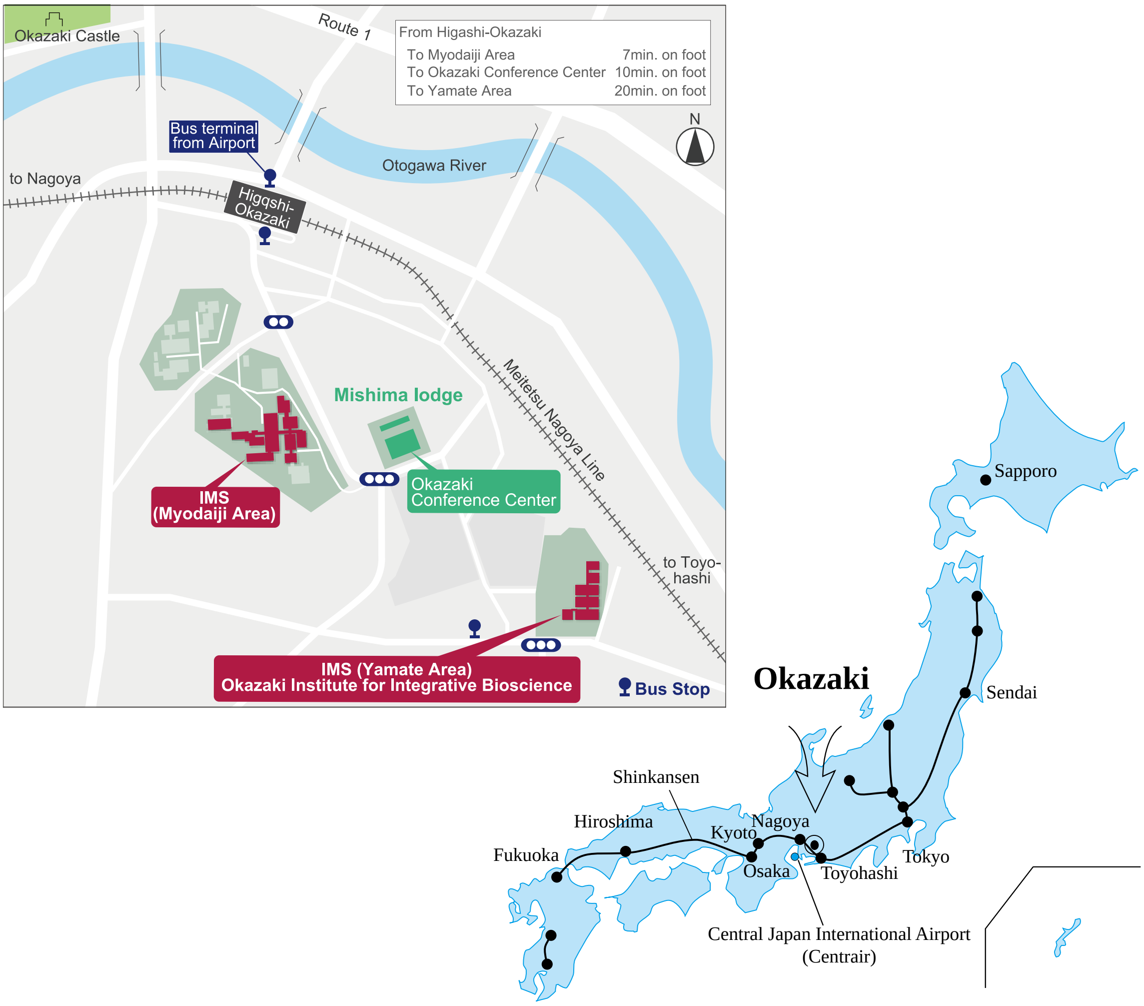
From Higashi-Okazaki

To Myodaiji Area	7min. on foot
To Okazaki Conference Center	10min. on foot
To Yamate Area	20min. on foot

NATIONAL INSTITUTES OF NATURAL SCIENCES
Institute for Molecular Science
Since 1975